GEOMETRIC DESIGN CONSIDERATIONS OF COMBINED HORIZONTAL AND VERTICAL HIGHWAY ALIGNMENTS

by

YASSER HASSAN
B.Sc., Cairo University, Egypt
M.Sc., Cairo University, Egypt

A thesis submitted to
the Faculty of Graduate Studies and Research
in partial fulfilment of
the requirements of the degree of

Doctor of Philosophy
in Civil Engineering

Department of Civil and Environmental Engineering
Carleton University
Ottawa, Ontario, Canada

The Doctor of Philosophy in Civil Engineering
is a joint program with the University of Ottawa
administered by the Ottawa-Carleton Institute for Civil Engineering

ISBN 0-612-19377-2

Name Tasser Hassan

Dissertation Abstracts International is arranged by broad, general subject categories. Please select the one subject which most nearly describes the content of your dissertation. Enter the corresponding four-digit code in the spaces provided.

Civil Engineering — SUBJECT TERM

0543 — SUBJECT CODE

U·M·I

Subject Categories

THE HUMANITIES AND SOCIAL SCIENCES

COMMUNICATIONS AND THE ARTS
Architecture 0729
Art History 0377
Cinema 0900
Dance 0378
Fine Arts 0357
Information Science 0723
Journalism 0391
Library Science 0399
Mass Communications 0708
Music 0413
Speech Communication 0459
Theater 0465

EDUCATION
General 0515
Administration 0514
Adult and Continuing 0516
Agricultural 0517
Art 0273
Bilingual and Multicultural 0282
Business 0688
Community College 0275
Curriculum and Instruction 0727
Early Childhood 0518
Elementary 0524
Finance 0277
Guidance and Counseling 0519
Health 0680
Higher 0745
History of 0520
Home Economics 0278
Industrial 0521
Language and Literature 0279
Mathematics 0280
Music 0522
Philosophy of 0998
Physical 0523
Psychology 0525
Reading 0535
Religious 0527
Sciences 0714
Secondary 0533
Social Sciences 0534
Sociology of 0340
Special 0529
Teacher Training 0530
Technology 0710
Tests and Measurements 0288
Vocational 0747

LANGUAGE, LITERATURE AND LINGUISTICS
Language
- General 0679
- Ancient 0289
- Linguistics 0290
- Modern 0291

Literature
- General 0401
- Classical 0294
- Comparative 0295
- Medieval 0297
- Modern 0298
- African 0316
- American 0591
- Asian 0305
- Canadian (English) 0352
- Canadian (French) 0355
- English 0593
- Germanic 0311
- Latin American 0312
- Middle Eastern 0315
- Romance 0313
- Slavic and East European 0314

PHILOSOPHY, RELIGION AND THEOLOGY
Philosophy 0422
Religion
- General 0318
- Biblical Studies 0321
- Clergy 0319
- History of 0320
- Philosophy of 0322

Theology 0469

SOCIAL SCIENCES
American Studies 0323
Anthropology
- Archaeology 0324
- Cultural 0326
- Physical 0327

Business Administration
- General 0310
- Accounting 0272
- Banking 0770
- Management 0454
- Marketing 0338

Canadian Studies 0385
Economics
- General 0501
- Agricultural 0503
- Commerce-Business 0505
- Finance 0508
- History 0509
- Labor 0510
- Theory 0511

Folklore 0358
Geography 0366
Gerontology 0351
History
- General 0578
- Ancient 0579
- Medieval 0581
- Modern 0582
- Black 0328
- African 0331
- Asia, Australia and Oceania 0332
- Canadian 0334
- European 0335
- Latin American 0336
- Middle Eastern 0333
- United States 0337

History of Science 0585
Law 0398
Political Science
- General 0615
- International Law and Relations 0616
- Public Administration 0617

Recreation 0814
Social Work 0452
Sociology
- General 0626
- Criminology and Penology 0627
- Demography 0938
- Ethnic and Racial Studies 0631
- Individual and Family Studies 0628
- Industrial and Labor Relations 0629
- Public and Social Welfare 0630
- Social Structure and Development 0700
- Theory and Methods 0344

Transportation 0709
Urban and Regional Planning 0999
Women's Studies 0453

THE SCIENCES AND ENGINEERING

BIOLOGICAL SCIENCES
Agriculture
- General 0473
- Agronomy 0285
- Animal Culture and Nutrition 0475
- Animal Pathology 0476
- Food Science and Technology 0359
- Forestry and Wildlife 0478
- Plant Culture 0479
- Plant Pathology 0480
- Plant Physiology 0817
- Range Management 0777
- Wood Technology 0746

Biology
- General 0306
- Anatomy 0287
- Biostatistics 0308
- Botany 0309
- Cell 0379
- Ecology 0329
- Entomology 0353
- Genetics 0369
- Limnology 0793
- Microbiology 0410
- Molecular 0307
- Neuroscience 0317
- Oceanography 0416
- Physiology 0433
- Radiation 0821
- Veterinary Science 0778
- Zoology 0472

Biophysics
- General 0786
- Medical 0760

EARTH SCIENCES
Biogeochemistry 0425
Geochemistry 0996
Geodesy 0370
Geology 0372
Geophysics 0373
Hydrology 0388
Mineralogy 0411
Paleobotany 0345
Paleoecology 0426
Paleontology 0418
Paleozoology 0985
Palynology 0427
Physical Geography 0368
Physical Oceanography 0415

HEALTH AND ENVIRONMENTAL SCIENCES
Environmental Sciences 0768
Health Sciences
- General 0566
- Audiology 0300
- Chemotherapy 0992
- Dentistry 0567
- Education 0350
- Hospital Management 0769
- Human Development 0758
- Immunology 0982
- Medicine and Surgery 0564
- Mental Health 0347
- Nursing 0569
- Nutrition 0570
- Obstetrics and Gynecology 0380
- Occupational Health and Therapy 0354
- Ophthalmology 0381
- Pathology 0571
- Pharmacology 0419
- Pharmacy 0572
- Physical Therapy 0382
- Public Health 0573
- Radiology 0574
- Recreation 0575
- Speech Pathology 0460
- Toxicology 0383

Home Economics 0386

PHYSICAL SCIENCES
Pure Sciences

Chemistry
- General 0485
- Agricultural 0749
- Analytical 0486
- Biochemistry 0487
- Inorganic 0488
- Nuclear 0738
- Organic 0490
- Pharmaceutical 0491
- Physical 0494
- Polymer 0495
- Radiation 0754

Mathematics 0405
Physics
- General 0605
- Acoustics 0986
- Astronomy and Astrophysics 0606
- Atmospheric Science 0608
- Atomic 0748
- Electronics and Electricity 0607
- Elementary Particles and High Energy 0798
- Fluid and Plasma 0759
- Molecular 0609
- Nuclear 0610
- Optics 0752
- Radiation 0756
- Solid State 0611

Statistics 0463

Applied Sciences

Applied Mechanics 0346
Computer Science 0984
Engineering
- General 0537
- Aerospace 0538
- Agricultural 0539
- Automotive 0540
- Biomedical 0541
- Chemical 0542
- Civil 0543
- Electronics and Electrical 0544
- Heat and Thermodynamics 0348
- Hydraulic 0545
- Industrial 0546
- Marine 0547
- Materials Science 0794
- Mechanical 0548
- Metallurgy 0743
- Mining 0551
- Nuclear 0552
- Packaging 0549
- Petroleum 0765
- Sanitary and Municipal 0554
- System Science 0790

Geotechnology 0428
Operations Research 0796
Plastics Technology 0795
Textile Technology 0994

PSYCHOLOGY
General 0621
Behavioral 0384
Clinical 0622
Developmental 0620
Experimental 0623
Industrial 0624
Personality 0625
Physiological 0989
Psychobiology 0349
Psychometrics 0632
Social 0451

The undersigned hereby recommend to
the Faculty of Graduate Studies and Research
acceptance of the thesis,

Geometric Design Considerations of Combined Horizontal and Vertical Highway Alignments

submitted by

Mr. Yasser Hassan, B.Sc., M.Sc.

in partial fulfilment of the requirements
for the degree of Doctor of Philosophy

Professor J.L. Humar, Chairman
Civil and Environmental Engineering

for. Professor A.O. Abd El Halim, Co-supervisor
Civil and Environmental Engineering

Said M. Hay

Professor S. Easa, Co-supervisor
Civil Engineering, Lakehead University

Professor J. Morrall, External Examiner
Civil Engineering, The University of Calgary

Carleton University

ABSTRACT

The process of highway design is a complex one where many phases are incorporated to achieve safe, efficient, economical, and aesthetically pleasant highways. Among these phases, geometric design is the most related to traffic safety. Highway efficiency, economics, and aesthetics depend on the decisions taken in the geometric design phase. Thus, design standards have been set to guarantee the achievement of the design objectives. However, these standards are based on 2-D modelling of highways where the horizontal alignment, vertical alignment, and cross-section are designed separately.

In this research, a framework is presented for 3-D combined highway alignments to jointly design all highway elements based on sight distance, vehicle stability, driver comfort, drainage, and aesthetics. Specifically, this research focuses on the daytime sight distance and its related aspects. First, a revised model for the required passing sight distance and minimum length of passing zones is developed, and the resulting passing sight distances show good agreement with field measurements. Second, a new concept for positioning the beginning and end of passing zones is presented and modelled analytically. Third, the available sight distance on complex 2-D horizontal and vertical alignments and 3-D alignments is modelled. Computer software are developed based on these analytical models, and each software is verified graphically or by field measurements. Applications of the developed models and software are presented in marking and design.

The application of the developed models for the required passing sight distance shows the need for revisions in the marking standards to ensure safety and efficiency of the traffic operation. The models for available sight distance provide a useful tool to replace the current graphical and field practices to establish the no-passing zones on two-lane highways. Such a tool would avoid the potential human errors, reduce the cost, and minimize the time required for marking. A comparison with the current design standards shows their inadequacy whether the highway is in cut or fill. The standards may compromise highway economics or traffic safety. As a result, the need for revisions in the design standards based on 3-D alignments is established.

ACKNOWLEDGMENTS

The author is grateful to William Hughes, Transportation and Works Department, Engineering Division, City of Thunder Bay; and Dennis Siezkar, Doug Robinson, and Angelo Tassone, Ministry of Transportation of Ontario, Thunder Bay District, for providing the field data and equipment that were used in this research. My sincere gratitude to Karen Williams, Lakehead University, Thunder Bay, for her assistance in producing this thesis; Kailash Bhatia and Ahmed Abo Taleb, Lakehead University, Thunder Bay, for their assistance in the field measurements; and Ahmed Shalaby, Carleton University, Ottawa, for his continuous help for almost three years. The financial support of Carleton University, the Transportation Association of Canada (TAC), and the Natural Sciences and Engineering Research Council of Canada (NSERC) is also gratefully acknowledged.

Finally, I would like to express my deepest gratitude to Dr. Said Easa, Lakehead University, Thunder Bay, and Dr. A.O. Abd El Halim, Carleton University, Ottawa, for their guidance, suggestions, help, support, and patience in supervising this thesis.

Yasser H.A. Hassan

TABLE OF CONTENTS

LIST OF TABLES

LIST OF FIGURES

CHAPTER 1

INTRODUCTION

Since ancient times, advancement and prosperity of civilizations have been very much dependent on the availability of a reliable transportation system, with roads representing a major component. Subsequently, it is not surprising to know that both the Roman and Persian Empires had built good roads which served not only as commercial tools but also as military and power instruments (Meijer and Van Nijf, 1992). Currently, in spite of the advancements in other transportation modes, highways are still holding their importance in both the economic and military fields. Realizing this fact, it was reported in a study published by the World Bank that a transport infrastructure is a prerequisite of economic development (Adler, 1987). It was also reported in the same study that it is not unusual for traffic growth to be two to three times as large as the rise in national income. Therefore, it has been the interest of the World Bank to encourage developing the transport sector in the less developed countries (Van Der Tak and Ray, 1971). Furthermore, the importance of highways increases even more in the US and Canada where, according to 1977 statistics, 5% of the world's population own 43% of the motor vehicles (Oglesbey and Hicks, 1982).

In Canada, highways have evolved from very primitive narrow trails made by natives to connect rivers and lakes, where the canoe was the basic transportation means, to one of the most advanced road networks in the world. The service provided by this network was described as "*today, no other country, in relation to its size and population,*

is better served" (Guillet, 1966) These roads served 93% of all domestic travel by Canadians in 1990 as well as the freight travel of more than 84 billion tonne-kilometres in 1988, with an expected continuous increase in these figures until the year 2000 (TAC, 1990). In the fiscal year 1988/89, the federal, provincial, and municipal expenditures on the road network, whose length totalled 879,530 2-lane kilometres, were more than $8.4 billion. In the US in the year 1994, federal, state, and local governments spent more than $90 billion on a total of 3,906,544 miles of highways (BTS, 1996). This latter highway network served 175,403,465 motor vehicle licensed drivers and a total of 133,929,661 cars; 3,718,427 motorcycles; 670,423 buses; and 63,445,280 trucks. Outperforming all other domestic transportation modes, in 1994, American highways accounted for 2,364,384 million vehicle-miles (98.5% of all domestic vehicle-milage) and 3,937,765 million passenger-miles (90.7% of all domestic passenger-milage). In addition to passenger travel, by carrying 908 billion ton-miles of freight (25.6% of all domestic ton-milage of freight), highways played a significant role in the American freight transportation.

However, one key element in designing modern highways is the increasing awareness of the possible highway and motor vehicle impacts. As a result, highway design has become a very complex process in which designers and agencies of different specialities and interests cooperate to account for traffic safety and efficiency, driver comfort, social and environmental impacts, highway aesthetics, and economic benefits. This complexity in the design process was reported by the Federal Highway Administration of the US (FHWA). It was stated that "*highway transportation goals*

become broader and more difficult to achieve as time goes" (FHWA, 1972). Subsequently, a rational highway design process should involve the following stages: planning, route selection, geometric design, and structural design.

1.1 Highway Design Process

The planning phase is a never-ending process whose main objective is "*the establishment of a highway network capable of accommodating all highway travel in an orderly, safe, efficient, and economical manner*" (Michael, 1960). Due to the increasing public concern about the social and environmental impacts of highways and motor vehicle transportation, the decisions made in this phase are usually influenced by public organizations and representatives. As a result, the decisions have to be acceptable not only professionally and economically but also politically. An approach for the planning phase including the decision-making process and the factors considered can be found in the literature (Khisty, 1990; Oglesbey and Hicks, 1982). If, at a certain time, a need for a highway between certain points is established, the possible alternative routes are compared to determine the most economical route for the highway to follow. Such an economic comparison must consider the costs of both construction and right-of-way and the existence of any control points (Young et al, 1960).

The highway geometric design is the phase which follows the route selection. As defined in the literature, highway geometric design is the proportioning of the visible elements of the highway (Easa, 1995; Garber and Hoel, 1988; King and Harkins, 1982; Noble, 1960; Wright and Paquette, 1979). The laws of motion (kinematics and

dynamics), the vehicle characteristics, and the ability and psychology of the road users are incorporated in this phase to produce safe and efficient highways. In order to ensure the safety and efficiency of the designed highways, each country has established a set of design standards to suite its traffic characteristics and environmental conditions. However, as reported by Krammes and Garnham (1995), the design standards used in most countries have far more similarities than differences. The most common set of design standards is found in the design guide developed by the American Association of State Highway and Transportation Officials, known as the AASHTO green book, (AASHTO, 1994). This design guide is used by the different states as a basis to develop their own standards. In Canada, the provinces use the *Manual of Geometric Design Standards for Canadian Roads* published by the Transportation Association of Canada (TAC, 1986), formerly known as the Roads and Transportation Association of Canada (RTAC), as their design standards or as a basis for their own. Another set of standards is used for highway marking and can be found in the *Manual of Uniform Traffic Control Devices* which is available in both Canadian and American editions (MUTCD, 1976; MUTCD, 1988).

Finally, the structural design of highways involves the selection of the materials used in the different pavement layers, including any required treatment for the subgrade, and thickness design for each layer. Accordingly, the designed pavement is expected to sustain the traffic loads and the environmental conditions during its design life. Detailed explanation of the principles of pavement structural design can be found in the literature (Huang, 1993; Yoder and Witczak, 1975). Also, design guides for flexible and rigid

pavements are given by AASHTO (1986) and the Portland Cement Association (PCA, 1984). Currently, extensive research work is being conducted mainly by US and partly by Canada to enhance the pavement design standards. The research program, known as the Strategic Highway Research Program (SHRP), lasted for five years and ended in 1993. Since then, FHWA, AASHTO, and the Transportation Research Board (TRB) have been working on the implementation of the new SHRP findings and products (FHWA, 1995).

Among the different phases of the highway design process, the geometric design phase is the most related to traffic safety. This phase is the broad subject of this research where the current standards of highway geometric design are reviewed. Then, extensions to these standards are suggested. The following sections explain the concerns with current standards and the objectives of this research.

1.2 Present Status of Geometric Design

Prior to the design of the different elements of the highway, traffic controls, such as the design speed and highway classification, are selected. Then, in the geometric design phase, the designer uses the standards to design the highway alignment and the cross section, including the roadside and other special elements such as acceleration, deceleration, and truck lanes. These design standards must ensure that the resulting highways satisfy sight distance, vehicle stability, driver comfort, drainage, and highway aesthetics. Also, the design must not violate the practical limitations of driver abilities, vehicle characteristics, and topography. Moreover, the design process should account for the variations in drivers' performances which result from the variations in education,

experience, and age. Each of the design bases and constraints influences the design of all highway elements, as shown in Figure 1.1.

However, although geometric design standards have been revised several times during the last 40 years, the theoretical bases and fundamentals of these standards have not changed since the first design guide issued in 1954 by the American Association of State Highway Officials (AASHO, 1954). For example, although the 3-D nature of highway geometric design is a well known fact, the highway alignment is still designed as separate 2-D horizontal and vertical alignments. On this point, it was reported that "*the alignment of a highway is a three-dimensional problem ... However, in highway design practice, three-dimensional design computations are cumbersome*" (Mannering and Kilareski, 1990). Convinced of the difficulty of establishing 3-D-based standards and recognizing the need for an assessment of the combined alignment, AASHTO and TAC design guides have offered general guidelines to enhance the coordination of horizontal and vertical alignments. However, these guidelines are far less than satisfactory. As a result, Smith and Lamm (1994) concluded that "*three-dimensional alinement, a very complex component in the highway geometric design process, still represents the weakest link in the overall design of highways*".

Moreover, the highway geometric design standards have been criticized by many researchers in studying certain areas. For example, Harwood and Glennon (1977) stated "*in the age of interactive graphics, automatic photogrammetric plotting, freeway surveillance and control ... the highway community still designs and marks passing zones on two-lane rural highways according to false and archaic principles*". Eleven years after

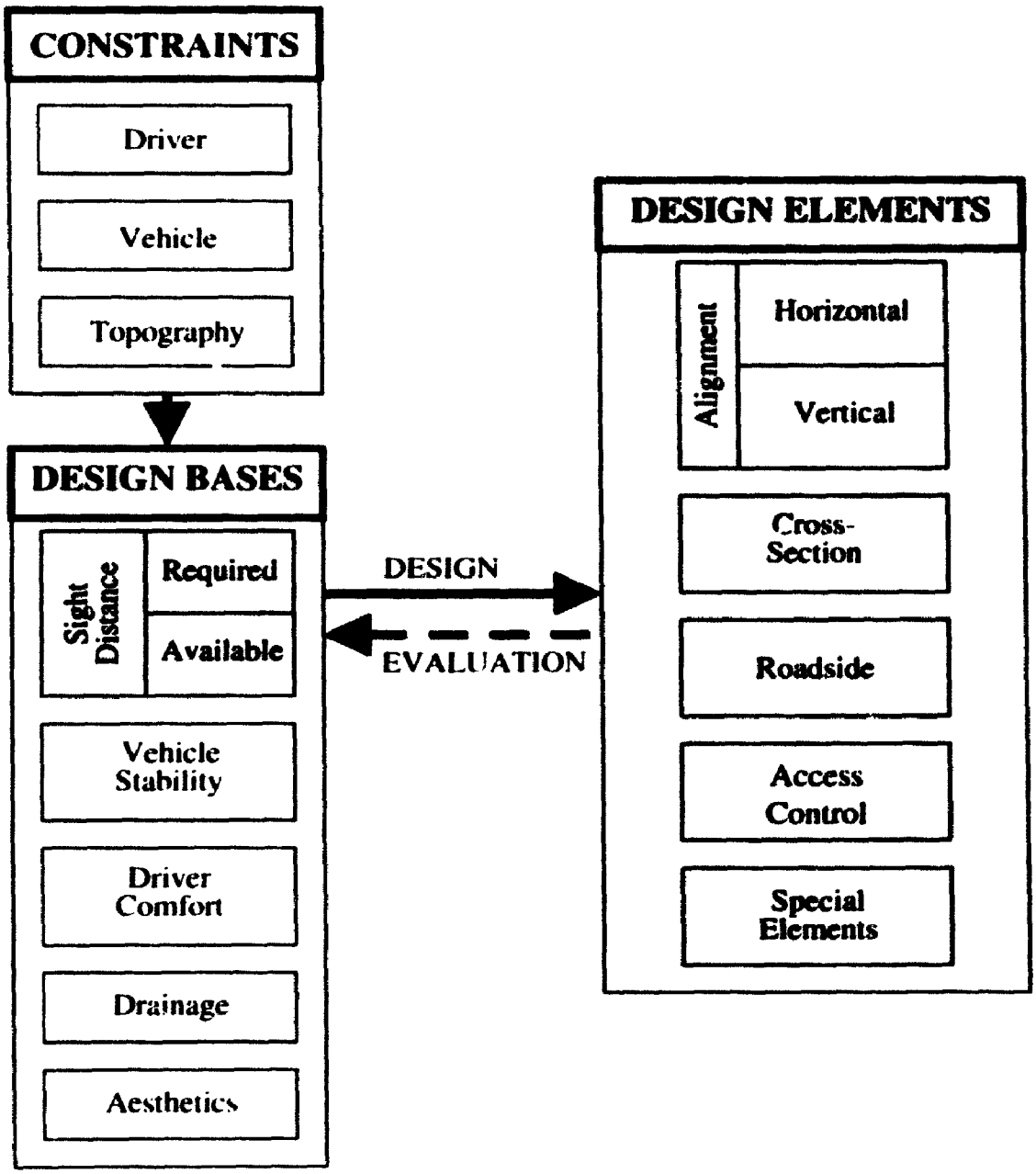

FIGURE 1.1: Framework for Highway Geometric Design.

this comment, it was repeated by Glennon (1988) on the same subject of passing zones that "*the highway community still clings to false and archaic principles*". The consideration of the stopping sight distance has also been criticized by Neuman (1989) who stated "*there is continuing, growing dissatisfaction among many design engineers with the current policy and general approach to the subject*". Furthermore, on the same point, Hall and Turner (1989) stated "*engineers are finding that it is expensive to comply with the current standards, especially in the reconstruction of existing highways*".

Generally, the observations of the deficiencies associated with the current standards have been summarized by Glennon (1989) who commented on the 1984 edition of the AASHTO design guide that "*efforts were inadequate to make the Green Book adequate reflection of the technology available at the time it was published*". Interestingly, most of the deficiencies pointed out by Glennon (1989) have not been addressed in the subsequent editions of the AASHTO green book, and the previous comment can still be applied to the most recent edition published in 1994.

1.3 Problem Definition

As stated earlier, this research focuses on the geometric design phase. The current practice and standards of highway geometric design are reviewed against the framework shown in Figure 1.1. As shown in the figure, all the design elements (horizontal and vertical alignments, cross-section, roadside, access control, and special elements such as acceleration lanes, climbing lanes, ...) should be designed jointly, if a new highway is being designed. Furthermore, when an existing highway is being evaluated, the effect of

all these elements should also be considered jointly. However, as mentioned earlier, one of the main deficiencies in the current practice of highway geometric design is that each element is designed separately instead of a combined alignment of all elements in 3-D analysis. As a result, complete achievement of the objectives of highway geometric design is not guaranteed with the use of the current standards, especially, if the designer is not very experienced. On the other hand, the consideration of the 3-D highway alignment should dramatically reduce the risk of any design deficiency and the associated costs for its subsequent fixation.

In summary, the concerns in the current geometric design standards can be stated as follows:

1. Current design standards are based on approximate and simplified consideration of each highway element in a 2-D projection and separately from the other elements
2. Moreover, in this simplified 2-D design, the current standards can deal only with an isolated simple curve, in a horizontal or vertical alignment.
3. Although other research works have considered compound and reverse curves, they have failed to consider general alignments with successive curves and short tangents
4. Oversimplified 2-D design standards do not guarantee a satisfactory highway design.
5. Highway alignment design should be based on 3-D analysis.
6. The 3-D nature of highway alignment has not been explored in design because of its complexity.

1.4 Objectives and Scope

Consequently, the main objectives of this research are:

1. To identify and evaluate the weakness in the current geometric design prac : where each element is designed separately in a 2-D projection.
2. To develop a design methodology to account for the 3-D nature of highway alignment.
3. To study the effect of 3-D analysis on different highway elements.
4. To quantify the difference between 2-D and 3-D alignment on highway marking and design.
5. To revise the available models for the required passing sight distance and the minimum required length of passing zones.

It should be noted that the scope of this research is limited to the design of rural highways. Also, as indicated by the hatching in Figure 1.1, the research focuses mainly on the sight distance and its impact on the different highway elements. In addition, since stopping sight distance is currently being addressed in the National Cooperative Highway Research Program (NCHRP) Project 3-42, it has not been included in this research.

The next chapters of this thesis are organized as follows:

- Chapter 2 presents a detailed review of the consideration of 3-D highway alignments with a greater focus on the work conducted in the field of sight distance and its relation to the different design elements.
- Chapter 3 explains the revised model developed in this research to determine the required passing sight distance. Also, developed models for the length of passing

zones and the profile of the required passing sight distance with the evolvement of the pass are presented.

- Chapter 4 explains the methodologies developed in this research to determine the available sight distance on complex 2-D horizontal and vertical alignments. Either alignment is considered separately from the other one.
- Chapter 5 explains a new methodology to determine the available sight distance on general 3-D combined horizontal and vertical alignments.
- Chapter 6 presents an application of the developed models for required and available sight distances in marking passing and no-passing zones. A practical example of a 7-km segment on Highway 61 is presented.
- Chapter 7 presents a further application of the developed models for available sight distance in alignment design with a quantification for the consequences of ignoring the 3-D nature of highway geometric design.
- Chapter 8 presents the main conclusions and findings of this research and recommendations for further research work required to establish 3-D design standards.

CHAPTER 2

REVIEW OF CURRENT DESIGN PRACTICE AND EXISTING RESEARCH WORK

In this chapter, the previous research work and the current practice of highway geometric design are reviewed against the framework presented in Figure 1.1. The review focuses on the design bases (sight distance, vehicle stability, driver comfort, drainage, and aesthetics) and how they affect the different design elements. Although the design constraints influence the design elements, they are not explicitly included in this review. As indicated by the hatching in the figure, more emphasis is put on the sight distance which is the main focus of this research.

2.1 Sight Distance

Ideally, geometric design should ensure that any object on the pavement surface is visible to the drivers within the normal eye sight distance. However, because topographical constraints make such a design impractical, roads are designed to provide drivers with at least the minimum sight distance required for safe and efficient operation. The sight distance is defined in the AASHTO guide (1994) as the length of the highway visible to the driver. The role of the sight distance in safe and efficient traffic operation has been emphasized in both AASHTO and TAC guides.

Although highway professionals agree on the correlation between sight distance and safety, many researchers have reported that not enough studies have been carried out

to quantify this relationship (TRB, 1987; Glennon, 1987; Olson et al, 1984). One of the main reasons for the difficulty associated with establishing such correlation is that sight distance is always associated with a horizontal and/or vertical curvature. Thus, it is difficult to separate sight distance effects from other highway elements. Moreover, the accidents resulting from deficient sight distance are event oriented. For such accidents to occur, a series of events must first take place at the critical section with deficient sight distance.

In the state-of-the art presented in Report 270 by the National Cooperative Highway Research Program (NCHRP), Olson et al (1984) summarized the findings of 20 studies on the relationship between highway elements, including sight distance, and safety. Among these studies, a weak relationship between sight distance and safety was reported in only one study while the remaining 19 concluded that safety increases as the alignment and sight distance improve. However, because all of these studies included the effect of the alignment, combined with sight distance, another study was conducted to neutralize this parameter (Olson et al, 1984). In this study, the accident counts on 10 matching pairs of vertical curves were compared. Each pair was selected so that the two curves had identical traffic and alignment features. One of the two curves had a limited sight distance while the other one had a sight distance more than the minimum required sight distance according to the 1965-AASHTO guide. The results showed that the accident counts on the control sections were significantly lower than the accident counts on the sections with limited sight distance.

Therefore, design standards state that designers must provide, at every point along the highway, a sight distance sufficient for a below-average driver or vehicle to stop before hitting an unexpected object on the pavement (AASHTO, 1994; TAC, 1986). Such a distance is known as the stopping sight distance (SSD). Moreover, a longer sight distance has been recommended in some situations where the driver has to make a complex decision. Such a distance is known as the decision sight distance (DSD). Design values for DSD are given in the AASHTO and TAC guides. However, DSD is extremely variable and must be analyzed on a single-situation-basis.

As for efficiency, "*if operational efficiency is to be built into the road, for higher traffic volumes, then lengths of road with sufficient sight distance may have to be provided for drivers to overtake slower vehicles safely*" (Kosasih et al, 1987). Clearly, since overtaking slower vehicles on multi-lane highways can be performed with a lane change without travelling in the lanes of the opposing traffic, this requirement is applicable for two-lane highways only. The role of the availability of sufficient passing sight distance (PSD) on the level-of-service of two-lane highways has been emphasized in the *Highway Capacity Manual* (HCM, 1994). As shown in the HCM, the volume-to-capacity ratio of two-lane rural highways may be reduced by more than 30% if the percentage of the length of no-passing zones increases from zero to 100%. Moreover, long stretches of two-lane rural highways with no opportunity for passing slower vehicles could cause drivers to carry out erratic and hazardous passing manoeuvres (Persaud, 1992). For example, in 1987, while the head-on non-intersection collisions on two-lane highways in Ontario, where erratic passing is the most probable cause, represented just

2% of all accidents, they accounted for 17% of the fatal accidents. Therefore, AASHTO and TAC guides have recommended providing sufficient PSD on two-lane rural highways at frequent intervals and for substantial portions of the highway length. The collisions due to erratic passing can also be reduced by a good marking of passing and no-passing zones to assist drivers, especially the less experienced, decide whether to pass or trail a slower vehicle. Such a marking is based mainly on sight distance requirements.

Realizing the importance of sight distance in highway geometric design, considerable research work has been directed to answer two vital questions: how long should the required sight distance be?, and how long is the actually available sight distance? In the following sections, the current models to determine the required sight distance are reviewed and discussed. Also, the existing models for the available sight distance, with the incorporation of these models in the highway design and evaluation, are presented.

2.1.1 Required Stopping Sight Distance (SSD)

As stated earlier, SSD is a major element in the safe operation on any highway. In the historical review of the development of the required SSD, Hall and Turner (1989) showed that the importance of SSD has been recognized as early as in 1914 (Agg, 1916; Blanchard and Drowne, 1914). In 1940, the AASHO policy on sight distance presented an analytical model for calculating the required SSD based on the laws of dynamics (AASHO, 1940). In this model, which is still in use until today, the SSD is measured from the driver eye to the highest point of a small stationary object on the road. The

required SSD in the model is the sum of the distance travelled during the perception-reaction time and the braking distance, *B.D.*, which can be calculated as follows:

$$B.D. = \frac{V^2}{254\ (f+G)} \tag{2.1}$$

where

V = initial speed of the vehicle (km/h),

f = coefficient of friction between the tires and the roadway, and

G = highway grade in decimal fraction (positive if upward and vice versa).

Although this model has not changed since then, many studies have been conducted to revise the values of its parameters. Among them is a comprehensive study conducted by Olson et al (1984). The study included the quantification of the perception-reaction time, height of the driver eye, height of the object, and the coefficient of friction. Furthermore, a new concept of deceleration with steering control for a passenger car and a truck was presented to ensure safety and comfort on horizontal curves. Also, a new and rational approach to determine the required SSD based on highway functional classification was suggested by Neuman (1989). However, the most recent edition of the AASHTO guide in 1994 failed to incorporate this approach in the design standards. A more recent comprehensive revision for the model is being conducted in the NCHRP Project 3-42 (Fambro et al, 1995).

2.1.2 Required Decision Sight Distance (DSD)

In some complex situation, the perception of information may be difficult and/or the appropriate action may be unexpected or unusual. In such situations, SSD is usually not enough to ensure traffic safety. As a result, the AASHTO guide recommends the provision of a longer sight distance known as the decision sight distance (DSD). The DSD has been defined in both AASHTO and TAC guides as "*the distance required for a driver to detect an unexpected or otherwise difficult-to-perceive information source or hazard in a roadway environment that may be visually cluttered, recognize the hazard or its threat potential, select an appropriate speed and path, and initiate and complete the required safety manoeuvre safely and efficiently*". A similar sight distance, called manoeuvre sight distance, is also recommended in the Australian standards presented by the National Association of Australian State Road Authorities (NAASRA, 1980). Although design values of the DSD are given in each of these design guides, DSD should be determined on a single-situation-basis. This is mainly due to the fact that it depends on the complexity of the situation and the volume of traffic.

2.1.3 Required Passing Sight Distance (PSD)

(i) AASHTO Model. Based on the results of field studies conducted in and before 1958 and as shown in Figure 2.1, AASHTO presented a model to calculate the PSD, S, as follows:

$$S = d_1 + d_2 + d_3 + d_4 \tag{2.2}$$

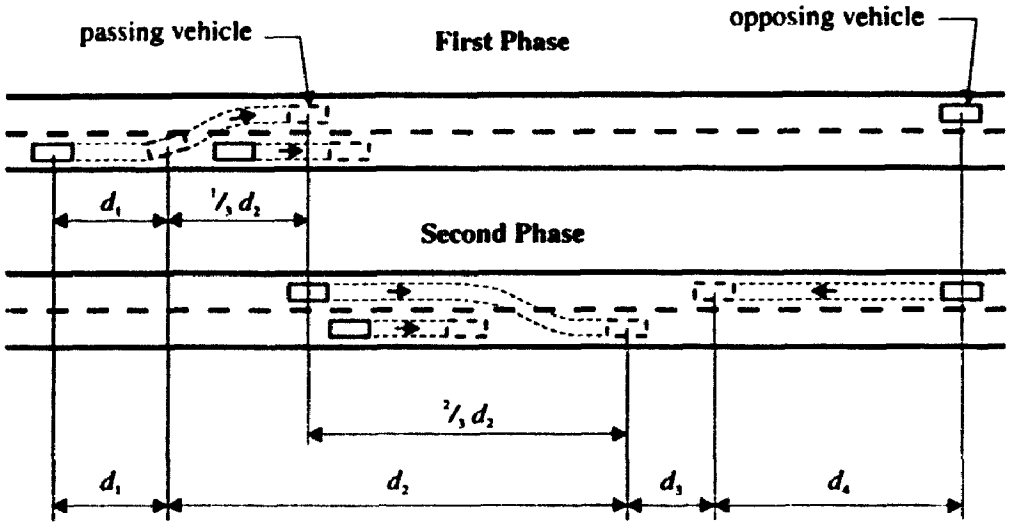

FIGURE 2.1 : Passing Manoeuvre According to AASHTO (1994).

d_2 = distance travelled by the passing vehicle while occupying the left lane (time elapsed = t_2),

d_3 = clearance distance between the passing and opposing vehicles at the end of the pass, and

d_4 = distance travelled by the opposing vehicle for two-thirds of the time the passing vehicle occupies the left lane = $\frac{2}{3}$ d_2 (time elapsed = t_4 = $\frac{2}{3}$ t_2).

Design values for these distances and PSD are given in the AASHTO and TAC design guides.

However, this model is not free of self-discrepancies. By taking $t_4=\frac{2}{3}t_2$ instead of t_1+t_2, the model accounts for the driver's ability to abort the pass if any opposing vehicle is seen ahead during the time $t_1 + \frac{1}{3}t_2$. At the mean time, by considering d_1 and all d_2 as parts of the PSD, the model assumes that the passing vehicle is committed to complete

However, this model is not free of self-discrepancies. By taking $t_4=\frac{2}{3}t_2$ instead of t_1+t_2, the model accounts for the driver's ability to abort the pass if any opposing vehicle is seen ahead during the time $t_1 + \frac{1}{3}t_2$. At the mean time, by considering d_1 and all d_2 as parts of the PSD, the model assumes that the passing vehicle is committed to complete the pass once it is initiated. Three additional flaws in the model and its design values were pinpointed by Harwood and Glennon (1977) as follows:

1. The model is incapable of determining the minimum length of the passing zone.
2. The model uses assumed average speeds rather than the design speeds, and subsequently it represents an average pass not a critical pass.
3. For high speeds, speed differentials between passing and passed vehicles were taken constant instead of being determined from field measurements.

In conclusion, Weaver and Glennon (1971) and Harwood and Glennon (1977) suggested that $\frac{2}{3}d_2+d_3+d_4$ would represent a more logical model for PSD. However, such a conclusion was very subjective and does not consider the other flaws in the model they criticized, and they themselves participated in developing another new model (Glennon, 1988; Harwood and Glennon, 1989).

(ii) MUTCD Design Values of PSD. Another discrepancy arises when comparing the PSD values given in the Canadian and American versions of MUTCD, which are used in pavement marking, and those given in design guides (AASHTO, 1994; TAC, 1986). A comparison between these values, as shown in Table 2.1, shows that the values used in pavement marking are much shorter than those presented in the design guides.

TABLE 2.1: Passing Sight Distance Requirements in Design and Marking Standards in Canada.

Speed (km/h)	Required PSD (m)	
	Design Standards (TAC, 1986)	Marking Standards (MUTCD, 1976)
50	340	160
60	420	200
70	480	240
80	560	275
90	620	330
100	680	400
110	740	475
120	800	565
130	860	---

Interestingly, it was reported by Harwood and Glennon (1977; 1989) that the reasons for selecting these minimum sight distances in the MUTCD are not stated, nor is the source given. However, they noted that these values are identical to those presented in the 1940-AASHO Guide. Since these values represent a subjective compromise between PSD for delayed and flying passes, Harwood and Glennon (1977; 1989) concluded that these values do not represent any particular passing situation.

(iii) Models Based on the Concept of Critical Position (Point of No Return). A new concept in modelling PSD was presented by Van Valkenberg and Michael (1971). As

shown in Figure 2.2, they considered that the distance travelled by the passing vehicle can be divided into two distances: S_0, the distance during which the vehicle can apply the brakes and pull back into the proper lane, and S_1, the distance required to complete the pass. The point beyond which the pass must be completed was called *the point of no return*, and based on personal judgement it was assumed to occur when the rear bumper of the passed vehicle is abreast of the middle of the passing vehicle. Then, the PSD was taken as the summation of S_1 and S_2 plus a clearance distance, where S_2 is the distance travelled by the opposing vehicle during the time required for the passing vehicle to travel the distance S_1. Although, Van Valkenberg and Michael (1971) presented design values for PSD based on field measurements, they did not present mathematical modelling for their work and subsequently, these measurements can be useful for highways with speeds and conditions within the range used in the field measurements only.

The same concept was used by Lieberman (1982) who called the point of no return the critical position. He defined the critical position as the point where "*the*

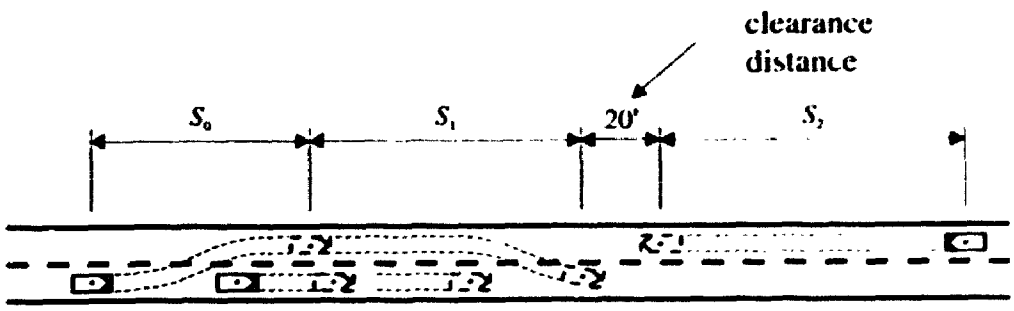

FIGURE 2.2 : Passing Manoeuvre According to Van Valkenberg and Michael (1971).

decision by the passing vehicle to complete the pass will afford it the same clearance relative to the oncoming vehicle as will the decision to abort the pass" (Lieberman, 1982). He incorporated this definition into a mathematical model to calculate the PSD but he assumed that the driver is committed to complete the pass, and therefore, he concluded that the AASHTO criteria for PSD were inadequate. In addition to this very conservative approach, other flaws in the modelling were identified by Glennon (1988) such as ignoring the direct effects of vehicle length and the perception-reaction time in aborted passes. Another attempt for modelling the PSD using the concept of the critical position was made by Saito (1984). However, as stated by Glennon (1988), Saito considered only the needs to abort the manoeuvre and ignored the trade-offs between the completed and aborted manoeuvres.

In 1988, Glennon (1988) presented the most comprehensive and closest modelling to the actual mechanism of the passing manoeuvre. He interpreted the definition of the critical position, or the point of no return, by having a minimum acceptable headway between the nearest points of each two vehicles involved in the manoeuvre at the end of either a completed or aborted pass (for example, the rear bumper of the passing vehicle and the front bumper of the impeding vehicle in a completed pass). Then, he developed a model based on the hypothesis that at the beginning of the pass, the sight distance required to abort the pass is much less than that required to complete it and vice versa by the end of the pass. In between, there is a point, the critical position, where the sight distance required to complete the pass is equal to that required to abort it. He called this sight distance the critical sight distance, S_c.

As shown in Figure 2.3, Glennon identified the time-space diagram for completed and aborted passes from the critical position. Equating the distances between the front bumper of the passing and impeding vehicles at the critical position, Δ_c and Δ_c', and the critical sight distance, S_c and S_c', and assuming a one-second minimum acceptable headway, the model was formulated as follows:

$$\Delta_c = L_P + m\left[\frac{2m + L_I + L_P}{2v - m} - \sqrt{\frac{4v(2m + L_I + L_P)}{d(2v - m)}}\right] \tag{2.3}$$

$$S_c = 2v\left[2 + \frac{L_P - \Delta_c}{m}\right] = 2v + \frac{2v(L_P + m - \Delta_c)}{m} \tag{2.4}$$

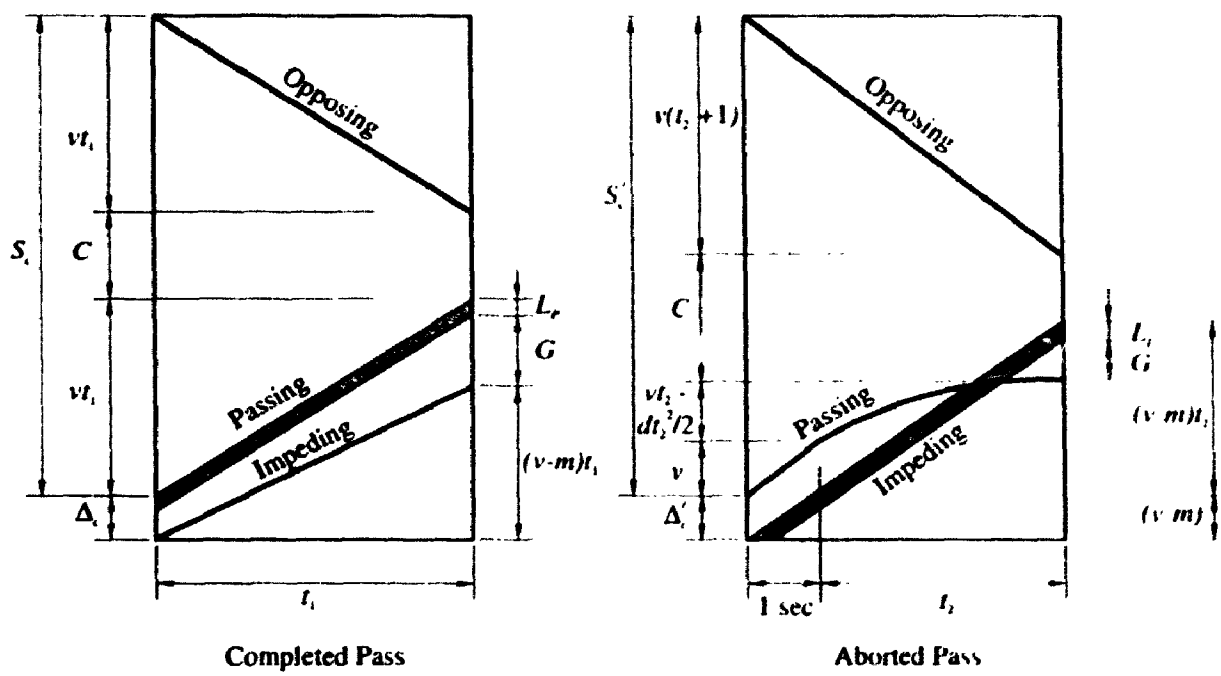

FIGURE 2.3: Time-Space Diagrams for Critical Passing Manoeuvre (Glennon, 1988).

where

v = design speed,

m = differential speed between passing and impeding vehicles,

L_p = length of passing vehicle,

L_i = length of impeding vehicle, and

d = deceleration rate.

Some of Glennon's assumptions were revised by Rillet et al (1990) and a modified model was developed. The main points addressed in this modified model are:

1. The value of G in either a completed or aborted pass was related to the speed (v-m) rather than the differential speed m used in Glennon's model.
2. In aborting the pass, the passing vehicle was assumed to decelerate to a minimum terminal speed, v_{min}, and then, maintain this speed until it is back in the right lane.
3. When reaching the critical position, the passing vehicle may have not completed the acceleration to reach the speed v yet.

The consideration of these assumptions resulted in PSD requirements much longer than those resulting from Glennon's model. Interestingly, due to the great complexity and conservatism associated with Rillet's model, some researchers have preferred using Glennon's model which is much simpler (Good et al, 1991; Sparks et al, 1993). However, a closer inspection of both models would establish a need for revising the assumptions involved in each of them. A detailed examination of these assumptions is given in the following chapter.

2.1.4 Minimum Length of Passing Zones

In order to ensure the safety of the passing manoeuvres, the American MUTCD states that the length of the passing zone must not be less than 122 m (100 m in the Canadian MUTCD). Also, as shown in Table 2.2, different lengths, depending on the speed limit, are used in Ontario (MUTCD, 1995). However, the basis for these lengths is not documented in any of the MUTCD editions.

TABLE 2.2: Minimum Length of Passing Zones Used in Ontario (MUTCD, 1995).

Operating Speed (km/h)	Minimum Length of a Passing Zone (m)
50	120
60	160
70	200
80	240
90	280
100	320
110	360

In the study conducted by Van Valkenberg and Michael (1971), the required minimum length of passing zones was suggested as ⅓ of the distance travelled by the passing vehicle, i.e., ½ the distance S_0 in Figure 2.2. Subsequently, lengths shorter than the 122 m stated in the MUTCD were suggested for speeds up to 96 km/h. However, no experimental or analytical evidence was presented to support this subjective

assumption. Moreover, these suggested short lengths were in disagreement with the findings of many studies as summarized by Harwood and Glennon (1977). For example, Jones (1970) studied the safety and efficiency of three short passing zones of 122, 195, and 268 m, with similar traffic and geometric features. In addition, the performance on these short zones was compared to the performance on two longer zones of 500 and 792 m length. With a speed limit of 113 km/h on all sites, fewer than 9% of the passing opportunities on the short zones were accepted by the drivers compared to 22.8 and 41.0% on the 500 and 792-m zones, respectively. Moreover, based on subjective rating, the 122-m zone experienced forced to violent returns in 63% of the passes compared to 45 and 10% on the 195 and 268-m zones, respectively. In conclusion, the short passing zones add very little to the quality of service of the highway and the passes performed on them are more hazardous than longer passing zones.

In another experimental study conducted by Weaver and Glennon (1971), the minimum length of passing zones was assumed as the sum of the distances travelled by the passing vehicle during the perception-reaction time and during occupying the left lane. The resulting suggested lengths were much higher than the values recommended in the MUTCD. However, the assumption is very conservative since, according to the concept of critical position, the passing vehicle can complete the pass safely once it passed the critical position. Therefore, a rational modelling of the minimum length of passing zones is unavailable.

2.1.5 Available Sight Distance

As mentioned earlier, due to topographical and economical considerations, the sight distance on some sections of the highway may be restricted to a certain length. On horizontal curves, the driver's sight line may be obstructed by lateral obstructions such as trees, buildings, and cut slopes. On crest vertical curves, the sight line may be obstructed by the vertical curve itself. Also, sight distance on sag vertical curves may be limited to the farthest point covered by the vehicle headlight. Furthermore, overpasses represent sight obstructions for the underneath traffic. Therefore, designers have to check the available sight distance against the required SSD on any highway and the required PSD on two-lane rural highways.

(i) 2-D Horizontal Alignments. For horizontal curves, many models have been developed to relate the available sight distance to the lateral clearance. Among these models is the one presented in the AASHTO guide for the case of $S \leq L$, where S is the sight distance on the curve and L is the curve length. The model, which can be used in case of continuous or single obstruction, is given as follows:

$$m = R \left[1 - \cos \left(\frac{90\ S}{\pi\ R} \right) \right] \tag{2.5}$$

where

R = curve radius, and

m = lateral clearance from the obstruction to the centerline of the inside lane.

This formula is the only analytical model presented by the AASHTO guide to relate the sight distance to horizontal alignment. Although the formula is easy and direct, it is "*of limited practical value except on long curves*" (AASHTO, 1990; 1994). Therefore, the AASHTO green book recommends that the designer must use graphical methods to check sight distance on horizontal curves. Furthermore, Neuman and Glennon (1984) and Glennon (1987) showed that the lateral clearance calculated by the AASHTO formula is needed only from the point at SSD/2 after the point of curve (PC) to the point at SSD/2 before the point of tangent (PT).

The other case, where the sight distance is greater than the curve length, has been studied by many researchers. Olson et al (1984), Waissi and Cleveland (1987), Berg et al (1989), and Easa (1991*a*) have developed different methods to check the required lateral clearance on simple horizontal curves. Easa (1993; 1994*a*) has also studied the case of a single lateral obstruction on compound and reverse curves and developed other formulas to relate the lateral clearance to the available sight distance.

Nevertheless, none of these models has considered the case of continuous obstructions. For example, according to the standards of MUTCD (1995), which is used by the Ministry of Transportation of Ontario (MTO) for establishing the no-passing zones, the available sight distance for the drivers in the inside lane is limited by a continuous obstruction represented by a theoretical shoulder of 3 m-width. Continuous obstructions may also be encountered due to cut slopes or trees and bushes. Moreover, none of the procedures mentioned above has been incorporated in the design standards by AASHTO or TAC.

(ii) 2-D Vertical Alignments. As for the case of vertical alignment, the AASHTO (1994) formulas can relate the available sight distance on a simple crest or sag curve with long tangents to the curve parameters as follows:

for a crest curve:

$$L = \frac{A\ S^2}{100\ (\sqrt{2h_1} + \sqrt{2h_2})^2} \qquad S < L \tag{2.6}$$

$$L = 2\ S - \frac{200\ (\sqrt{h_1} + \sqrt{h_2})^2}{A} \qquad S > L \tag{2.7}$$

for a sag curve:

$$L = \frac{A\ S^2}{120 + 3.5\ S} \qquad S < L \tag{2.8}$$

$$L = 2\ S - \frac{120 + 3.5\ S}{A} \qquad S > L \tag{2.9}$$

where

L = length of vertical curve,

S = sight distance,

A = algebraic difference in grades, percent,

h_1 = height of driver eye, and

h_2 = height of object.

These formulas are to be used in designing vertical curves to satisfy SSD, and can also be used to evaluate the PSD requirements on two-lane highways. However, using

these formulas to evaluate the available sight distance would produce only the minimum sight distance rather than the sight distance profile. Therefore, only the conclusion of whether a sight distance deficiency exists or not can be reached. Yet, the exact portion of the highway with deficient sight distance cannot be determined. Moreover, the previous formulas can be used only in the case of a simple vertical curve with long tangents.

For the case of unsymmetrical (compound) crest or sag curves and reverse vertical curves, the available sight distance can be determined using the models developed by Easa (1991*b*; 1991*c*; 1994*a*). Also, sight-hidden dips, which may develop if a crest curve is followed by a sag curve, has been modelled by Easa (1994*b*). Using this latter model, the designer can check the existence of a sight-hidden dip and determine the portion of the highway experiencing this sight-hidden dip. Moreover, an account of sight obstructions resulting from non-centred overpasses has been modeled (Easa, 1992). Yet, all the available models for sight distance on vertical alignments are valid only for the daytime sight distance, and no work has been conducted regarding the nighttime (headlight) sight distance on complex alignments.

(iii) 3-D Combined Alignments. Although computer programs for 3-D highway visualization have been available for a long time, none has been directed to the 3-D analysis of sight distance. With the recent advancements of computers, more software packages have been developed and have been available to highway professionals (Tanton et al. 1986). Nevertheless, as stated by Jull and Murray (1984), "*as with all computer*

programs, ITEDS (a computer software for highway design) *does not provide any new revelations in the theory of highway design*".

In a recent study, Sanchez (1994) studied the interaction between the sight distance and the 3-D combined alignment of interchange connectors. The methodology used in this study can be summarized in three main steps. First, the alignment was idealized into a net of triangular planes using a software called *InRoads*. Second, a perspective view of the idealized net was created by the computer, and the sight line was drawn from the driver eye to the object. Then, from the different views generated by the computer (top, side, and driver's perspective), the operator was able to determine the obstruction impeding the sight line. Also, the available sight distance was calculated using a spreadsheet. Although this methodology was successful in achieving the objectives of the study, it is clear that it is very time consuming because: (1) a large number of small planar triangular elements is required to model horizontal and/or vertical curvatures and (2) the available sight distance is determined graphically (not analytically). Therefore, such a methodology cannot be used to establish 3-D geometric design standards. As a result, the need for accurate analysis of the sight distance in 3-D alignments has been pointed out by Easa (1994*a*).

2.2 Vehicle Stability and Driver Comfort

It is essential for the highway designers to account for the stability of the vehicle on the road to avoid situations which impose excessive forces on the vehicle and may lead to single or multiple vehicle collisions. For example, the centrifugal forces imposed on a

vehicle negotiating a horizontal curve may cause a single vehicle collision if the vehicle skids laterally or rolls over. Also, a multiple vehicle collision can result if the vehicle moves to another lane due to lateral skidding or loss of control. Similarly, a centrifugal force experienced on vertical curves must be accounted for in the design of vertical curves. In addition to the vehicle stability, the forces should not be high enough to cause a driver discomfort even if the vehicle can maintain its stability. The need to satisfy the two conditions of vehicle stability and driver comfort is one of the basic requirements in the design of horizontal alignments, vertical alignments, and cross-sections.

In the design of horizontal alignments, AASHTO has presented a simple formula to determine the minimum radius of horizontal curves that would satisfy driver comfort and vehicle stability as follows:

$$R = \frac{V^2}{127\,(f_s + e)} \tag{2.10}$$

where

V = design speed, km/h,

f_s = coefficient of side friction, and

e = superelevation rate.

The values of f_s were determined based on the driver comfort criterion using a ball-bank indicator (AASHTO, 1994). It is assumed that drivers who travel at speeds higher than the design speed will experience some level of discomfort, and therefore will reduce their speeds before any significant risk of lateral skidding. Thus, the resulting radii are expected to be higher than the limiting values beyond which the vehicle stability

is questioned. However, Harwood and Mason (1994) have noticed that the values of f_s were developed 50 years ago, and since then, vehicle design has changed significantly. Therefore, they pointed out the need to reevaluate the levels of driver comfort used by AASHTO.

In respect to vertical alignments, a significant difference can be noted between the centrifugal forces on crest and sag vertical curves. On crest curves, the centrifugal force is acting upward in an opposite direction to the vehicle's weight. Therefore, the developed forces are always too small to cause driver discomfort or vehicle instability within the limits of normal highway speeds and conditions. On sag curves, however, the centrifugal force is acting downward in the same direction of the vehicle's weight. Although there is no risk of vehicle instability, the combination of the centrifugal force and the vehicle's weight may cause driver discomfort. Therefore, AASHTO recommends an absolute minimum length of sag curves that will limit the centrifugal acceleration to less than 0.3 m/sec^2 using the following formula:

$$L = \frac{A \quad V^2}{395} \tag{2.11}$$

It should be noted, however, that the resulting length is around 50% of the length required to satisfy the headlight sight distance. Subsequently, the previous formula does not control the design unless the highway is well lighted.

Finally, the vehicle dynamics is an important consideration in the cross-section design. The pavement cross-slope on horizontal curves (superelevation rate) is selected mainly to help overcome a portion of the centrifugal force experienced on the curve, and

thus enhance the vehicle stability and driver comfort. However, a maximum limit for the superelevation rate is set to avoid having slow and stationary vehicles skidding into the inside of the curve, especially in icy conditions. Such a maximum limit is set by each country according to the prevailing weather conditions (Krammes and Garnham, 1995).

The weakness of this current design practice has been addressed by several researchers. An important shortcoming is that the effect of the grades or vertical curves combined with the horizontal curve is completely overlooked. In addition, the main formula for horizontal curve design has a number of rough approximations which make it far from accurate. First, the vehicle is approximated into a point mass rather than a body. As a result, the variation in the distribution of the friction forces between the rear and front tires and between the inner and outer tires is totally ignored. Second, as mentioned by Harwood and Mason (1994), the AASHTO formula assumes that drivers follow a path of constant radius equal to the curve radius. However, based on field studies, it was found that drivers tend to oversteer at some point of the curve, and subsequently follow a more critical path (Glennon and Weaver, 1972). Third, the formula considers only one case of driving, namely, driving with a constant speed. Therefore, it does not consider the reduction in the side friction supply in case the vehicle's brakes are applied and some longitudinal friction is used. TAC, however, pays attention to the interaction between longitudinal and side frictions by recommending increasing the stopping sight distance on horizontal curves. More detailed consideration of this interaction is found in the German design standards (Lamm, 1984). Finally, AASHTO design guide does not consider the risk of rollover due to excessive centrifugal forces.

Although this may be justified for passenger cars which have small heights, it may not be the case for trucks. Because of their high centre of gravity, trucks usually have a higher potential for rollover (Harwood and Mason, 1994).

In a research to evaluate the adequacy of the AASHTO standards, Harwood and Mason (1994) defined the margin of safety against skidding as the difference between the available tire friction and the friction demand on the curve. In order to avoid the weaknesses in the AASHTO formula, and based on field data, the friction demand for trucks was taken 10% higher than that for passenger cars to account for the tire-to-tire friction variation. Also, the friction generated by trucks was taken as 70% of that generated by passenger cars. The margin of safety against rollover was defined as the additional lateral acceleration the vehicle can undergo before rolling which was assumed to occur at a lateral acceleration of 1.2 g for passenger cars and 0.27 to 0.40 g for trucks. In conclusion, passenger cars were found to have adequate margins of safety against skidding and rollover. On the other hand, it was found that trucks with high centre of gravity would roll over before they would skid off a dry pavement. However, the margins of safety for trucks against skidding and rollover were still adequate if they do not exceed the curve design speed. Although Harwood and Mason (1994) concluded that the AASHTO standards do not need revisions for safety concerns, it should be noted that the interaction of the vertical and horizontal alignments was not included nor was the reduction in the side friction supply when the vehicle's brakes are applied. Also, an accurate consideration of the variation of the friction forces from tire to tire was not included.

The interaction between downgrades and upgrades and horizontal curves was a part in a study aiming at developing guidelines for highway geometry and pavement surface characteristics to ensure adequate vehicle control during different manoeuvres. Dunlap et al (1978) studied the accident data on two turnpikes in Ohio and Pennsylvania and found that neither the horizontal curvature nor the combining vertical grade has an effect on the accident rate on horizontal curves. The abilities of three different types of passenger cars to perform three different manoeuvres (cornering under traction, cornering and lane change, and cornering and lane change plus braking) were studied using computer simulation. The highway grade was found to have a very little influence while the curvature influenced the cornering under traction only. Although the AASHTO point mass formula was found to be adequate for vehicles driving at a constant speed (cornering under traction), it was far from conservative if an emergency manoeuvre would be performed on the curve.

Although Dunlap et al (1978) provided field and analytical evidence on the insignificance of the effect of grades combined with horizontal curves, it should be noted that the field evidence was limited to the range of grades on the two turnpikes, namely, -3 to +2% on Ohio Turnpike and -3 to +3 on Pennsylvan' Turnpike. In addition, Kontaratos et al (1994) disputed the analytical evidence because Dunlap et al used a sliding coefficient of friction between 0.3 to 0.5 which is too high according to established road safety criteria. Furthermore, Dunlap et al (1978) did not consider the case of a vertical curve combined with the horizontal curve.

In a more accurate model than the AASHTO point-mass formula, Kontaratos et al (1994) simulated the vehicle-road interaction using a bicycle model (Figure 2.4). The model can consider the combining effect of grade, horizontal curve, and superelevation and the interaction between longitudinal and side frictions. The vehicle used in the model is a passenger car and is modelled as a body with a specific height. The variation in friction forces between rear and front axles is considered depending on the type of vehicle drive while interior and exterior tires are assumed to have equal friction forces. Assuming that the vehicle is travelling at a constant speed, the model was used to determine the minimum required radius of a horizontal curve combined with an upgrade or downgrade.

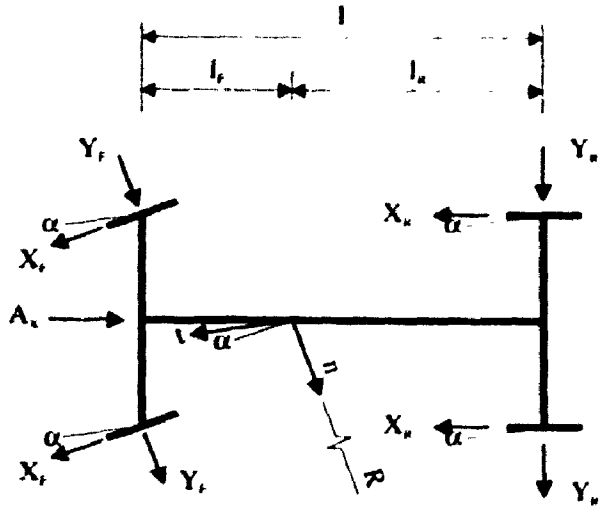

FIGURE 2.4: Forces Acting on a Passenger Car in a Bicycle Model (Kontaratos et al, 1994).

The results showed that the AASHTO formula would yield conservative radii when the horizontal curve was combined with a downgrade. On the other hand, if the curve was combined with an upgrade, the required minimum radius increased with the increase of the upgrade. Depending on the design and operating speeds, there would be an upgrade beyond which the AASHTO formula would underestimate the required horizontal curve radius. Although this may seem to contradict the intuition that downgrades are more critical than upgrades, it was explained that this would be true in the braking mode. However, in the driving mode assumed in this analysis, Kontaratos et al (1994) explained that "*as the vehicle moves upgrade, greater longitudinal forces act on it, demanding greater reserves of friction. Consequently, fewer reserves of friction remain to be used in the lateral direction*". An interesting observation in the results Kontaratos et al (1994) is that the effect of the upgrade tends to compromise the safety of curves designed according to the AASHTO formula when the grade is higher than 3%. These grades were beyond the limits of the two turnpikes investigated by Dunlap et al (1978). Therefore, there is no contradiction between the two opposite conclusions regarding the effect of upgrades by Dunlap et al (1978) and Kontaratos et al (1994).

Although the model by Kontaratos et al (1994) is far superior to the AASHTO point-mass formula, it should be noted that the study did not include the braking driving mode, emergency manoeuvres performed on curves, or the effect of combining vertical curves. A more complex and comprehensive vehicle dynamics model (VDM) has been developed by Allen et al (1995). The model can simulate passenger cars, trucks, and articulated vehicles. With a total of 17 degrees of freedom (Figure 2.5), the model can

MASS	MOTION VARIABLES	D.O.F.
Sprung Mass (m_s)	θ_s, ϕ_s, z_s, a_{zs}	4
Total Mass (m)	ψ, u	2
Front Unsprung (m_{uF})	z_{uF}, ϕ_{uF}, a_{zuF}	3
Rear Unsprung (m_{uR})	z_{uR}, ϕ_{uR}, a_{zuR}	3
Wheel rotational inertial (I_w)	ω (spin mode, 4 wheels)	4
Wheel inertia about steer axis (I_{zw})	δ_{wF}	1
TOTAL DEGREES OF FREEDOM		17

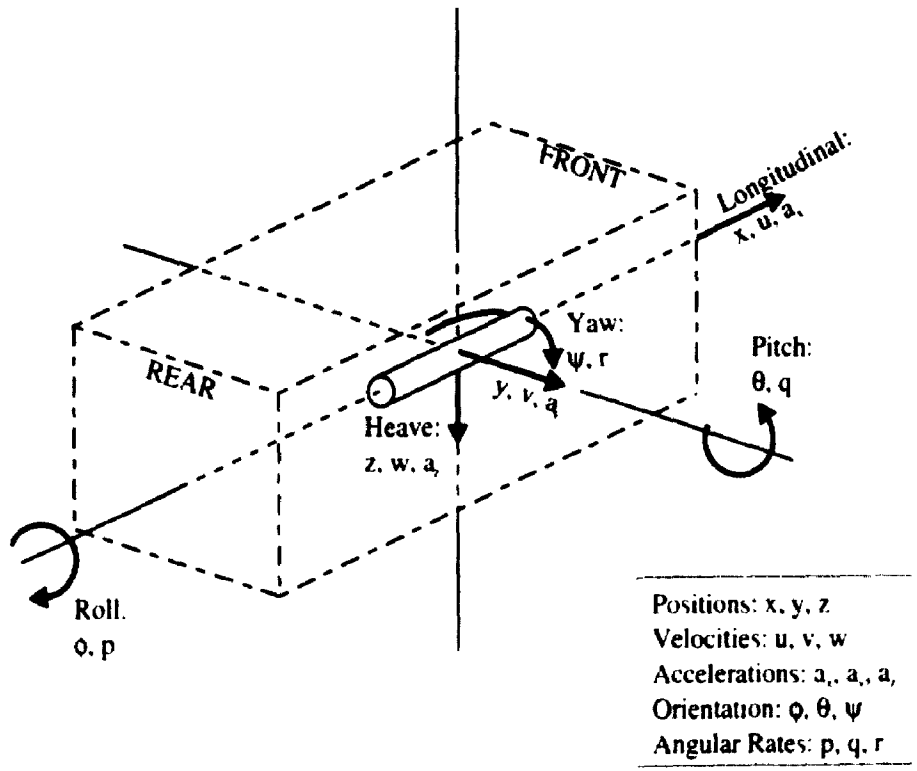

FIGURE 2.5: Vehicle Dynamics Model Axis System and Degrees of Freedom (Allen et al, 1995).

cover virtually all types of lateral, longitudinal, and angular motions. The model is also claimed to be able to simulate "*virtually all driver induced maneuvering up through and including limit performance conditions defined by tire saturation characteristic (plowout, spinout) and rollover*". The model has been incorporated as a main module in the Interactive Highway Safety Design Model (IHSDM) being created by the US Federal Highway Administration (Reagan, 1995). This module will permit highway designers to simulate any of the AASHTO design vehicles and drive them through the alignment. Thus, a complete speed profile, data on lateral accelerations, and the potential of accidents will be available for the designer to evaluate the available alignment alternatives (Reagan, 1994).

In summary, it can be stated that the AASHTO point-mass formula for designing horizontal curves is far from accurate and can be far from conservative (Dunlap et al, 1978). Ignoring the 3-D nature of highway alignment may lead to erroneous decisions regarding the selection of horizontal curve radii (Kontaratos et al, 1994). On the other hand, more accurate models are currently available for a more reliable alignment design based on 3-D analysis. However, more research for accurate quantification of the side frictions is still needed (Fitzpatrick, 1994; Harwood and Mason, 1994; Kontaratos et al, 1994).

2.3 Drainage

Drainage of storm water off the road is an integral part of highway geometric design. Water on the pavement surface reduces the available friction between the road and the

vehicle's tires, and therefore compromises the vehicle stability and increases the risk of collisions. Moreover, high rainfall intensity combined with poor pavement surface drainage may cause complete hydroplaning where the pavement surface and the tires are separated by a thin film of water. Therefore, safe traffic operation requires highway designers to coordinate horizontal and vertical alignments and cross-sections to ensure adequate surface drainage. In addition to the pavement surface drainage, drainage facilities such as bridges, culverts, channels, curbs, and gutters are used to carry storm water across the right-of-way. The design of this latter type of drainage provisions is explained in separate manuals (AASHTO 1991; 1993), rather than being included in the AASHTO green book, and is beyond the scope of this review.

As mentioned above, poor pavement surface drainage will accumulate a significant water depth on the pavement and may lead to complete hydroplaning. However, it should be noted that the majority of wet-weather skidding accidents occurs at water depths well below that required for complete hydroplaning (Dunlap et al, 1978). For example, for a specific smooth tire and pavement surface texture, Staughton and Williams (1970) reported that the tire brake force coefficient at 96 km/h (60 mph) was less than 0.05 at a water depth of 0.762 mm (0.03 in). The corresponding water depth required for a complete hydroplaning was estimated as 3.81 mm (0.15 in). Therefore, pavement surface drainage provisions should be designed not only to avoid significant water depths which will cause complete hydroplaning but also to avoid low water depths which will jeopardize traffic safety.

Both AASHTO and TAC design guides recommend general guidelines for pavement surface drainage. In designing the cross-section, a range of pavement cross-slopes is suggested based on the pavement type. High-type two-lane highways crowned at the centre can have the lowest rate of cross-slope (1.5 to 2.0%). As the pavement surface type gets more inferior and water can be drained more difficultly, the rate of the cross-slope should be increased. For multi-lane highways, gradual increase in the cross-slope of each lane relative to the preceding one is recommended. Moreover, the advantages and disadvantages of the different cross-slope arrangements should be weighed to determine the best overall arrangement. For example, when the lanes of each travelling direction are sloped in both the median and shoulder directions, the pavement surface drainage will be more effective and less water depths will be encountered. However, drainage facilities are required to collect the water from three points (both shoulders and median). On the other extreme, if all lanes are sloped in the median direction, less expenses are required for the drainage facilities since water is collected from one point only. However, such arrangement will result in greater water depths in the inside lane which carries the traffic with higher operating speeds.

In addition to the design of the cross-slope, some caution should be practiced in designing the vertical alignment. Although level or flat grade is allowed on uncurbed highways with adequate cross-slope for drainage, a minimum grade of 0.5 (or 0.3% in case of high-type pavement) is recommended. In addition, crest and sag vertical curves should allow a minimum grade of 0.3% at a point 15 m away from the level point. This criterion allows for a maximum K of 51 m per percent change of grade which

corresponds to a maximum design speed of 80 and 100 km/h for crest and sag curves, respectively. However, if a higher design speed is to be reached, flatter curves should be used and special attention is needed for proper pavement drainage.

Although the coordination of vertical alignments and cross-slope for adequate drainage is implicitly included in the design standards, again, a clear and quantified coordination is lacking. For example, a further enhancement of pavement drainage can be accomplished by good coordination of horizontal and vertical alignments so that the revolving points in both alignments are approximately coinciding (Smith and Lamm, 1994). As shown in Figure 2.6, by placing approximately equal-length horizontal and vertical curves at approximately the same locations, the maximum superelevation rate will coincide with the minimum longitudinal grade and vice versa. This combination would not only add to the highway aesthetics but also enhance the pavement drainage significantly. Moreover, the current design guides which base the superelevation

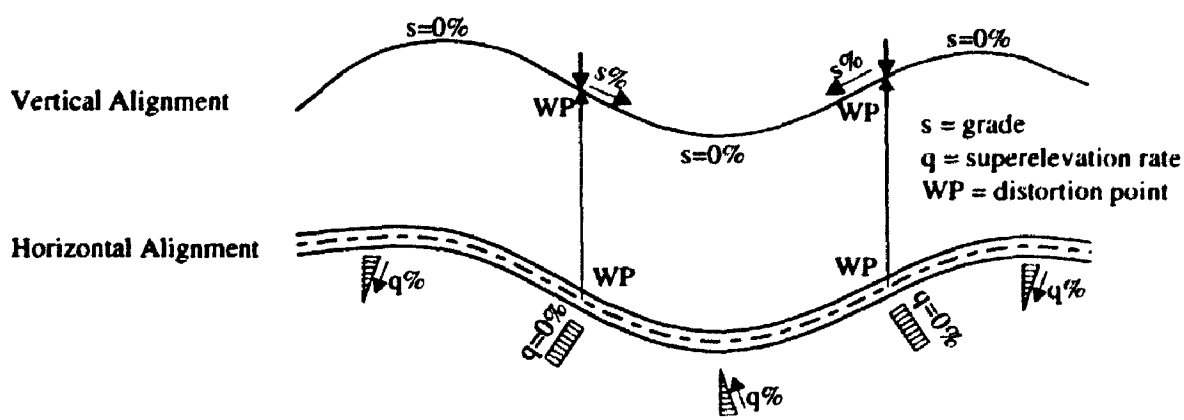

FIGURE 2.6: Coordination of Distortion Points in Horizontal and Vertical Alignments (Smith and Lamm, 1994).

primarily on the vehicle stability alone may produce curves with long radii and low superelevation rates. With all lanes sloped in the same direction (to the inside of the curve), such a situation may deteriorate the pavement surface drainage significantly (Dunlap et al, 1978).

A more quantitative analysis for pavement surface drainage can be carried out using existing formulas to predict the water depth over the pavement surface (Gallaway et al, 1971; Ross and Russam, 1968; Yeager, 1971; Yeager and Miller, 1971). According to these formulas, the primary factors affecting the water depth are the road width, the superelevation (cross-slope) rate, and to a less extent, pavement surface texture. On the other hand, longitudinal grade has no or little effect. This can be explained by the fact that the grade increases the slope and the run-off length. Although the former reduces the water depth, the second increases it with a net result of almost zero (Dunlap et al, 1978). Using these formulas, Dunlap et al (1978) suggested a methodology to account for pavement drainage and the loss in friction forces on horizontal curves relative to tangent sections. Depending on the superelevation rate, rainfall intensity, drainage length, and longitudinal grade, the required increase in the pavement skid resistance on horizontal curves to overcome the loss in friction is recommended.

Dunlap et al (1978) also investigated the correlation between pavement surface drainage and traffic safety. In a comprehensive investigation of a 1° horizontal curve (R=1746 m) on Ohio Turnpike with significantly high accident rate, it was found that the wet-weather accidents were over-represented. The percentage of wet-weather accidents represented 79 and 62% of the total accidents when the pavement was made of portland

cement and asphalt cement, respectively. Observing that the superelevation rate was relatively low (1.56%) which was equal to the crown slope on the tangent, the water depth on the curved section was predicted to be almost twice that on the tangent. Thus, the curve experienced a considerable sudden loss in the available friction. Subsequently, the safe operating speed on the curve was significantly less than that on the tangent. Although drivers expect a lower safe operating speed on curves than on tangents, such a sudden and significant drop in the safe operating speed was beyond their expectations, and therefore they failed to adjust their speed properly.

In summary, it can be seen that the current design standards include implicit correlation between vertical alignment and cross-section in providing proper pavement surface drainage. However, a clear coordination is not included explicitly. Also, the current provisions of the superelevation rate can be misinterpreted to produce unsafe horizontal curves during wet weather. Further research is still needed to establish a clear correlation between pavement surface drainage and traffic safety. Quantitative analysis and guidelines for the effect of combined alignments on providing proper pavement surface drainage are still needed.

2.4 Highway Aesthetics

Although highways' essential function is to provide safe and rapid mobility for goods and people, their pleasing appearance should not be overlooked. The interrelationship between highway aesthetics and traffic safety has been emphasized (ASCE, 1977; Smith and Lamm, 1994); though has not been well quantified. Poor coordination of horizontal and

vertical alignment may violate the driver expectations or cause an erroneous perception of information. For example, in viewing existing highways from the driver's point of view, Mori et al (1995) concluded that the alignment coordination may cause the drivers to perceive the alignment wrongly. Such a wrong perception may be hazardous if the driver perceives a sharp curve as a flat curve. Therefore, the AASHTO green book emphasizes the need for a comprehensive study of the alignment coordination during the design phase to avoid the excessive costs associated with any deficiency that may be noticed later.

However, unfortunately, "*the exact adherence to preceding* (specific) *design standards does not guarantee obtaining a satisfactory and aesthetically pleasing design*" (Easa, 1995). This statement summarizes, in simple terms, a widely spread conviction among highway professionals and researchers. The main reason for this conviction is the current design practice in which each of the horizontal and vertical alignments are designed separately. Since the drivers do not view the highway in 2-D but rather in 3-D, there is no guarantee that the resulting combined alignment will be satisfactory. Moreover, in designing either alignment, both AASHTO and TAC design guides pay attention to a single element (curve or tangent) at a time. Such practice may cause further violations to highway aesthetics and design consistency (Lamm and Smith, 1994).

In order to achieve a better coordination between horizontal and vertical alignments, AASHTO and TAC provide general guidelines which should enhance the aesthetics of the combined alignment. In following these guidelines, the designer must depend on his/her ability to visualize the highway in 3-D using the 2-D drawings of the

plan and profile. Such a task is believed to be achievable by an experienced designer. Yet, the AASHTO design guide recommends using physical models in complex situations where using the 2-D maps for 3-D visualization may be difficult.

As an easier alternative for 3-D highway visualization, computer simulation models can be used. This computerized visualization has been approached as early as in the 1960's (Geissler, 1968; Park et al, 1968). With the recent advancements in computers, the simulation and visualization of 3-D highway alignments have been much easier and more accurate using computer-aided drafting and design packages (CADD). Currently, many highway agencies in the US and Canada, governmental and private, are using 3-D computer visualization in reviewing the highway alignment before construction or reconstruction (Larson, 1996). Taking the time as a fourth dimension to create short movies, the available packages are also used to generate 4-D visualization to the highway from the driver's point of view. This 3-D and 4-D visualization can help detect any alignment deficiencies before it is too late or too expensive to fix them. Moreover, it is proved to be a fast, understandable, and relatively inexpensive way for highway agencies to communicate with the public. 3-D visualization is also a main module in the IHSDM being created by the US Federal Highway Administration (Reagan, 1994).

Still, however, further research is needed for good quantification of the effect of highway aesthetics on traffic safety. Similarly, research on the effect of alignment coordination on the driver's perception of information is needed. Under the heading "*An Interesting Phenomenon*", Smith and Lamm (1994) mentions a specific case of alignment coordination that needs further research. This case is the driver's perception of horizontal

curves when superimposed with sag vertical curves (Figure 2.7). Using CADD, the hypothesis that sag vertical curves cause horizontal curves to appear flatter than what they really are can be examined. Such an erroneous perception of information would cause drivers to travel at higher speeds than what they should adopt, and, subsequently, would increase the risk of collisions.

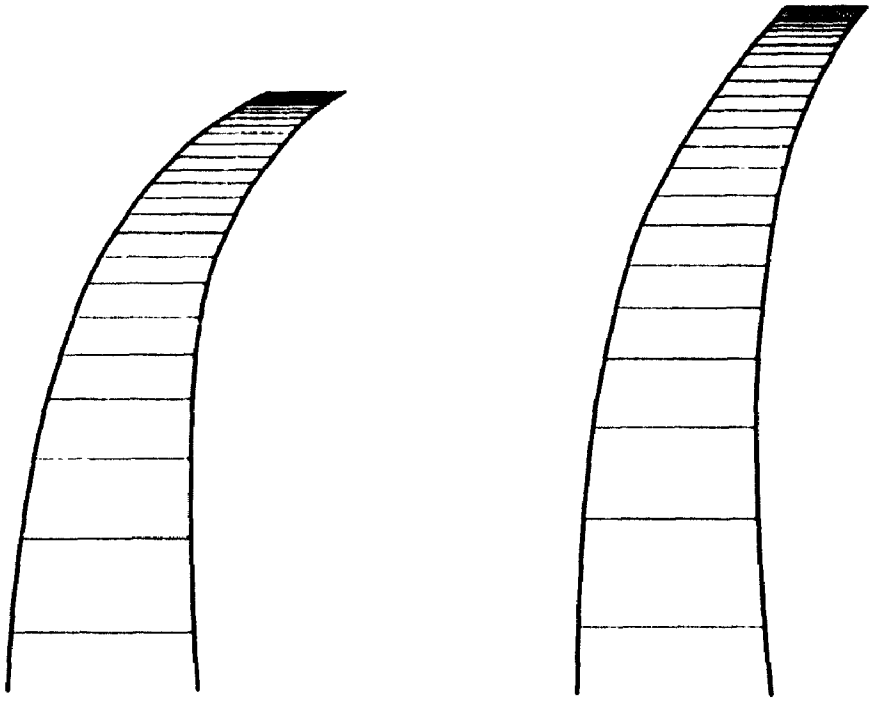

(a) Horizontal Curve

(b) Horizontal Curve with Superimposed Sag Vertical Curve

FIGURE 2.7: Effect of Superimposed Sag Vertical Curves on Appearance of Horizontal Curves (Smith and Lamm, 1994).

2.5 Summary of Review

To sum up, the previous review shows clearly that the current highway geometric design standards are based entirely on 2-D separate alignments. Moreover, in the 2-D alignment, only a single element is looked at, separately from the other alignment components. Although analytical models are currently available for a better consideration of more complex 2-D alignments, they have not been included in the design standards. The 3-D analysis of combined highway alignments, however, has been thought to be complex and cumbersome. As a result, not much research work has been directed at designing highways in 3-D alignments or quantifying the effect of ignoring the 3-D nature of highway alignments. Consequently, the margin of safety or risk on highways designed according to the current standards cannot be quantified. Therefore, the highway community agrees that a considerable research work is needed to establish 3-D highway geometric design standards. As stated by Krammes and Garnham (1995) "*Several issues seem particularly fertile for fruitful discussions among a worldwide audience: ... Considering the interrelationships among horizontal and vertical alignment and roadway cross section*".

CHAPTER 3

MODELLING REQUIRED PASSING SIGHT DISTANCE AND PASSING ZONES

In this Chapter, based on the examination of the current design and marking practices and existing research work related to the required PSD and based on the critique of the available models presented below, a model is developed to simulate the entire passing manoeuvre (Hassan, et al 1996*a*; 1995*a*). In addition to the required PSD, the model can be used to determine the location and the minimum length of passing zones. The mechanism of the passing manoeuvre upon which the model is based is presented first. Then, the values of the required PSD using this model, referred to as the revised model, are validated using field measurements made by Van Valkenberg and Michael (1971). Finally, practical design considerations for PSD and passing zones are discussed.

3.1 Critique of Existing Models for PSD

3.1.1 Glennon's Model

Referring to Chapter 2, two parameters in Glennon's model are worth of closer investigation. The first parameter is the clearance, C, between the passing and opposing vehicles at the end of the pass. Although the concept of the point of no return is basically the same as that of the critical position, Van Valkenberg and Michael (1971) identified the point of no return by producing the same *safety factor* whether the pass is completed or aborted while Lieberman (1982) identified the critical position by producing

the same *clearance* for completed and aborted passes. In the completed pass, the passing vehicle will maintain its speed, v, while decelerating in aborted passes, and thus, having a final speed lower than v. Therefore, if the clearance distance is the same in both cases, the clearance headway will be greater in aborted passes than that in completed passes. Undoubtedly, the safety factor depends on the time headway not on the clearance distance. For example, two stationary vehicles will maintain an infinite safety factor even if the clearance between them is almost zero because the time headway in this case is infinity. Therefore, the definition given by Van Valkenberg and Michael (1971), and interpreted by Glennon (1988) by assuming a minimum acceptable headway between the two vehicles at the end of the pass, appears to be more reasonable. However, in his model's derivation, Glennon (1988) considered that the clearance C is constant for completed and aborted passes. This of course is in disagreement with the more reasonable definition for the critical position and its interpretation by a minimum acceptable headway. Generally, if two vehicles are travelling in opposite directions with speeds v_1 and v_2, the clearance C which makes them reach the same point after a headway h will be $(v_1+v_2)h$.

The second parameter is the gap, G, between the passing and impeding vehicles at the end of the pass. In the model's derivation, Glennon (1988) stated "*assuming a minimum acceptable headway of one second for G, then G = m*", where m is the differential speed and is equal to the difference between the speed of the impeding vehicle and the design speed. Although this equality may theoretically be true in some special cases, it seems very unrealistic. As shown in Figure 3.1, knowing that the total time

required to abort the pass is t_2+1 sec (for perception-reaction time) and the time required to complete the pass is t_1, for the value of G to equal m (times 1 sec), one has to assume:

1. For a completed pass, at time $t=t_1-1$, the rear bumper of the passing vehicle is abreast of the front bumper of the impeding vehicle. Then, from this position, the driver of the passing vehicle will initiate the lateral shift of one lane width, to return back to the right lane, and complete it in 1 sec.
2. For an aborted pass, at time $t=t_2$, the rear bumper of the impeding vehicle is abreast of the front bumper of the passing vehicle and the passing vehicle will travel at a constant speed of (v-2m) for the remaining second (note that the speed of the impeding vehicle is v-m). Also, the driver of the passing vehicle will initiate the lateral shift from this position and complete it in 1 sec. Another possible scenario for an aborted pass is as follows: the passing vehicle will continue decelerating during the entire time period t_2. Obviously, G, in this case, cannot be related to m.

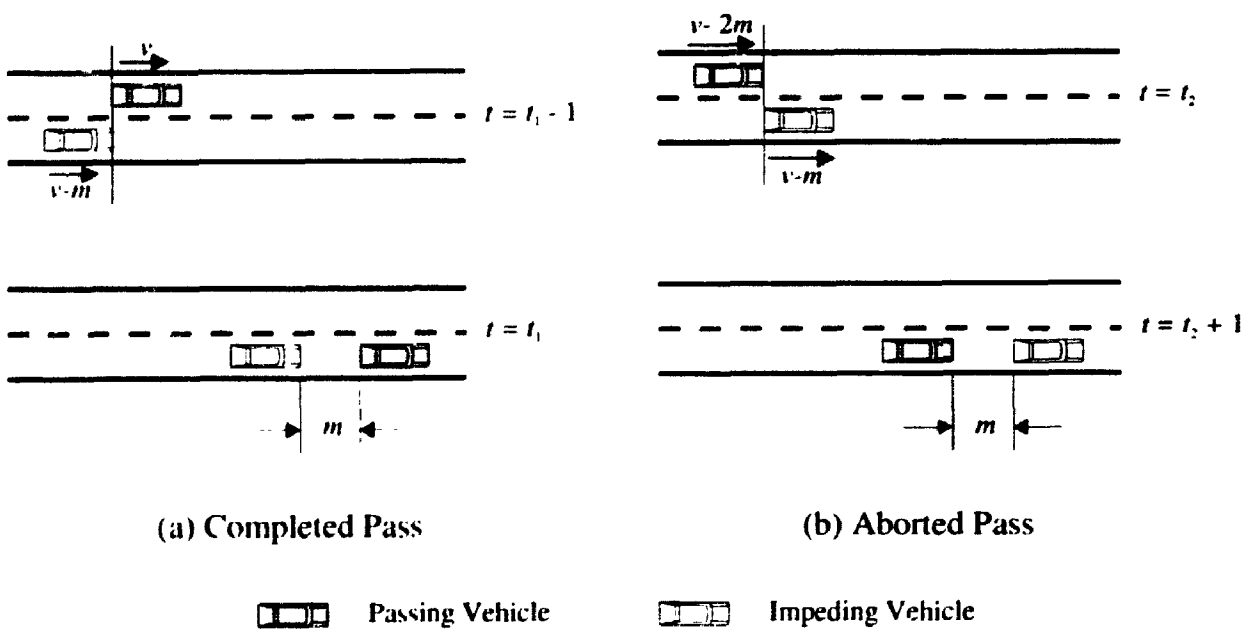

FIGURE 3.1: Assumptions Required for *G=m*.

The above assumptions are extremely difficult to justify or accept. It is obvious that initiating the lateral shift from the positions stated in both assumptions is very hazardous. Actually, the driver of the passing vehicle will maintain some gap distance between his/her vehicle and the impeding vehicle before starting shifting to the right lane. Subsequently, for G to equal m, the driver has to complete the lateral shift in a time much less than a second.

Moreover, as defined in the HCM (1994), the headway is the time between successive vehicles as they pass a point on a lane or roadway. The headway, as stated in the HCM (1994), can be measured using stopwatch observations as vehicles pass a point on the roadway. As shown in Figure 3.2, if an observer measures the time spacing between the passage of the passing and impeding vehicles at the end of a completed pass, it will be $m/(v\text{-}m)$ which is much lower than 1 sec for speeds higher than $2m$. For an aborted pass, the time spacing will be m/v_f , where v_f is the final speed of the passing vehicle due to deceleration. Although the time spacing in this latter case is greater than the corresponding time for a completed pass, it will remain less than the one second minimum acceptable headway, assumed by Glennon (1988), for high speeds where $v_f > m$. The physical interpretation of such very low headway is that the driver of the trailing vehicle will not have any opportunity to decelerate if the leading vehicle stops suddenly unless his/her perception-reaction time approaches zero. As shown in Figure 3.3, a more reasonable gap distance, G, between two vehicles having different speeds, v_1 and v_2, where $v_1 > v_2$ and v_1 is the speed of the leading vehicle, and for a headway of h

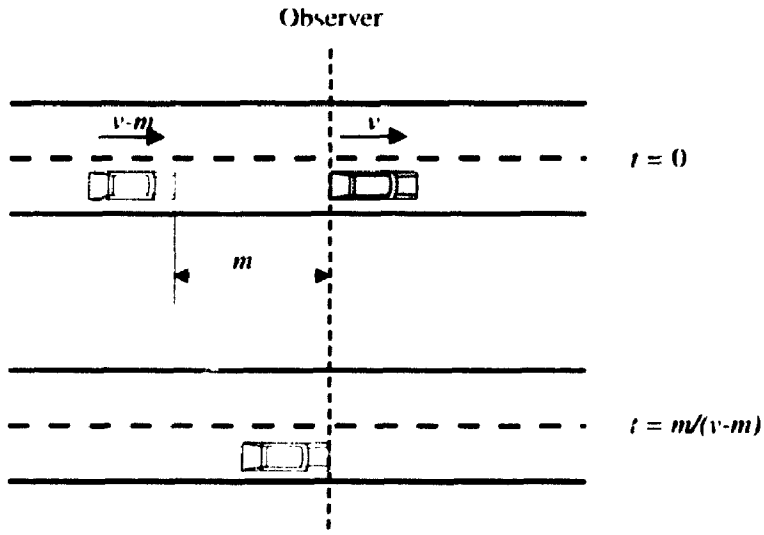

FIGURE 3.2 : Actual Headway at the End of a Completed Pass.

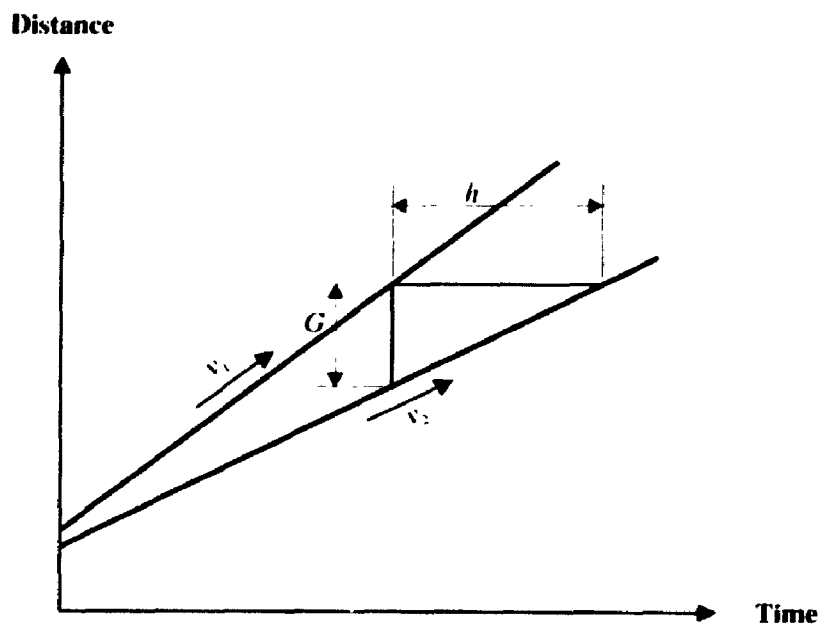

FIGURE 3.3: Time-Space Relationship for Two Vehicles with Speeds v_1 and v_2.

seconds, is v_2h. Therefore, the values of C and G in the model should be based on the speeds of the vehicles involved.

3.1.2 Rillet et al's Model

A closer inspection of the modified model by Rillet et al (1990) reveals the following:

1. In developing the model, Rillet et al (1990) stated "*a correct approach would be to multiply the time headway by the speed of the slower moving vehicle, (v-m)*". However, since the passing vehicle in aborted passes decelerates to a speed lower than the speed of the impeding vehicle, (v-m) in this case will correspond to the faster vehicle. Therefore, a more correct approach would be to multiply the time headway by the speed of the trailing vehicle.
2. The assumption of a minimum terminal speed appears to be too conservative. In a study conducted by TAC, Good et al (1991) stated "*it seems illogical to assume that drivers, having determined that a situation exists in which there is potential for an accident (i.e., an oncoming vehicle), will decelerate gradually, and then stop decelerating even though they are not in a position to re-integrate themselves into the traffic stream*".
3. This conservative approach in considering the aborted passes pushes the critical position back, i.e. closer to the beginning of the pass, as the design speed increases. Consequently, the possibility of having the passing vehicle reached the critical position while still accelerating increases. This explains the observation "*the*

acceleration at the critical point is still occurring at design speeds of up to 100 km/h when the impeding vehicle is a car (5 m long)" (Rillet et al, 1990).

4. Although the model successfully considered the acceleration occurring at and beyond the critical position in completed passes, it failed to consider the same event in aborted passes. Instead, the speed of the passing vehicle during the perception-reaction time in aborted passes was taken constant (Rillet et al, 1990).

Based on the above discussion, a revision for the models of required PSD is needed. A revised model based on the mechanism of the passing manoeuvre, explained in the following section, is developed in the subsequent sections.

3.2 Mechanism of the Passing Manoeuvre

An ideal passing manoeuvre should proceed as follows:

First, the manoeuvre is initiated as follows:

- The impeding and opposing vehicles are travelling at constant speeds of v-m and v, respectively, during the entire manoeuvre.
- At the beginning of the pass, the passing vehicle is trailing the impeding vehicle and travelling at a speed of v-m. A minimum headway, h, is maintained between the front bumper of the passing vehicle and the rear bumper of the impeding vehicle.
- Then, the passing vehicle accelerates with a constant rate, a, to a speed v while shifting to the left lane. The sight distance required at this stage is minimal and corresponds to aborting the pass safely.

- As the pass builds up, the sight distance required for the passing vehicle to abort the pass increases and that required to complete the pass decreases.

Second, if the manoeuvre cannot be completed safely, it should be aborted as follows:

- If, at any instance, the driver of the passing vehicle decides to abort the pass, a minimum headway, h_l, should be maintained between the front bumper of the passing vehicle and the rear bumper of the impeding vehicle. Similarly, a minimum headway, h_O, should be maintained between the front bumper of the passing vehicle and the front bumper of the opposing vehicle.
- In aborting the pass, the driver of the passing vehicle takes a perception-reaction time, P, before applying the brakes. During this perception-reaction time, the speed profile of the passing vehicle is assumed not to be influenced by the need to abort the pass. This means that the passing vehicle will continue its acceleration until it reaches the design speed, v, or to the end of P, whichever is first.
- Then, the vehicle keeps decelerating with a constant rate, d, until it is back in the right lane.

Finally, at a certain point, the critical position, the sight distance required to abort the pass equals that required to complete it. The sight distance at this point is called the critical sight distance.

- By passing the critical position, the passing vehicle can complete the pass safely.
- At the end of the completed pass, the minimum headways, h_O and h_l, should be maintained between the front bumpers of the passing and opposing vehicles and

between the rear bumper of the passing vehicle and the front bumper of the impeding vehicle, respectively.

The model derivation, presented in the following sections, includes the determination of the critical position, the critical sight distance, the minimum length of passing zones and the profile of the required sight distance with the evolvement of the pass.

3.3 Critical Position and Critical Sight Distance

Figure 3.4 shows the time-space diagram for a completed and an aborted pass beginning from the critical position. Referring to the completed pass,

$$\Delta_c + x_1 + v\,t_1 = L_P + G_1 + (v-m)(t_a+t_1) \tag{3.1}$$

or

$$\Delta_c = L_P + G_1 - x_1 + (v-m)t_a - m\,t_1 \tag{3.2}$$

where

L_P = length of passing vehicle,

t_1 = time required to complete the pass after accelerating to the speed v,

G_1 = distance between the rear bumper of the passing vehicle and the front bumper of the impeding vehicle at the end of a completed pass,

t_a = time required to complete the acceleration from the critical position,

x_1 = distance travelled by the passing vehicle during the time t_a, and

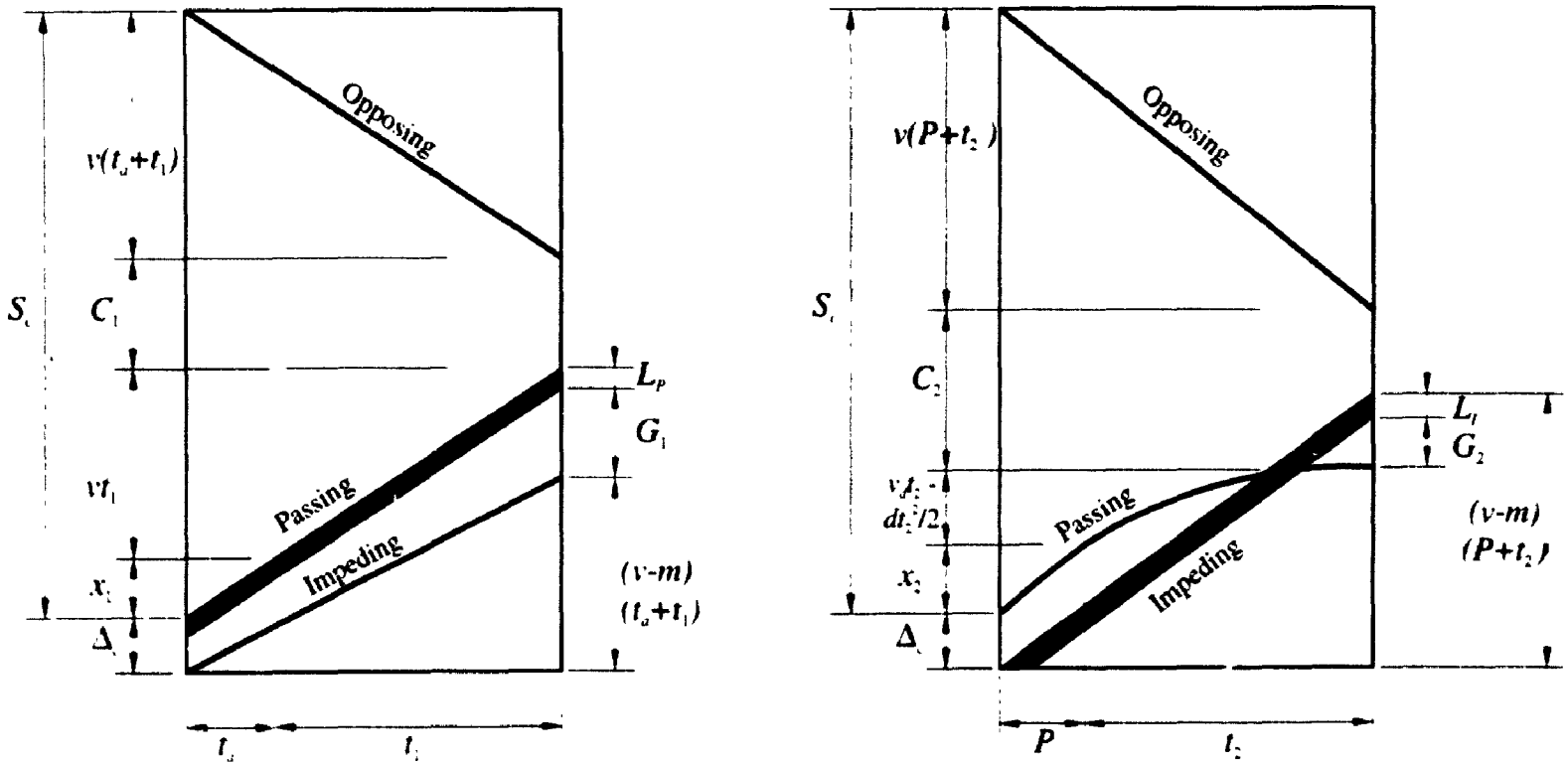

(a) Completed Pass

(b) Aborted Pass

FIGURE 3.4: Time-Space Diagrams of Aborted and Completed Passes.

Δ_c = distance between the front bumpers of the impeding and passing vehicles at the critical position.

Similarly, for an aborted pass,

$$\Delta_c + x_2 + v_d t_2 - \frac{d\, t_2^2}{2} = (v-m)(P+t_2) - L_I - G_2 \tag{3.3}$$

or

$$\Delta_c = \frac{d\, t_2^2}{2} + (v-m-v_d)t_2 + (v-m)P - L_I - G_2 - x_2 \tag{3.4}$$

where

L_I = length of the impeding vehicle,

P = perception-reaction time,

t_2 = time required to abort the pass from the critical position (after the perception-reaction time),

G_2 = distance between the front bumper of the passing vehicle and the rear bumper of the impeding vehicle at the end of an aborted pass,

v_d = speed of the passing vehicle after the perception-reaction time, and

x_2 = distance travelled by the passing vehicle during the perception-reaction time.

By equating Δ_c in Equations 3.2 and 3.4,

$$t_1 = \frac{L_P + L_I - x_1 + x_2 + (v-m)(t_a-P) + G_1 + G_2 - (v-m-v_d)t_2 - d\, t_2^2/2}{m} \tag{3.5}$$

By equating the critical sight distance, S_c, for the completed and aborted passes,

$$v(2t_1+t_a) + x_1 + C_1 = v(P+t_2) + x_2 + v_d\, t_2 - \frac{d\, t_2^2}{2} + C_2 \tag{3.6}$$

or

$$t_1 = \frac{v(P-t_a) + x_2 - x_1 + C_2 - C_1 + (v+v_d)t_2 - d\, t_2^2/2}{2\, v} \tag{3.7}$$

where

C_1 = distance between the front bumpers of the passing and opposing vehicles at the end of a completed pass, and

C_2 = distance between the front bumpers of the passing and opposing vehicles at the end of an aborted pass.

As explained earlier and knowing that the speed of the passing vehicle at the end of an aborted pass equals $(v_d - dt_2)$, the values of G_1, G_2, C_1, and C_2 will be as follows:

$$G_1 = (v - m)\, h_I$$

$$G_2 = (v_d - d\, t_2)\, h_I$$

$$C_1 = 2\, v\, h_O$$

$$C_2 = (v + v_d - d\, t_2)\, h_O$$

From Equations 3.5 and 3.7 and substituting for the values of G_1, G_2, C_1, and C_2,

$$t_2^2 \left[\frac{d(2v-m)}{4\, v\, m}\right] + t_2 \left[\frac{v+v_d-dh_O}{2\, v} + \frac{v-m-v_d+dh_I}{m}\right] + \left[\frac{v_d h_O - v(t_a-P+h_O)+x_2-x_1}{2\, v} - \frac{L_P+L_I+(v-m)(t_a-P+h_I)+v_d h_I+x_2-x_1}{m}\right] = 0 \tag{3.8}$$

which can be solved to get the value of t_2. Then, the values of t_1 and Δ_t can be determined using the previous equations. Finally, S_t can be formulated as:

$$S_c = v(2t_1 + t_a + 2h_0) + x_1 \tag{3.9}$$

However, to determine the distances x_1 and x_2 in the previous equations, the speed of the passing vehicle at the critical position, v_c, must be known. Therefore, an iterative procedure can be followed as follows:

1. Assume an initial value of v_c as the design speed v. In this case, t_a and x_1 will vanish and v_d and x_2 will be equal to v and vP, respectively.
2. Use the model to determine Δ_c.
3. Knowing the acceleration rate of the passing vehicle, a, determine the time t_{cc} required for accelerating from the speed $(v\text{-}m)$ to the speed v_c as:

$$t_{cc} = \frac{v_c - (v-m)}{a} \tag{3.10}$$

4. Determine the time t_{cv} during which the passing vehicle is travelling with a speed equal to or greater than v_c before reaching the critical position. Referring to Figure 3.5, t_{cv} can be calculated as:

$$t_{cv} = \frac{\Delta_c + L_l + (v-m)h - a\, t_{cc}^2/2}{v_c - (v-m)} \tag{3.11}$$

5. If t_{cv} is negative, reduce the value of v_c and make another iteration. In this case, the values of t_a, x_1, x_2, and v_d will be as follows:

$$t_a = \frac{v - v_c}{a} \tag{3.12}$$

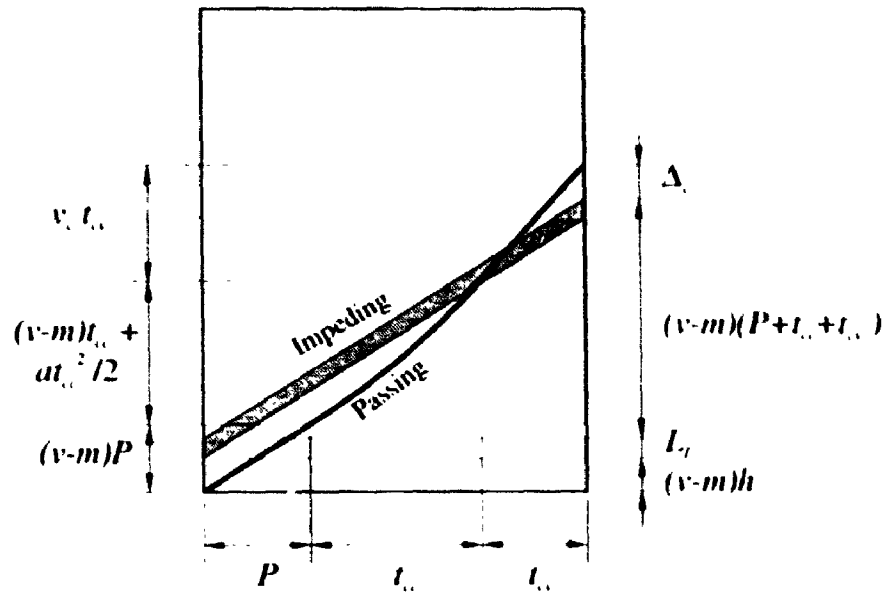

FIGURE 3.5: Time-Space Diagram for the Passing Manoeuvre Between Pass Initiation and Critical Position.

$$x_1 = v_c\, t_a + \frac{a\, t_a^2}{2} \tag{3.13}$$

$$x_2 = \begin{cases} v_c\, P + \dfrac{a\, P^2}{2} & t_a \geq P \\ v_c\, t_a + \dfrac{a\, t_a^2}{2} + v(P - t_a) & t_a < P \end{cases} \tag{3.14}$$

$$v_d = \begin{cases} v_c + a\, P & t_a > P \\ v & t_a \leq P \end{cases} \tag{3.15}$$

6. Iterations should end if $t_{cv} \geq 0$ and $v_c = v$ or $t_{cv} = 0$ and $v_c < v$.

The solution of the previous equations may produce a positive value of Δ_c which means that the passing vehicle is ahead of the impeding vehicle. This can be interpreted

as that a safe passing manoeuvre may, in some situations, require the driver of the passing vehicle to abort the pass after being ahead of the impeding vehicle. Practically, drivers should not be expected to abide to such a requirement. Therefore, it is recommended to provide the passing vehicle with the sight distance required to complete the pass when its front bumper is abreast of the front bumper of the impeding vehicle, i.e., at $\Delta=0$ at most, where Δ is the distance between the front bumpers of the impeding and the passing vehicles. Substituting for $\Delta_c=0$ in Equation 3.2, the time required to complete the pass in this case, t_1^*, can be calculated as follows:

$$t_1^* = \frac{(v-m)(h_j+t_a^*) + L_p - x_1^*}{m} \tag{3.16}$$

where

t_a^* = time required to complete the acceleration from the critical position, and

x_1^* = distance travelled by the passing vehicle during the time t_a^*.

t_a^* and x_1^* can be determined using Equations 3.10 to 3.13.

Then, Equation 3.9 can be rewritten as follows:

$$S_c = \begin{cases} v(2t_1+t_a+2h_0) + x_1 & \Delta_c \le 0 \\ v(2t_1^*+t_a^*+2h_0) + x_1^* & \Delta_c > 0 \end{cases} \tag{3.17}$$

It should be noted that although L_l and L_p are not explicit parameters in the formula for S_c, they affect the values of t_1, t_2, Δ_c, and in turn S_c.

3.4 Minimum Length of Passing Zone

The models based on the concept of the critical sight distance, including the model developed in this research, determine the required sight distance at the critical position. However, it is obvious that the passing manoeuvre should be initiated a certain time and distance before reaching the critical position. Therefore, the distance travelled by the passing vehicle from the beginning of the pass until reaching the critical position, l_p, would represent the absolute minimum length of the passing zone required for safe passes. This length would guarantee that at least one pass can be initiated on the passing zone and reach the critical position before the passing zone ends. The time, t_p, required for the passing vehicle to reach the critical position (after the initial perception reaction time) can be calculated by adding the times t_{c_1} and t_{c_2} from Equations 3.10 and 3.11, where t_{c_2} may be equal to zero. The distance l_p, can be calculated as follows:

$$l_p = (v-m)(P + t_{c_1}) + a\, t_{c_2}^2/2 + v\, t_{c_2} \tag{3.18}$$

3.5 Profile of Required PSD

In order to study the safety of the passing manoeuvre comprehensively, the required sight distance profile should be determined. The portion of the profile prior to the critical position must be checked to satisfy the needs to abort the pass at any time $t_b < t_p$ if it cannot be completed safely (where both t_b and t_p are times elapsed after the initial perception-reaction time). Although the passing vehicle can complete the pass safely once it reaches the critical position, this portion of the profile beyond the critical position should be checked to ensure that the opposing vehicle is visible to the driver of the

passing vehicle at any time $t_b > t_f$. Therefore, this section presents the derivation of the required sight distance, S, at any time t_b. The derivation of the required sight distance depends on whether t_b is less or greater than t_f, where t_f is the time required for the passing vehicle to complete its acceleration and reach the full design speed, v, and equals m/a. Generally, three cases can be encountered.

Case 1: $(t_b + P) \leq t_f$. In this case, in aborted passes, the passing vehicle is assumed to keep accelerating during the entire perception-reaction time, P. The speed of the passing vehicle at the beginning and end of the perception-reaction time, v_1 and v_2, will be $(v-m+at_b)$ and $(v-m+at_b+aP)$, respectively. As shown in Figure 3.6a, the distance between the front bumpers of the passing and the impeding vehicles, Δ, can be calculated as follows:

$$(v-m)t_b + a\,t_b^2/2 - \Delta = (v-m)h + L_f + (v-m)t_b \tag{3.19}$$

or

$$\Delta = -L_f - (v-m)h + a\,t_b^2/2 \tag{3.20}$$

If $t_b < t_f$, the pass should be aborted. Referring to Equation 3.3, the values of Δ_c, v_d, and v_2 can be replaced by Δ, v_2, and $(v_1P + aP^2/2)$, respectively. Then, the time t_2 required to abort the pass can be calculated as follows:

$$(v-m)(P+t_2) = L_f + G_2 + v_2\,t_2 - d\,t_2^2/2 + v_1\,P + a\,P^2/2 + \Delta \tag{3.21}$$

or

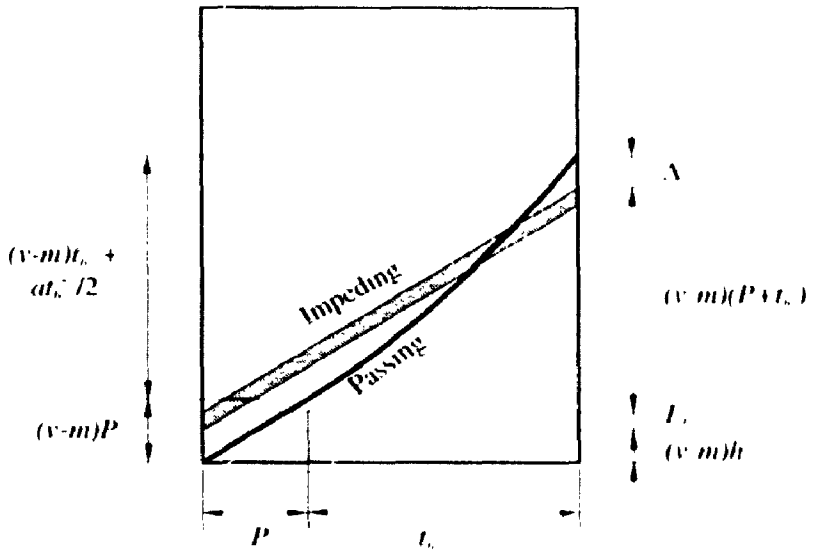

(a) $t_p \leq t_l$

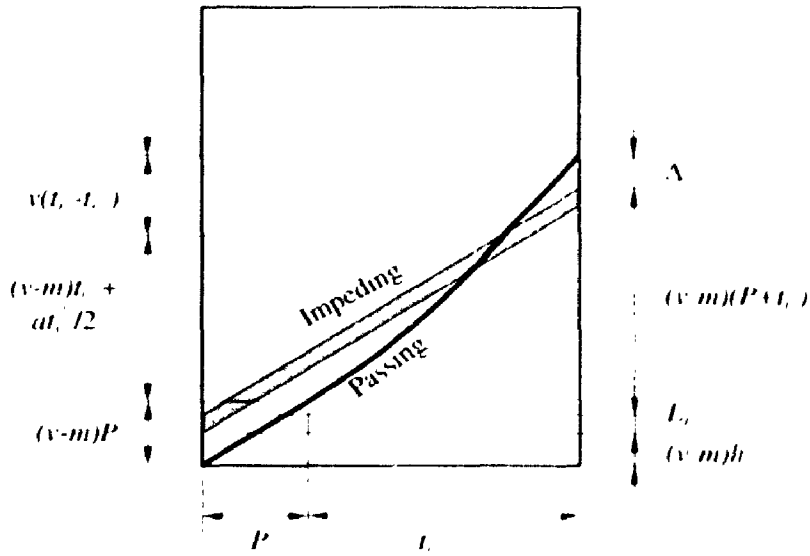

(b) $t_l > t_p$

FIGURE 3.6: Relative Positions of the Passing and Impeding Vehicles up to Time t_p after Pass Initiation.

$$d\ t_2^2/2 + [d\ h_l - a(t_b+P)]t_2 + \left[(v-m)(h-h_l) - \frac{a}{2}(t_b+P)(t_b+P+2h_l)\right] = 0 \quad (3.22)$$

Then, S can be formulated as:

$$S = (v_1 P + aP^2/2) + (v_2 t_2 - d t_2^2/2) + (v+v_2-d t_2)h_O + v(P+t_2) \quad (3.23)$$

On the other hand, if $t_b > t_f$, the pass should be completed, and the time t_1 required to complete the pass can be calculated by substituting for Δ_c and x_1 in Equation 3.1 with Δ, and $(v_1 t_a + a t_a^2/2)$, respectively, as follows:

$$\Delta + (v_1 t_a + a t_a^2/2) + v\ t_1 = (v-m)(t_a+t_1) + (v-m)h_l + L_p \quad (3.24)$$

or

$$t_1 = \frac{L_l + L_p + (v-m)(h+h_l) - \frac{a}{2}(t_a+t_b)^2}{m} \quad (3.25)$$

Then, S can be formulated as:

$$S = (v_1 t_a + a t_a^2/2) + v\ t_1 + v(t_a+t_1) + 2\ v\ h_O \quad (3.26)$$

Case 2: $t_b < t_f$ and $(t_b + P) > t_f$. In this case, in aborted passes, the passing vehicle is assumed to keep accelerating during a portion P_1 of the perception-reaction time and then, maintain its constant speed, v, during the remaining portion P_2, where $P_1 = m/a - t_b$ and $P_2 = P - P_1$. The speed of the passing vehicle at the beginning of the perception-reaction time, v_1, will be $(v-m+at_b)$. The distance Δ in this case can be calculated as in Case 1.

Then, if $t_b < t_Z$, the pass should be aborted, and the time t_2 can be calculated by substituting for Δ_t, v_d, and x_2 in Equation 3.3 with Δ, v, and $(v_1P_1 + aP_1^2/2 + vP_2)$, respectively, as follows:

$$(v-m)(P+t_2) = L_f + G_2 + v\ t_2 - d\ t_2^2/2 + v\ P_2 + v_1\ P_1 + a\ P_1^2/2 + \Delta \quad (3.27)$$

or

$$d\ t_2^2/2 + [d\ h - m]t_2 + \left[\frac{m^2}{2\ a} - m(h+P+t_b) + v(h-h_f)\right] = 0 \quad (3.28)$$

Then, S can be formulated as:

$$S = (v_1P_1+aP_1^2/2) + vP_2 + (vt_2-dt_2^2/2) + (2v-dt_2)h_o + v(P+t_2) \quad (3.29)$$

If $t_b > t_Z$, the pass should be completed, and t_1 and S can be calculated as in Case 1.

Case 3: $t_b \geq t_f$. As shown in Figure 3.6*b*, the distance Δ can be calculated as follows:

$$(v-m)t_f + a\ t_f^2/2 + v(t_b-t_f) - \Delta = (v-m)h + L_f + (v-m)t_b \quad (3.30)$$

or

$$\Delta = -L_f - v\ h - \frac{m^2}{2\ a} + m(t_b+h) \quad (3.31)$$

If $t_b < t_Z$, the time required to abort the pass, t_2, can be calculated by substituting for Δ_t, v_d, and x_2 in Equation 3.3 with Δ, v, and vP, respectively, as follows:

$$(v-m)(P+t_2) = L_f + G_2 + v\ t_2 - d\ t_2^2/2 + v\ P + \Delta \quad (3.32)$$

or

$$d\ t_2^2/2 + [d\ h_l - m]t_2 + \left[v(h-h_l) + \frac{m^2}{2\ a} - m(h+P+t_b)\right] = 0 \tag{3.33}$$

Because the speed of the passing vehicle at the beginning of the deceleration is v, as in Case 2, the formulas of t_2 in the two cases are similar. However, the resulting t_2 will not be the same due to the change in the value of t_b in the two formulas.

Then, S can be formulated as:

$$S = v\ P + (vt_2 - dt_2^2/2) + (2v - dt_2)h_O + v(P+t_2) \tag{3.34}$$

If $t_b > t_Z$, both t_a and x_1 in Equation 3.1 will vanish, and substituting for Δ_c with Δ, the time t_1 required to complete the pass can be calculated as follows:

$$\Delta + v\ t_1 = (v-m)t_1 + (v-m)h_l + L_P \tag{3.35}$$

or

$$t_1 = \frac{L_l + L_P + (v-m)(h+h_l)}{m} + \frac{m}{2a} - t_b \tag{3.36}$$

Then, the required sight distance can be calculated as follows:

$$S = 2\ v(t_1 + h_O) \tag{3.37}$$

3.6 Model Simplification

The model derived above can be simplified by assuming that, by reaching the critical position, the passing vehicle has completed its acceleration to the design speed, v. In this case, the time-space diagram for the completed and aborted pass can be simplified as shown in Figure 3.7. Following the same technique, the model can be derived as follows:

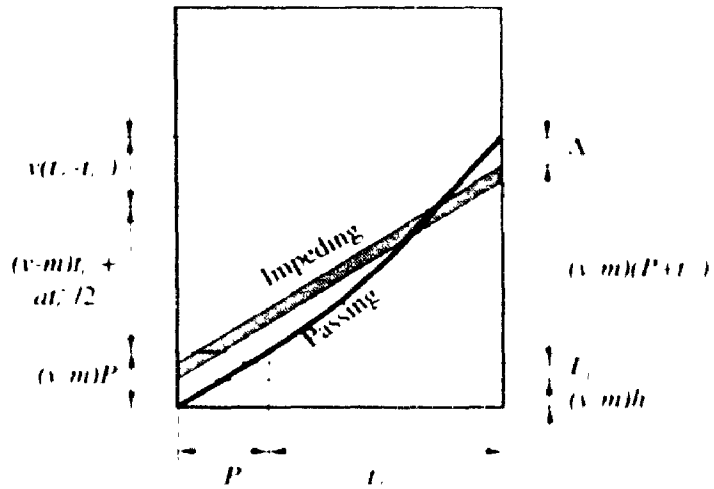

(a) Before the Critical Position

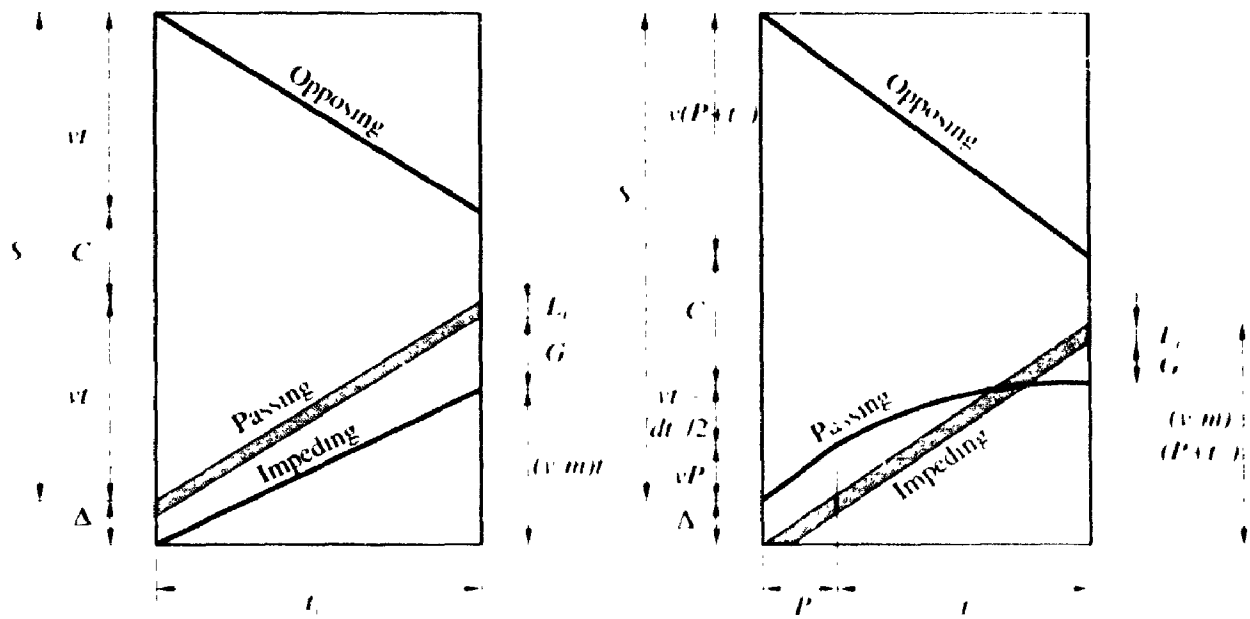

(b) Beyond the Critical Position.

FIGURE 3.7: Time-Space Diagrams for the Simplified Model.

For a completed pass,

$$\Delta_c + v\,t_1 = L_P + G_1 + (v-m)t_1 \tag{3.38}$$

or

$$\Delta_c = L_P + G_1 - m\,t_1 \tag{3.39}$$

Similarly, for an aborted pass,

$$\Delta_c + v\,P + v\,t_2 - \frac{d\,t_2^2}{2} = (v-m)(P+t_2) - L_I - G_2 \tag{3.40}$$

or

$$\Delta_c = \frac{d\,t_2^2}{2} - m(P+t_2) - L_I - G_2 \tag{3.41}$$

By equating Δ_c in Equations 3.39 and 3.41,

$$t_1 = P + t_2 - \frac{d\,t_2^2}{2\,m} + \frac{L_P + L_I + G_1 + G_2}{m} \tag{3.42}$$

By equating S_c for the completed and aborted passes,

$$2\,v\,t_1 + C_1 = v\,P + v\,t_2 - \frac{d\,t_2^2}{2} + C_2 + v(t_2+P) \tag{3.43}$$

or

$$t_1 = P + t_2 - \frac{d\,t_2^2}{4\,v} - \frac{C_1-C_2}{2\,v} \tag{3.44}$$

From Equations 3.42 and 3.44,

$$t_2^2 \left[\frac{d(2v-m)}{4\,v\,m}\right] = \frac{L_P + L_I + G_1 + G_2}{m} + \frac{C_1 - C_2}{2\,v} \tag{3.45}$$

Substituting for the values of G_1, G_2, C_1, and C_2 and solving for t_2:

$$t_2 = -\frac{2vh_I - mh_O}{2v - m} + \sqrt{\left[\frac{2vh_I - mh_O}{2v - m}\right]^2 + \frac{4v\,[L_P + L_I + (2v - m)h_I]}{d\,(2v - m)}} \tag{3.46}$$

Note that the other possible value of t_2 is negative and thus inadmissible. Then, the values of t_1, Δ_c, and S_c can be formulated as:

$$t_1 = P + t_2 - \frac{d\,t_2}{4\,v}\,(t_2 + 2\,h_O) \tag{3.47}$$

$$\Delta_c = L_P + (v - m)h_I - m\,t_1 = \frac{d\,t_2^2}{2} - m(P + t_2) - L_I - (v - d\,t_2)h_I \tag{3.48}$$

$$S_c = 2\,v\,(t_1 + h_O) = 2\,v\,(P + t_2 + h_O) - \frac{d\,t_2^2}{2} - d\,t_2\,h_O \tag{3.49}$$

If $h_O = h_I = h$, Equations 3.46 through 3.49 can be written as follows:

$$t_2 = -h + \sqrt{h^2 + \frac{4v\,[L_P + L_I + (2v-m)h]}{d\,(2v-m)}} \tag{3.50}$$

$$t_1 = P + t_2 - \frac{d\,t_2}{4\,v}\,[t_2 + 2\,h] \tag{3.51}$$

$$\Delta_c = L_P + (v-m)h - m\,t_1 = \frac{d\,t_2^2}{2} - m(P+t_2) - L_I - (v-d\,t_2)h \tag{3.52}$$

$$S_c = 2\,v\,(t_1 + h) = 2\,v\,(P + t_2 + h) - \frac{d\,t_2^2}{2} - d\,t_2\,h \tag{3.53}$$

If $\Delta_c > 0$, as shown previously, the time required to complete the pass in this case, t_1^*, can be calculated by substituting for the value of $\Delta_c = 0$ in Equation 3.48 as follows:

$$t_1^* = \frac{(v-m)h_l + L_P}{m} \tag{3.54}$$

Then, Equation 3.49 can be written as follows:

$$S_c = \begin{cases} 2\,v\,(t_1 + h_o) & \Delta_c \le 0 \\ 2\,v\,(t_1^* + h_o) & \Delta_c > 0 \end{cases} \tag{3.55}$$

The derivations for t_Z and l_Z can also be simplified using the same assumption that the passing vehicle has completed the acceleration before reaching the critical position. In this case, the time-space diagram for the pass before the critical position will be as shown in Figure 3.7*a*, and t_Z and l_Z can be formulated as follows:

$$t_Z = \frac{m}{2a} + \frac{\Delta_c - L_l + v\,h}{m} - h \tag{3.56}$$

$$l_Z = \Delta_c + (v-m)(P + t_Z + h) + L_l \tag{3.57}$$

The derivations for the profile of the required sight distance will not be affected by this assumption. However, in this case, Cases 1 and 2 will not be applicable for completed passes.

3.7 Selection of Model Parameters

Differential Speed (m): In the AASHTO design guide, the differential speed, m, is set as a constant value of 15 km/h regardless of the design speed, v. On the other hand, based on field studies, speed dependant values of m were assumed by Glennon (1988) and Harwood and Glennon (1989). These values can be related to the design speed, V, using the following formula:

$$m = 24 - V/10 \tag{3.58}$$

where m and V are in km/h.

Deceleration Rate (d): Although the deceleration rate of the passing vehicle, d, in the presented model is assumed constant, an iterative procedure can be used to account for a speed-dependent deceleration rate as follows:

1. Assume an initial value for the deceleration rate, d.
2. Calculate t_2 as shown previously.
3. Calculate the final speed of the passing vehicle, v_f, as $(v_d - dt_2)$, or $(v - dt_2)$ according to the simplified model.
4. Select an appropriate model for the speed-dependent deceleration rate (AASHTO, 1994; Olson et al, 1984; French, 1982) and determine the average deceleration rate corresponding to these initial and final speeds.
5. Continue the iterations until the change in the value of d in two successive iterations is within the required accuracy.

Among the different available models for deceleration, the model presented by Olson et al (1984) for a worn tire to 1.59 mm (2/32 inches) and operation with steering control should provide a sufficient braking distance for virtually all the vehicles on a highway. Therefore, it is recommended in this research. According to this model, the average deceleration rate from the design speed, v, to the final speed, v_f , can be calculated as follows:

$$d = \frac{v^2 - v_f^2}{2\ (BD_0 - BD_f)} \tag{3.59}$$

where BD_0 and BD_f are the braking distances (in metres) corresponding to v and v_f , respectively.

Table 3.1 shows the braking-distance data for a passenger car with a worn tire and decelerating with steering control. The braking distance corresponding to any speed can be calculated using Gauss interpolation. However, because these data were developed assuming a locked-wheel condition for speeds lower than 32 km/h (20 mph) (Olson et al, 1984), only the braking distance corresponding to higher speeds are to be used in calculating d. This can be done by imposing a maximum deceleration rate that corresponds to deceleration from the design speed to 32 km/h. Finally, to avoid the situation where the passing vehicle decelerates to unreasonably low speed, the final speed at an aborted pass can be set to a minimum value, v_f . This can be done by reducing the value of d to allow deceleration during the entire time interval t_2 and maintaining the final speed v_f .

TABLE 3.1: Braking Distance for a Passenger Car with Tires Worn to 2/32 inch in Operation with Steering Control (Olson et al, 1984).

Speed (km/h)	Braking Distance (m)
32	13.72
42	33.53
64	65.84
80	115.82
97	188.67
113	287.43
129	416.05

Acceleration Rate (a): The values of a can be directly taken from the AASHTO design guide (Table 3.2). Another model was developed by Glauz et al (1980) and can also be used. According to this model, the acceleration rate, a (m/s^2), can be calculated at an arbitrary speed, v_a (m/s), as follows:

$$a_0 = 1.14 \left[\frac{2 - e^{(-42.55\,R)}}{1 - e^{(-42.55\,R)}} \right] \tag{3.60}$$

$$v_m = \frac{a_0}{0.085} \tag{3.61}$$

$$a = a_0\,(1 - v_a/v_m) \tag{3.62}$$

where

R = mass-to-power ratio (kg/W),

a_0 = maximum acceleration (m/s^2), and

v_m = maximum speed (m/s).

However, because the speed increases continuously upon acceleration, an average speed (v-m/2) can be used to calculate the acceleration rate. Also, a low power-to-mass ratio of 40 W/kg which represents a relatively poor performance is recommended for passenger cars to account for most of the vehicles. However, because such a vehicle cannot operate on high speeds (the maximum speed 121.9 km/h) and because this model tends to underestimate acceleration capability at high speeds (Glauz et al, 1980), the acceleration rate corresponding to a 160-km/h design speed can be assumed to be the same for higher speeds.

TABLE 3.2: Initial Acceleration in Passing Manoeuvres (AASHTO, 1994).

Speed Group of Passing Vehicle (km/h)	Average Acceleration (km/h/sec)
50 - 65	2.25
66 - 80	2.30
81 - 95	2.37
96 - 110	2.41

Vehicle Length: The vehicle length is extremely variable. However, a design length of 5 m can be assumed for passenger cars. On the other hand, the length of a design truck

can be taken as 25 m which is the maximum truck length on Canadian roads (Good et al. 1991).

3.8 Model Validation

In order to test the derived model against its simplification, both of them were used to determine the required PSD and length of passing zones for design speeds ranging from 50 to 130 km/h. The length of the impeding vehicle was taken as 5 and 25 m to represent a passenger car and the longest truck on Canadian roads (Good et al. 1991). The results of S_i and l_p were identical for all the speeds higher than 50 km/h. Moreover, the difference at the speed 50 km/h was less than 1.0 m. Therefore, the complexity involved in considering the acceleration is not justified. The simplified version of the model will be used here on and is referred to as the revised model.

The validity of the developed model was tested by comparing the PSD requirements resulting from Glennon's model (1988), the modified model (Rillet et al. 1990), and the revised model with the field measurements presented by Van Valkenberg and Michael (1971). In the study by Van Valkenberg and Michael (1971), the distance travelled by the passing vehicle from the point of no return until it is back in the right lane and the time elapsed during this distance were measured for three different speeds of the passed vehicle. The measurements were classified into four types of passes: accelerative with voluntary return, accelerative with forced return, flying with voluntary return, and flying with forced return. Then, the sight distance was calculated assuming

2

PM-1 3½"x4" PHOTOGRAPHIC MICROCOPY TARGET
NBS 1010a ANSI/ISO #2 EQUIVALENT

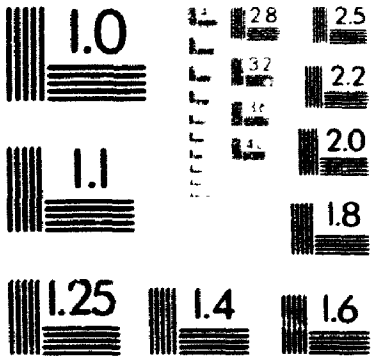

PRECISION℠ RESOLUTION TARGETS

an opposing vehicle travelling with a speed greater than the average speed by 11.2 km/h (7 mph) and a head-on clearance of 6.1 m (20 ft) at the end of the pass

The three models were used to determine the required PSD for each speed of the passed vehicle according to the following assumptions:

1. Only the accelerative passes were considered because all the models assume that the passing vehicle is trailing the passed vehicle at the beginning of the manoeuvre.
2. The deceleration rate was taken so as to simulate the operation with steering control for a passenger car with tires worn to 2/32 inches modeled by Olson et al (1984). These rates were 2.14, 1.88, and 1.55 m/s^2 for the speeds 77.25, 90.12, and 111.04 km/h, respectively.
3. The speed differential, m, was calculated using equation 3.58. The values of m were 16.3, 15.0, and 12.9 km/h for the speeds 77.25, 90.12, and 111.04 km/h, respectively.
4. The clearance between the passing and opposing vehicle at the end of the pass was taken as $2v/h$ instead of the 6.1 m (20 ft) assumed by Van Valkenberg and Michael.
5. The acceleration rate used in the modified model (Rillet et al, 1990) was assumed according to the values given by AASHTO (1994) for the initial acceleration in the passing manoeuvre (Table 3.2).

As shown in Figure 3.8, the PSD requirements resulting from Glennon's model are closer to the forced return performance indicating uncomfortable or unsafe manoeuvring. On the other hand, the PSD requirements resulting from Rillet's modified model are much longer than those required for safe and comfortable manoeuvring indicating that the model is too conservative. These conservative results are not justified

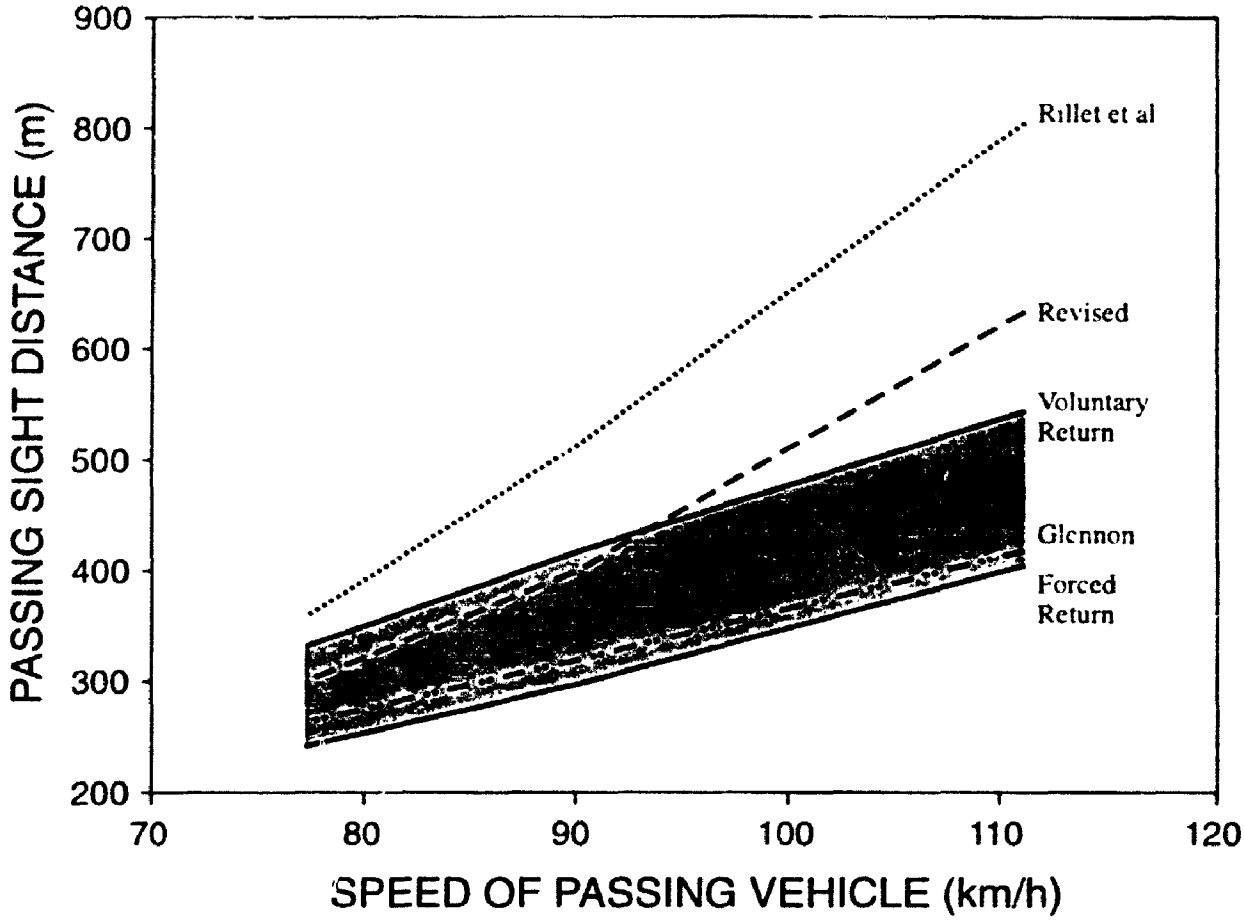

FIGURE 3.8: Validation of the Model for Required PSD.

by field observations. The revised model, however, provides PSD requirements that are very close to the voluntary return field data, and therefore ensures safe and comfortable passing manoeuvres. Interestingly, the margin of safety and comfort of PSD requirements produced by the revised model increases as the design speed increases, and thus, the degree of potential hazards due to human errors or shifting from the model's assumptions increases. An example of shifting from the model's assumptions is a higher perception-

reaction time due to any type of impairments such as fatigue. This margin of safety would overcome these hazards.

3.9 Practical Considerations

3.9.1 Design Values for Required PSD

The revised model presented here was used to develop design values for the required PSD on two-lane highways, as shown in Figure 3.9. The PSD requirements when the impeding vehicle is a truck are longer than those when the impeding vehicle is a passenger car for speeds up to 110 km/h. For higher speeds, there is no difference because the critical position was set as Δ=0 instead of Δ_c which was positive at higher

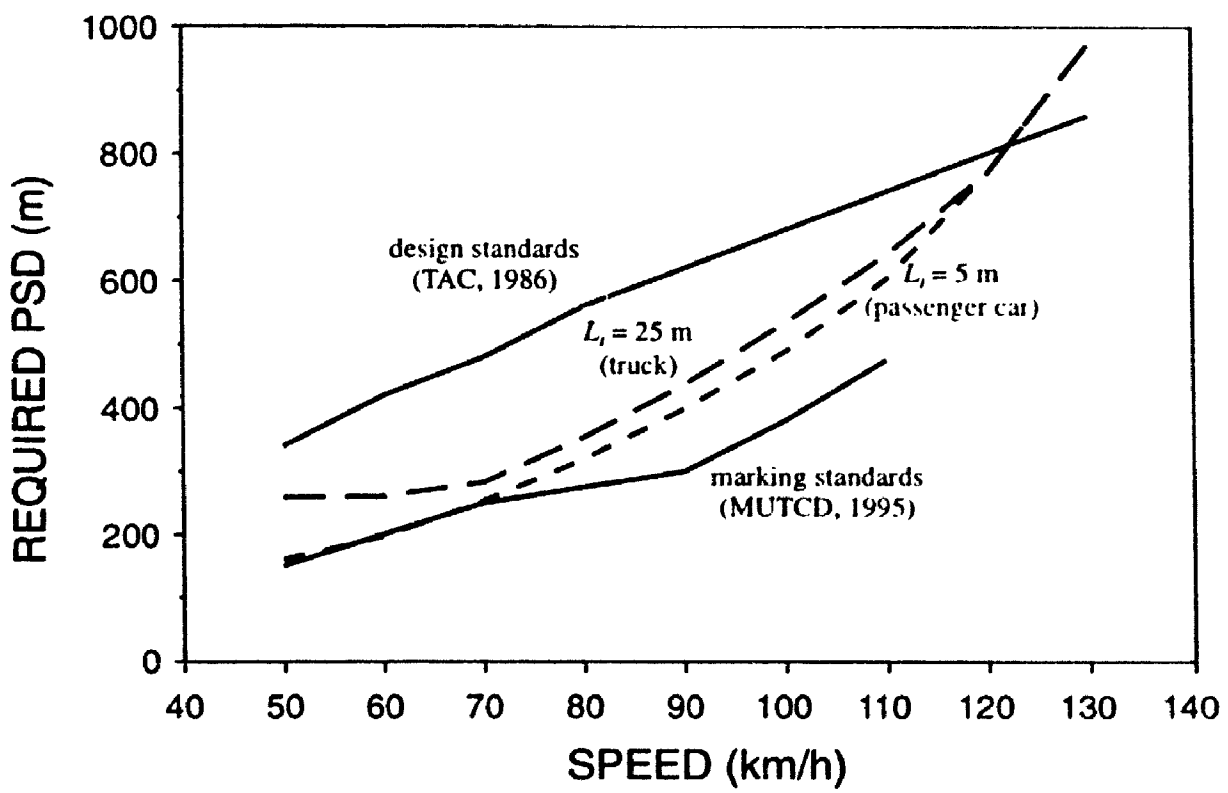

FIGURE 3.9: Comparison of Required PSD of the Model and Current Practice.

speeds. As expected, this process would produce PSD requirements which are independent of the characteristics of the impeding vehicle. On the other hand, since the values recommended in the design and the marking standards are to be used for any highway regardless of the traffic composition, both standards fail to consider the effect of the vehicle length. The results also show, in addition to the great difference between the two standards, that the PSD requirements in neither of them would help achieve safe and economic roads. Although following the design standards would guarantee the safety of the passing manoeuvres for all passes up to a 120-km/h design speed, this safety would be achieved in an expensive way. On the other hand, following the MUTCD standards would jeopardize the passes involving passenger cars when the design speed is higher than 70 km/h. If the impeding vehicle is a long truck, safety would not be achieved for all speeds. It is clear, therefore, that the MUTCD marking standards need major revisions to account for the traffic composition on any specific highway and to ensure safety and comfort in all passing manoeuvres.

3.9.2 Design Values for Minimum Length of Passing Zones

Similar to the required PSD, the marking standards fail to consider the traffic characteristics in setting the minimum length of passing zones. Figure 3.10 shows the minimum length of passing zones developed using the model presented earlier and the values recommended in the MUTCD (1976; 1995). The values recommended in the MUTCD (1995) and used for marking in Ontario are higher than the required length for low speeds, and this difference can be related to practical considerations. Moreover, the

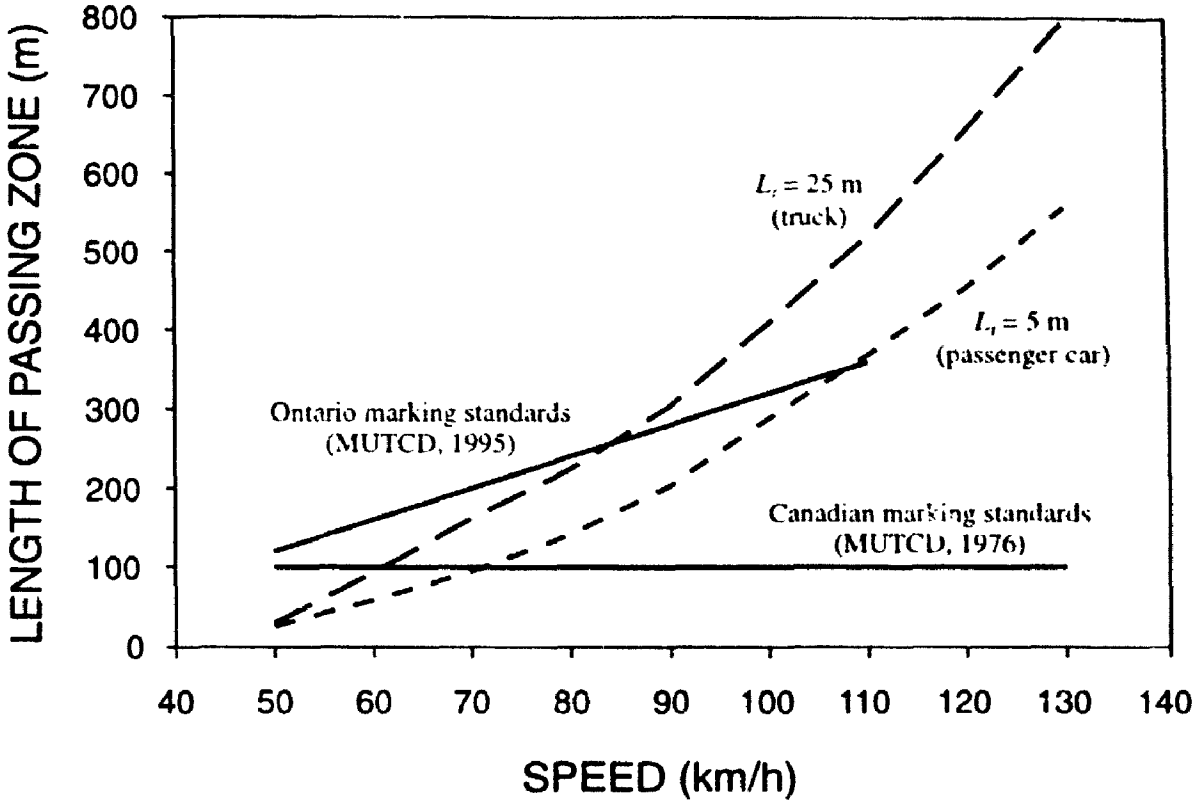

FIGURE 3.10: Comparison of Minimum Length of Passing Zones of the Model and Current Practice.

values are satisfactory for all speeds if the manoeuvre involves passenger cars only. However, if the impeding vehicle is a truck, these values are not sufficient for speeds higher than 90 km/h. On the other hand, the constant minimum lengths of 100 m and 122 m (400 ft) recommended in Canadian and American MUTCD (1976; 1988) seem unrealistic.

3.9.3 Beginning and End of Passing zones

As mentioned earlier, the profile of required PSD with the evolvement of the pass is useful in checking the safety of the manoeuvre from its beginning to its end. Figure 3.11 shows an example of this profile for a 90 km/h design speed. The profile of the required

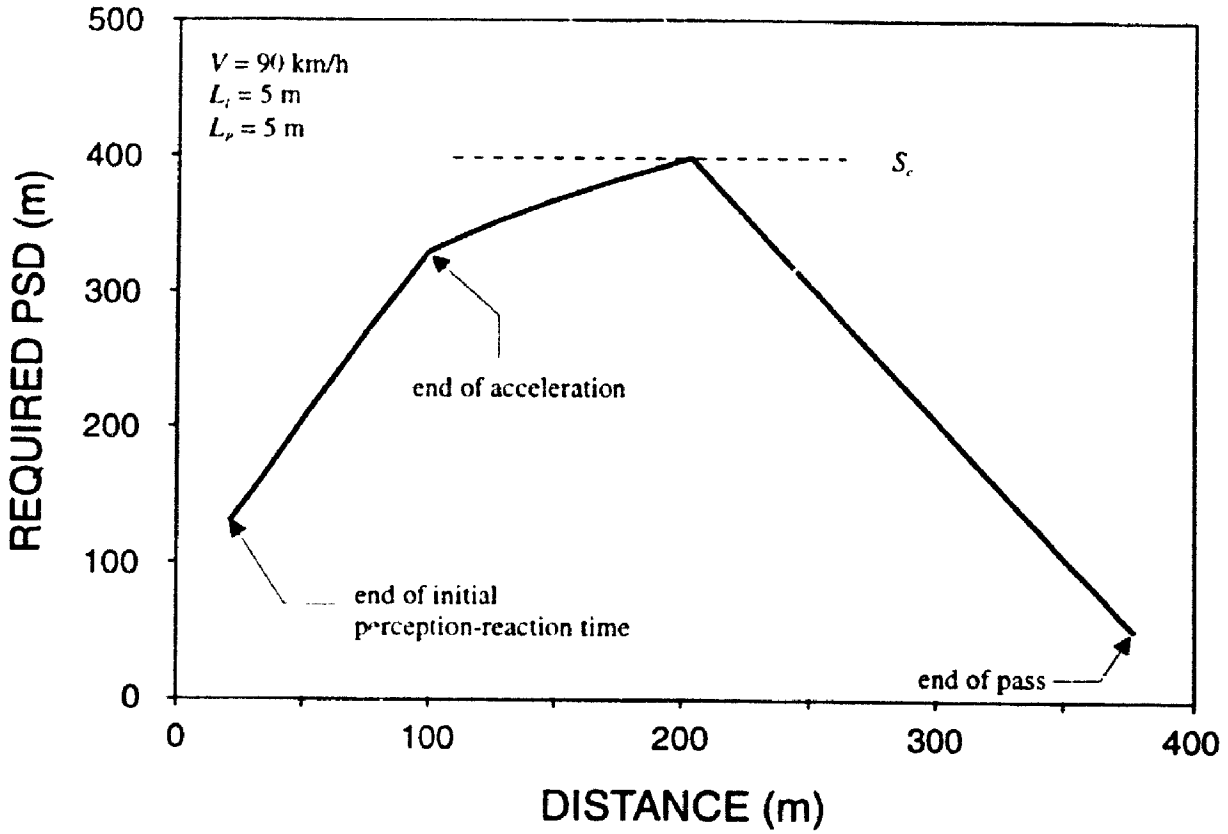

FIGURE 3.11: Example for the Profile of Required PSD.

PSD consists of three distinct zones. The first zone extends from the end of the initial perception-reaction time to the end of the passing vehicle's acceleration time. In this zone, the required PSD is minimum at the end of the initial perception-reaction time, and corresponds to aborting the pass. Although the passing vehicle at this point has not begun the acceleration yet, it is assumed that the driver will keep accelerating for a complete perception-reaction time before decelerating again if the pass is to be aborted. The rate of increase of the required PSD in this first zone is relatively high because the speed of the passing vehicle is increasing.

The second zone extends from the end of acceleration to the critical position. The required PSD in this zone corresponds also to aborting the pass. The speed of the passing

vehicle in this zone is constant. Therefore, the rate of increase of the required PSD is lower than that in the first zone. Finally, the third zone extends from the critical position to the end of the pass. The required PSD in this zone corresponds to completing the pass. Therefore, it decreases as the distance travelled by the passing vehicle increases. At the end of the pass, the required PSD is just two times the headway spacing between the passing and opposing vehicle.

The use of the profile of required PSD to check the safety of the pass during the entire manoeuvre is shown in Figure 3.12 for different profiles of the available PSD (dashed lines), referred to as profiles **1** to **4**. Profiles **1** to **3** can result near the end of a horizontal or a vertical curve where the available sight distance is increasing. On the other hand, profile **4** can result near the beginning of the curves where the available sight distance is decreasing. For any profile of available PSD between profiles **1** and **2**, a passing zone can begin prior to the point with available sight distance greater than the critical sight distance, S_c. On the other hand, doing the same with profile **3** would hide the potential opposing vehicles during a portion of the pass. Therefore, the beginning of the passing zone must be shifted so that the required PSD at any time is less than the available PSD. Moreover, although the available sight distance in profile **4** is higher than S_c, the potential opposing vehicle may be hidden during a portion of the manoeuvre. This would give a false sense of safety for the passing driver, and therefore may produce head-on collisions between the passing and opposing vehicles. Subsequently, such a passing manoeuvre should be prohibited by an early marking of a no-passing zone.

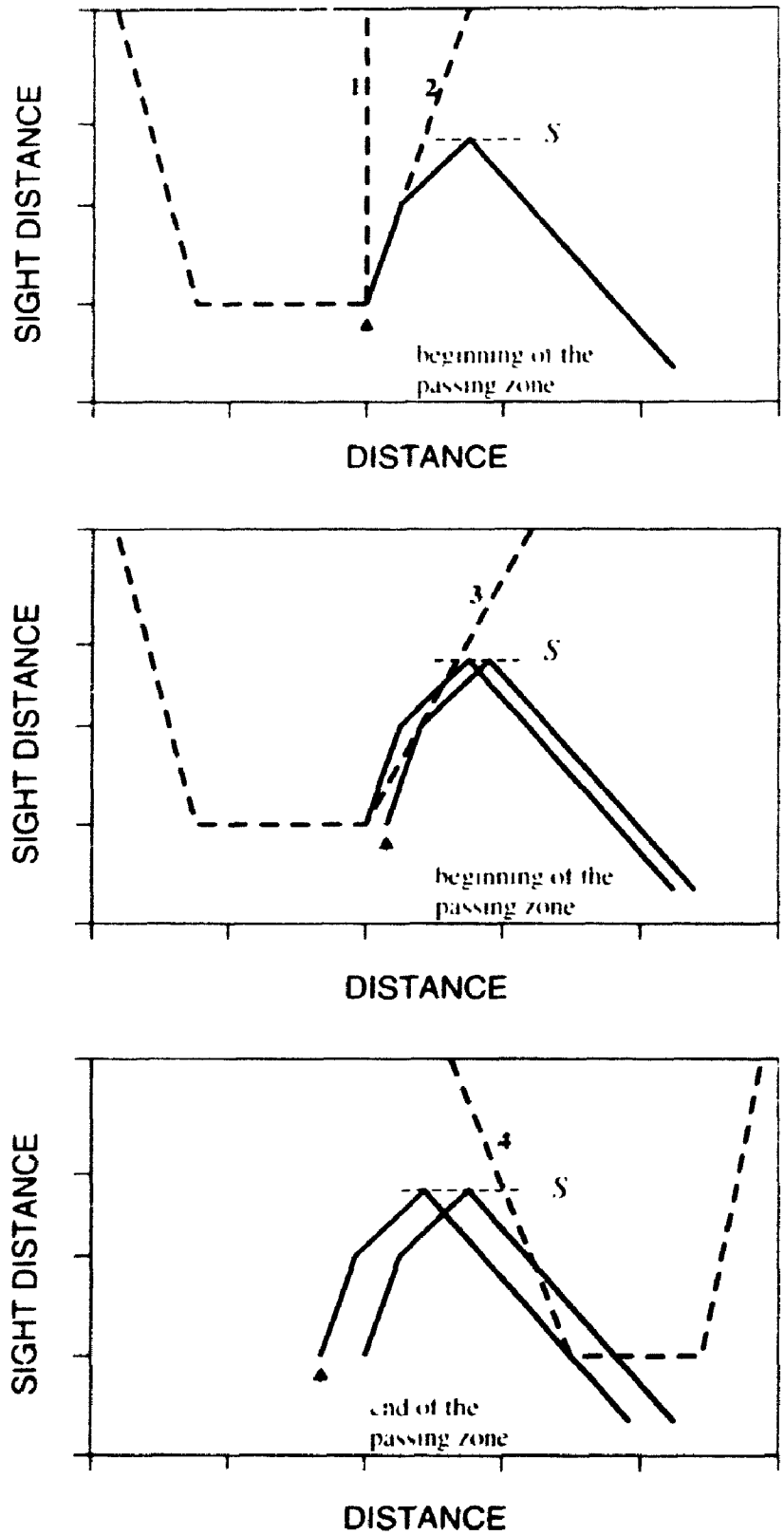

FIGURE 3.12: Determination of the Beginning and End of Passing Zones.

CHAPTER 4

AVAILABLE SIGHT DISTANCE ON 2-D SEPARATE ALIGNMENTS

As shown in Chapter 2, current analytical models for available sight distance cannot consider complex 2-D alignments. In addition, in order to evaluate the effect of considering the combined alignment in design, separate horizontal and vertical alignments are studied first. Therefore, this chapter presents general analytical models to evaluate sight distance on horizontal alignments for both cases of continuous and single obstructions (Hassan et al. 1995*b*; 1995*d*). Also, models for available sight distance on vertical alignments, where the obstruction may be the crest curves or the overpasses on sag curves, are presented (Hassan et al. 1995*c*; 1995*d*). The term *horizontal alignment* is used herein to refer to any combination of the horizontal highway components which are straight segments, circular curves, and clothoid spiral curves. Similarly, the term *vertical alignment* is used to refer to any combination of the highway vertical components which are straight segments with constant grade and parabolic sag and crest vertical curves. Finally, computer models are developed to determine the profile of available sight distance, and in turn the no-passing zones, on two-lane rural highways

4.1 Horizontal Alignment with Continuous Obstruction

Assuming a constant lane width and lateral clearance, the continuous obstruction will be parallel to, and will have the same geometry of, the highway centerline, and the sight

distance is restricted by having the sight line tangent to the obstruction. The point of tangency may be located on a circular curve, spiral curve, or the point of intersection of two successive straight segments without curves. The following sections present general procedures which can be used to determine the available sight distance regardless of the components of the horizontal alignment. Then, special relationships are presented for the special alignments of simple circular curves and intersecting long tangents. In both of the general procedures and special relationships, the lateral clearance between the obstruction and the centre of the lane is assumed constant and referred to as m.

In the following sections, the azimuth of a line, defined as the angle between the north direction and the line, measured clockwise, is used and referred to as Φ. Also, the east and north coordinates of a point are used and referred to as (x, y), respectively. However, since it is the relative positioning of the points to each other, not the absolute positions, which determines the available sight distance, the coordinates and azimuths can be taken relative to any reference point and direction.

4.1.1 General Procedure: Sight Line Tangent to Circular Curve

As shown in Figure 4.1, the obstruction restricting the sight line in this case is a circular curve. In general, the beginning and the end of the sight line may be positioned on any horizontal highway segment (straight, circular curve, or spiral curve). The general procedure, developed in this research, is iterative, where the sight distance is initially assumed as S. Then, S is checked and decreased or increased until the sight line becomes tangent to the obstruction. The procedure involves the following steps:

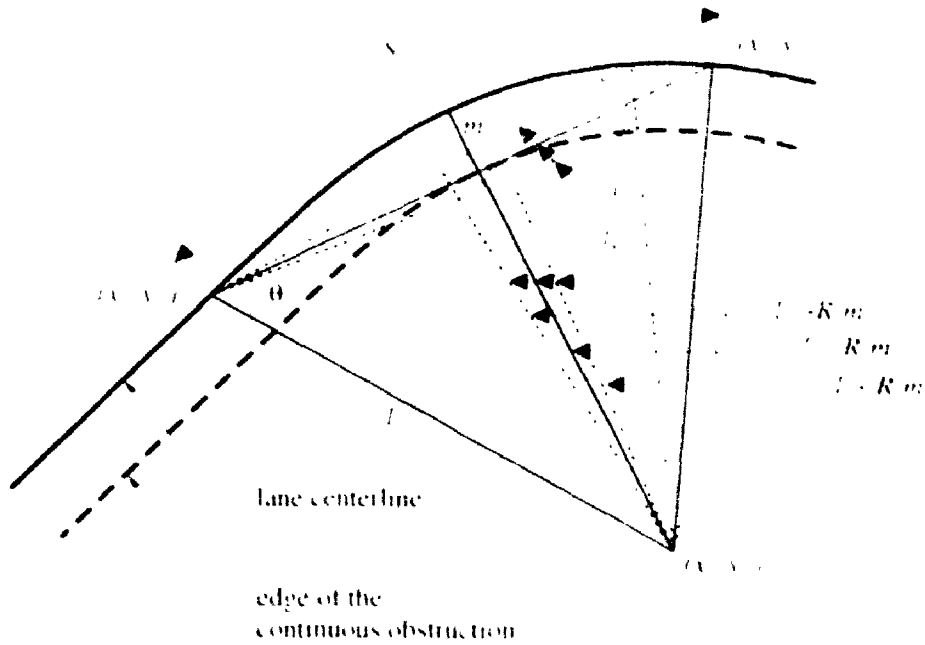

FIGURE 4.1: General Procedure: Sight Line Tangent to Circular Curve. (Continuous Obstruction)

1. Determine the coordinates of the beginning of the sight line and the centre of the curve, (x_1, y_1) and (x_c, y_c), respectively.

2. Calculate the length l_1 as:

$$l_1 = \left[(x_1 - x_c)^2 + (y_1 - y_c)^2\right]^{1/2} \tag{4.1}$$

3. Determine the coordinates of the end of the sight line, (x_2, y_2)

4. Calculate l_2 and l_3 similar to l_1.

5. Calculate the angle θ as:

$$\theta = \cos^{-1}\left(\frac{l_1^2 + l_3^2 - l_2^2}{2\, l_1\, l_3}\right) \tag{4.2}$$

6. Calculate the length l_4 as:

$$l_4 = l_1 \sin\theta \tag{4.3}$$

7. If $l_4 < R\text{-}m$, S is greater than the actual sight distance. Decrease S and repeat steps 3-6.
8. If $l_4 > R\text{-}m$, S is less than the actual sight distance. Increase S and repeat steps 3-6.
9. If $l_4 = R\text{-}m$, S is equal to the actual sight distance. End of iterations.

Although the lengths l_1, l_2, and l_3 can be calculated without using the coordinates, a unique sequence of calculations is required for each possible combination of horizontal segments. On the other hand, using the coordinates of the points makes the procedure applicable regardless of the positions of the beginning and end of the sight line and also makes it easier for programming.

4.1.2 General Procedure: Sight Line Tangent to Spiral Curve

Generally, the spiral curve is a curve with varying radius, beginning with a straight segment ($R \rightarrow \infty$), and as the curve length increases, the corresponding radius decreases. Many mathematical formulas can be used to represent spiral curves and can be found in mathematics textbooks (Drábek, 1969). Among these formulas, Euler's spiral, known as the clothoid spiral, is the most commonly used in road design (AASHTO, 1994; TAC, 1986). Defining l as a segment length of a spiral curve beginning at the point of tangent-spiral (TS), R as the corresponding radius, and δ as the deflection angle of this segment in radian, Euler's spiral is formulated as follows:

$$A^2 = l \cdot R = \frac{l^2}{2\delta} = R^2 \cdot 2\delta \qquad (4.4)$$

where A is a constant known as the spiral parameter

As shown in Figures 4.2 and 4.3, this case is similar to the previous case but the obstruction restricting the sight line is a spiral curve. The beginning and the end of the sight line may be positioned on any horizontal highway segment (straight, circular curve, or spiral curve). In this case, the developed general procedure involves the following steps:

1. Determine the coordinates of the beginning of the sight line, (x_s, y_s)
2. Determine the coordinates of the end of the sight line, (x_e, y_e)

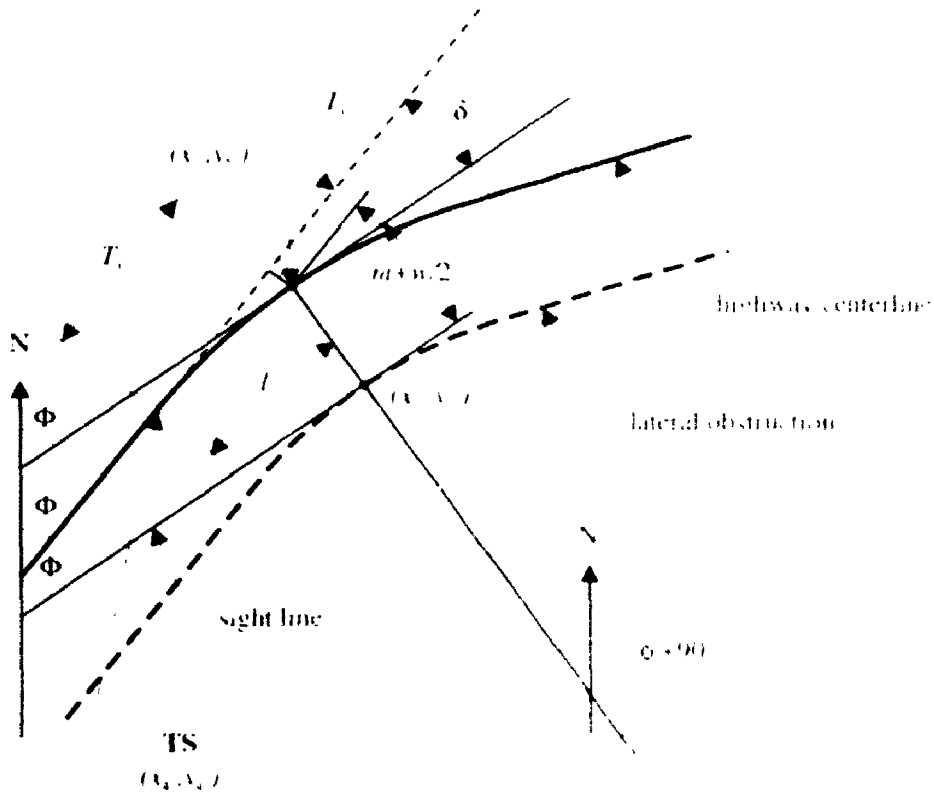

FIGURE 4.2: Determination of Coordinates on Spiral Curves.

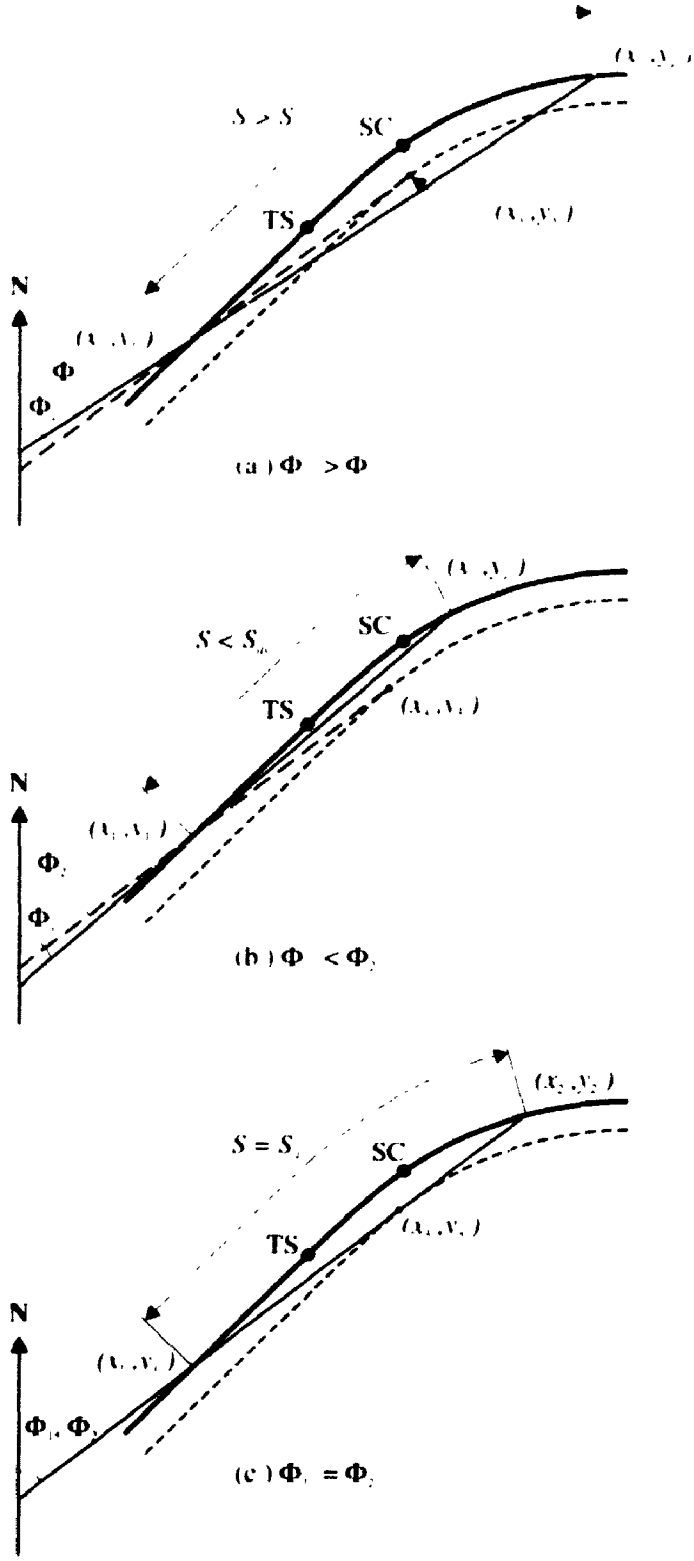

Figure 4.3: General Procedure: Sight Line Tangent to Spiral Curve. (Continuous Obstruction)

3. Calculate the azimuth of the sight line, Φ_1, as:

$$\Phi_1 = \tan^{-1}\left[\frac{x_2 - x_1}{y_2 - y_1}\right] \tag{4.5}$$

4. Knowing the azimuth of the tangent to the spiral, Φ_0, determine the coordinates of the point of tangency of a line having an azimuth Φ_1 and the given obstruction, (x_3, y_3). For right turn spirals beginning with a straight segment, (x_3, y_3) can be determined by considering another point (x_5, y_5) defined as the point of tangency of a line having an azimuth Φ_1 and the highway centerline. As shown in Figure 4.2, the coordinates (x_5, y_5) can be determined as follows:

$$\delta = (\Phi_1 - \Phi_0) \times \frac{\pi}{180°} \tag{4.6}$$

Using the spiral formula presented in Equation 4.4,

$$l_\delta = A \times \sqrt{2\delta} \tag{4.7}$$

From the general characteristics of Euler's spiral (Drábek, 1969),

$$T_x = A\sqrt{2\delta}\left[1 - \frac{\delta^2}{5\ .\ 2!} + \frac{\delta^4}{9\ .\ 4!} - \frac{\delta^6}{13\ .\ 6!} + \ldots\right] \approx l_\delta - \frac{l_\delta\,\delta^2}{10} \tag{4.8}$$

$$T_y = A\sqrt{2\delta}\left[\frac{\delta}{3} - \frac{\delta^3}{7\ .\ 3!} + \frac{\delta^5}{11\ .\ 5!} - \ldots\right] \approx \frac{l_\delta\,\delta}{3} \tag{4.9}$$

Defining (x_4, y_4) as the coordinates of the tangent-spiral (TS) point on the centerline of the highway, then

$$x_5 = x_4 + T_x \sin\Phi_0 + T_y \cos\Phi_0 \tag{4.10}$$

$$y_5 = y_4 + T_x \cos\Phi_0 - T_y \sin\Phi_0 \tag{4.11}$$

Defining w as the lane width, the line from (x_5, y_5) to (x_3, y_3) will have an azimuth of $\Phi_1+90°$ and a length of $m+w/2$. Therefore, (x_3, y_3) can be calculated as follows:

$$x_3 = x_5 + (m+w/2) \sin(\Phi_1+90°) \tag{4.12}$$

$$y_3 = y_5 + (m+w/2) \cos(\Phi_1+90°) \tag{4.13}$$

5. Calculate the azimuth of the line between points 1 and 3, Φ_2.
6. For right turn curves, If $\Phi_1 > \Phi_2$ (if $\Phi_1 < \Phi_2$, for left turn curves), S is greater than the actual sight distance (see Figure 4.3 for illustration). Decrease S and repeat steps 2-5.
7. For right turn curves, If $\Phi_1 < \Phi_2$ (if $\Phi_1 > \Phi_2$, for left turn curves), S is less than the actual sight distance (see Figure 4.3 for illustration). Increase S and repeat steps 2-5.
8. If $\Phi_1 = \Phi_2$, S is equal to the actual sight distance (see Figure 4.3 for illustration). End of iterations.

Since, the azimuth is always less than 360°, some caution is required in the last check if, for right turn curves, Φ_1 is slightly greater than zero and Φ_2 is slightly less than 360° (or if Φ_2 is slightly greater than zero and Φ_1 is slightly less than 360°, for left turn curves). For example, for right turn curves, if Φ_2 is slightly less than 360° and S is greater than the available sight distance, Φ_1 may be slightly greater than zero. In this case, S should be decreased and another iteration is required.

4.1.3 General Procedure: Sight Line Passing Through Point of Intersection

In this case, only two long straight segments are intersecting at a small deflection angle, as shown in Figure 4.4. Although no circular or spiral curves are involved in this case, it represents a possible horizontal alignment and, therefore, it is considered in this research. In general, the beginning and the end of the sight line may be located on any horizontal highway segment. However, the straight segments in this case are usually long enough for the beginning and the end of the sight line to be located on the two intersecting straight segments. Though, for the comprehensiveness of the research, a general iterative procedure is presented here to determine the available sight distance regardless of the beginning and end of the sight line.

As shown in Figure 4.4, the sight line will pass through the point of intersection of the two straight segments, PI. The general iterative procedure involves the following steps:

1. Determine the coordinates of the beginning of the sight line, (x_1, y_1).
2. Determine the coordinates of the point of intersection (PI) at the lane centerline and at the obstruction, (x_3, y_3) and (x_4, y_4), respectively.
3. Determine the coordinates of the end of the sight line, (x_2, y_2).
4. Calculate the area of the triangle 123 and the traverse 1324, *AREA1* and *AREA2*, respectively
5. If *AREA1* > *AREA2*, *S* is greater than the actual sight distance. Decrease *S* and repeat steps 3 and 4.

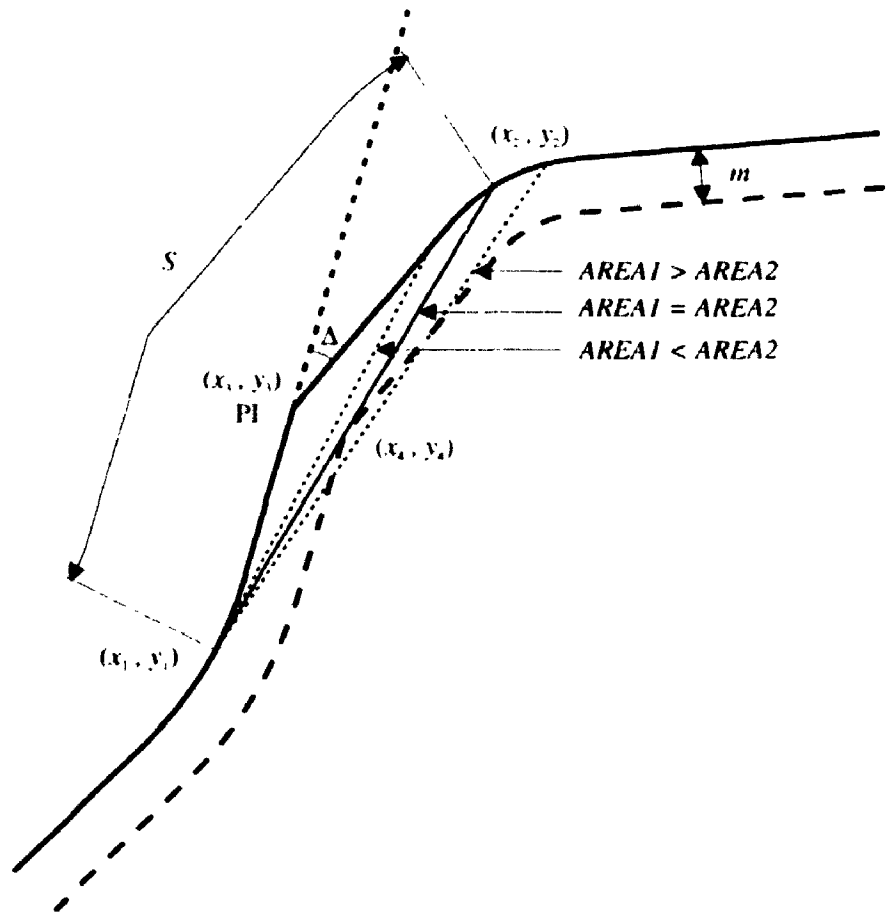

FIGURE 4.4: General Procedure: Intersecting Straight Segments Without Curves. (Continuous Obstruction)

6. If *AREA1* < *AREA2*, *S* is less than the actual sight distance. Increase *S* and repeat steps 3 and 4.

7. If *AREA1* = *AREA2*, *S* is equal to the actual sight distance. End of iterations.

4.1.4 Special Case: Simple Circular Curve

In this case, the horizontal curve consists of a simple circular curve, having a radius *R*, with two straight segments (tangents) at the two ends. Obviously, the sight line can only

presented previously can be applied. However, other closed form relationships have been developed for this special case to determine the available sight distance more easily and accurately. These formulas can be considered extensions to the work of Easa (1991*a*) which considered only a single (or multiple) lateral obstruction.

For the case of a simple curve, there are four possibilities regarding the beginning and the end of the sight line touching the obstruction:

(i) Sight line begins on first tangent and ends on curve.

(ii) Sight line begins on first tangent and ends on second tangent.

(iii) Sight line begins and ends on curve.

(iv) Sight line begins on curve and ends on second tangent.

Case (i): Sight line begins on first tangent and ends on curve. As shown in Figure 4.5*a*,

$$l_2 = (R^2 + l_1^2)^{1/2} \tag{4.14}$$

where l_1 is the distance between the driver and the point of curve (PC).

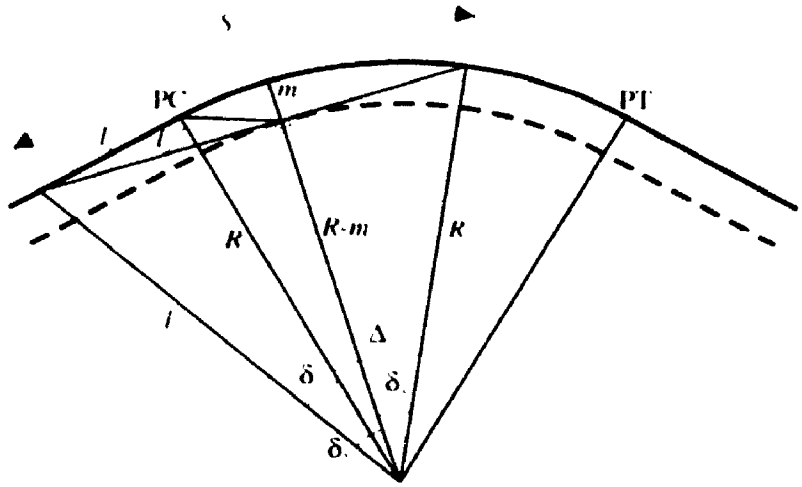

(a) Sight Line Begins on Tangent and Ends on Curve.

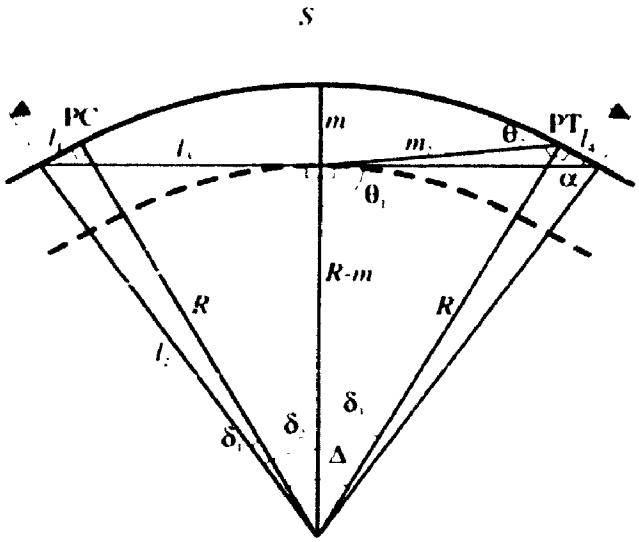

(b) Sight Line Begins and Ends on Tangents.

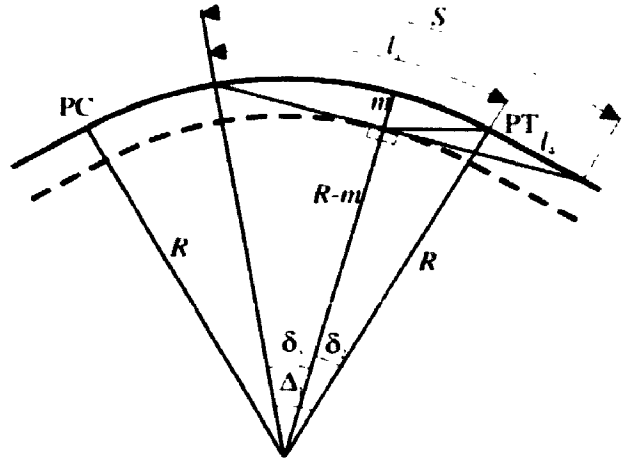

(c) Sight Line Begins on Curve and Ends on Tangent.

FIGURE 4.5: Special Case: Simple Horizontal Curve. (Continuous Obstruction)

$$\delta_1 = \sin^{-1}(l_1/R) \tag{4.15}$$

$$\delta_2 = \cos^{-1}\left[\frac{R - m}{l_2}\right] \tag{4.16}$$

$$\delta_3 = \cos^{-1}\left[1 - \frac{m}{R}\right] \tag{4.17}$$

$$\Delta_1 = \delta_2 - \delta_1 + \delta_3 \tag{4.18}$$

Then, the available sight distance is:

$$S = l_1 + R \ \Delta_1 \times \frac{\pi}{180°} \tag{4.19}$$

Case (ii): Sight line begins on first tangent and ends on second tangent. As shown in Figure 4.5*b*, δ_1 and δ_2 can be determined as in case (i). Defining Δ as the total deflection angle of the curve, then:

$$\delta_3 = \Delta + \delta_1 - \delta_2 \tag{4.20}$$

$$m_2 = \left(R^2 + (R-m)^2 - 2\ R\ (R-m)\ \cos\delta_3\right)^{1/2} \tag{4.21}$$

$$\theta_1 = \sin^{-1}\left(R \ \sin\delta_3/m_2\right) \tag{4.22}$$

$$\theta_2 = \sin^{-1}\left[(R-m) \ \sin\delta_3/m_2\right] \tag{4.23}$$

$$\alpha = 180 - \theta_1 - \theta_2 \tag{4.24}$$

$$l_4 = m_2 \sin(\theta_1 - 90°)/\sin\alpha \tag{4.25}$$

Then, the available sight distance is:

$$S = l_1 + R \Delta \times \frac{\pi}{180°} + l_4 \tag{4.26}$$

Case (iii): Sight line begins and ends on curve. In this case, the formula presented by AASHTO can be applied as follows:

$$S = 2 R \times \cos^{-1}(1 - m/R) \times \frac{\pi}{180°} \tag{4.27}$$

Case (iv): Sight line begins on curve and ends on second tangent. The relationships involved in this case are backward derivations for case (i). As shown in Figure 4.5*c*, the angle δ_3 can be calculated as in case (i). Knowing the distance l_1 and the radius R, the angle Δ_1 and subsequently δ_2 can be calculated. Then, l_4 can be calculated as in case (ii). Finally, S equals the sum of l_1 and l_4.

4.1.5 Special Case: Intersecting Long Straight Segments

This case, as shown in Figure 4.6, is a special case of *sight line passing through point of intersection* where two straight segments are intersecting at a deflection angle Δ. The straight segments are long enough for the beginning and end of the sight line to be located at the first and second segment, respectively. The driver is at a distance l_1 from

PI. As shown, the sight line will touch the continuous obstruction at its PI. From Figure 4.6,

$$l_3 = m/\tan\frac{180° - \Delta}{2} \tag{4.28}$$

$$\alpha = \tan^{-1}\left[m/(l_1 - l_3)\right] \tag{4.29}$$

$$\beta = \Delta - \alpha \tag{4.30}$$

$$l_2 = l_1 \sin\alpha/\sin\beta \tag{4.31}$$

Then, the available sight distance is:

$$S = l_1 + l_2 \tag{4.32}$$

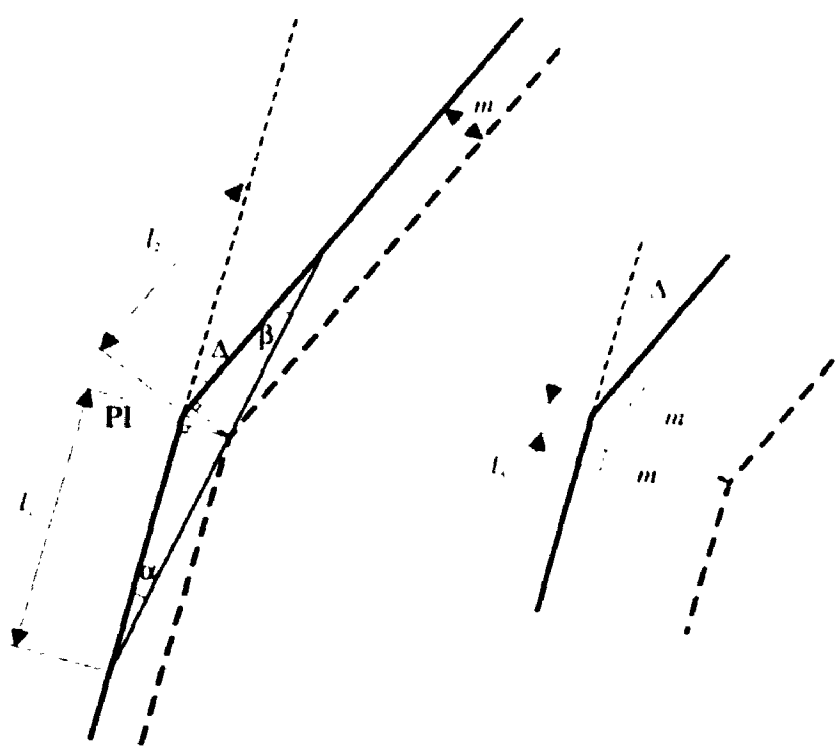

FIGURE 4.6: Special Case: Intersecting Straight Segments Without Curves. (Continuous Obstruction)

4.2 Horizontal Alignment with Single Obstructions

As mentioned previously, the case of a single obstruction has been extensively studied by many researchers. Formulas relating the available sight distance to the lateral clearance on simple horizontal curves already exist. In this research, two general iterative procedures have been developed to check the available sight distance regardless of the components of the horizontal curve and the positions of the beginning and end of the sight line.

The first procedure uses the areas as explained in the general procedure of sight line passing through point of intersection while the second procedure uses the azimuths of the lines in a way similar to the general procedure of the continuous obstruction with the sight line tangent to a spiral curve. In the first procedure, the coordinates of an intermediate point on the highway between points 1 and 2 can replace the coordinates (x_3, y_3) and the coordinates of the obstruction are used instead of (x_4, y_4). In the second procedure, the coordinates of the obstruction are directly used instead of the point of tangency (x_3, y_3).

4.3 Vertical Alignment

Generally, vertical alignment may obstruct the sight line in three possible ways. First, if the sight line from the driver eye to the object should pass over a crest curve, it may intersect with the road itself. The points of intersection may be on a tangent segment, a crest curve, or a sag curve. Subsequently, the sight distance is limited by having the sight line tangent to the crest curve. Second, although sag curves do not represent a

sight obstruction at daytime, the available SSD at nighttime is limited to the farthest point covered by the vehicle headlights. However, this restriction is not applied for the available PSD since the driver can always detect the opposing vehicles by their own headlights. Therefore, the case of headlight sight distance is beyond the scope of this research. Third, overpasses existing on sag curves may obstruct the sight line which must be limited by passing under these overpasses.

In considering the separate vertical alignment, as in the general practice of highway vertical alignment design, the profile of the highway is drawn using a system of axes X-Z with the first axis going through the highway centerline. Therefore, the coordinates of any point (x, z) represent the point station and elevation, respectively. It should be noted also that, in the following sections, the grade of a tangent segment or the instantaneous grade at a point on a curve is used as a percentage and referred to as g. The sign of g is positive if the grade is upward and negative if it is downward. The algebraic difference in grades of vertical curves, which is always a positive value, is used as a percentage and referred to as A. Finally, h_1 and h_2 are referring to the heights of the driver's eye and the object, respectively.

4.3.1 Geometric Characteristics of Vertical Alignment Elements

Elements' Equations. Three main elements are encountered when studying sight distance on vertical alignments at daytime. These elements are the sight line, tangent segments, and sag and crest vertical curves.

The sight line is a straight line whose equation is:

$$\frac{z - z_1}{x - x_1} = \frac{z_2 - z_1}{x_2 - x_1} \tag{4.33}$$

where (x_1, z_1) and (x_2, z_2) are the coordinates of any two points on the sight line and will be taken in this research as its beginning and end, respectively.

The previous equation can be simplified as:

$$z = c_1 \cdot x + c_2 \tag{4.34}$$

where

$$c_1 = \frac{z_2 - z_1}{x_2 - x_1}$$
$$c_2 = z_1 - c_1 \cdot x_1 \tag{4.35}$$

Tangent segments are also straight lines, and can be represented by Equation 4.33 or 4.34 but with (x_1, z_1) and (x_2, z_2) representing the coordinates of any two points on the segment. However, to distinguish between the equations of the sight line and that of a tangent segment, the la. .t will be written as:

$$z = c_3 \cdot x + c_4 \tag{4.36}$$

It can be noted that since c_3 in Equation 4.36 represents the slope of the line, it can be taken directly as the decimal grade of the segment, $g/100$.

Highway vertical curves are always taken as second degree parabolas. If the coordinate origin is taken at the point of beginning of vertical curve (BVC), the curve equation can be written as:

$$\textit{for a crest curve:} \quad z = \frac{g_1}{100} x - \frac{A}{200 L} x^2$$
$$\textit{for a sag curve:} \quad z = \frac{g_1}{100} x + \frac{A}{200 L} x^2 \tag{4.37}$$

where

g_1 = grade of the first tangent,

A = algebraic difference in grades of the curve, and

L = curve length.

Using an arbitrary origin of the coordinate system so that the coordinates of the BVC are (x_1, z_1), Equation 4.37 can be written as:

$$z = c_5 x^2 + c_6 x + c_7 \tag{4.38}$$

where

$$c_5 = -\frac{A}{200 L} \quad (\textit{crest curve})$$
$$c_5 = +\frac{A}{200 L} \quad (\textit{sag curve}) \tag{4.39}$$

$$c_6 = \frac{g_1}{100} - 2 c_5 x_1 \tag{4.40}$$

$$c_7 = z_1 - \frac{g_1}{100} x_1 + c_5 x_1^2 \tag{4.41}$$

Intersection with Sight Line. As will be shown later, determining the point(s) of intersection between the sight line and the vertical alignment elements is a key step in the procedure developed for determining the available sight distance. If the element

considered is a tangent segment, it can have only one point of intersection with the sight line. Solving Equations 4.34 and 4.36, the X-coordinate of the point of intersection , x_i can be written as:

$$x_i = \frac{c_4 - c_2}{c_1 - c_3} \qquad (c_1 \neq c_3) \tag{4.42}$$

It should be noted that if $c_1 = c_3$, the two lines are either parallel or coinciding. In either case, this specific segment does not obstruct the sight line.

If the element is a curve, it can nave two points of intersection with the sight line. Solving Equations 4.34 and 4.38, these points can be determined as:

$$x_i = \frac{(c_1 - c_6) \pm \sqrt{M}}{2\, c_5} \qquad (M \geq 0) \tag{4.43}$$

where

$$M = (c_6 - c_1)^2 - 4\, c_5\, (c_7 - c_2) \tag{4.44}$$

However, the sign of M should be checked first before applying Equation 4.43. If $M < 0$, there are two *imaginary* points of intersection; i.e., the curve does not intersect with the sight line. If $M > 0$, there are two real points of intersection whose X-coordinates can be determined using Equation 4.43. Finally, if $M = 0$, the two points of intersection will coincide and represent a single point of tangency. This last case is the limiting condition for the sight distance and occurs on crest vertical curves only.

4.3.2 Road as Sight Obstruction

As stated previously, the road itself may obstruct the sight line if the latter should pass over a crest curve. As shown in Figure 4.7, for such obstruction to happen, there must be at least two points of intersection between the sight line and the highway segments within the limits of the sight line. Although the road cannot obstruct the sight line unless there is a crest curve, the points of intersection may be on the crest curve, a sag curve, or a tangent segment. The procedure developed in this research to determine the available sight distance is carried out assuming an initial value for the sight distance, S. Then, any existing intersection between the highway segments and the sight line is checked, and S is increased or decreased until the sight line becomes a tangent to a crest curve. The following steps explain how the procedure can be carried out.

1. Determine the coordinates of the beginning of the sight line, (x_1, z_1).
2. Determine the coordinates of the end of the sight line, (x_2, z_2).
3. Establish the equation of the sight line as in Equation 4.34.

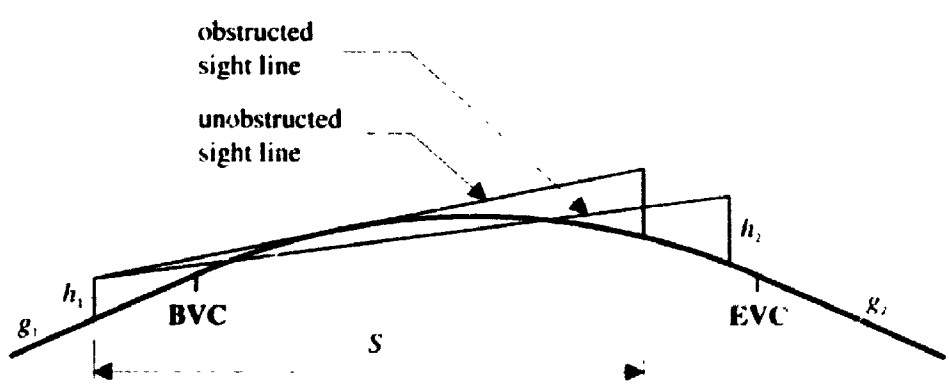

FIGURE 4.7: Sight Distance Limited by Crest Vertical Curve.

4. Check the existence of any point of intersection between the sight line and all the highway segments between the beginning and end of the sight line.
5. If ANY segment intersects with the sight line within the segment limits, S is greater than the actual sight distance. Decrease S and repeat steps 2-4.
6. If NO segment intersects with the sight line within the segment limits, S is less than the actual sight distance. Increase S and repeat steps 2-4.
7. If the sight line is tangent to a crest curve, S is equal to the actual sight distance. End of iterations.

4.3.3 Sight-Hidden Dips

As shown in Figure 4.8, sight-hidden dips may exist if a crest curve is followed by a sag curve (with or without an intermediate tangent segment). Using the model developed by Easa (1994*b*), the existence of the sight-hidden dips can be checked and its length can be determined. However, a simple iterative procedure, easily programmable, is presented here to check the existence of a sight-hidden dip and to determine the available sight distance in such cases. This procedure should follow the determination of the

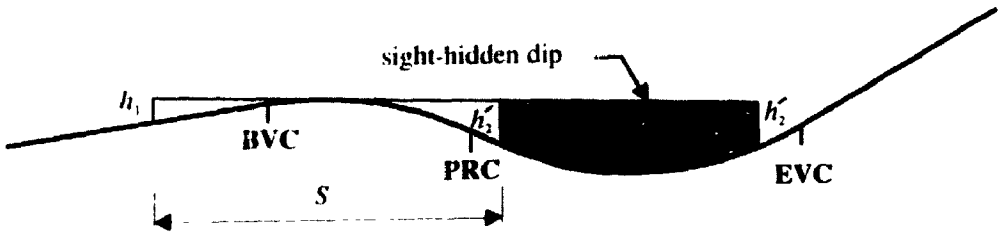

FIGURE 4.8: Development of Sight-Hidden Dips.

farthest point seen by the driver as explained in the previous section. The procedure involves the following steps:

1. Determine the unobstructed sight distance, S, as explained previously.
2. Establish the equation of the sight line as in Equation 4.34.
3. For a number of points between the two limits of the sight line and taken at a fine step, determine the vertical clearance between the sight line and the highway surface. The clearance at a certain point can be obtained as the elevation obtained from Equation 4.34 minus that obtained from Equation 4.36 or 4.38, depending on the segment type.
4. Determine the maximum clearance, z_h, and the station at this point, x_h.
5. If $z_h \leq h_2$, NO sight-hidden dip exists. End of procedure.
6. If $z_h > h_2$, check the existence of any point of intersection between a sight line from the driver eye to an object at x_h and the different highway segments.
7. If there is NO point of intersection, no sight-hidden dip exists. End of procedure.
8. If there is ANY point of intersection, a sight-hidden dip exists. Take $S = x_h - x_1$ and repeat the procedure in Section 4.3.2.

It should be noted that if a sight hidden dip is detected, the height of the object may be reduced by a factor called the visibility factor, f_v. The use of this factor was recommended by Easa (1994*b*). The object height used in this case will be, $h_2' = (1 - f_v)\, h_2$, where $f_v = 0.1$ to 0.3.

4.3.4 Overpasses as Sight Obstructions

As shown in Figure 4.9, the existence of overpasses on sag curves may obstruct the sight line. To check the existence of such an obstruction, the elevation of the sight line at the station of the overpass is compared to the elevation of the lowest point in the overpass. If the elevation of the sight line is higher than that of the overpass, an obstruction exists. S should be reduced and another iteration is performed until the elevation of the sight line is lower than that of the overpass. However, it should be noted that the sight line in this case should be taken as the line connecting the driver's eye to the minimum height required for the object to be detected, h_{min}. Although this height may be theoretically set as zero, it is preferred to be of a certain minimum height. In determining the available PSD, and because drivers use the headlight of the opposing vehicles to detect them at night, it is recommended here to take this minimum height as the height of the headlight. Finally, if the overpass is relatively wide, the sight line may be obstructed by the two bottom edges of the overpass. In this case, the obstruction should be modelled by two points over the highway profile.

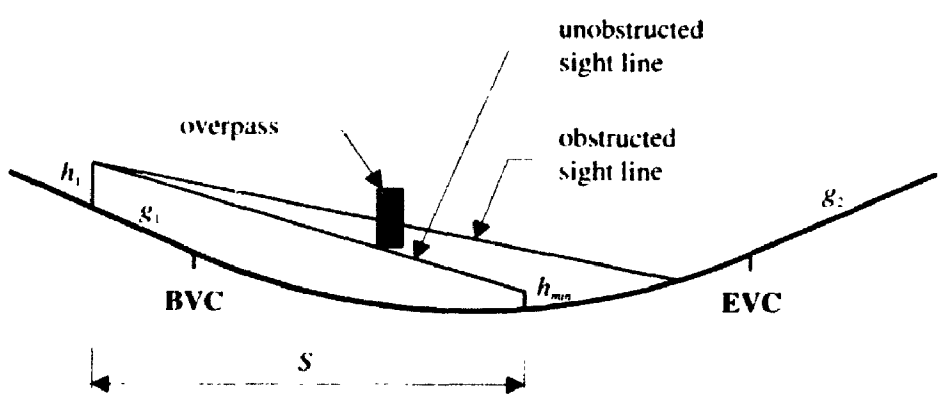

FIGURE 4.9: Sight Distance Limited by Overpass on Sag Vertical Curve.

4.4 Unified Methodology for Separate Horizontal and Vertical Alignments

In the models presented above, each type of sight obstructions is dealt with in a unique way, and thus, computer programming is not an easy task. Also, in dealing with continuous obstructions on horizontal alignments, the lane width has to be constant. As a result, lane widening could not be considered. In addition, spline grades in vertical alignments, where the alignment is given as stations and elevations, do not have an explicit mathematical equation and cannot be modelled. More importantly, it is extremely difficult to extend these models to 3-D combined alignments. In this section an analytical model that can deal with separate 2-D alignments and can overcome these disadvantages is presented. The model is an application of the finite element method where sight obstructions are modelled using finite elements, and the intersection between the sight line and these elements is checked to determine the available sight distance.

In the following sections, a background for the parametric elements in 2-D alignments, upon which the model is based, will be presented. Then, the model itself will be explained. It should be noted that the coordinates of any point will be referred to as (x, y) which represent the east and north coordinates of the point (in horizontal alignments) or the station and elevation of the point (in vertical alignments). The reference point can be anywhere because the sight distance is governed by the relative, not the absolute, positioning of the points.

4.4.1 Background to Parametric Elements

The model developed here depends on the characteristics of the parametric elements which have been used in the structural analysis using the finite element method since the 1960's (Cook et al, 1989; Zienkiewicz and Taylor, 1991). The basic idea in using the parametric elements is to transform distorted straight or curved lines (in a global coordinate system, X-Y) to regular one-dimensional straight lines (in a local coordinate system, η) using a number of points with known coordinates (*nodes*). The coordinates of any point within the element can be interpolated among the nodes using interpolation functions. These functions along with a specific number of nodes can define a unique element geometry (shape), and therefore they are referred to as *shape functions*. The interpolation in 2-D can be expressed as:

$$
\begin{aligned}
x &= \sum_{i=1}^{n} N_i \, x_i \\
y &= \sum_{i=1}^{n} N_i \, y_i
\end{aligned}
\tag{4.45}
$$

where

n = total number of element nodes,

x, y = global cartesian coordinates of any point,

x_i , y_i = global cartesian coordinates of node i, and

N_i = shape function of node i.

The shape functions, N_i , for an element with a specific number of nodes can be obtained by Gauss interpolation. For example, referring to Figure 4.10, for a 2-node

element with its nodes at the local coordinates η of -1 and +1, respectively, the shape functions will be:

$$N_1 = \frac{1}{2}(-\eta + 1)$$
$$N_2 = \frac{1}{2}(\eta + 1) \tag{4.46}$$

Similarly, the 3-node element shown in Figure 4.10 (with its nodes at the local coordinates η of -1, 0, and +1, respectively) will have shape functions as follows:

$$N_1 = \frac{1}{2}(\eta^2 - \eta)$$
$$N_2 = -(\eta^2 - 1) \tag{4.47}$$
$$N_3 = \frac{1}{2}(\eta^2 + \eta)$$

As shown in Equation 4.46, the shape functions of the 2-node element are linear. As a result, applying Equation 4.45 to calculate the coordinates of any point in the element will represent a linear interpolation between the two nodes. This element can exactly model straight lines only, and is referred to here as the *linear element*. On the other hand, the shape functions of the 3-node element are quadratic functions, and therefore such an element can model exactly second-degree parabolic curves. This element is referred to as the *quadratic element*. Also, higher order elements with higher number of nodes can be used to model higher degree curves.

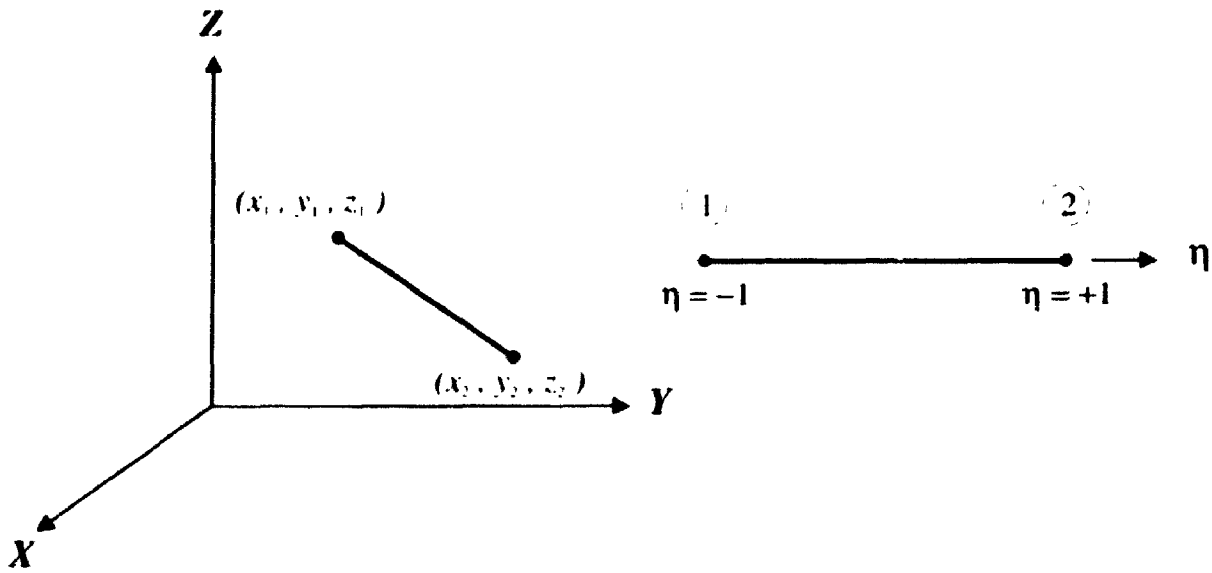

(a) 2-Node Linear Element.

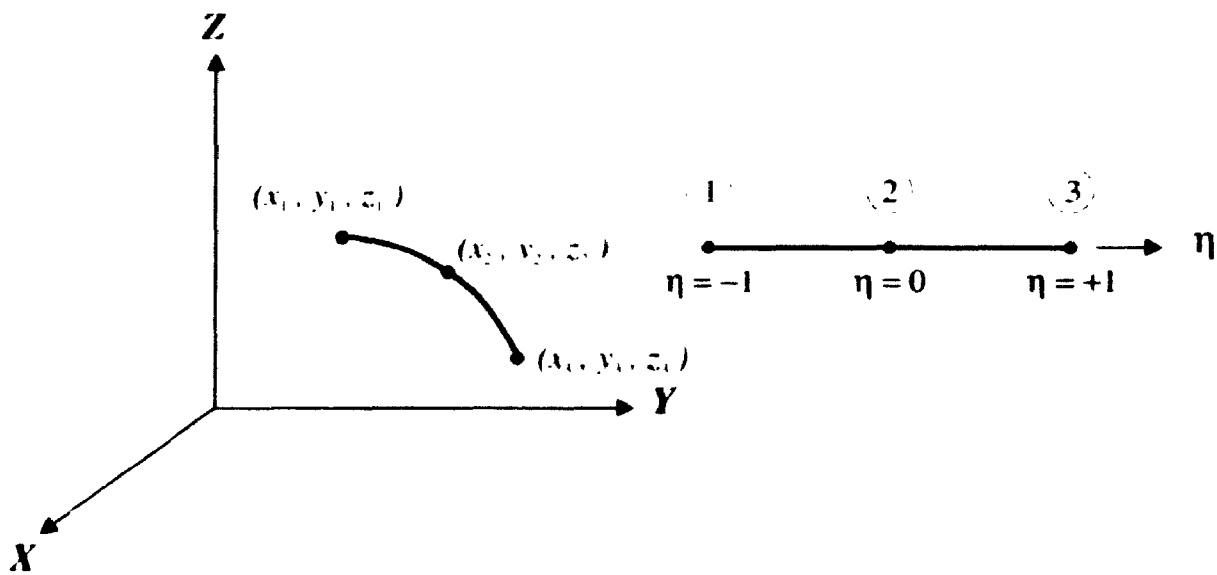

(b) 3-Node Quadratic Element.

FIGURE 4.10: Parametric Elements for 2-D Horizontal and Vertical Alignments.

4.4.2 Alignment Idealization

According to this model, sight obstructions in horizontal and vertical alignments are idealized into a series of parametric elements. The elements which can be used for each sight obstruction are as follows:

Horizontal Alignment. As shown in Figure 4.11, the different types of sight obstructions modelled in horizontal alignments are:

1. Continuous obstructions on straight segments (tangents) are straight lines, and therefore they are exactly modelled using linear elements.
2. Although the equation of horizontal spiral curves is an infinite series, it is usually approximated to a second degree equation only. Therefore, continuous obstructions parallel to spiral curves are modelled using quadratic elements. However, the smaller the element size, the higher the modelling accuracy. Therefore, the elements used to model continuous obstructions on spiral curves will be referred to as short quadratic elements.
3. Circular curves are not parabolic, and therefore cannot be exactly modelled using the quadratic element. However, since they are second degree curves, they can be reasonably modelled using short quadratic elements. Generally, the smaller the element size the higher the accuracy and the more the time required to determine the available sight distance. Although more accurate modelling can be achieved by increasing the number of nodes in the element, such elements are not used here because of the difficulty expected in using such elements in 3-D analysis. As a

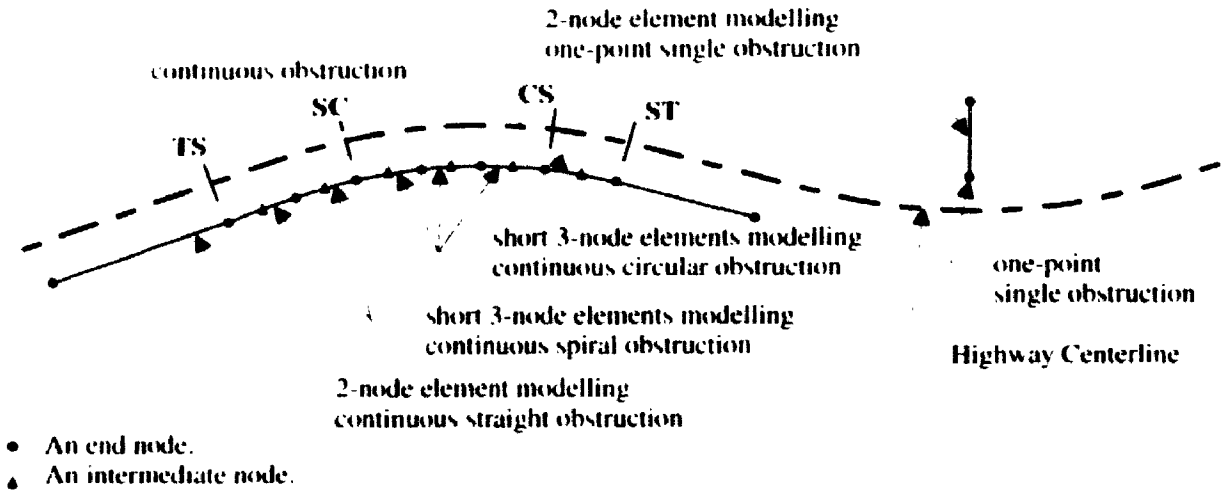

(a) Continuous and One-Point Single Obstructions.

(b) Two-Point Obstruction

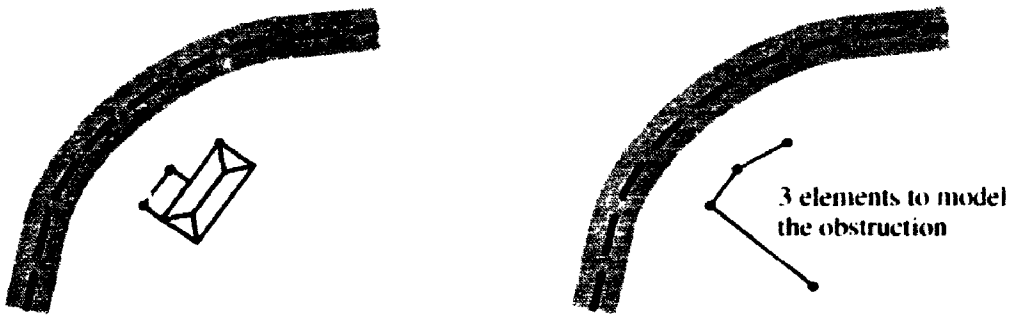

(c) Three-Point Obstruction

FIGURE 4.11: Idealization of Horizontal Alignment.

result, continuous obstructions parallel to circular curves are modelled using a number of short quadratic elements.

4. Single obstructions, although defined by a single point, are represented by a linear element. The first node of the element is the point defining the obstruction while the element extends away from the highway. Sometimes, the obstruction has considerably large dimensions and cannot be modelled properly as a single point but rather with two or three points. In this case, a number of elements should be used as shown in Figure 4.11*b* and *c*.

Vertical Alignment. As shown in Figure 4.12, the different types of sight obstructions modelled in vertical alignments are:

1. Straight segments (slopes) are straight line, and therefore they are exactly modelled using linear elements.
2. Vertical curves are parabolic curves, and therefore, they are exactly modelled using a quadratic element for each curve, regardless of its length. These elements will be referred to as long quadratic elements.
3. In some cases, vertical curves are not perfect parabolas but rather spline grades defined by the station and elevation of a number of points on the curve. This type of curvature does not have an explicit mathematical formula and cannot be considered in the model presented in Section 4.3. However, in using the parametric elements, spline grades can be modelled using short quadratic elements similar to horizontal curves.

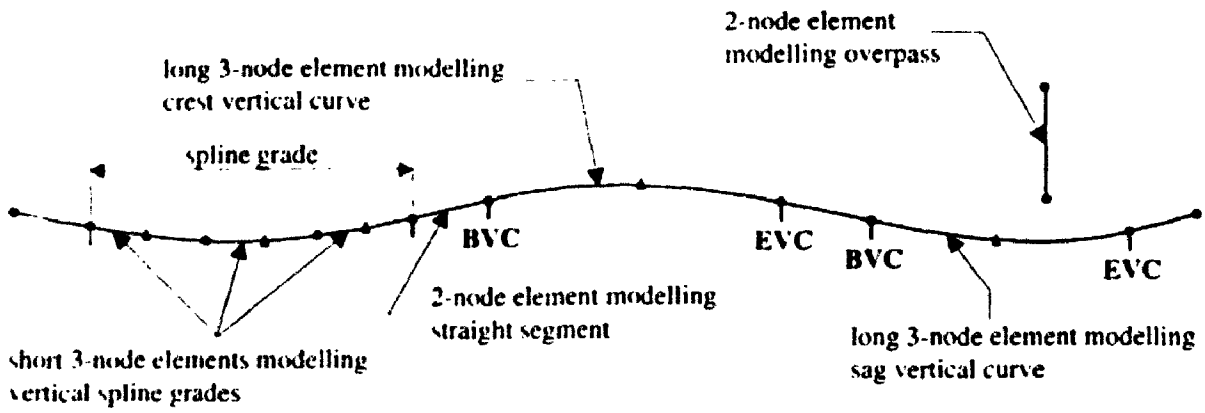

- An end node.
- An intermediate node.

FIGURE 4.12: Idealization of Vertical Alignment.

4. Overpasses are modelled similar to the single obstructions in horizontal alignments. This is by using a linear element with the first node at the lowest point of the overpass, and the element extends up. As mentioned previously, if the overpass is relatively wide, two consecutive elements, at the limits of the overpass, should be used in modelling the obstruction.

4.4.3 Intersection Between Sight Line and Parametric Elements

As will be explained later, the model depends mainly on the intersection between the sight line and the highway elements, mapped into linear and quadratic parametric elements. In this section, (x_{s1}, y_{s1}) and (x_{s2}, y_{s2}) refer to the cartesian coordinates of any two points on the sight line. Usually, these two points are taken as its beginning and end. Similarly, (x_i, y_i) refer to the cartesian coordinates of node i. The parameter a_i refers to

a constant defined at node i while the parameters τ and c refer to unique constants in the equation.

In a 2-D alignment, the equation of the sight line is:

$$\frac{x - x_{s1}}{y - y_{s1}} = \frac{x_{s2} - x_{s1}}{y_{s2} - y_{s1}} \qquad (y_{s1} \neq y_{s2}) \qquad (4.48)$$

or

$$x - S_{xy}\, y + (S_{xy}\, y_{s1} - x_{s1}) = 0 \qquad (y_{s1} \neq y_{s2}) \qquad (4.49)$$

where

$$S_{xy} = (x_{s2} - x_{s1})/(y_{s2} - y_{s1})$$

If $y_{s1} = y_{s2} = y_s$, the equation of the sight line becomes:

$$y - y_s = 0 \qquad (y_{s1} = y_{s2} = y_s) \qquad (4.50)$$

Since the point(s) of intersection between the sight line and the element must satisfy the equations of both, then

$$\sum N_i\, a_i + \tau = 0 \qquad (4.51)$$

where

$$a_i = x_i - S_{xy}\, y_i \qquad (y_{s1} \neq y_{s2})$$

$$a_i = y_i \qquad (y_{s1} = y_{s2})$$

$$\tau = -x_{s1} + S_{xy}\, y_{s1} \qquad (y_{s1} \neq y_{s2})$$

$$\tau = -y_s \qquad (y_{s1} = y_{s2})$$

Equation 4.51 represents a polynomial in one variable, η, which can be obtained by substituting for the values of N_i as shown in Equations 4.46 and 4.47. For a linear element, Equation 4.51 can be written in terms of η as follows:

$$c_1 \eta + c_2 = 0 \tag{4.52}$$

where

$$c_1 = -a_1 + a_2$$

$$c_2 = a_1 + a_2 + 2\tau$$

The solution of Equation 4.52 may produce:

1. No solution, if the equation is trivial ($c_1 = c_2 = 0$). This case can happen only if the sight line is parallel to or coincident with the linear element. As a result, no sight obstruction exists.
2. One real root, $\eta = -c_2/c_1$. In this case, one point of intersection exists whose cartesian coordinates can be calculated using Equation 4.45.

If the element considered is quadratic, Equation 4.51 can be written in terms of η as follows:

$$c_1 \eta^2 + c_2 \eta + c_3 = 0 \tag{4.53}$$

where

$$c_1 = a_1 - 2a_2 + a_3$$

$$c_2 = -a_1 + a_3$$

$$c_3 = 2a_2 + 2\tau$$

The solution of Equation 4.53 may produce:

1. No solution, if the equation is trivial ($c_1 = c_2 = c_3 = 0$). No sight obstruction exists.
2. Two imaginary roots, if $c_2^2 - 4\, c_1\, c_3 < 0$. This case also represents no intersection.
3. One real root, if $c_1 = 0$ and $c_2 \neq 0$. In this case, one point of intersection exists whose cartesian coordinates can be calculated using Equation 4.45.
4. Two different real roots, if $c_2^2 - 4\, c_1\, c_3 > 0$. In this case, two points of intersection exist, and their cartesian coordinates can be calculated using Equation 4.45.
5. Two identical real roots, if $c_2^2 - 4\, c_1\, c_3 = 0$. In this case, the two points of intersection coincide and represent one point of tangency. The cartesian coordinates of this point can be calculated using Equation 4.45.

4.4.4 Iterative Procedure for Available Sight Distance

Based on the mathematical formulation presented above, an iterative procedure has been developed to determine the available sight distance on any horizontal or vertical alignment. In this procedure, the sight distance is initially assumed as S, and then S is decreased or increased until the sight line becomes tangent to an element representing a sight obstruction. The following steps summarize the procedure:

1. Idealize the sight obstructions to a series of elements as explained previously.
2. Determine the coordinates of the beginning of the sight line.
3. Determine the coordinates of the end of the sight line.
4. Check the intersection between the sight line and the elements which are used to idealize the sight obstructions. The point of intersection which represents a sight

obstruction must be within the limits of both the sight line and the element. A point is within the limits of the element, linear or quadratic, if its local coordinate satisfies the condition: $-1 \leq \eta \leq +1$. A point is within the limits of the sight line if the length of the sight line equals the length of the two lines connecting the point and the two extremes of the sight line (the beginning and the end).

5. If the sight line intersects with any element, S is greater than the available sight distance. Decrease S and repeat steps 3 and 4.
6. If the sight line does not intersect with any element, S is less than the available sight distance. Increase S and repeat steps 3 and 4.
7. If the sight line is tangent to any element, S is equal to the available sight distance. End of iterations.

4.5 Software for Marking No-Passing Zones

4.5.1 Description of Developed Software

The theoretical procedures, presented in Sections 4.1-4.3, have been translated into two computer programs, *MARKH* and *MARKV*, written in Microsoft QuickBasic. The two programs can determine the profile of available passing sight distance, and in turn no-passing zones, on two lane highways due to separate horizontal and vertical alignments, respectively.

The software *MARKH* uses the MUTCD (1995) standards for no-passing zones which are used by the Ministry of Transportation of Ontario (MTO). For horizontal alignments, the sight line of a driver on the inside lane, the lane nearer to the centre(s)

of the curve(s), is limited by the edge of a theoretical shoulder of 3-m width. The sight line of a driver on the outside lane can cross the right-of-way and is limited only by any existing lateral obstruction (single or continuous). In both cases, the sight distance is measured along the centerline of the lane. Therefore, for the inside lane, the software determines the available sight distance due to the theoretical 3 m-width shoulder specified by the MUTCD. For the outside lane, the software determines the available sight distance due to user specified obstructions. In the case of the existence of more than one obstruction, the software will check the available sight distance against each obstruction and determine the minimum available sight distance.

For vertical alignments, although the MUTCD has set the values of both h_1 and h_2 as 1.05 m and has not mentioned using h_{min} or f_v, the software *MARKV* adopts these heights as parameters entered by the user. This would provide higher degree of flexibility in determining S_{av} according to any other specifications, or if any modifications are adopted in the MUTCD specifications. It should also be noted that the adoption of 1.05 m height for both the driver eye and the object in the MUTCD is set basically to mark the two lanes at the same time and to reduce the amount of work. Such a problem is not experienced in using *MARKV*.

For both programs, the user specifies the minimum sight distance, S_m, required to be checked. If the available sight distance is less than S_m, each of the two programs determines the available sight distance, S_{av}, at every user-specified step, STEP, and for a user-specified accuracy, ACC. Otherwise, the current station will be skipped and the available sight distance at the next station will be checked.

In addition to *MARKH* and *MARKV*, another computer software, *MARKS*, has also been developed based on the methodology presented in Section 4.4. The software determines the profile of available sight distance similar to *MARKH* and *MARKV*. However, it has a number of additional features which are: (1) it is a single software that can deal with 2-D horizontal or vertical alignments, (2) it can consider variable lane width on horizontal alignment and spline grades on vertical alignments, and (3) it can create the lateral continuous obstruction in horizontal alignments based on the data of the side-slopes. It should be noted that this last feature could not be included in *MARKH* because of the limitation of constant lateral clearance which is not applicable for *MARKS*.

4.5.2 Software Verification

The developed procedures and software were verified by comparing the results obtained by the software with those obtained graphically using numerical examples having different alignments. The parameters specified for the software were as follows: S_m = 250 m, STEP = 20 m, and ACC = 0.1 m. The actual available sight distances were determined by drawing the same curves using Autocad. Then, for horizontal alignments, the available sight distances on the inside lane were determined by drawing sight lines tangent to the theoretical shoulder. On the outside lane, the sight lines were drawn passing through certain obstructions input to the software. For vertical alignments, the available sight distances were determined graphically considering the existing crest vertical curves and assuming certain locations for the overpasses on sag vertical curves.

The alignments used in the verification and samples for the input files and the output results are given in the reports published by the Transportation Research Centre, Lakehead University (Hassan et al, 1994*a* and 1994*b*). Figure 4.13 shows an example for the horizontal and vertical alignments that were used in the verification. Also, a sample of the results calculated by the computer programs and those measured graphically is shown in Table 4.1. The results obtained by the programs for all cases were in excellent agreement with those obtained graphically.

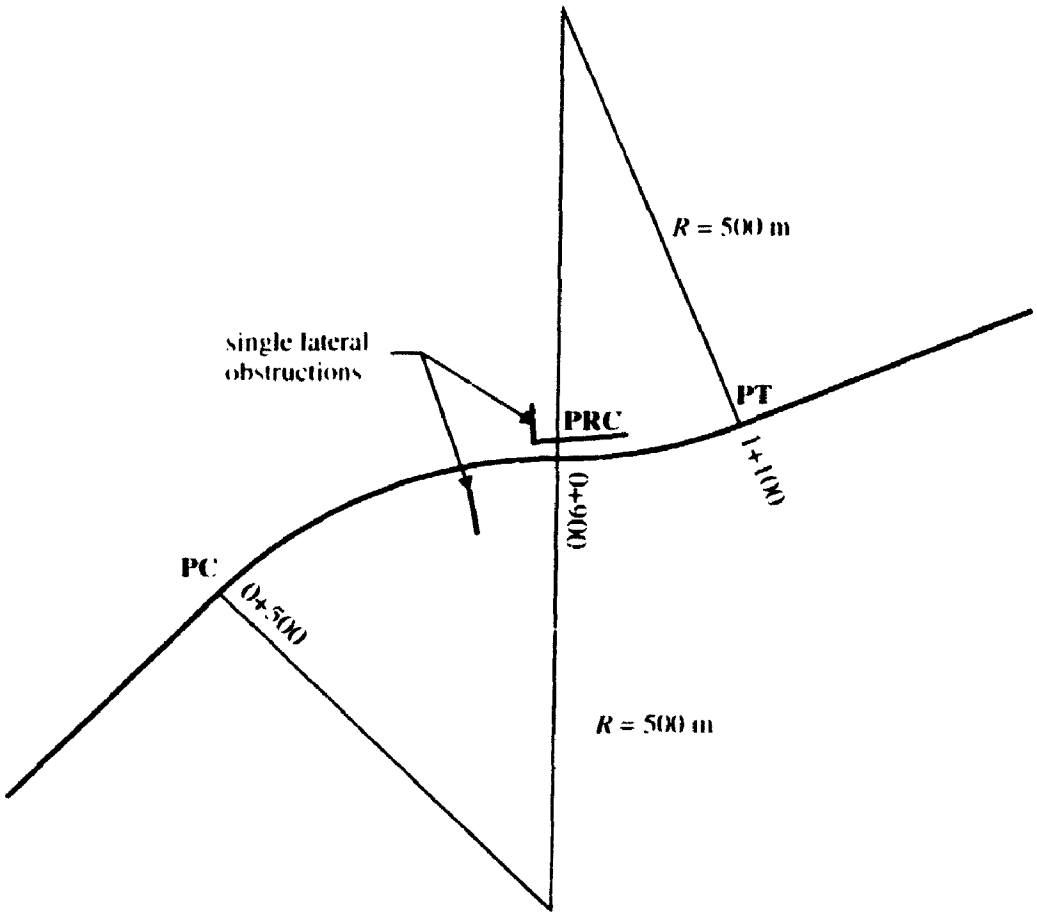

(a) Horizontal Alignment.

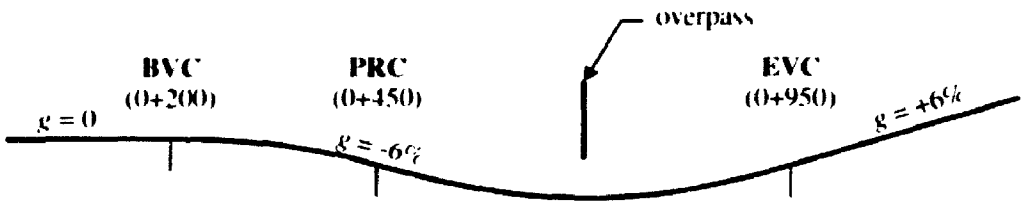

(b) Vertical Alignment.

FIGURE 4.13: Example of 2-D Verification Alignments.

TABLE 4.1: Sample of Measured and Calculated Values of 2-D Available Sight Distance.[a]

2-D Horizontal Alignment[b]					2-D Vertical Alignment[c]		
Station	S_{av} (m)[d]		S_{av} (m)[e]		Station	S_{av} (m)	
	Calculated	Measured	Calculated	Measured		Calculated	Measured
0+100	474.9	474.9	-----[f]	-----	0+000	332.5	332.6
0+200	376.9	376.9	-----	-----	0+100	248.7	248.8
0+300	280.6	280.6	-----	-----	0+200	205.3	205.4
0+400	190.5	190.5	415.5	415.5	0+300	-----	-----
0+500	138.1	138.1	323.6	323.6	0+400	425.4	425.5
0+600	138.1	138.1	236.1	236.1	0+500	376.7	376.9
0+700	138.1	138.1	172.9	172.9	0+600	469.2	469.6
0+800	258.9	258.9	286.4	286.4			
0+900	181.5	181.5	213.3	213.3			

[a] Sight distance is given on the right lane (relative to a driver travelling in the direction of increasing stations)
[b] Results of *MARKH* and *MARKS*
[c] Results of *MARKV* and *MARKS*
[d] Case of vertical continuous lateral obstructions at both sides (lateral clearance = 6.5 m)
[e] Case of single lateral obstructions (Figure 4.13)
[f] Sight distance is 500 m or more

CHAPTER 5

AVAILABLE SIGHT DISTANCE ON 3-D COMBINED ALIGNMENTS

This chapter presents an analytical model for determining the available sight distance on 3-D combined horizontal and vertical alignments (Hassan et al, 1996*b*). The model is an extension to the 2-D model presented in Section 4.4 and is based on idealizing the highway surface and sight obstructions into a net of finite elements that can model planar, curved, and warped surfaces. Then, the sight line, which is a straight line between the driver's eye and the object, is checked against all the possible sight obstructions. If any element representing a sight obstruction intersects with the sight line, the sight line is obstructed. Otherwise, it is an unobstructed sight line. The references used here are Cook et al (1989) and Zienkiewicz and Taylor (1991).

5.1 Elements in 3-D Alignment

Generally, two approaches can be adopted in idealizing the highway alignment into a net of elements: using a large number of simple and small size (micro) elements or using a small number of more accurate and large size (macro) elements. Although the mathematical modelling involved in the second approach is more complicated, this approach produces better accuracy and may require less overall run-time due to the smaller number of elements. Therefore, this approach has been adopted in the developed

model. Consequently, the elements that are used to idealize the alignment should be able to represent the geometry of planar, warped, and curved highway segments.

Similar to the 2-D elements, the 3-D elements which can have a relatively complex geometry in the global *X-Y-Z* coordinate system can be represented by a number of points with known coordinates (*nodes*). The coordinates of any point within the element can be interpolated among the nodes using the shape functions as follows:

$$
\begin{aligned}
x &= \sum_{i=1}^{n} N_i \, x_i \\
y &= \sum_{i=1}^{n} N_i \, y_i \\
z &= \sum_{i=1}^{n} N_i \, z_i
\end{aligned}
\tag{5.1}
$$

where

n = total number of element nodes,

x, y, z = global cartesian coordinates of the point,

x_i, y_i, z_i = global cartesian coordinates of node i, and

N_i = shape function of node i.

As explained earlier, because the shape functions in the global cartesian coordinates can be very complex, the original element in the global coordinates (*parent element*) can be transformed to a simpler element (*transformed or parametric element*) in an arbitrary local coordinate system. For example Figure 5.1 shows three parent elements, each has four edges, and the parametric element used for each of them. As

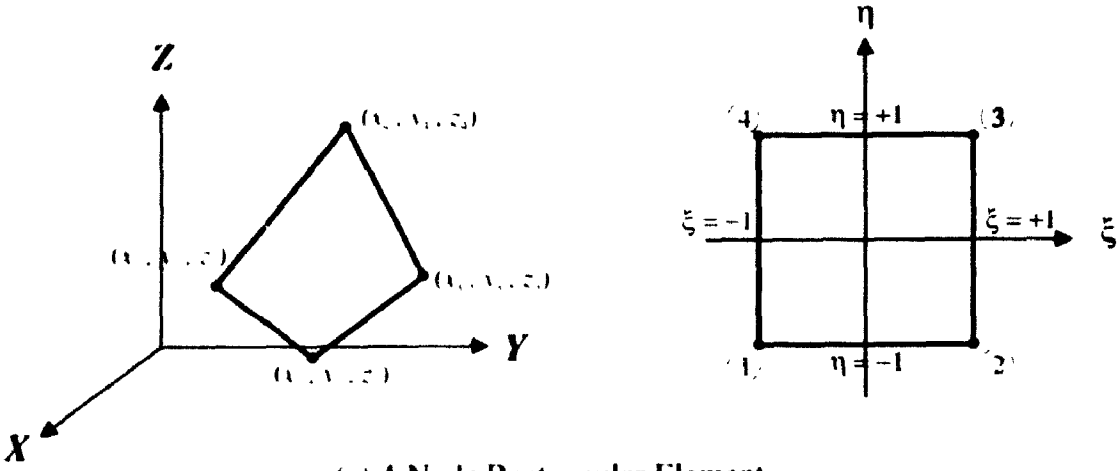

(a) 4-Node Rectangular Element.

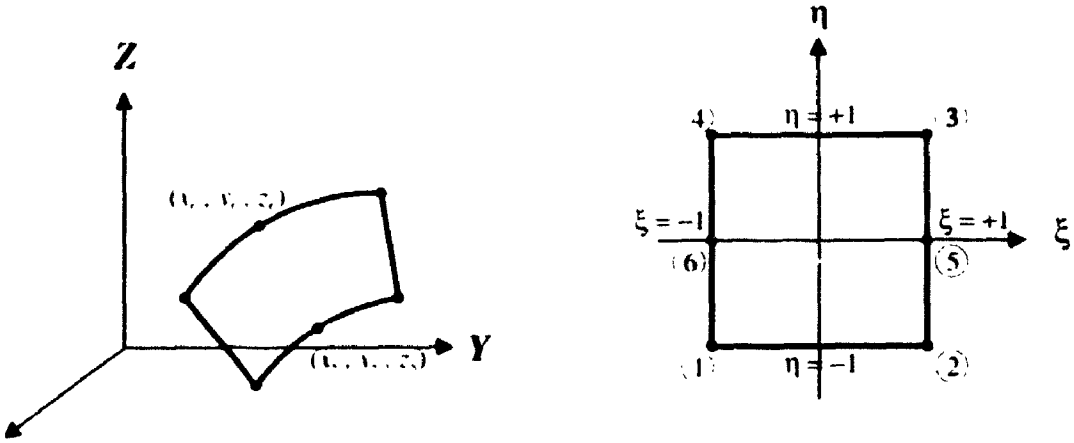

(b) 6-Node Rectangular Element.

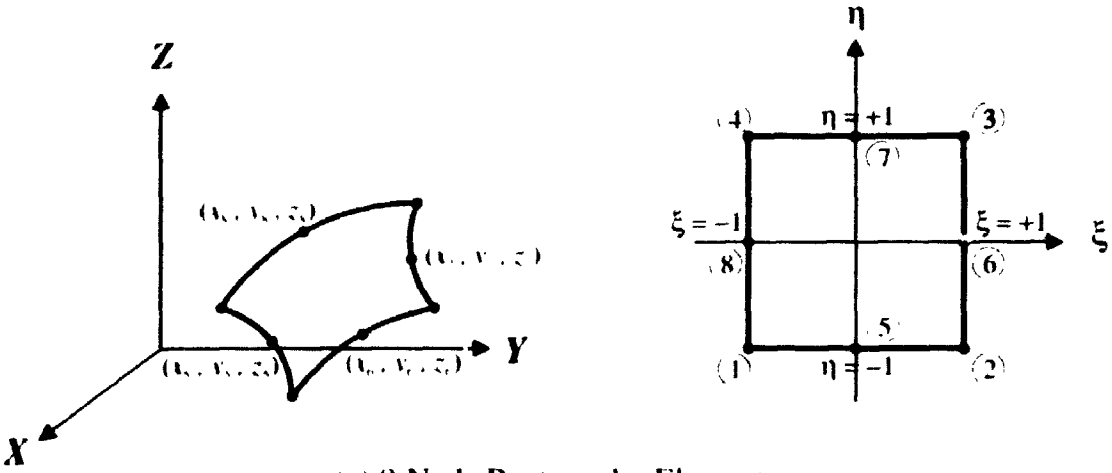

(c) 8-Node Rectangular Element.

FIGURE 5.1: Rectangular Parametric Elements.

shown in the figure, the three parametric elements are rectangles in a local ξ-η coordinate system.

First, the 4-node rectangular element has a node at each corner, and thus there are two nodes on each edge. Subsequently, the interpolation along any edge will be linear. Therefore, the interpolation is expected to be exact if and only if all the element's four edges are straight lines, which is the case for highway segments which have no vertical or horizontal curvature. However, due to the interpolation in two directions, the surface does not have to be planar; instead, it can be warped. Such feature is particularly useful when modelling segments along which the cross-section changes, e.g., straight segments before horizontal curves which are used for the superelevation development.

Second, the 6-node rectangular element has four nodes at its four corners in addition to an extra node at the middle of two parallel edges (parallel to η-axis). Such an arrangement results is two edges that have three nodes each (parallel to η-axis) while the remaining two edges have two nodes each (parallel to ξ-axis). As a result, the interpolation in the η-direction is expected to be quadratic (second degree polynomial) while the interpolation in the ξ-direction is still linear. Since a second degree polynomial (parabola) can be defined by three points, the interpolation in the η-direction will be exact if the edges of the parent element are parabolic. However, because of the linear interpolation in the ξ-direction, the other two edges of the element must be straight lines. Such surfaces can be experienced on highway segments which have horizontal and/or vertical curvature and have non-curved cross-sections.

Finally, the 8-node rectangular element is similar to the 6-node element but has an intermediate node on all edges. Following the same argument, the 8-node element can model surfaces that have four curved edges. Such surfaces can be experienced on highway segments which have horizontal and/or vertical curvature and have curved cross-secti ıs.

In addition to the rectangular elements, triangular elements can also be used. Figure 5.2 shows two types of triangular elements that are transformed into parametric elements in a different local coordinate system. As explained above, since the 3-node element has two nodes along each edge, it can model surfaces with straight edges. However, unlike the 4-node rectangular element, since any three intersecting lines can exist in only one plane, the 3-node triangular element cannot model warped surfaces. As for the 5-node element, it can model surfaces with two curved edges and one straight edge. Similar to the 6-node element, this element can be used on curved segments with non-curved cross-sections. In addition, a 6-node triangular element can be generated from the 5-node element by adding a node at the middle of the third edge. This latter element is similar to the 8-node element and can be used on curved segments with curved cross-sections.

5.2 Alignment Idealization into Parametric Elements

The five different elements presented previously can be used in modelling sight obstructions which consist of the highway surface, lateral obstructions, and overpasses. Although all of these elements can be used, selecting an improper element will reduce

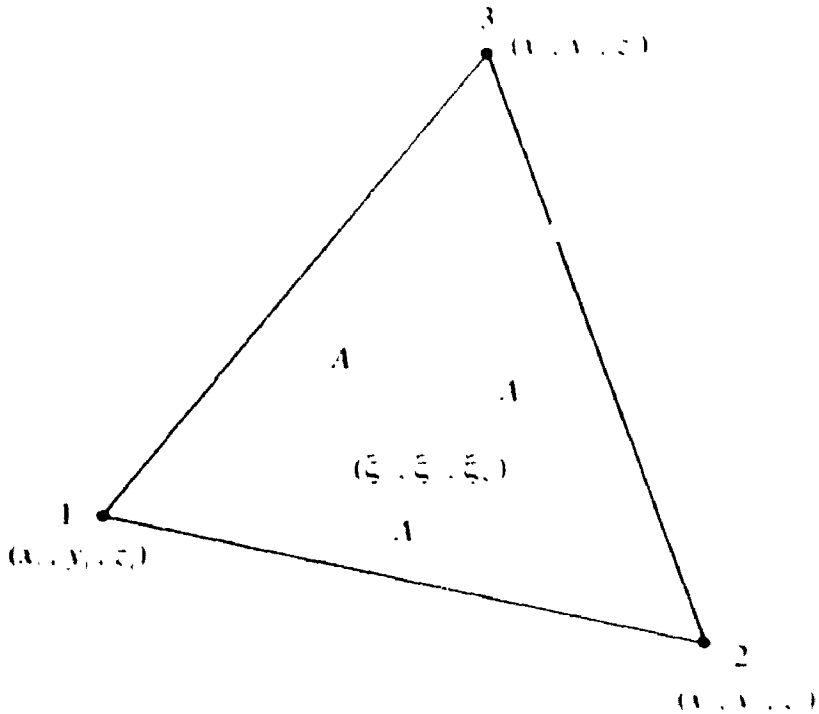

(a) 3-Node Triangular Element.

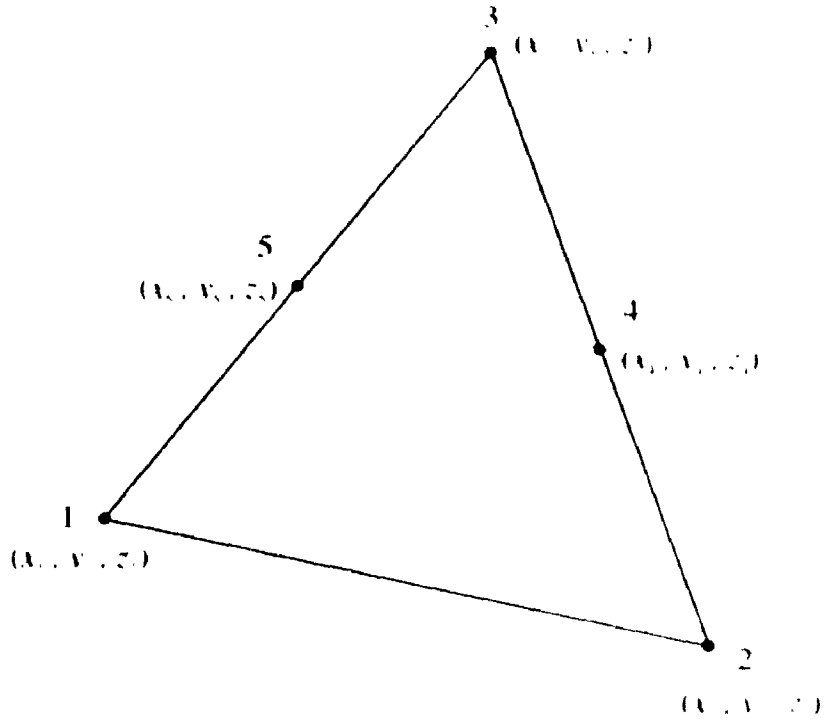

(b) 5-Node Triangular Element.

FIGURE 5.2: Triangular Elements.

the accuracy or increase the complexity of the modelling. Therefore, a good modelling requires a good understanding of the capabilities and limitations of each element.

Surfaces with straight edges can be exactly modelled using the 4-node element where the methodology for the intersection between the sight line and the element is very simple. Therefore, this element can be used to model the highway segments which have no horizontal or vertical curves. Figure 5.3*a* shows how tangent segments are modelled by the 4-node rectangular elements. As shown in the figure, only one element is required along the whole segment. However, because of the breaks in the segment's cross-section, a number of transversally adjacent elements is required so that every breaking edge will represent the edge of two adjacent elements. Although, the 3-node element has a similar capability, the idealization of the highway into a net of rectangles will produce one-half the number of elements required for a net of triangles. Therefore, finding the intersection between the sight line and the rectangular elements will consume almost one-half the time required for triangular elements In addition, the 4-node element can model the warped surface which cannot be modelled by the 3-node element.

As discussed earlier, the 6-node element can model surfaces with two straight edges and two curved edges. Therefore, this element can be used for highway segments with horizontal and/or vertical curves and with non-curved cross-sections. This modelling will be exact if the two curved edges are parabolic, which is the case for curvature due to the vertical alignment. Subsequently, if the curvature is due to a vertical curve only, one element can be used to model the segment regardless of its length. These elements are referred to here as large elements. Figure 5.3*a* shows also

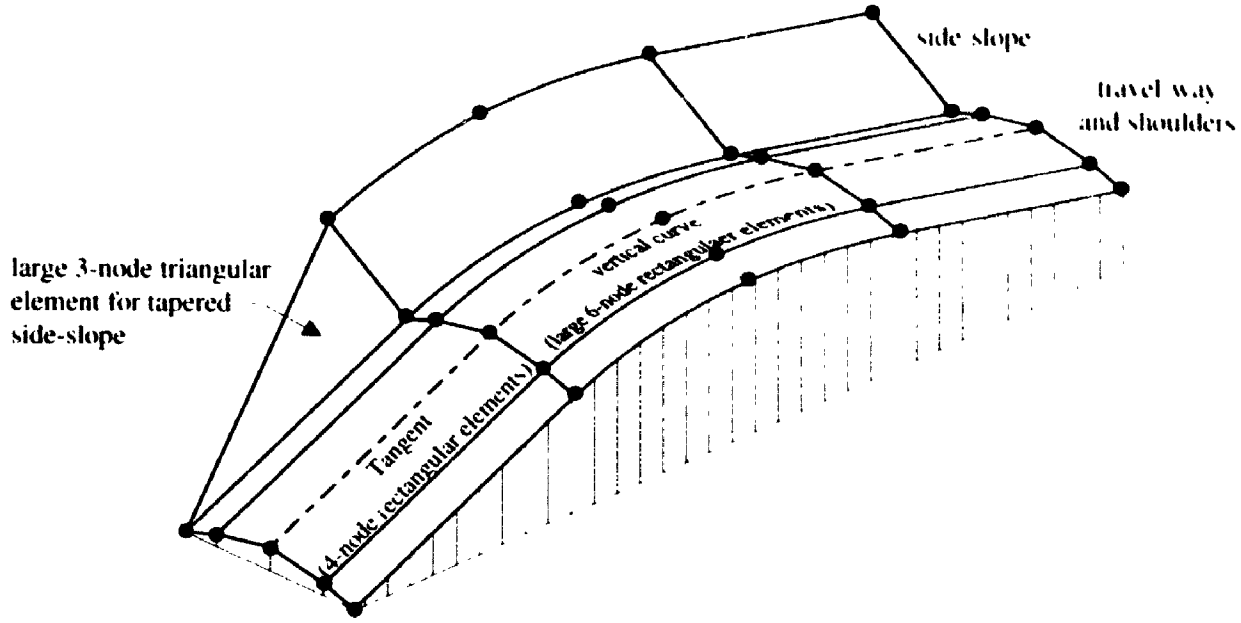

(a) Vertical Curve and Tangent.

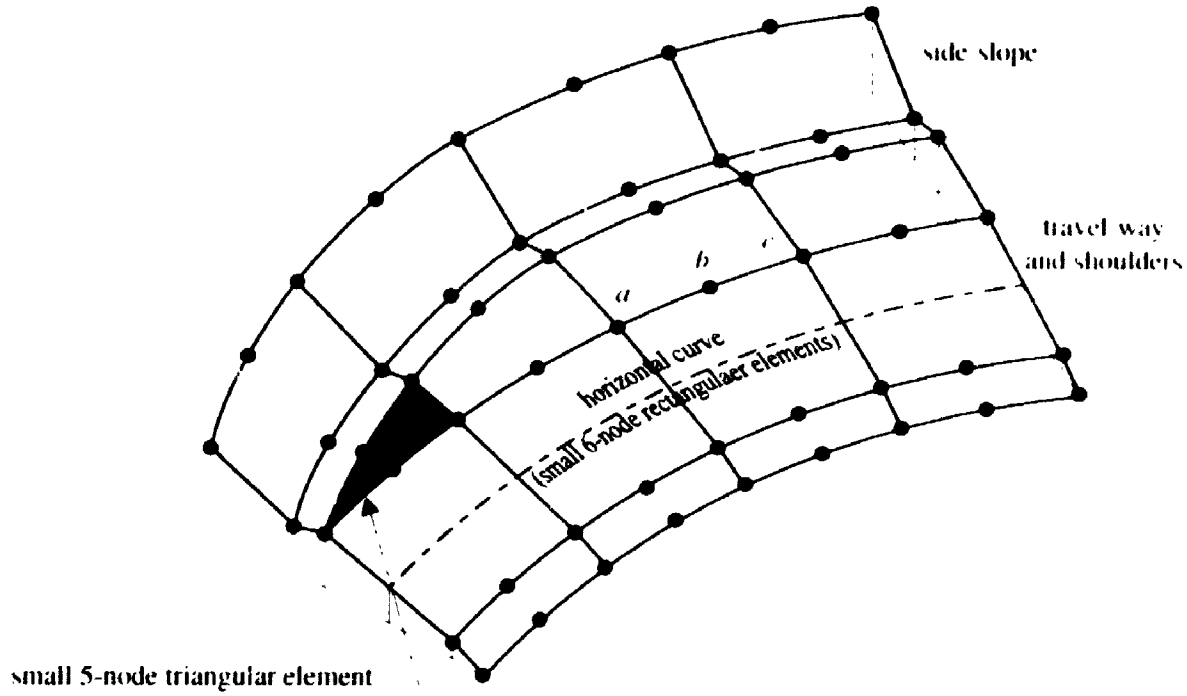

(b) Horizontal Curve.

FIGURE 5.3: Idealization of Tangents, Vertical Curves, and Horizontal Curves into Parametric Elements.

an example of a crest vertical curve modelled by large 6-node rectangular elements. The elements extend longitudinally from the beginning to the end of the curve. However, similar to the tangent segment, a number of transversally adjacent elements is required so that every breaking edge will represent the edge of two adjacent elements. As shown also in the figure, the continuous lateral obstruction, represented by a side-slope, is also modelled by a 4-node or large 6-node rectangular element if it is on a tangent segment or a vertical curve, respectively. In addition to the parabolic vertical curves, the vertical alignment may include spline grades which do not have explicit mathematical formulas. In this case, small 6-node elements should be used. Generally, the smaller the element size, the greater the modelling accuracy.

On the other hand, since the curvature due to the horizontal alignment is circular or spiral, rather than parabolic, the 6-node element can only provide approximate modelling. The accuracy of this approximation will depend on the element size. Generally, the smaller the element size, the greater the accuracy. Therefore, if the curvature involves a horizontal curve (circular or spiral), the curve should be modelled by a series of 6-node rectangular elements referred to here as small elements. Nonetheless, the element size is still larger than what should be used if the curvature is modelled by planar elements. As shown in Figure 5.3*b*, a segment on a horizontal curve (or a continuous lateral obstruction on a horizontal curve) is modelled by a number of small 6-node elements where, for example, the circular arc *ac* is approximated to a parabola (second-degree polynomial) passing through the two ends *a* and *c* and the midpoint *b*. However, it should be noted that in using the 6-node rectangular element

(for vertical or horizontal curves), the cross-section of the highway segment should be linear. If the highway has a parabolic curved cross-section, the 8-node element will be more accurate.

Triangular elements can be beneficial, however, in modelling pavement widening or narrowing when a new lane is added to or removed from the highway. If the extra lane has a cross-slope different from that of the adjacent lane, the widening should be modelled by triangular elements. Triangular elements can also be used in modelling the side-slope, if there is a tapered segment with an increasing (or decreasing) width. As shown in Figure 5.3, a 3-node triangular element should be used if the widening is on a straight segment while a 5-node would be more accurate if the widening is on a horizontal or/and vertical curve with non-curved cross-section. Similar to the rectangular elements, the modelling accuracy will not depend on the element size if it is on a straight segment or a vertical curve, and large elements can be used. If the curvature is due to a horizontal curve, a small element size should be used.

Figure 5.4 shows a highway segment where a part of a horizontal curve coincides with a part of a vertical curve. To idealize this segment into parametric elements, first, 4-node rectangular elements are required for the segment *ab* because it is a tangent segment in both horizontal and vertical alignments. Second, since segment *bc* has a vertical curvature only, large 6-node rectangular elements should be used. Then, small 6-node rectangular elements should be used on segment *cd* (which has horizontal and vertical curvatures) and segment *de* (which has horizontal curvature only). Finally, segment *ef* is modelled by 4-node rectangular elements similar to segment *ab*. If a

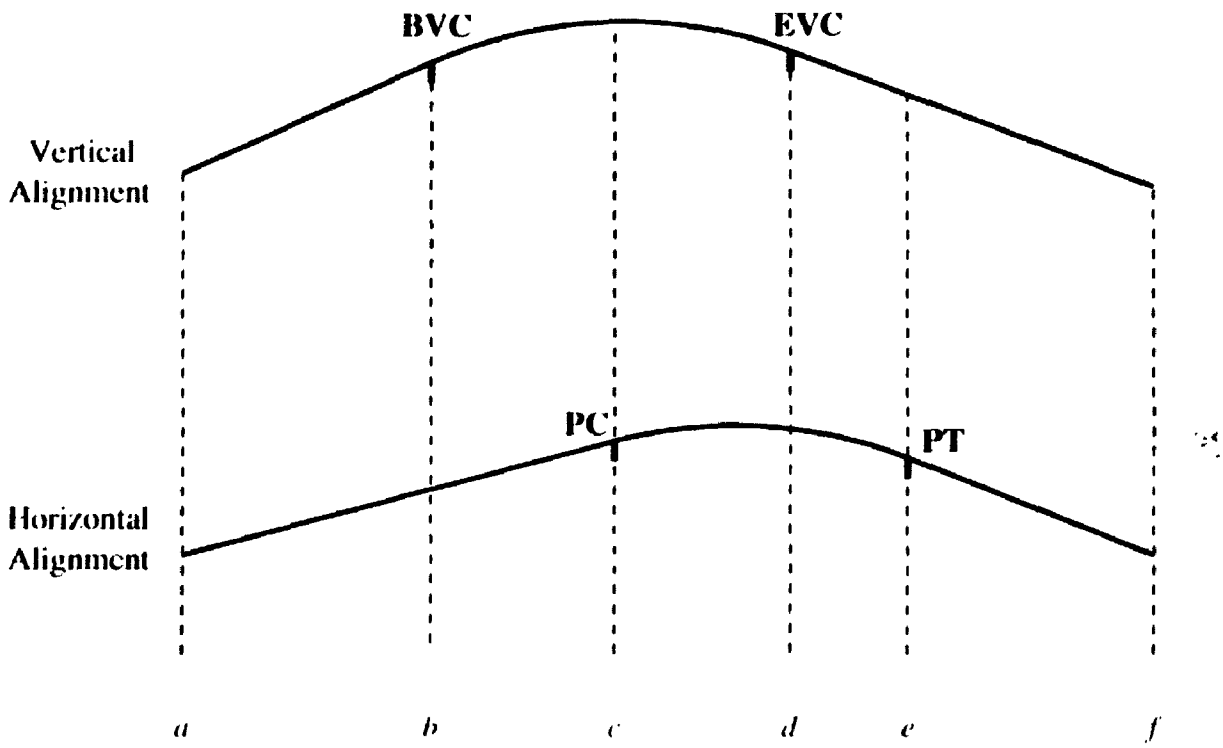

PC = Point of Curve
PT = Point of Tangent
BVC = Beginning of Vertical Curve
EVC = End of Vertical Curve

FIGURE 5.4: Idealization of Combined Vertical and Horizontal Alignment.

tapered element is encountered on segment *ab* or *ef*, a 3-node triangular element would used. On the other hand, a large 5-node element should be used if the tapered element is on segment *bc*. Finally, a small 5-node element should be used if the tapered element is on segment *cd* or *de*.

Single lateral obstructions, which are usually on the inside of a horizontal curve and are represented by a single point in the plan with coordinates (x, y), can be modelled by a 4-node rectangular element. As shown in Figure 5.5*a*, the first edge of this element coincides with the coordinates (x, y) and extends vertically while the element itself extends to the inside of the curve. The element should have vertical and horizontal dimensions large enough to obstruct the sight line if passes beyond the obstruction. In some cases, however, the lateral obstruction cannot be modelled properly using one-point obstruction. Figure 5.6*b* and *c* shows schematic representations for other cases where the obstruction cannot be modelled properly with one-point obstruction. In such cases, a number of elements will be required depending on whether the obstruction can be modelled with two or three points.

Similarly, overpasses on sag vertical curves, with a minimum elevation of z, can be represented by 4-node rectangular elements. As shown in Figure 5.6*a*, the first edge of the element will have an elevation of z and extends from the beginning to the end of the overpass. Then, the element extends vertically to an elevation large enough to obstruct the sight line if lies above the overpass. If the overpass is too wide to be modelled by one vertical element, two successive elements can be used instead. The spacing between the two elements will equal the width of the overpass. In addition to

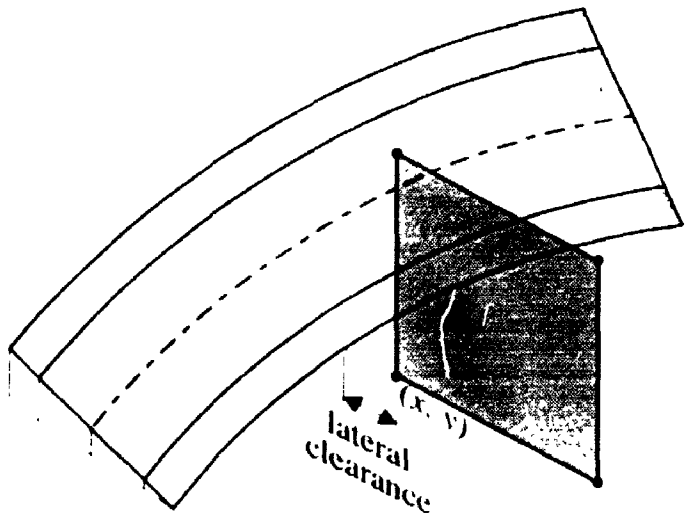

(a) One-Point Single Lateral Obstruction on Horizontal Curve.

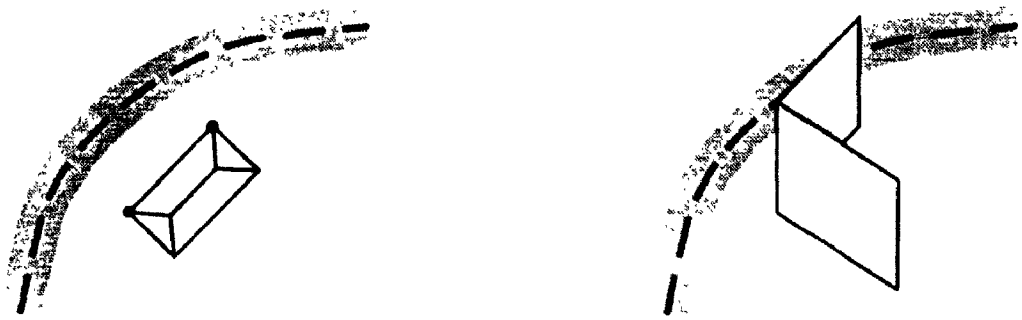

(b) Two-Point Obstruction.

(c) Three-Point Obstruction.

FIGURE 5.5: Lateral Obstructions and Their Representation by 4-Node Elements.

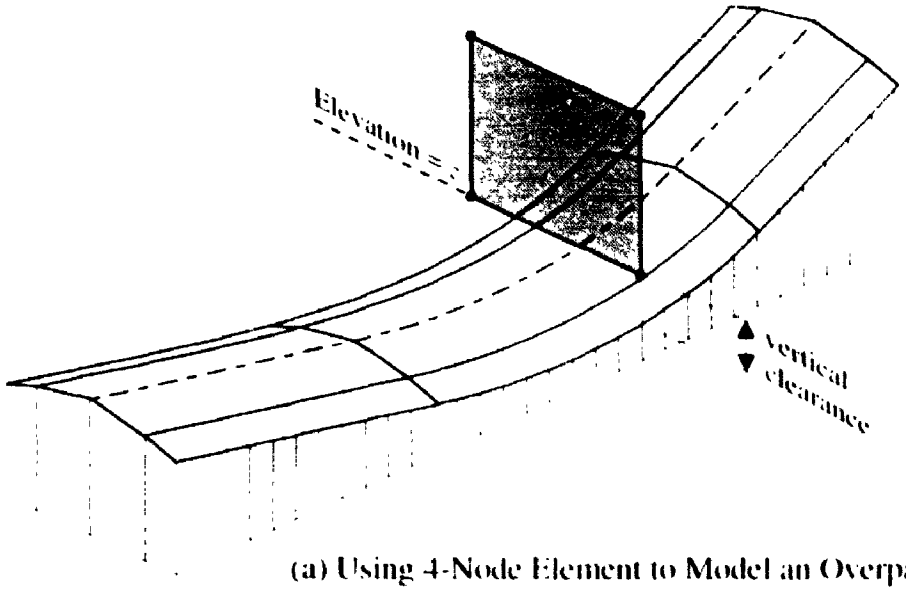

(a) Using 4-Node Element to Model an Overpass.

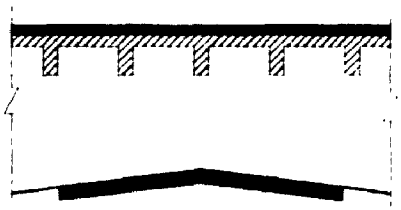

(b) Overpass with Constant Vertical Clearance.

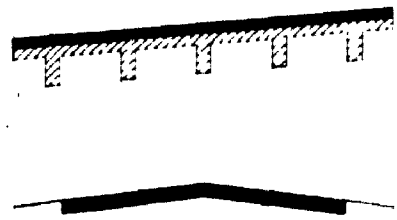

(c) Overpass with Variable Vertical Clearance.

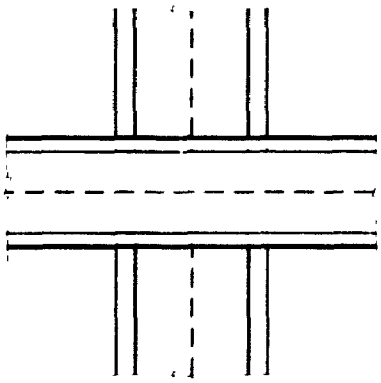

(d) Overpass at Right Angle with the Highway.

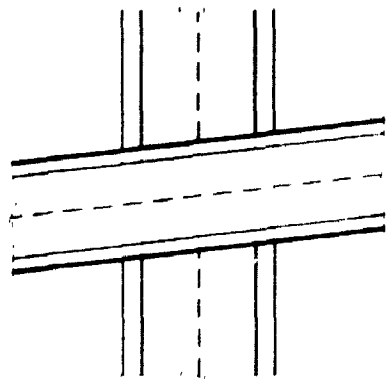

(e) Skewed Overpass.

FIGURE 5.6: Modelling of Overpasses.

the overpass width, a proper positioning of the element nodes enables modelling the different types of overpasses, such as overpass with variable vertical clearance or overpasses at skewed angles with the highway (see Figure 5.6 for illustration).

5.3 Mathematical Modelling

The mathematical modelling required for the developed iterative procedure is based on checking the intersection of the sight line, which is a straight line, and the elements used to model the highway alignment. In this modelling, a global system of *X-Y-Z* coordinates is used to define the 3-D highway alignment. The coordinates (x_{s1}, y_{s1}, z_{s1}) and (x_{s2}, y_{s2}, z_{s2}) refer to the cartesian coordinates of any two points on the sight line. Usually, these two points are taken as its beginning and end. Similarly, (x_i, y_i, z_i) refer to the cartesian coordinates of node i. Also, the parameters a_i and b_i refer to constants defined at node i while the parameters τ and c_i refer to unique constants in the equations.

5.3.1 The 4-Node Rectangular Element

Referring to Figure 5.1*a*, the 4-node rectangular element has a node at each of its four corners. The local coordinates are set so that for any point within the element, $-1 \leq \xi \leq +1$ and $-1 \leq \eta \leq +1$. For this local coordinate system and referring to the node numbering system in the figure, the element's shape functions are given as:

$$N_1 = \frac{1}{4}(1 - \eta - \xi + \eta\,\xi)$$
$$N_2 = \frac{1}{4}(1 - \eta + \xi - \eta\,\xi)$$
$$N_3 = \frac{1}{4}(1 + \eta + \xi + \eta\,\xi) \qquad (5.2)$$
$$N_4 = \frac{1}{4}(1 + \eta - \xi - \eta\,\xi)$$

As discussed in the previous chapter for the linear element, the shape functions of the 4-node element are linear in both η and ξ directions. Thus, this element can accurately model surfaces with straight edges only.

The point(s) of intersection between the sight line and the element can be determined by enhancing the methodology applied in 2-D analysis as follows:

First, the equation of the sight line in 3-D space will be:

$$\frac{x - x_{s1}}{x_{s2} - x_{s1}} = \frac{y - y_{s1}}{y_{s2} - y_{s1}} = \frac{z - z_{s1}}{z_{s2} - z_{s1}} \qquad (5.3)$$

which represents the following two linear equations:

$$x - S_{xy}\,y + (S_{xy}\,y_{s1} - x_{s1}) = 0 \qquad y_{s1} \neq y_{s2} \qquad (5.4)$$

$$x - S_{xz}\,z + (S_{xz}\,z_{s1} - x_{s1}) = 0 \qquad z_{s1} \neq z_{s2} \qquad (5.5)$$

where

$$S_{xy} = (x_{s2} - x_{s1})/(y_{s2} - y_{s1})$$

$$S_{xz} = (x_{s2} - x_{s1})/(z_{s2} - z_{s1})$$

If $y_{s1} = y_{s2} = y_s$, Equation 5.4 becomes:

$$y - y_s = 0 \qquad (y_{s1} = y_{s2} = y_s) \tag{5.6}$$

Similarly, if $z_{s1} = z_{s2} = z_s$, Equation 5.5 becomes:

$$z - z_s = 0 \qquad (z_{s1} = z_{s2} = z_s) \tag{5.7}$$

Since the point(s) of intersection between the sight line and the element must satisfy the equations of both, then

$$\sum N_i \, a_i + \tau_1 = 0 \tag{5.8}$$

$$\sum N_i \, b_i + \tau_2 = 0 \tag{5.9}$$

where

$$a_i = x_i - S_{sy} \, y_i \qquad (y_{s1} \neq y_{s2})$$

$$a_i = y_i \qquad (y_{s1} = y_{s2})$$

$$b_i = x_i - S_{sz} \, z_i \qquad (z_{s1} \neq z_{s2})$$

$$b_i = z_i \qquad (z_{s1} = z_{s2})$$

$$\tau_1 = - x_{s1} + S_{sy} \, y_{s1} \qquad (y_{s1} \neq y_{s2})$$

$$\tau_1 = - y_s \qquad (y_{s1} = y_{s2})$$

$$\tau_2 = - x_{s1} + S_{sz} \, z_{s1} \qquad (z_{s1} \neq z_{s2})$$

$$\tau_2 = - z_s \qquad (z_{s1} = z_{s2})$$

Substituting for the element shape functions, Equations 5.8 and 5.9 can be written in terms of η and ξ as:

$$c_1 + c_2\,\eta + c_3\,\xi + c_4\,\eta\,\xi = 0 \tag{5.10}$$

$$c_5 + c_6\,\eta + c_7\,\xi + c_8\,\eta\,\xi = 0 \tag{5.11}$$

where

$$c_1 = 4\tau_1 + a_1 + a_2 + a_3 + a_4$$

$$c_2 = -a_1 - a_2 + a_3 + a_4$$

$$c_3 = -a_1 + a_2 + a_3 - a_4$$

$$c_4 = a_1 - a_2 + a_3 - a_4$$

c_5 to c_8 are similar to c_1 to c_4, respectively, with replacing a_i by b_i and τ_1 by τ_2.

Equations 5.10 and 5.11 are two polynomials in two unknowns η and ξ, and can be solved numerically or analytically. Using the software MAPLE-V to solve the equations analytically, ξ is given as the roots of the polynomial:

$$(c_3\,c_8 - c_4\,c_7)\,\xi^2 + (c_1\,c_8 - c_2\,c_7 + c_3\,c_6 - c_4\,c_5)\,\xi + (c_1\,c_6 - c_2\,c_5) = 0 \tag{5.12}$$

Then, η is as follows:

$$\eta = -\frac{c_5 + c_7\,\xi}{c_6 + c_8\,\xi} \tag{5.13}$$

This solution can produce:

1. No solution, if the equation is trivial or due to division by zero. This case represents a sight line parallel to or coincident with the element, and no sight obstruction exists.
2. Two imaginary roots. This case also represents no intersection.

3. One real root, if $c_3 c_8 - c_4 c_7 = 0$. In this case, one point of intersection exists whose cartesian coordinates can be calculated using Equation 5.1. For this case to represent a sight obstruction, the point of intersection must be within the limits of the element. This happens only if $-1 \leq \xi \leq +1$ and $-1 \leq \eta \leq +1$.
4. Two real roots (different or identical). This case can happen only with distorted elements, and therefore, it is not applicable in this research.

5.3.2 The 6-Node Rectangular Element

As shown in Figure 5.1*b*, the 6-node element is similar to the 4-node element but with an additional node at the middle of each of any two parallel edges. For the node numbering shown in Figure 5.1*b*, the shape functions of this element are:

$$
\begin{aligned}
N_1 &= \frac{1}{4}(-\eta + \eta\xi + \eta^2 - \eta^2\xi) \\
N_2 &= \frac{1}{4}(-\eta - \eta\xi + \eta^2 + \eta^2\xi) \\
N_3 &= \frac{1}{4}(\eta + \eta\xi + \eta^2 + \eta^2\xi) \\
N_4 &= \frac{1}{4}(\eta - \eta\xi + \eta^2 - \eta^2\xi) \\
N_5 &= \frac{1}{2}(1 + \xi - \eta^2 - \eta^2\xi) \\
N_6 &= \frac{1}{2}(1 - \xi - \eta^2 + \eta^2\xi)
\end{aligned}
\tag{5.14}
$$

The shape functions of the 6-node element shown in Figure 5.1*b* are quadratic in the η-direction and linear in the ξ-direction. Subsequently, this element can accurately model surfaces with two curved and two straight edges.

Following the same derivation as in the case of the 4-node element, the coordinates of the points of intersection between the sight line and the element can be given as the roots of the following two polynomials:

$$c_1 + c_2\,\eta + c_3\,\xi + c_4\,\eta^2 + c_5\,\eta\,\xi + c_6\,\eta^2\,\xi = 0 \tag{5.15}$$

$$c_7 + c_8\,\eta + c_9\,\xi + c_{10}\,\eta^2 + c_{11}\,\eta\,\xi + c_{12}\,\eta^2\,\xi = 0 \tag{5.16}$$

where

$$c_1 = 4\tau_1 + 2a_5 + 2a_6$$

$$c_2 = -a_1 - a_2 + a_3 + a_4$$

$$c_3 = 2a_5 - 2a_6$$

$$c_4 = a_1 + a_2 + a_3 + a_4 - 2a_5 - 2a_6$$

$$c_5 = a_1 - a_2 + a_3 - a_4$$

$$c_6 = -a_1 + a_2 + a_3 - a_4 - 2a_5 + 2a_6$$

c_7 to c_{12} are similar to c_1 to c_6, respectively, with replacing a_i by b_i and τ_1 by τ_2.

a_i, b_i, τ_1, and τ_2 are as given previously.

Using the software MAPLE-V to solve Equations 5.15 and 5.16 analytically, η is given as the roots of the polynomial:

$$\begin{aligned}&(-c_{10}\,c_6 + c_{12}\,c_4)\,\eta^4 + (-c_{10}\,c_5 - c_8\,c_6 + c_{11}\,c_4 + c_{12}\,c_2)\,\eta^3\\ &\quad + (-c_{10}\,c_3 - c_7\,c_6 - c_8\,c_5 + c_{11}\,c_2 + c_{12}\,c_1 + c_9\,c_4)\,\eta^2\\ &\quad + (-c_7\,c_5 - c_8\,c_3 + c_{11}\,c_1 + c_9\,c_2)\,\eta + (-c_7\,c_3 + c_9\,c_1) = 0\end{aligned} \tag{5.17}$$

which can be solved numerically (Goult et al, 1973). Then, ξ is as follows:

This solution can produce:

$$\xi = -\frac{c_1 + c_2\,\eta + c_4\,\eta^2}{c_3 + c_5\,\eta + c_6\,\eta^2} \tag{5.18}$$

1. No solution, if the equation is trivial or due to division by zero. This case represents a sight line parallel to or coincident with the element, and no sight obstruction exists.
2. Imaginary roots only. This case also represents no intersection.
3. One real root. In this case, one point of intersection exists whose cartesian coordinates can be calculated using Equation 5.1. For this case to represent a sight obstruction, the point of intersection must be within the limits of the element. This happens only if $-1 \leq \xi \leq +1$ and $-1 \leq \eta \leq +1$.
4. Two different real roots. In this case, two points of intersection exist, and the comments made above are applicable.
5. Two identical real roots. This case represents a point of tangency. No sight obstruction exists.
6. More than Two real roots. This case can happen only with distorted elements, and therefore, it is not applicable in this research.

5.3.3 The 8-Node Rectangular Element

As shown in Figure 5.1*c*, the 8-node element is similar to the 4-node and 6-node elements but with an additional node at the middle of each edge. For the node numbering shown in Figure 5.1*c*, the shape functions of this element are:

$$
\begin{aligned}
N_1 &= \frac{1}{4}(-1 + \eta\,\xi + \eta^2 + \xi^2 - \eta^2\,\xi - \eta\,\xi^2) \\
N_2 &= \frac{1}{4}(-1 - \eta\,\xi + \eta^2 + \xi^2 + \eta^2\,\xi - \eta\,\xi^2) \\
N_3 &= \frac{1}{4}(-1 + \eta\,\xi + \eta^2 + \xi^2 + \eta^2\,\xi + \eta\,\xi^2) \\
N_4 &= \frac{1}{4}(-1 - \eta\,\xi + \eta^2 + \xi^2 - \eta^2\,\xi + \eta\,\xi^2) \\
N_5 &= \frac{1}{2}(1 - \xi^2 - \eta + \eta\,\xi^2) \\
N_6 &= \frac{1}{2}(1 + \xi - \eta^2 - \eta^2\,\xi) \\
N_7 &= \frac{1}{2}(1 - \xi^2 + \eta - \eta\,\xi^2) \\
N_8 &= \frac{1}{2}(1 - \xi - \eta^2 + \eta^2\,\xi)
\end{aligned}
\tag{5.19}
$$

The shape functions of the 8-node element are quadratic in both η and ξ directions. Subsequently, this element can accurately model surfaces with all edges curved.

Following the same derivation as in the case of the 4-node and 6-node elements, the coordinates of the points of intersection between the sight line and the element can be given as the roots of the following two polynomials:

$$c_1 + c_2\,\eta + c_3\,\xi + c_4\,\eta^2 + c_5\,\xi^2 + c_6\,\eta\,\xi + c_7\,\eta^2\,\xi + c_8\,\eta\,\xi^2 = 0 \tag{5.20}$$

$$c_9 + c_{10}\,\eta + c_{11}\,\xi + c_{12}\,\eta^2 + c_{13}\,\xi^2 + c_{14}\,\eta\,\xi + c_{15}\,\eta^2\,\xi + c_{16}\,\eta\,\xi^2 = 0 \tag{5.21}$$

where

$$c_1 = 4\tau_1 - a_1 - a_2 - a_3 - a_4 + 2a_5 + 2a_6 + 2a_7 + 2a_8$$

$$c_2 = -2a_5 + 2a_7$$

$c_3 = 2a_6 - 2a_8$

$c_4 = a_1 + a_2 + a_3 + a_4 - 2a_6 - 2a_8$

$c_5 = a_1 + a_2 + a_3 + a_4 - 2a_5 - 2a_7$

$c_6 = a_1 - a_2 + a_3 - a_4$

$c_7 = -a_1 + a_2 + a_3 - a_4 - 2a_6 + 2a_8$

$c_8 = -a_1 - a_2 + a_3 + a_4 + 2a_5 - 2a_7$

c_9 to c_{16} are similar to c_1 to c_8, respectively, with replacing a_i by b_i and τ_1 by τ_2. a_i, b_i, τ_1, and τ_2 are as given previously.

Equations 5.20 and 5.21 were also solved using the software MAPLE-V to produce the solution in terms of c_1 to c_{16}. However, because the solution is too long and, as explained earlier, this element will not be used, the solution is not given here.

5.3.4 The 3-Node Triangular Element

As discussed earlier, rectangular elements provide an easier and better modelling of the highway alignment than triangular elements. However, this element can be particulary important in modelling tapered elements on straight segments. Moreover, the analytical modelling of this element should provide an automated tool for the methodology followed by Sanchez (1994).

Referring to Figure 5.2*a*, the 3-node element is a triangle with 3 nodes at its apexes. The main difference between this element and the rectangular elements is the system of local coordinates used in each element. The coordinate system in the triangular element is the area coordinates (ξ_1, ξ_2, and ξ_3) which can be defined as follows:

$$\xi_i = \frac{A_i}{A} \qquad (i = 1 \text{ to } 3) \tag{5.22}$$

where A is the area of the triangle and A_i are the areas of the subtriangles as shown in Figure 5.2.

The shape functions of this element are simply the area coordinates. From Equation 5.22, it can be proven that:

$$\xi_1 + \xi_2 + \xi_3 = 1 \tag{5.23}$$

To determine the coordinates of the point(s) of intersection between the sight line and the element, three equations are required. The first two equations can be obtained by substituting for the shape functions in the equations of the sight line, Equations 5.8 and 5.9, as follows:

$$\xi_1 a_1 + \xi_2 a_2 + \xi_3 a_3 = -\tau_1 \tag{5.24}$$

$$\xi_1 b_1 + \xi_2 b_2 + \xi_3 b_3 = -\tau_2 \tag{5.25}$$

where a_i, b_i, τ_1, and τ_2 are as given previously.

Equations 5.23, 5.24, and 5.25 are three linear equations in three unknowns, and can be solved to calculate the area coordinates of the point(s) of intersection. The solution of the three equations can produce:

1. No solution, due to singularity. This case represents a sight line parallel to or coincident with the element, and no sight obstruction exists.
2. One real solution. In this case, one point of intersection exists whose cartesian coordinates can be calculated using Equation 5.1. For this case to represent a sight

obstruction, the point of intersection must be within the limits of the element. Referring to Equation 5.22, this happens only if $0 \leq \xi_i \leq +1$.

5.3.5 *The 5-Node Triangular Element*

As shown in Figure 5.2*b*, the 5-node element is a triangle with 3 nodes at its apexes and one node at the middle of two edges. As mentioned earlier, this element can replace the 3-node element if the pavement widening or narrowing occurs on curved sections in horizontal and/or vertical alignments.

For this element, the same area coordinate system used for the 3-node triangular element is still the best parametric coordinate system. Therefore, Equation 5.23 is still valid. However, the shape functions, for the node numbering shown in Figure 5.2*b*, will be as follows:

$$
\begin{aligned}
N_1 &= \xi_1 (1 - 2\,\xi_3) \\
N_2 &= \xi_2 (1 - 2\,\xi_3) \\
N_3 &= \xi_3 (2\,\xi_3 - 1) \\
N_4 &= 4\,\xi_2\,\xi_3 \\
N_5 &= 4\,\xi_1\,\xi_3
\end{aligned}
\tag{5.26}
$$

To determine the coordinates of the point(s) of intersection between the sight line and the element, three equations are required. Equation 5.23 represents the first equation and the other two can be obtained by substituting for the shape functions in the equations of the sight line, Equations 5.8 and 5.9. Solving the three equations using MAPLE-V, ξ_3 is the roots of:

$$c_0 + c_1 \xi_3 + c_2 \xi_3^2 + c_3 \xi_3^3 = 0 \tag{5.27}$$

where

$$\begin{aligned}
c_0 &= a_1(-\tau_2 - b_2) + a_2(\tau_2 + b_1) + \tau_1 b_1 \\
c_1 &= a_1 (5b_2 + b_3 - 4b_4 \quad 2\tau_2) + a2(-5b_1 - b_3 + 4b_5 - 2\tau_2) + a_3(-b_1 + b_2) \\
&\quad + a_4(4b_1 + 4\tau_2) + a_5(-4b_2 + \tau_2) + \tau_1(-2b_1 + 2b_2 - 4b_4 + 4b_5) \\
c_2 &= a_1(-8b_2 - 4b_3 + 12b_4) + a_2(8b_1 + 4b_3 - 12b_5) + a_3(4b_1 - 4b_2 + 4b_4 - 4b_5) \\
&\quad a_4(-12b_1 - 4b_3) + a_5(12b_2 - 16b_4 + 16b_5) \\
c_3 &= a_1(4b_2 + 4b_3 - 8b_4) + a_2(-4b_1 - 4b_3 + 8b_5) + a_3(-4b_1 + 4b_2 \quad 8b_4 + 8b_5) \\
&\quad a_4(8b_1 + 8b_3 - 16b_5) + a_5(-8b_2 - 8b_3 + 16b_4)
\end{aligned} \tag{5.28}$$

Then ξ_2 and ξ_1 can be given as follows:

$$\begin{aligned}
\xi_2 &= - \frac{(-2b_1 - 2b_3 + 4b_5)\xi_1^2 + (3b_1 + b_3 - 4b_5)\xi_3 + (-b_1 - \tau_2)}{(-2b_1 + 2b_2 - 4b_4 + 4b_5)\xi_3 + (b_1 - b_2)} \\
\xi_1 &= 1 - \xi_2 - \xi_3
\end{aligned} \tag{5.29}$$

This solution can produce:

1. No solution, if Equation 5.27 is trivial or due to division by zero. This case represents a sight line parallel to or coincident with the element, and no sight obstruction exists.

2. One real root (note that a cubic equation must have at least one real root). In this case, one point of intersection exists whose cartesian coordinates can be calculated using Equation 5.1. For this case to represent a sight obstruction, the point of intersection must be within the limits of the element. This happens only if $0 < \xi_i < +1$.

3. Two different real roots (the third root must be real and repeated). In this case, two points of intersection exist, and the comments made above are applicable.
4. Identical real roots. This case represents a point of tangency. No sight obstruction exists.
5. Three different real roots. This case can happen only with distorted elements, and therefore, it is not applicable in this research.

5.4 Iterative Procedure for Available Sight Distance

Based on the mathematical formulation presented above, an iterative procedure can be used to determine the available sight distance on 3-D combined horizontal and vertical alignments. In this procedure, the sight distance is initially assumed as S, and then S is decreased or increased until the sight line becomes tangent to an element representing a sight obstruction. The following steps summarize the procedure:

1. Idealize the highway surface and the sight obstructions into a series of elements as explained previously. Since, it is the relative positioning, not the absolute positioning, that controls the sight distance, the cartesian coordinates of each node can be referred to any arbitrary point of origin.
2. Position the driver's eye at the station where the available sight distance is required and determine the coordinates of the beginning of the sight line. These coordinates should be calculated relative to the same point of origin.
3. Position the object at a distance S ahead to the driver's eye and determine the coordinates of the end of the sight line relative to the same point of origin.

4. Check the intersection between the sight line and the elements which are used to idealize the highway surface and the sight obstructions. The point of intersection which represents a sight obstruction must be within the limits of both the sight line and the element.
5. If the sight line intersects with any element, S is greater than the available sight distance. Decrease S and repeat steps 3 and 4.
6. If the sight line does not intersect with any element, S is less than the available sight distance. Increase S and repeat steps 3 and 4.
7. If the sight line is tangent to any element, S is equal to the available sight distance. End of iterations.

5.5 Software for Marking No-Passing Zones

5.5.1 Description of Developed Software

The theoretical procedure, presented above, has been translated into a computer program, ***MARKC***, written in Microsoft QuickBasic. The program can determine the profile of available passing sight distance, and in turn no-passing zones, on two lane highways due to 3-D combined horizontal and vertical alignments. This first version of ***MARKC*** is based on the 4-node and 6-node rectangular elements only. The main inputs for ***MARKC*** are the alignment, cross-section data, and sight obstructions and the main output is the profile of available sight distance on both lanes of the highway. This profile can be used to determine the passing and no-passing zones in both directions. A brief explanation of

the input data, data processing, and the output results of *MARKC* is presented below, and more detailed explanation with numerical examples can be found in Hassan et al (1995*e*).

Input Data. The input data are entered to *MARKC* through a data file prepared by the user before running the program. The data file includes description of the highway alignment, cross-section data, and sight obstructions. In addition, similar to the 2-D computer programs, the input file contains user-specified parameters that determine the accuracy required in determining the sight distance, the stations at which the sight distance will be determined, the minimum value of the sight distance to be checked, S_m, and the heights of the driver eye and the object.

The horizontal alignment of the highway centerline is input as a series of straight segments (tangents) and circular and spiral curves. These segments may be arranged in any order. Thus, *MARKC* can deal with simple and complex alignments. The information required to define the alignment are the station of every point between two successive elements and the turning direction and the radius of each curve. If the element is a spiral curve, the radii at the beginning and end should be identified. Thus, *MARKC* can consider spiral curves connecting two circular curves.

Similarly, the vertical alignment of the highway centerline is input as a series of straight segments (slopes) and crest and sag parabolic curves. The segments may be arranged in any order. In addition, the user can identify certain segments as spline grades rather than parabolic vertical curves. Although, spline grades are not used in the design of new highways, this feature allows the application of *MARKC* to existing highways that

have such type of alignment. The spline grades are modelled by small 6-node elements similar to the horizontal curves.

The cross-section data include the width and cross-slope of each of the two travel-lanes, width and cross-slope of each shoulder, and the side-slope data (whether in a cut or fill section). A total of four segments can be entered on each side of the highway, and each segment is defined by width and slope (horizontal-to-vertical). If the side-slope is positive, it will indicate a cut-section, and will be considered as a continuous lateral sight obstruction. A zero value for the slope indicates a cut section with vertical side-slope, and will be interpreted as a continuous lateral sight obstruction. On the other hand, a negative value for the slope indicates a fill section. Since horizontal-to-vertical slope cannot define flat segments, a very flat slope will have to be used (for example, 1:1000). Generally, a set of cross-section data should be entered to the software at any station with a change of any of these data. Widths and slopes at intermediate stations are estimated by linear interpolation between the two bounding points.

Finally, in addition to the continuous sight obstructions represented by the cut slopes, the user can identify the existence of single lateral obstructions and overpasses which can obstruct the sight distance. Single lateral obstructions (one-, two-, and three-point) are defined to *MARKC* as stations and lateral clearances from the highway centerline. In all cases, the sight line is allowed only to pass within the lateral clearance. If the sight line passes through or beyond the obstruction, it will be considered obstructed. In case of overpasses, the user can specify the station, vertical clearance, and width of each overpass. Skewed overpasses and/or overpasses with variable vertical clearance can

also be defined to the software. Similar to lateral obstructions, the sight line must be below the overpass; otherwise, it will be considered obstructed.

Data Processing. The main modules that are incorporated in *MARKC* are the idealization module and the sight distance module. In the idealization module, *MARKC* automatically idealizes the alignment and the obstructions into a series of 4-node and 6-node elements according to the concept presented perviously. In the second module, *MARKC* assumes a relatively low value for the available sight distance S_{av}. Then, S_{av} is increased gradually with checking the existence of any sight obstruction until the actual S_{av} is determined at the specified accuracy. However, if S_{av} becomes greater than S_m, no more iterations are conducted at this station. Since S_{av} is determined as the difference between the stations of the driver eye and the object, it will be a distance projected on the highway centerline. Subsequently, a subroutine is added to the software to project this distance on the lane centerline. Therefore, the final S_{av} is a distance projected on the lane centerline similar to the MUTCD (1995) standards. The module carries on this procedure for all the stations on which the available sight distance is required.

Output Results. The final output is shown first on the computer screen with options of sending it to a data file or to a printer. The output contains first a display of the input data and then the available sight distance on the right and left lane, where the right and left lanes are relative to a driver travelling in the direction of increasing stations. It should be noted also that the available sight distance is given only if it is less than S_m.

5.5.2 *Verification*

The developed software, *MARKC*, was verified in two steps (Hassan et al. 1996c). In the first step, *MARKC* was verified using a series of separate horizontal and vertical alignments. In preparing the data input, a straight segment was used as the vertical alignment when a horizontal alignment was used for verification, and vice versa. In either case, the cross-section was assumed constant along the alignment. The results showed that *MARKC* can determine the available sight distance on separate alignments accurately. In the second step, the software was verified using a combined alignment. Two alternatives were suggested: to build a physical model according of an assumed alignment, or to measure the available sight distance in the field on an actual alignment. Because the longitudinal and cross-slopes of highways are relatively small, a small error in building the physical model or in measuring the available sight distance would magnify significantly. Therefore, the option of field measurements of an actual alignment was favoured.

In order to get an actual combined alignment with dimensions feasible to measuring the available sight distance in the field and with the sight obstructions easy to locate, an overpass was selected, namely the Marina Park Overpass in the City of Thunder Bay, Ontario (Figure 5.7). The overpass maps were provided by the City of Thunder Bay, Engineering Division, and the as-built horizontal and vertical alignments are shown in Figure 5.8. Nonetheless, it was noticed that considerable pavement settlements had taken place in the fill immediately after the bridge deck. A limited levelling was carried out to this section to determine the centerline's elevation every 5 m. Figure 5.9 shows

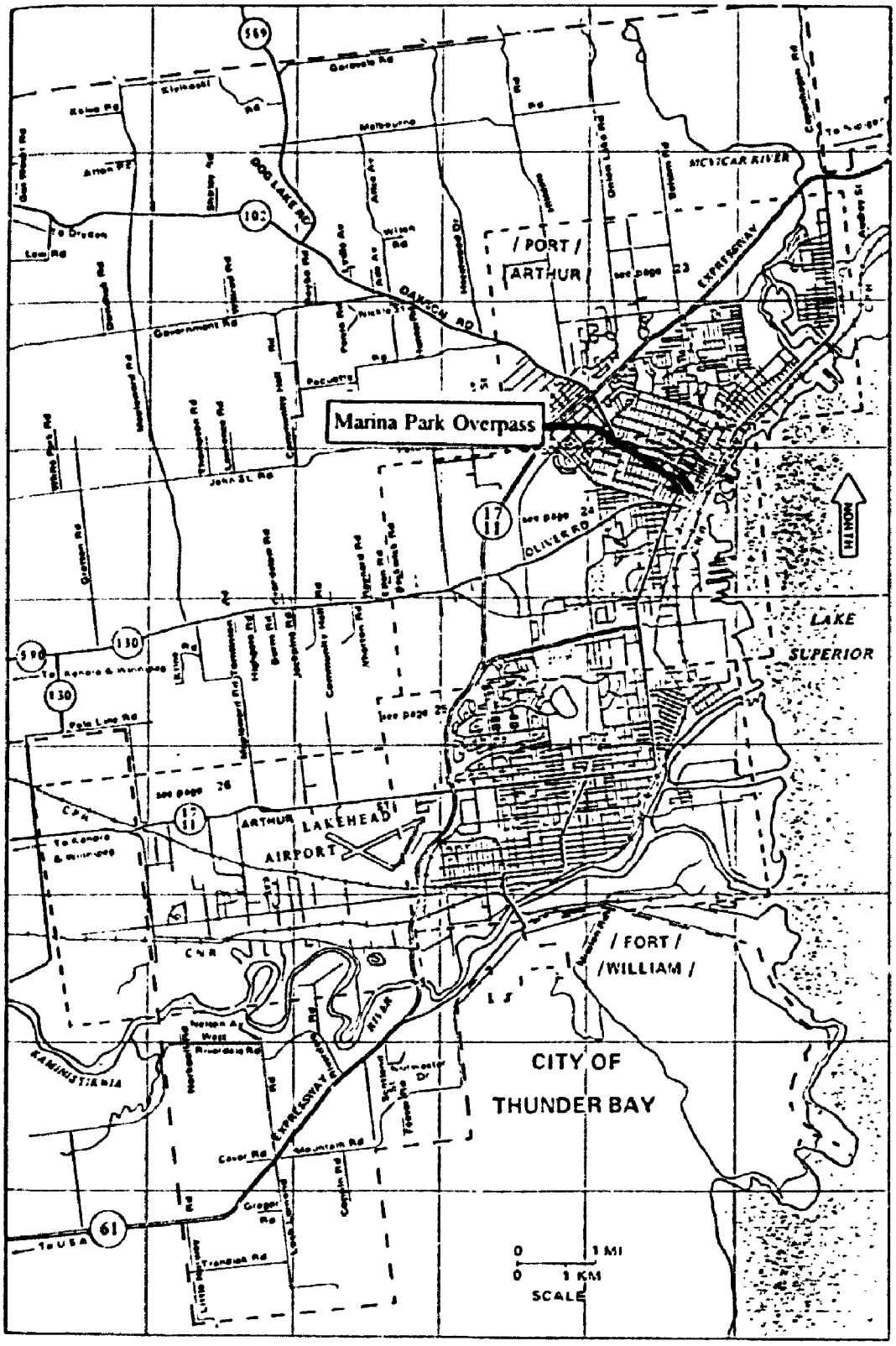

FIGURE 5.7: Location of Marina Park Overpass.

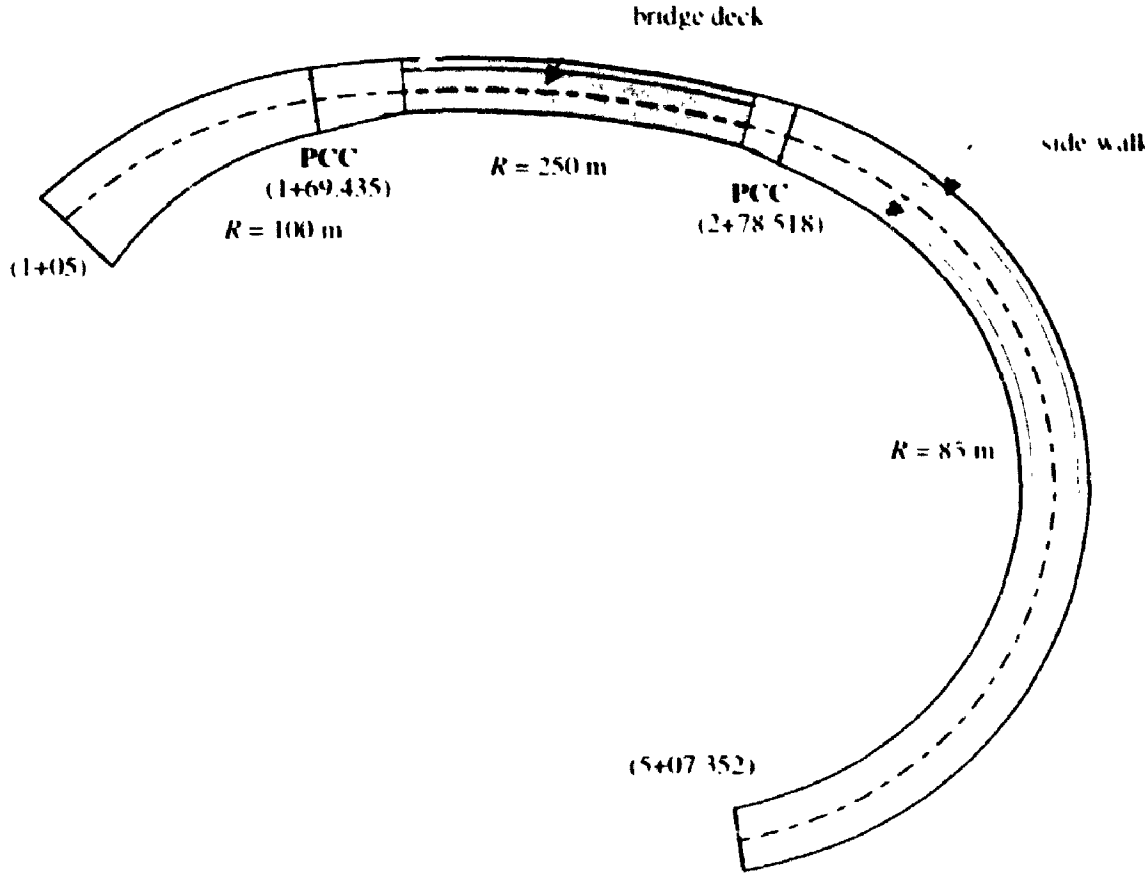

(a) Horizontal Alignment

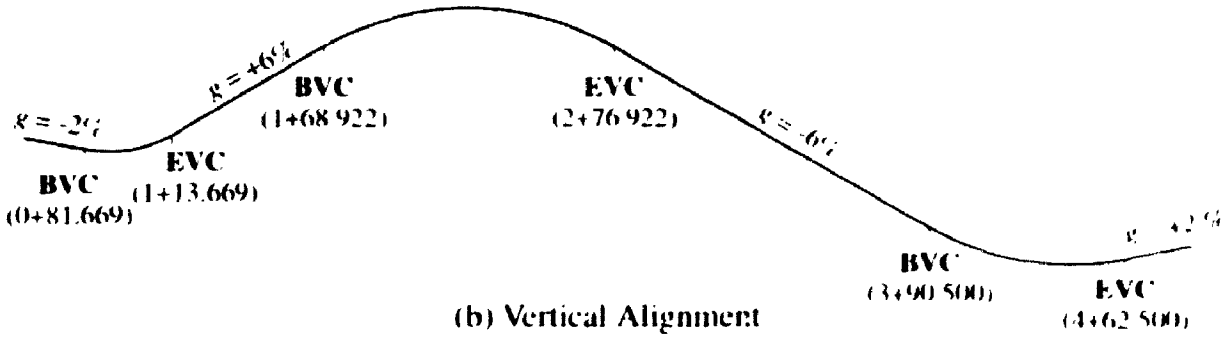

(b) Vertical Alignment

Stations are every 100 m.

FIGURE 5.8: As-Built Horizontal and Vertical Alignments of Marina Overpass, Thunder Bay, Ontario.

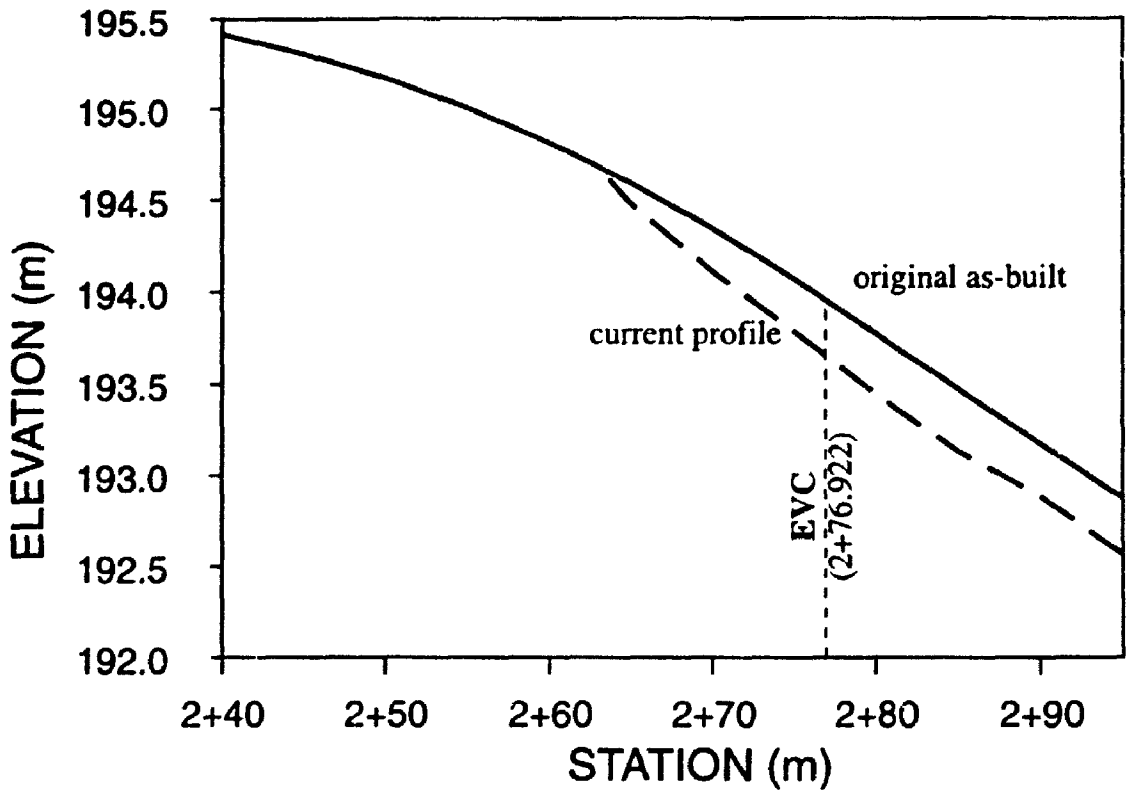

FIGURE 5.9: Original As-Built and Current Vertical Alignments After Bridge Deck.

the centerline's original and current profiles. The cross-section data can be classified into four distinct segments: prior to the bridge deck (variable lane width and lateral clearance), the bridge deck (constant lane width and lateral clearance), immediately after the bridge deck (constant lane width and variable lateral clearance), and the last segment (constant lane width and lateral clearance). Field measurements were carried out to determine the lane width and lateral clearance on the four segments every 10 m. The entire overpass had, however, a constant superelevation rate, namely 4%.

The available sight distance in the field was determined using a pair of targets used by the Ministry of Transportation of Ontario (MTO) in marking passing and no-

passing zones in the field. As shown in Figure 5.10, each of the two targets consists of a rod with two discs, and each disc has an opening. The heights of the two openings were measured and found 0.305 and 1.14 m. One of the two targets was used as the driver eye (at the height of 1.14 m) and the other was used as the object (at the height of 0.305 m). Based on the advice of the MTO field crew, side levels were fixed at the two targets to ensure their vertical setup. Then, the available sight distance on the inside lane was measured every 10 m beginning at station (1+05) and ending at station (2+85) for a total of 29 measurements. The alignment data were fed to the program and the available sight distances at the same stations were determined to the nearest 0.01 m. Setting the maximum element size as 25 m, the element net created by *MARKC* to model the overpass is shown in Figure 5.11.

As shown in Table 5.1, the calculated and measured sight distances were in good agreement for 25 stations where the absolute difference was less than 1 m (maximum percentage difference was 1.448%). However, a considerable error was observed at the stations which had the object immediately after the bridge deck, specially at stations (2+05) and (2+15). Another observation was that the sight distance at these two stations were limited by the crest vertical curve in the field while the software showed that they were limited by the lateral obstruction. The reason for these differences was mainly due to the settlements observed after the bridge deck (see Figure 5.9). This settlement would reduce the effective object height which was estimated as 0.101 and 0.040 m for stations (2+05) and (2+15), respectively. Therefore, the vertical alignment after the bridge was assumed as a series of broken slopes, as measured in the field, and the available sight

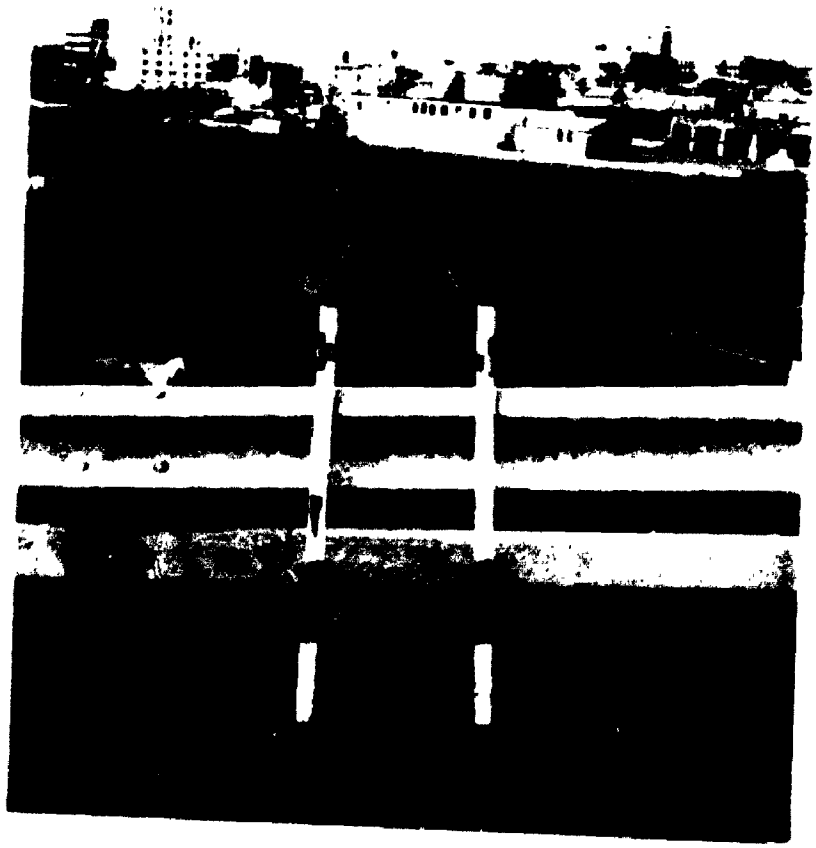

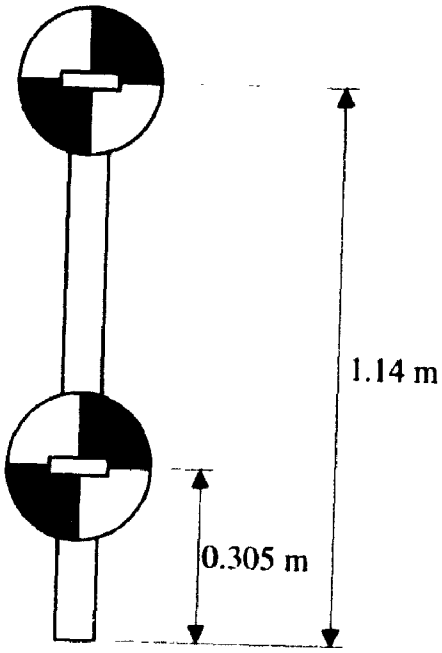

FIGURE 5.10: Sight Distance Targets Used in Field Measurements.

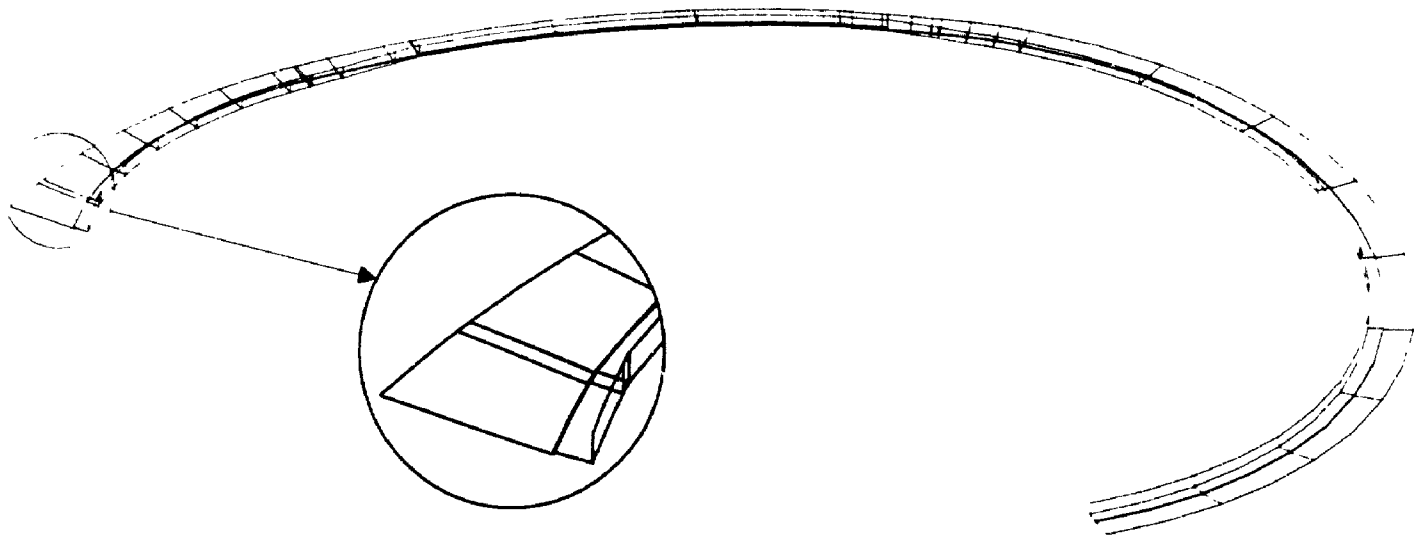

FIGURE 5.11: The Element Net for Modelling Marina Overpass.

TABLE 5.1: Measured and Calculated Values of the Available Sight Distance.

Station (m)	S_{av} (m)		Absolute Difference (m)	Difference (%)
	Measured (Field)	Calculated (Software)		
1 + 05	60.95	60.57	-0.38	-0.627
1 + 15	60.09	59.47	-0.62	-1.043
1 + 25	63.02	62.66	0.36	-0.575
1 + 35	70.11	69.97	-0.14	-0.200
1 + 45	65.97	66.47	+0.50	+0.752
1 + 55	67.20	67.81	+0.61	+0.900
1 + 65	71.94	71.48	-0.46	-0.644
1 + 75	71.42	70.91	-0.51	-0.719
1 + 85	72.06	71.12	-0.94	-1.322
1 + 95	**69.50**	**71.12**	**+1.62**	**+2.278**
2 + 05	**63.74**	**71.12**	**+7.38**	**+10.377**
2 + 15	**57.70**	**70.08**	**+12.38**	**+17.666**
2 + 25	67.53	66.81	-0.72	-1.078
2 + 35	61.25	62.15	+0.90	+1.448
2 + 45	59.07	58.50	-0.57	-0.974
2 + 55	59.45	60.01	+0.56	+0.933
2 + 65	61.05	61.61	+0.56	+0.909
2 + 75	59.26	59.94	+0.68	+1.134
2 + 85	59.55	59.87	+0.32	+0.534
2 + 95	59.47	59.87	+0.40	+0.668
3 + 05	59.52	59.87	+0.35	+0.585
3 + 15	59.54	59.87	+0.33	+0.551
3 + 25	59.40	59.87	+0.47	+0.785
3 + 35	59.65	59.87	+0.22	+0.367
3 + 45	59.47	59.87	+0.40	+0.668
3 + 55	59.55	59.87	+0.32	+0.543
3 + 65	60.44	59.87	-0.57	-0.952
3 + 75	60.27	59.87	-0.40	-0.668
3 + 85	60.35	59.87	-0.48	-0.802

distances at these points were recalculated. As shown in Table 5.2, the difference between the measured and calculated sight distances had dropped to an acceptable level

TABLE 5.2: Results of the Modified Vertical Alignment.

Station (m)	S_{ia} (m)		Absolute Difference (m)	Difference (%)
	Measured (Field)	Calculated (Software)		
1 + 95	69.50	69.58	+0.08	+0.115
2 + 05	63.74	63.36	-0.38	-0.600
2 + 15	57.70	57.46	-0.24	-0.418

However, it should be noted that the verification, so far, is based on the measured available sight distance at each station which is one reading belonging to a population of readings. Normally, because the measurement errors are unbiased, some of these readings should be greater than the actual sight distance while the others should be less. However, since the alignment, obstruction, and cross-section on the segment after station (2+85) were the same, the available sight distance should also be the same (this was the case for the calculated sight distance). Therefore, it can be assumed that the measured sight distance at these stations belong to the same population. Because the number of readings, sample size, was small (n = 11), it was assumed that they would follow the t distribution The sample's average sight distance, $\bar{x}$, was 59.75 m and the sample's standard deviation, s, was 0.3968 m. A statistical test of hypothesis was carried out for the null hypothesis that the actual mean of the sample, μ, was 59.87 m (as calculated by the software) and

the difference between the actual mean and the sample's average was due to the measurement errors. As shown in Table 5.3, the hypothesis is acceptable for a level of significance, α, of 5%.

TABLE 5.3: Test of Hypothesis for Available Sight Distance.

Item	Value
Sample's average, $\bar{x}$	59.75 m
Sample's standard deviation, s	0.3968 m
Sample size, n	11
Degree of freedom, $r = n - 1$	10
Level of significance, α	5% (two-sided test)
Null hypothesis, H_0	the population mean, $\mu = 59.87$ m
Calculations	$t_0 = \pm 2.228$ (from the t-distribution)
	$t_c = \dfrac{\mu - \bar{x}}{s/\sqrt{n - 1}} = 0.9563$
	$t_c < t_0$
Conclusion	Accept the hypothesis, H_0

CHAPTER 6

UTILIZATION OF DEVELOPED MODELS IN MARKING TWO-LANE HIGHWAYS

In this chapter the models for 2-D and 3-D available sight distance, presented in Chapters 4 and 5, are used to determine the profile of available sight distance on a real segment of a two-lane highway. A discussion about the programs applicability and accuracy and a comparison between 2-D and 3-D sight distances are presented. Then, the profiles of 2-D and 3-D available sight distances are used to determine the proper marking of passing and no-passing zones according to the MUTCD standards and according to the revised model developed in Chapter 3. Finally, a comparison among the different methods of marking and the existing marking in the field is presented.

6.1 Alignment Data

The segment used in the application is a 7-km stretch on Highway 61 (station 10+000 to 17+000, township of Crooks) between the Canada-US borders and the City of Thunder Bay (Figure 6.1). The highway is a two-lane facility with a passing lane added to the right lane (relative to a driver travelling in the direction of increasing stations) from station 10+740 to 12+550 (including tapers). Another passing lane is added to the left lane from station 19+200 to 16+420 (including tapers). However, since the application is limited to station 17+000, only the portion from 17+000 to 16+420 is considered. The speed limit on Highway 61 is 90 kph while the design speed is 110 kph. According to

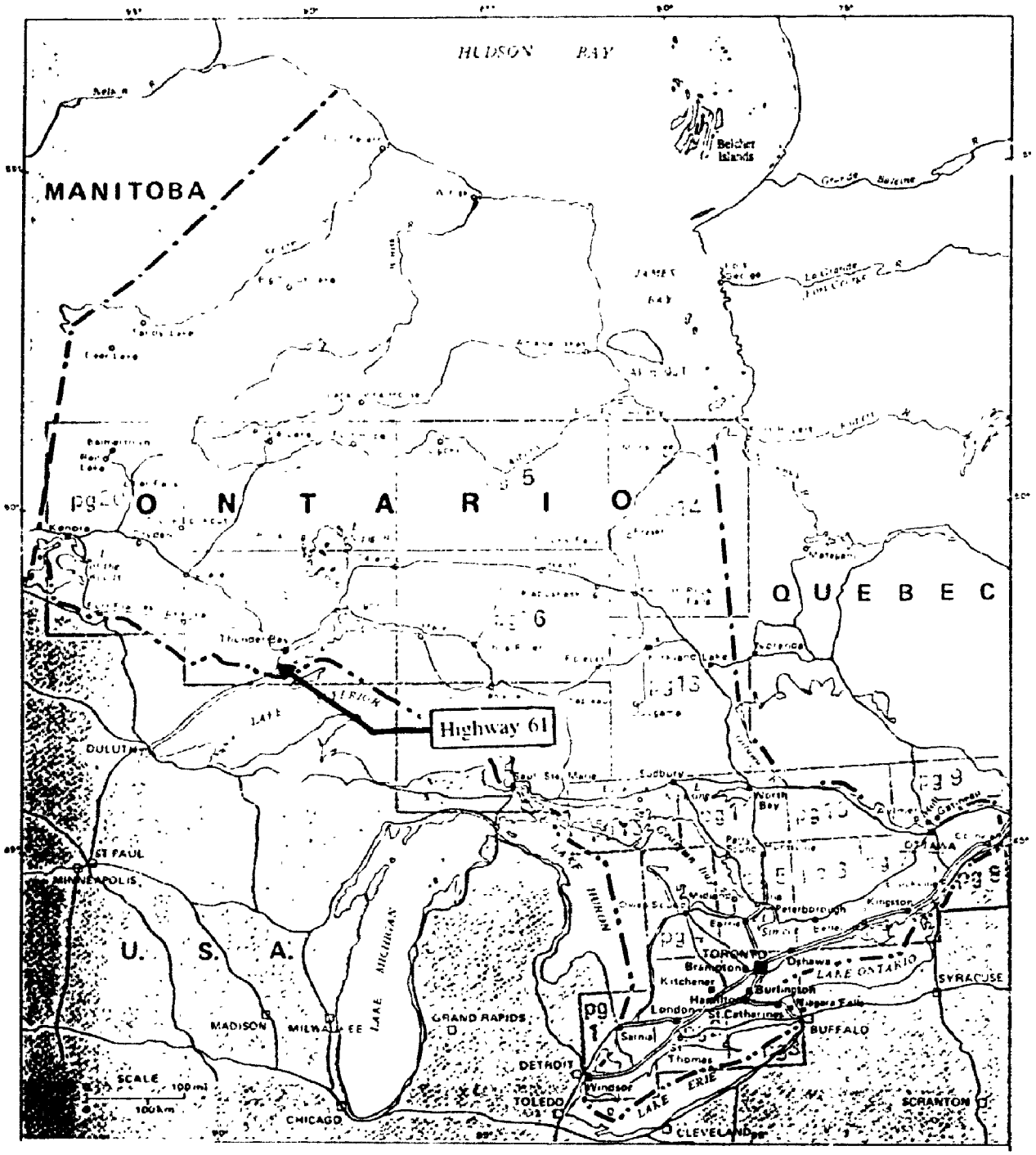

FIGURE 6.1: Location of Highway Segment.

the 1992-traffic count, the average annual daily traffic (AADT) on the segment was 2250 vpd. The alignment data were provided by the Ministry of Transportation of Ontario (MTO). Nonetheless, the data of single lateral sight obstructions were not available in MTO, and there are no overpasses crossing the segment to represent potential sight obstructions. Therefore, sight obstructions on the segment consist mainly of the highway surface and the cut-slopes in cut sections.

Figure 6.2 shows the segment's horizontal alignment. As shown in the figure, the alignment includes a wide variety of horizontal curves such as curves with and without spirals, separate curves with long tangents, successive curves with short tangents, broken back, reverse, and compound curves. As shown in Figure 6.3, the segment's vertical alignment is a continuous curvilinear profile with successive crests and sags. Also, with the exception of the four vertical curves shown in the figure (and short tangents before and after each curve), the alignment consists mainly of successive spline grades. The spline grades are defined by a total of 400 points with known stations and elevations. In defining the alignment to the computer software, it was divided into a total of 29 segments (4 curves, 7 tangents, and 18 spline grades).

In addition to the elevation of the highway centerline, detailed cross section data are available at each of the 400 points. From these data, complete cross section information; such as pavement width and cross-slope, shoulder width and cross slope, and cut and fill side-slopes; can be obtained. The pavement width is mainly 7.50 m (3.75 m for each lane) and varies along the segment due to pavement widening on curves and due to adding passing lanes. Normal crown-slope of the pavement is 2% and changes on

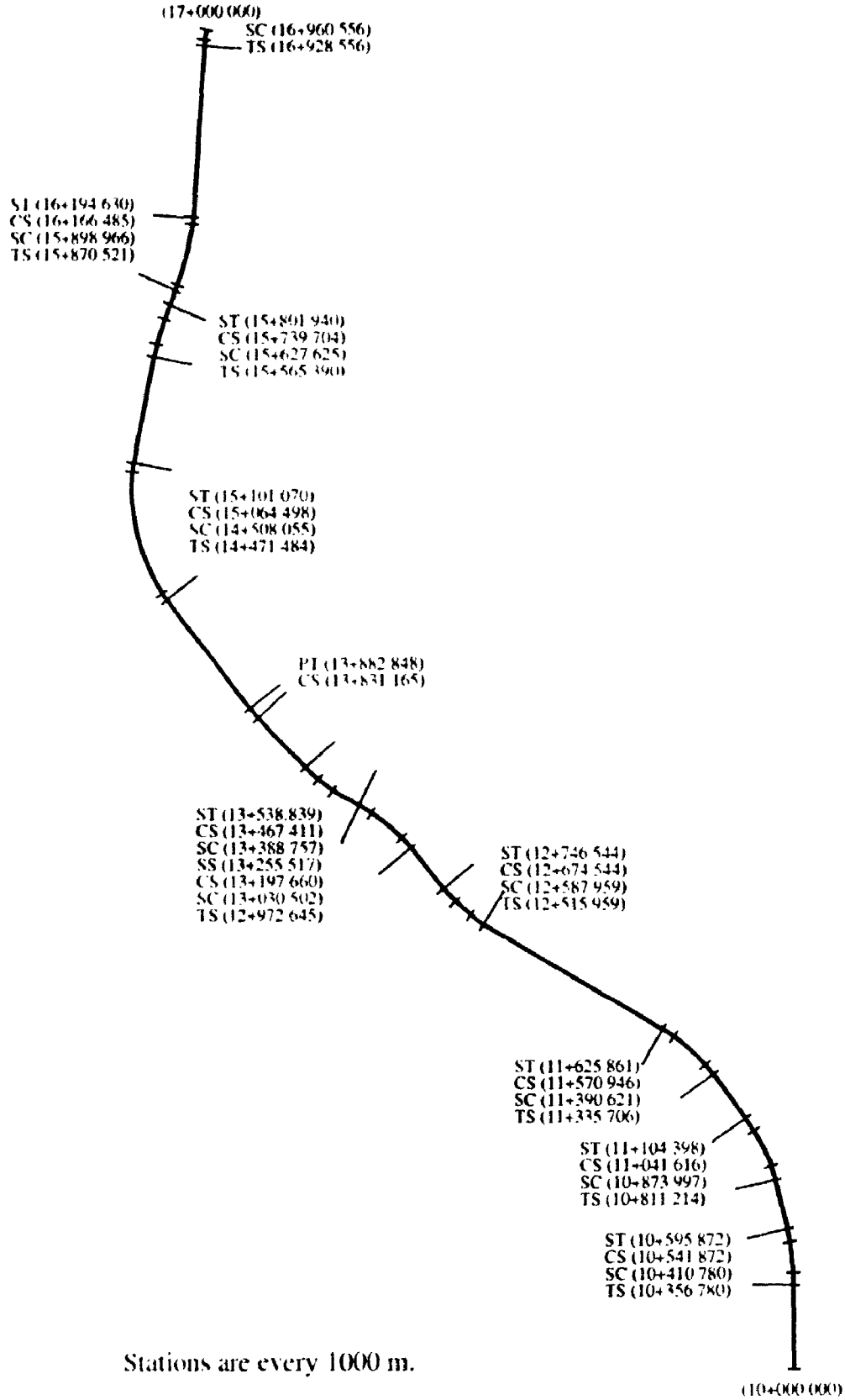

Stations are every 1000 m.

FIGURE 6.2: Horizontal Alignment of Highway Segment.

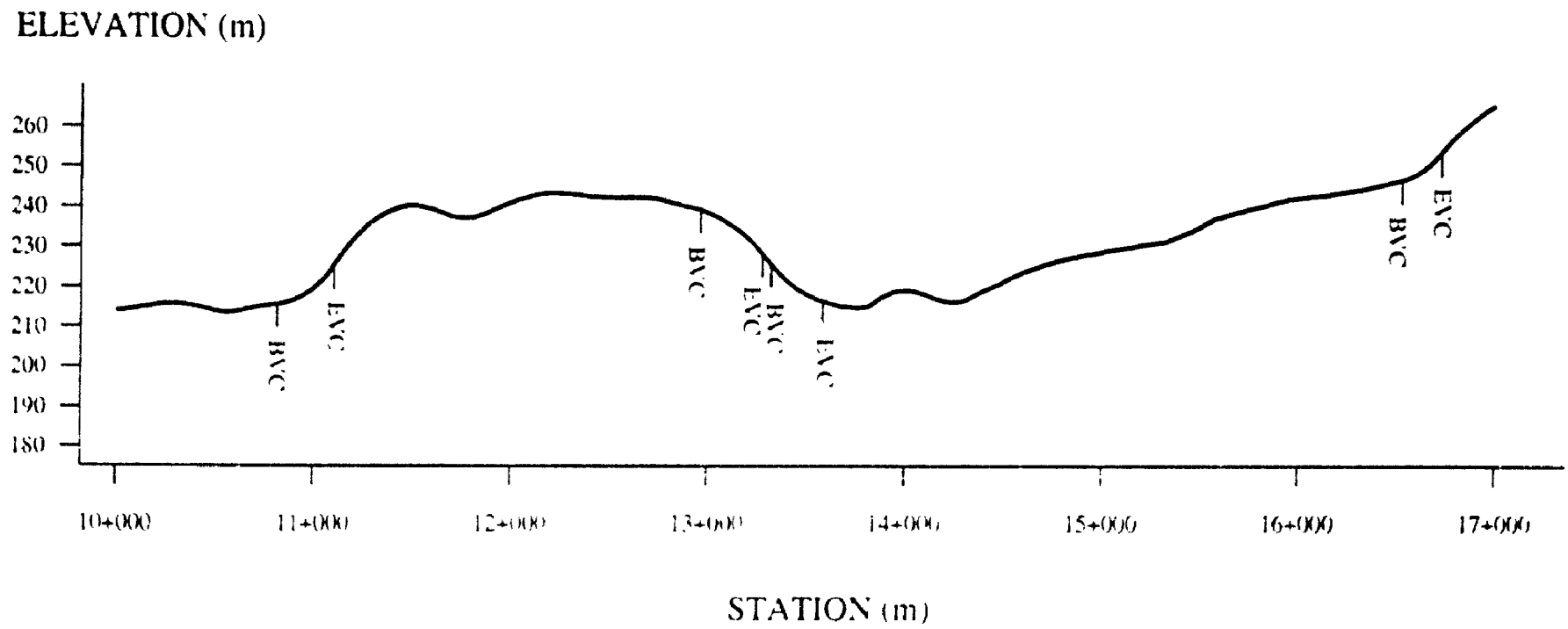

Stations are every 1000 m.

FIGURE 6.3: Vertical Alignment of Highway Segment.

curves to the superelevation rate (up to 5.90%). Shoulder width is mainly 2.5 m but varies up to 1.5 m. Shoulder cross-slope is mainly 6% and varies on curves depending on the superelevation rate. Finally, side-slopes vary widely and include fill in both sides, cut in both sides, fill in one side and cut in the other, and vertical cut in rock areas. However, in cut sections, a down-slope (with or without a ditch) is introduced before the up-slope. Figure 6.4 shows examples for four different cross-sections. In defining the cross section data to the computer software, a total of 189 points (out of the original 400 points) were used. The cross-section data for any other point is estimated by linear interpolation.

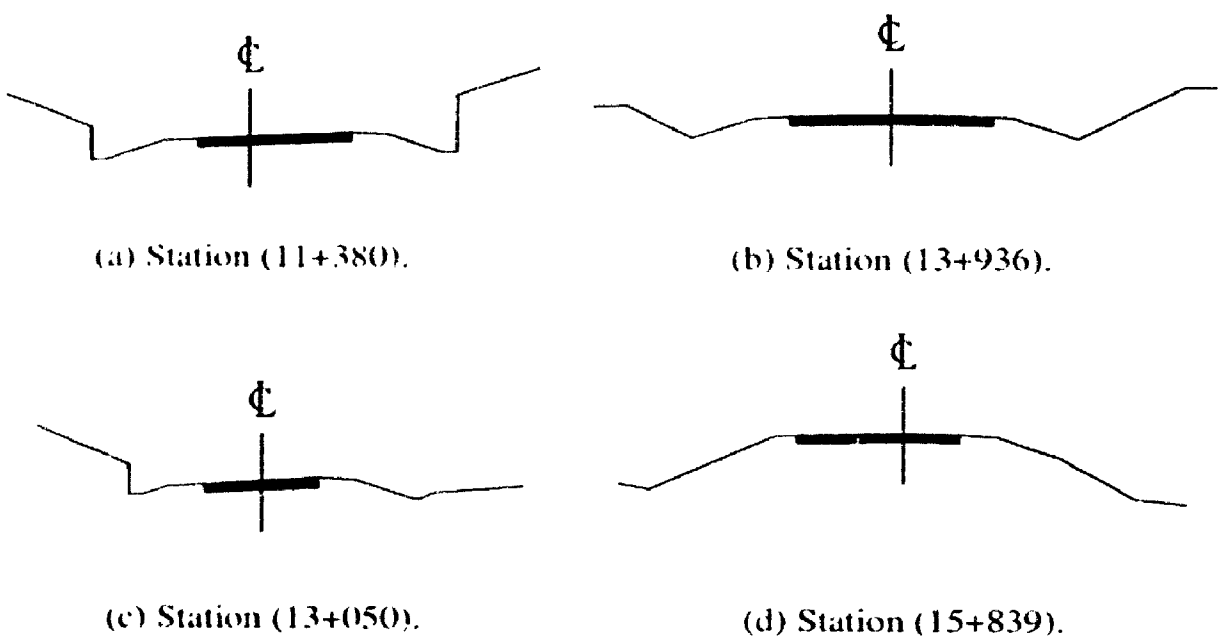

(a) Station (11+380). (b) Station (13+936).

(c) Station (13+050). (d) Station (15+839).

FIGURE 6.4: Examples for Different Cross-Sections of Highway Segment.

As shown in the figures, there is no separate curve (horizontal or vertical) with long tangents along most of the alignment. Subsequently, the available models for sight distance cannot be used to evaluate the sight distance on the segment. Currently, the available sight distance on such alignment can be determined only graphically using approximate 2-D projections or in the field using sight distance targets (Figure 5.10). Both techniques are adopted in the current marking standards (MUTCD, 1998), and obviously, both techniques are time consuming, expensive, and subject to human errors. In addition, two more important disadvantages are: (1) the designer (in case of a new design or modifying an existing highway) does not have the flexibility to change the alignment and check the gains or losses in passing zones and (2) the decision of allowing or prohibiting passing manoeuvres on any specific segment is in the hands of the field crew, and engineers do not have proper tools to oversee these decisions.

6.2 Application Objectives and Procedure

6.2.1 Application Objectives

The disadvantages of the current marking practice, mentioned above, can be overcome using the analytical models and computer software developed in this research. Therefore, an application example for using the computer software in marking passing and no passing zones is presented here. The main objectives of the marking application are:

1. To demonstrate the applicability of the developed analytical models and computer software and their ability to evaluate the available sight distance on real highway segments.

3 OF/DE 3

PM-1 3½"x4" PHOTOGRAPHIC MICROCOPY TARGET
NBS 1010a ANSI/ISO #2 EQUIVALENT

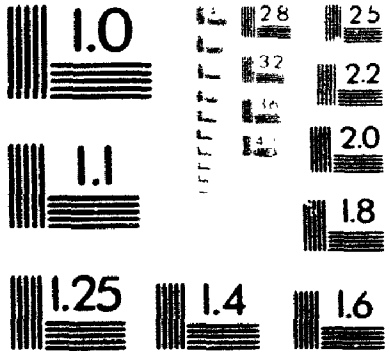

PRECISION℠ RESOLUTION TARGETS

2. To pinpoint the important points that should be taken care of when using the developed software, specifically, alignment preparation, element size, and computer run-time.
3. To compare between the 2-D and 3-D available sight distances and to quantify the range of error associated with ignoring the 3-D nature of highway alignments.
4. To compare the marking obtained by the developed software with the current marking in the field.
5. To compare the marking according to the MUTCD (1995) standards with that according to the criteria developed in this research (Chapter 3).

6.2.2 Computer Programs and User-Specified Parameters

Because of the changes in the pavement width and lateral obstruction due to cut slopes (horizontal alignment) and because of the spline grades (vertical alignment), both ***MARKH*** and ***MARKV*** could not be used in this application. Thus, ***MARKS*** was used in this application to evaluate the available sight distance, S_m, on 2-D separate horizontal and vertical alignments. On the other hand, ***MARKC*** was used to evaluate S_m on the 3-D combined alignment. As explained previously, in both programs, the user specifies certain parameters which control the minimum sight distance to be checked, S_m, accuracy of the calculated sight distance, ACC, and the range of stations on which the sight distance should be evaluated (first and last station and step between each two successive stations).

Although the current marking standards specifies a 300-m minimum PSD corresponding to a speed limit of 90 kph (MUTCD, 1995), S_m was specified as 400 m which corresponds to the minimum PSD developed in the research (Figure 3.9). Therefore, the range of stations on which S_m could be calculated was 10+000 to 16+600, for the right lane, and 10+400 to 17+000, for the left lane. The step between each two successive stations, STEP, was set as 10 m. Thus, S_m was determined on a total of 661 stations on each lane. Finally, ACC was set as 1.0 m. However, to speed up the computer runs, S_m was checked using 100-m jumps. If the sight distance was obstructed, the finer 1.0-m jump was used to determine S_m to the required accuracy.

6.2.3 Experimental Design

Referring to the parameters set above, a single computer run involved the calculation of S_m to the nearest 1.0 m on a total of 1322 stations. In order to achieve the objectives listed earlier, a four-phase study was carried out as follows.

Phase (1): Effect of Element Size. Reducing the element size increases both the modelling accuracy and the computer run-time. While the former is desirable, the latter is not. Therefore, different element sizes were used to study the trade-offs between the modelling accuracy and computer run-time in 2-D and 3-D alignments. Three element sizes; namely, 10, 25, and 50 m; were used to evaluate S_m in 2-D separate horizontal alignment, 2-D separate vertical alignment, and 3-D combined alignment (total of 9 runs). It should be noted, however, that these element sizes are the maximum size that can be

used for any small element (on horizontal curves or vertical spline grades). The real element size is variable and depends on the length of each segment between two successive points used to define the horizontal alignment, the vertical alignment, or the cross-section. Also, this element size does not control the long elements used on straight segments or parabolic vertical curves. The heights of the driver eye and the object, h_1 and h_2, were taken as 1.05 and 1.30 m, respectively (TAC, 1986).

Phase (2): 2-D Versus 3-D Sight Distances. The same runs in the first phase can be used to compare the 2-D and 3-D sight distances. Thus, the effect of ignoring the 3-D nature of highway alignment regrading the sight distance can be quantified.

Phase (3): Comparison with Existing Marking in the Field. According to the current marking standards (MUTCD, 1995), a no-passing zone should begin on vertical alignments when a 1.05-m object is not visible to a driver eye at 1.05-m height. However, the same no-passing zone should end when a 0.30-m object is visible to a driver eye at 1.05-m height. On horizontal alignments, a constant object height of 0.30 m is used. Therefore, two computer runs with 1.05 and 0.30-m object heights were carried out on the 2-D separate vertical alignment. Another run with a 0.30-m object height was carried out on the 2-D separate horizontal alignment (total of 3 runs). In this last case, a continuous lateral obstruction after a 3-m shoulder is added on right-turn curves to simulate the MUTCD (1995) standards used by MTO. The element size in each of these runs was taken as the optimum size determined in the first phase.

Phase (4): Marking Using Profiles of Available and Required PSD. In this phase, practical marking considerations developed for marking passing and no-passing zones (Chapter 3) are used with the profile of S_a to establish the optimum marking. The driver eye and object heights were taken as 1.05 and 1.30 m, respectively. It should be noted that the object height of 1.05 m is set in the MUTCD standards to mark the two lanes at the same time and reduce the amount of work, which is not a matter of concern when using the computer software. Since these runs were already included in the first phase, no additional runs are require in this phase.

In summary, a total of 12 runs were conducted in this application. The main parameters in these runs are summarized in Table 6.1.

TABLE 6.1: Summary of Experimental Design.

Parameter	2-D Separate Alignment		3-D Combined Alignment
	Horizontal	Vertical	
Software	*MARKS*	*MARKS*	*MARKC*
Element size (m)	10, 25, 50	10, 25, 50	10, 25, 50
Height of driver eye, h_1 (m)	1.05	1.05	1.05
Height of object, h_2 (m)[a]	1.30, 0.30	1.30, 1.05, 0.30	1.30
Number of runs	4	5	3

[a] Only h_2 of 1.30 m is used with the three element sizes. Other values of h_2 are used with a specific element size

6.3 Results and Analysis

6.3.1 Phase 1: Effect of Element Size

The nine computer runs, where the main variable is the element size, were carried out. Figure 6.5 shows the element net created by *MARKS* to model the lateral obstructions due to the cut-slopes in the 2-D horizontal alignment using a 25-m maximum element size, while the element net to model the highway surface in the 2-D vertical alignment is shown in Figure 6.3. An example for the element net created by *MARKC* to model the highway surface and side-slopes in the 3-D combined alignment using a 25-m maximum element size is shown in Figure 6.6.

The computer run-time for each run is shown in Table 6.2. The table shows also the effect of the element size on the calculated available sight distance, S_{av}. The smallest element size of 10 m is used as a reference and the effect of any other specific element size, *Eff*, is defined as:

$$Eff = \frac{S_{av}\ (specific\ element\ size) - S_{av}\ (10\text{-}m\ element\ size)}{S_{av}\ (10\text{-}m\ element\ size)} \times 100 \qquad (6.1)$$

where *Eff* can be positive or negative.

As shown in the table, expectedly, reducing the element size increases the computer run-time. However, the rate of increase in run-time varies in each of the three cases shown in the table (2-D horizontal, 2-D vertical, and 3-D combined). First, since most of the vertical alignment is spline grade, and is modelled by short elements, reducing the element size will increase the number of elements and run-time with almost the same ratio. However, because the parabolic curves and tangents are modelled with

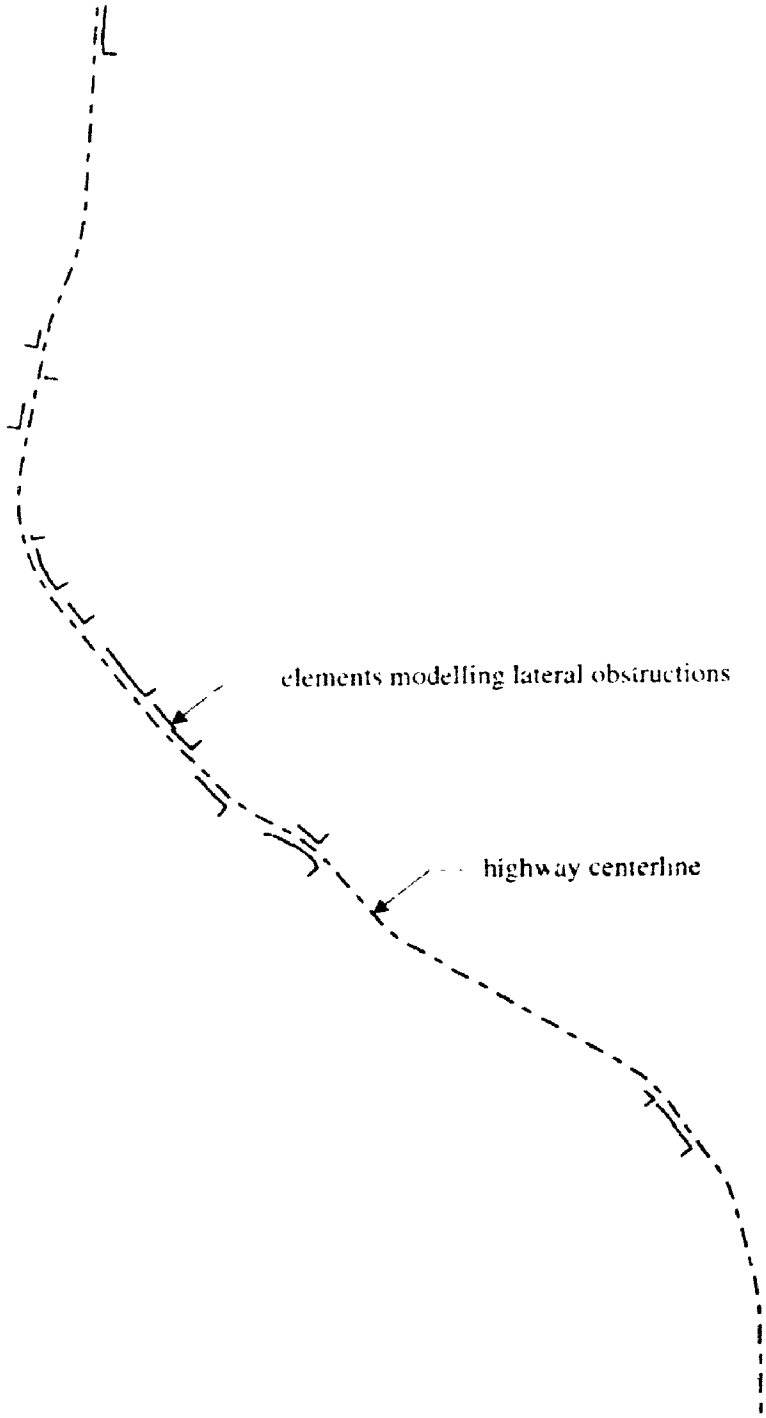

FIGURE 6.5: Element Net for 2-D Horizontal Alignment.

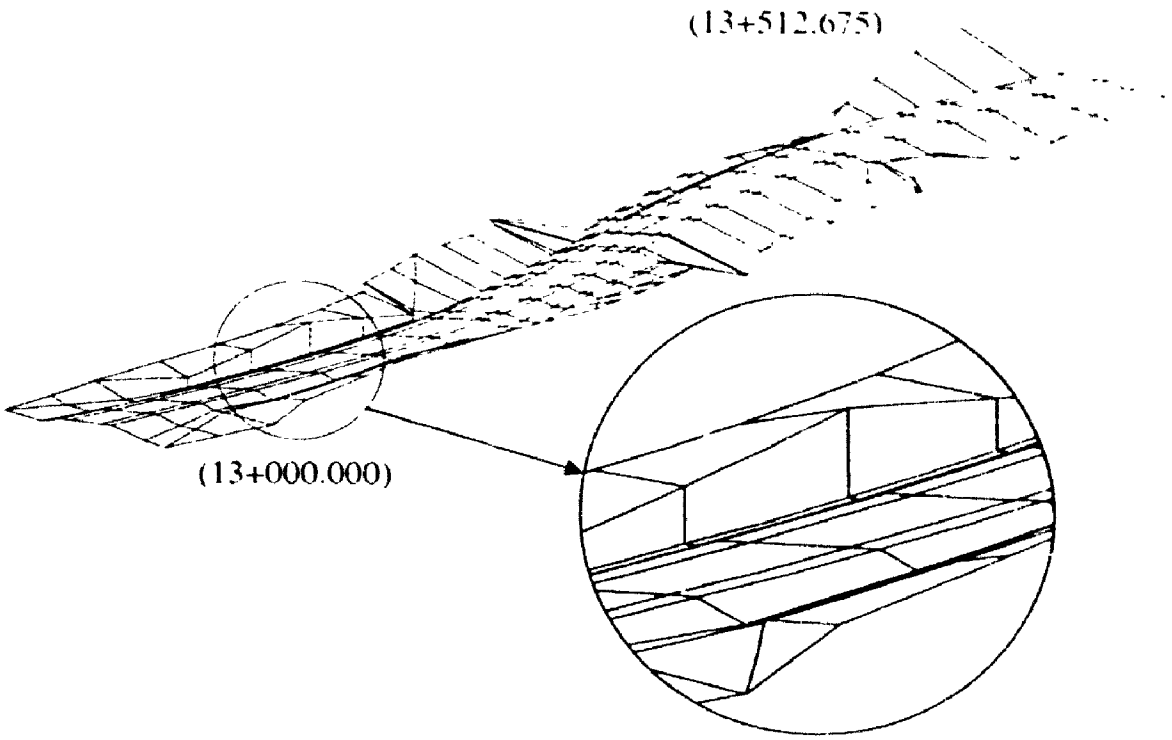

FIGURE 6.6: Example of Element Net for 3-D Combined Alignment.

TABLE 6.2: Effect of Element Size.

Element Size	2-D Separate Alignment		3-D Combined Alignment
	Horizontal	Vertical	
(a) Computer Run-Time (minutes)[a].			
10 m	3.77	7.38	342.02
25 m	2.77	3.28	164.53
50 m	2.55	1.88	117.78
(b) *Eff* (Equation 6.1).			
25 m	-2.20 to +0.90%	-0.48 to +1.02%	-0.46 to +0.51%
50 m	-2.19 to +50.57%	-0.98 to +3.11%	-1.13 to +0.86%

[a] Using a 486-PC with 66 MHZ speed

one element each, regardless of the maximum element size, the rates of increase in number of elements and run-time are slightly less than the rate of reduction in element size. As for the horizontal alignment, a large portion of the alignment consists of tangents where the element size does not depend on the maximum size. In addition, each point used to define the horizontal alignment or the cross-section must fall at the end of an element and the beginning of a new element. The large number of points used in defining the cross-section data (189 points) would produce an average element length of 37.2 m regardless of the maximum size. Therefore, the rates of increase in number of elements and run-time are considerably less than the rate of reduction in element size. The same argument is also valid for the 3-D combined alignment.

As shown also in the table, the low values of *Eff* indicates that increasing the element size from 10 to 25 m would result in slight reduction in the modelling accuracy of 2-D and 3-D alignments. The same argument is also valid for 2-D vertical alignment and 3-D combined alignment when the element size is increased from 10 to 50 m. On the other hand, the 50-m maximum element size produced a considerably high value of *Eff* (50.57%) in case of 2-D horizontal alignment. This high value of *Eff* occurred at one station only (13+050 on the right lane), and the next highest value of *Eff* was 6.17%. The reason for this high value of *Eff* can be referred to the modelling of the lateral obstruction between station 13+100 to 13+150. Cross-section data are defined at both stations and are interpolated for any intermediate station. The exact lateral clearance from the highway centerline to the left lateral obstruction produced by the cut-slope is constant (9.41 m) from station 13+100 to 13+140.8, and then increasing gradually to 12.212 m at

station 13+150. As shown in Figure 6.7, this profile of lateral clearance was modelled almost exactly using 5 elements of 10 m element size each. However, for a 50 m element size, only one element was generated to model the obstruction. Although the element had the exact lateral clearance at 13+100, 13+125, and 13+150, using a single curve to fit these three points slightly underestimated the lateral clearance from station 13+100 to 13+125 and overestimated it from station 13+125 to 13+150. This latter overestimation of the lateral clearance caused the sight distance on station 13+050 to be overestimated from 266 m to unobstructed (400 m).

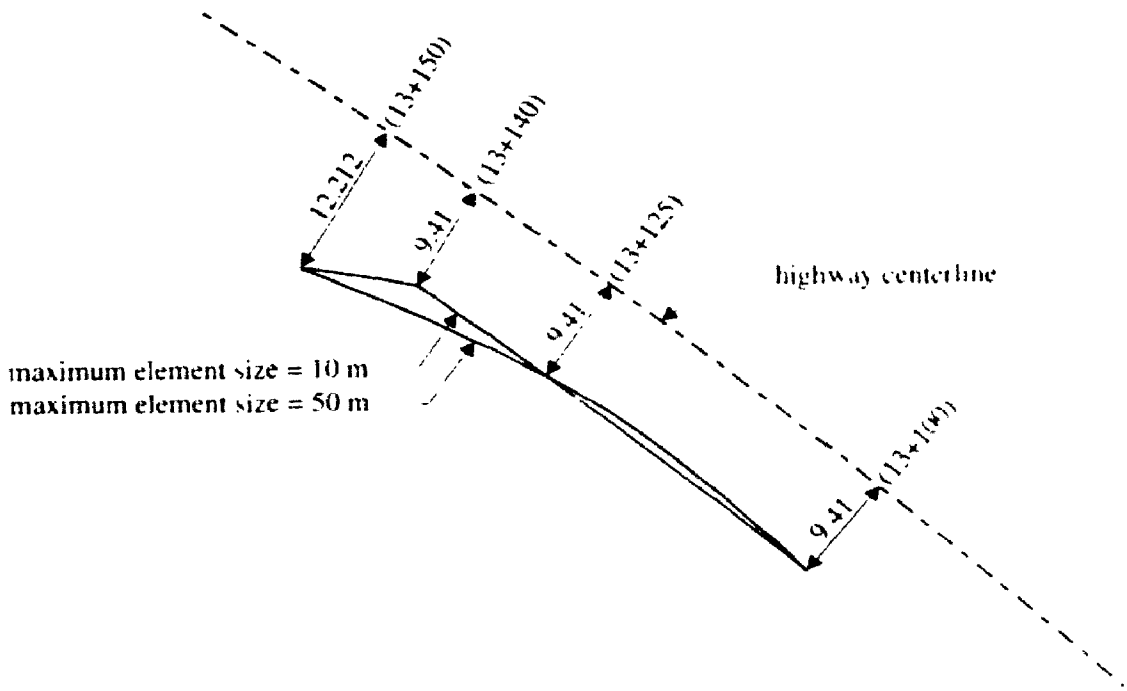

FIGURE 6.7: Lateral Obstruction in 2-D Horizontal Alignment from Station (13+100) to Station (13+150).

It should be noted, however, that this problem was associated with the 2-D horizontal alignment with variable side-slope data. For the 3-D combined alignment, using surfaces to model the side-slopes did not cause the same accuracy problem. Moreover, the values of *Eff* in the case of 3-D combined alignment were considerably less than those in both 2-D horizontal and vertical alignments. This shows that the 3-D modelling produces a relatively better accuracy which is less dependent on the element size.

In summary, a caution should be practiced in selecting the element size in 2-D horizontal alignments. Noting that the run-time in this case is significantly short, small element size is recommended if the side-slope data vary along short distances. On the other hand, the element size does not have a significant effect on the modelling accuracy of 2-D vertical alignments or 3-D combined alignments. For this specific segment, a 25-m element size represents the best compromise between the run-time and the accuracy.

6.3.2 Phase 2: 2-D Versus 3-D Sight Distances

In this phase, the results of sight distance obtained in the first phase for a 25-m element length are used to compare the 2-D and 3-D alignments. At any station, the 2-D sight distance or 2-D PSD refers to the minimum of the two values of passing sight distance (PSD) determined from 2-D horizontal and vertical alignments. The corresponding sight distance determined from the 3-D combined alignment is referred to as the 3-D sight distance or 3-D PSD. Profiles of both 2-D and 3-D PSD are shown in Figure 6.8, and

the percentage difference, *Diff*, is shown in Figure 6.9. The percentage difference, *Diff*, is used to compare the 2-D and 3-D sight distances, and is defined as

$$Diff = \frac{(2\text{-}D\ sight\ distance) - (3\text{-}D\ sight\ distance)}{(3\text{-}D\ sight\ distance)} \times 100 \qquad (6.2)$$

The 3-D sight distance is a more accurate value, and, as shown in Equation 6.2, it is takes as the reference of comparison. Thus, a negative value of *Diff* indicates that the 2-D alignment underestimates the available sight distance, while a positive value indicates that the 2-D alignment overestimates the available sight distance.

As shown in Figure 6.9, the absolute value of *Diff* is considerably high for both lanes. *Diff* can be as low as -51.00% indicating that designing the highway alignment based on 2-D analysis compromises the economics of the project due to using horizontal and vertical curves that are flatter than need. In the marking of passing and no passing zones, passing may be prohibited on segments with adequate sight distance causing unjustified reduction of the highway capacity. On the other hand, *Diff* can be as high as 11.51% indicating that designing the highway alignment based on 2-D analysis compromises the traffic safety due to using horizontal and vertical curves that are sharper than needed. In the marking of passing and no-passing zones, passing may be allowed on segments with inadequate sight distance generating unsafe passing manoeuvres.

A close investigation of *Diff* with the horizontal and vertical alignment and cross section data showed that the positive values of *Diff* were encountered at combined horizontal and crest vertical curves in cut sections. In such cases, the crest vertical curves cause both the driver eye and the object to *sink* relative to the lateral obstruction. Thus,

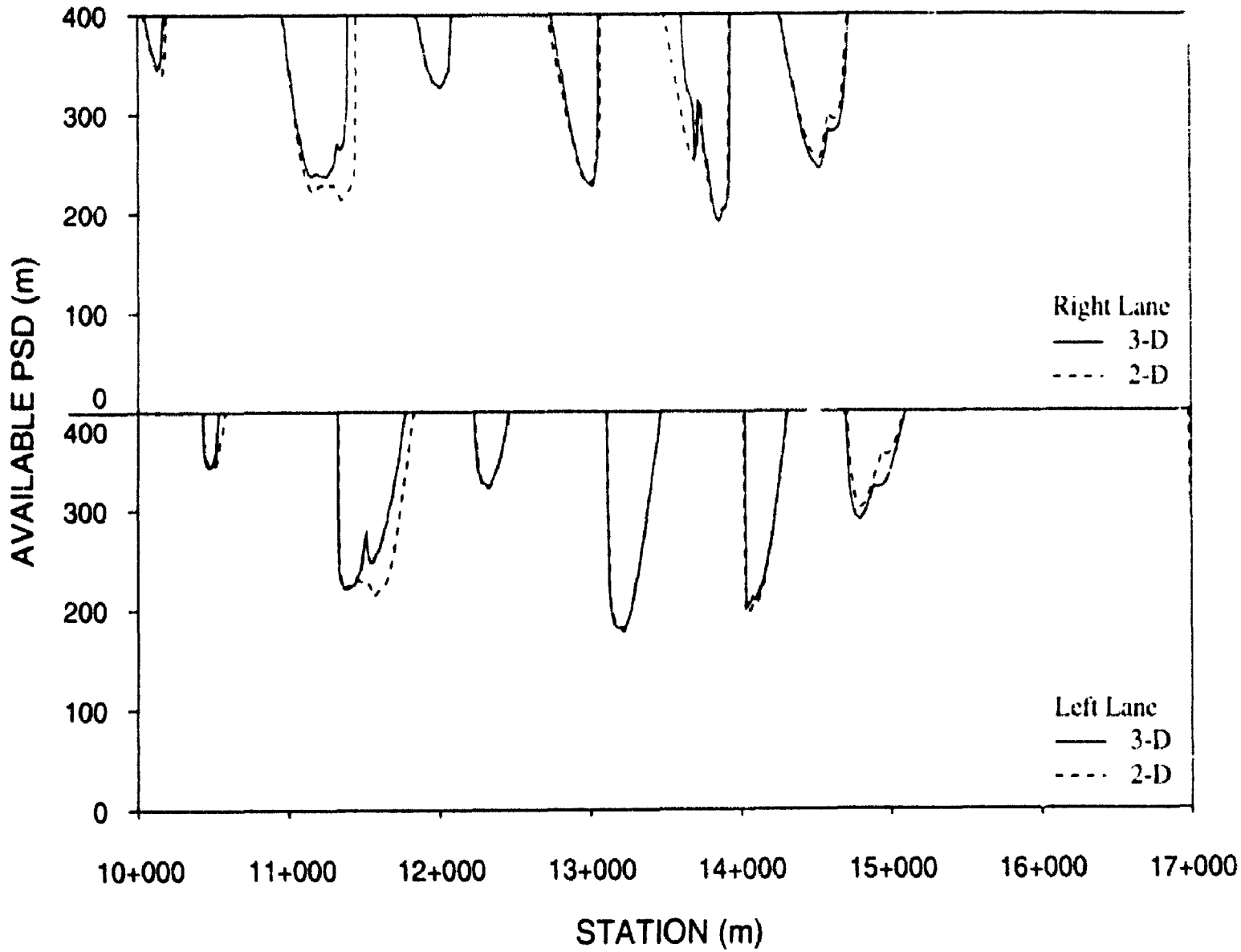

FIGURE 6.8: Profile of Available PSD in 2-D and 3-D Alignments.

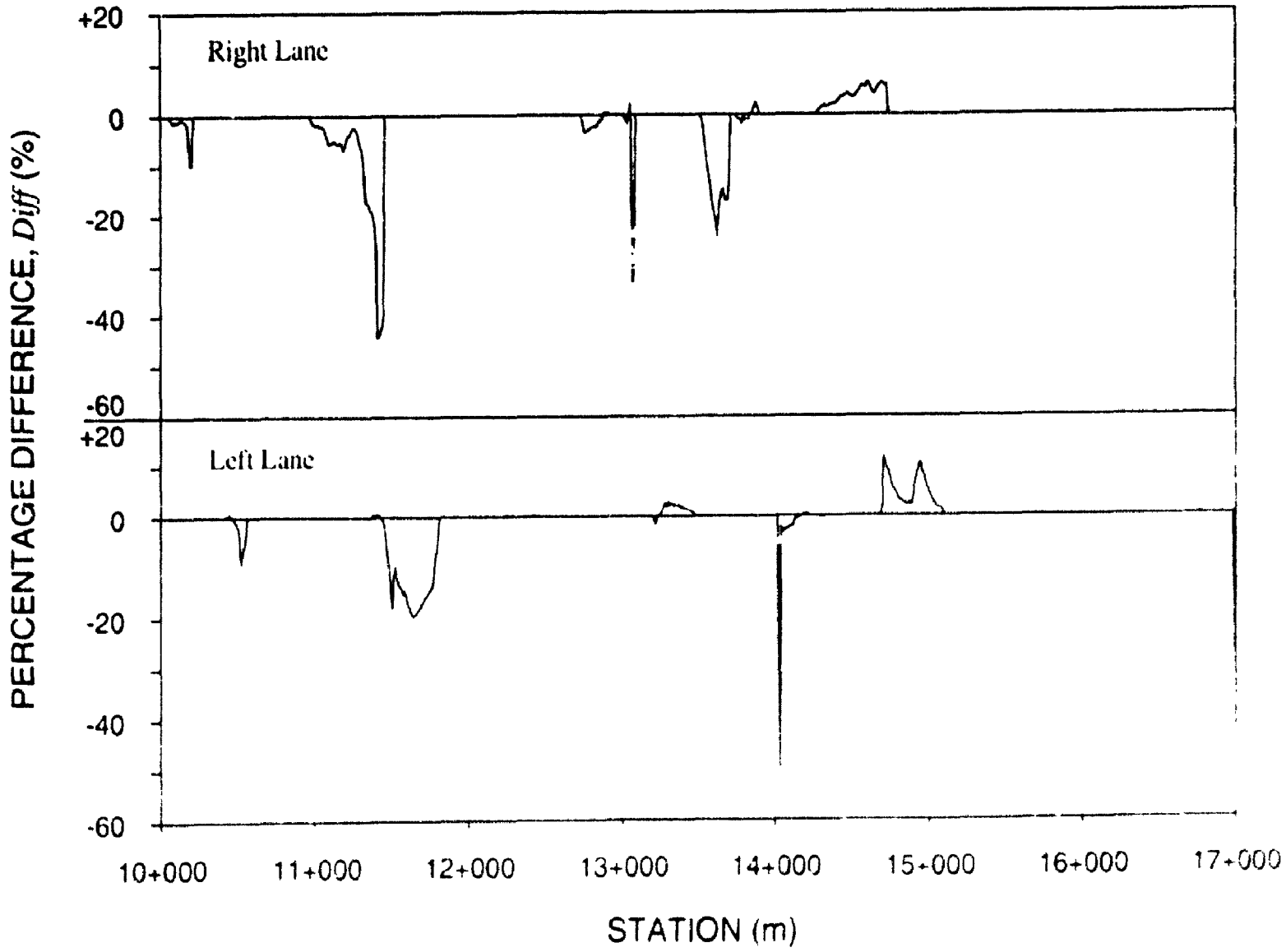

FIGURE 6.9: Percentage Difference Between 2-D and 3-D Sight Distances.

the lateral clearance at which the sight line becomes tangent to the lateral obstruction is less than the lateral clearance calculated at the average height between the driver eye and the object in 2-D horizontal alignment. On the other hand, the negative values of *Diff* were encountered at two situations, combined horizontal and sag vertical curves in cut sections and combined horizontal and crest vertical curves in fill sections. The first case is the opposite of the case with positive *Diff*, where the sag curve causes the effective lateral clearance to be greater than that calculated at the average height between the driver eye and the object in 2-D horizontal alignment. In the second case, the superelevation on the horizontal curve lowers the highway surface relative to the sight line. Therefore, the crest vertical curve becomes less critical than it looks to be in 2-D vertical alignment. These three cases are discussed in more detail in Chapter 7.

6.3.3 Phase 3: Comparison with Existing Marking in the Field

As explained earlier, the profile of available PSD obtained by *MARKS* and *MARKC* can be used to determine the marking of passing and no-passing zones on two-lane highways. Figure 6.10 shows the profile of available PSD in 2-D alignments according to MUTCD (1995) standards used by MTO. According to these standards, the minimum required PSD, corresponding to a 90-kph speed limit, is 300 m. The available PSD at any specific station is the lower of PSD on horizontal and vertical alignments. In calculating the PSD on the horizontal alignment, the object height, h_2, is set as 0.30 m and a vertical continuous obstruction after a 3-m shoulder is added on right-turn curves. For the vertical alignment, h_2 is initially set as 1.05 m. If a no-passing zone is detected (S_{av} < 300 m),

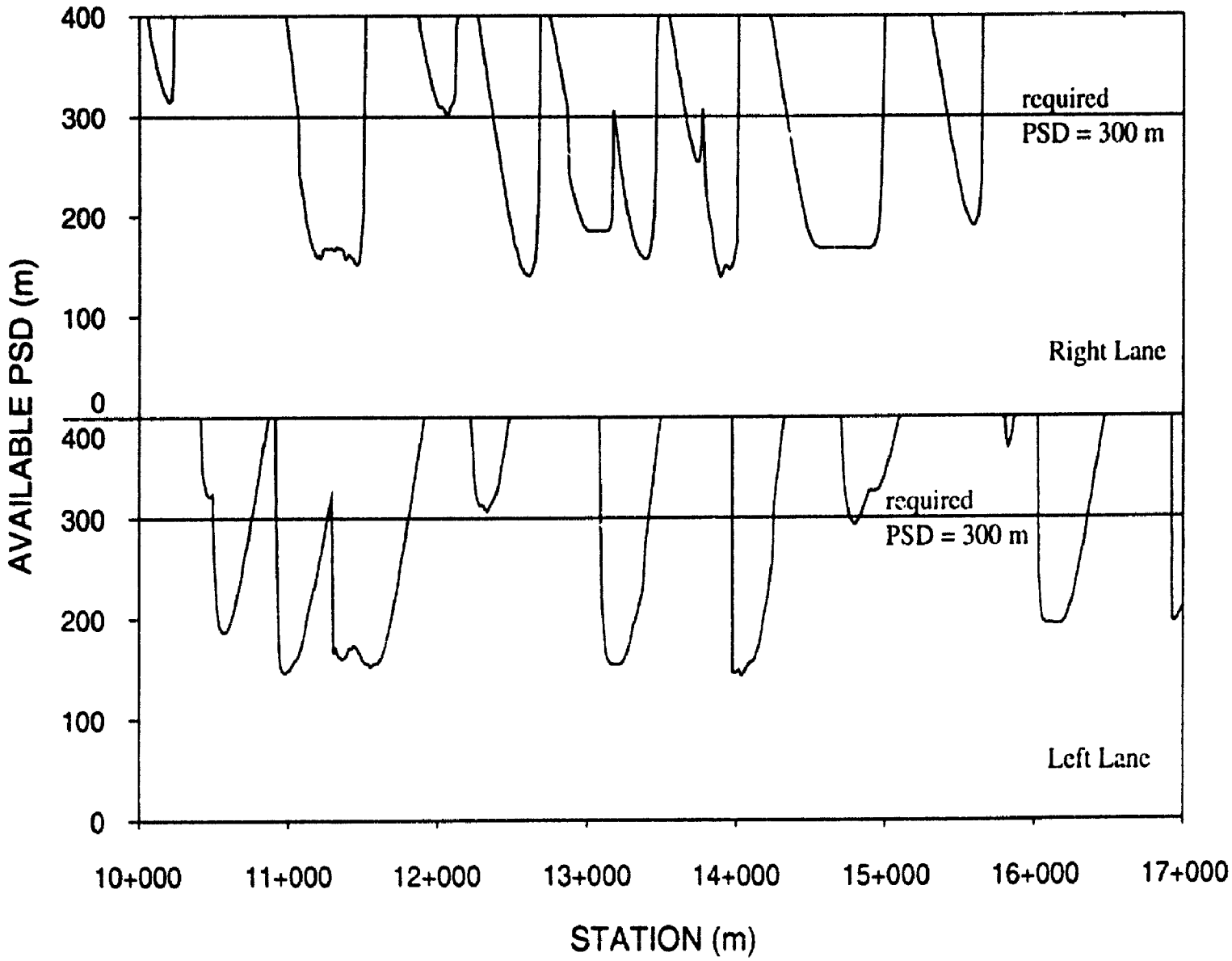

FIGURE 6.10: Profile of Available PSD According to MUTCD (1995) Standards.

h_2 is set as 0.30 m until the no-passing zone ends where h_2 is re-set as 1.05 m. As shown in the figure, a no-passing zone should be marked wherever the available PSD drops below the 300-m minimum required PSD.

Additional considerations in marking passing and no-passing zones are (MUTCD, 1995):

1. The minimum length of passing zones, l_Z, is 280 m. If a passing zone has a length less than 280 m, passing should be prohibited and a no-passing zone is warranted. This warrant was not considered at the segment's both ends.
2. The minimum length of no-passing zones is 150 m. If a no-passing zone has a length less than 150 m, an additional length should be added to the beginning of the no-passing zone This warrant was not considered at the segment's both ends.
3. When a passing or a truck climbing lane is added in a specific direction, a no-passing zone should be marked in the same direction. The no-passing zone begins 100 m before the beginning of the widening taper and ends at the end of the narrowing taper (if the sight distance is unobstructed). However, the opposite direction can be marked as passing or no-passing depending on the available PSD. Therefore, a no-passing zone is warranted from station 10+640 to 12+550 on the right lane and from station 17+000 to 16+420 on the left lane.
4. A no-passing zone should be marked on bridges which are not 1.25 m or more wider than the approach pavement. The no-passing zone begins 120 m before the bridge structure and ends at its end (if the sight distance is unobstructed). Therefore, a no-

passing zone is warranted from station 13+630 to 13+776 on the right lane and from station 13+896 to 13+750 on the left lane.

A summary for the marking of passing and no-passing zones obtained using the profile of available PSD is shown in Table 6.3. If a no-passing zone is warranted at a specific segment, the warrant is given in the table. The actual marking in the field was recovered by the MTO Traffic Section, and is shown in Table 6.4. Comparing the marking in Tables 6.3 and 6.4 shows that the marking based on the profile of PSD matched all the passing zones in the field. However, a considerable length that is safe for passing according to MUTCD (1995) standards is marked as no-passing in the field. Although, ignoring the single obstructions in the computer runs may contribute to this difference, the consideration of a continuous obstruction after a 3-m shoulder on right curves reduces this possibility significantly. On the other hand, there are some no-passing zones where the warrants are not obvious and could not be lateral obstructions. For example, on the right lane in the field, a no-passing zone begins at station 16+532 while the segment remains straight in the horizontal alignment until station 16+928.556. In the vertical alignment, the segment consists of a sag curve followed by a tangent and a smooth crest curve that does not obstruct the sight distance until station 16+680. In addition, no intersections are encountered at this specific section. Thus, this loss of almost 150-m passing zone is not justified.

TABLE 6.3: Marking Using Profile of Available PSD and MUTCD (1995) Standards.

Right Lane			Left Lane		
Station	Marking		Station	Marking	
	P or N	Warrant[a]		P or N	Warrant[a]
10+000			17+000		
	P	-----		N	PSD
10+640			16+920		
	N	passing lane		N	passing lane
11+020			16+370		
	N	PSD		N	PSD
11+470			16+020		
	N	passing lane		P	-----
12+320			14+900		
	N	PSD		N	length of no-passing zone
12+640			14+850		
	N	length of passing zone		N	PSD
12+820			14+750		
	N	PSD		P	-----
13+420			14+250		
	N	length of passing zone		N	PSD
13+610			13+970		
	N	PSD		N	length of passing zone
13+970			13+896		
	P	-----		N	bridge
14+290			13+750		
	N	PSD		P	-----
14+290			13+420		
	P	-----		N	PSD
15+410			13+080		
	N	PSD		P	-----
15+650			11+810		
	P	-----		N	PSD
16+600			10+920		
				N	length of passing zone
			10+760		
				N	PSD
			10+490		
				P	-----
			10+400		

P = passing zone, N = no-passing zone
Right and left lanes are relative to the direction of increasing stations
[a] Warrant for no-passing zones

TABLE 6.4: Segment Marking in the Field.

Right Lane		Left Lane	
Station	Marking	Station	Marking
10+000		17+000	
	P		N
10+050		15+700	
	N		P
16+024		15+286	
	P		N
16+532		10+460	
	N		P
17+000		10+000	

P = passing zone, N = no-passing zone
Right and left lanes are relative to the direction of increasing stations

6.3.4 Phase 4: Marking Using Profiles of Available and Required PSD

As explained in Chapter 3, there are a number of safety concerns associated with the marking of passing and no-passing zones according to MUTCD standards. First, the current standards fail to consider the effect of the traffic characteristics on the minimum required PSD. A 300-m PSD is set for the 90-kph speed limit regardless of the vehicles' acceleration and deceleration capabilities or length. On the other hand, the revised model, presented in Chapter 3, can consider these traffic characteristics. For a passenger car passing a passenger car (both are 5 m long) and for the acceleration and deceleration capabilities discussed in Chapter 3, the required PSD is 398.9 m. Second, the same argument is valid for the minimum length of passing zones. For the same assumptions for PSD, the minimum length of passing zones is 203.3 m compared to the 280-m length

recommended in the standards. Third, according to the MUTCD standards, passing zones should end when the available PSD becomes less than the required PSD. However, since the maximum sight distance is required some distance after the pass initiation (at the critical position), the available PSD at this position will be significantly less than the required PSD. Subsequently, a pass that begins legally near the end of a passing zone will not have a sufficient sight distance for safe manoeuvring. On the other hand, the revised model uses the profile of available and required PSD to ensure that any specific pass beginning at a passing zone will have a sufficient PSD along the entire pass.

In this phase, the profiles of 2-D and 3-D available sight distance shown in Figure 6.8 and the profile of required PSD shown in Figure 3.11 are used to establish the passing and no-passing zones. A computer program was written to automate the comparison between available and required PSD as explained in Chapter 3 (Figure 3.12). The resulting markings for 2-D and 3-D alignments, referred to as the 2-D and 3-D marking, are shown in Tables 6.5 and 6.6, respectively.

Comparing Tables 6.5 and 6.6 shows that the 2-D and 3-D markings are almost the same. According to the 2-D marking, a total of 130 m (4.5% of the 2900-m total length of passing zones on the segment), where passing can be achieved safely, are marked as no-passing on the right lane (this total should have been 220 m if the warrant for passing lane is not applicable). The corresponding length on the left lane is 100 m (3.2% of the 3090-m total length of passing zones on the segment). On the other hand, just 10 m on the right lane (0.3% of the length of passing zones) are marked as passing while the 3-D marking indicates that passing manoeuvres are unsafe. This last condition

TABLE 6.5: Marking Using Profiles of Required and 2-D Available PSD.

Right Lane			Left Lane		
Station	Marking		Station	Marking	
	P or N	Warrant[a]		P or N	Warrant[a]
10+000			17+000		
	N	PSD		N	passing lane
10+050			16+420		
	P	-----		P	---
10+640			15+290		
	N	passing lane		N	PSD
10+750			14+840		
	N	PSD		P	-
11+370			14+520		
	N	passing lane		N	PSD
11+640			14+070		
	N	PSD		N	length of passing zone
11+950			13+896		
	N	passing lane		N	bridge
12+520			13+750		
	N	PSD		N	length of passing zone
13+000			13+680		
	P	-----		N	PSD
13+300			13+180		
	N	PSD		P	-- --
13+880			12+670		
	N	length of passing zone		N	PSD
14+070			12+370		
	N	PSD		P	-- --
14+590			12+020		
	P	-----		N	PSD
16+600			11+390		
				P	--
			10+770		
				N	PSD
			10+560		
				P	-----
			10+400		

P = passing zone, N = no-passing zone
Right and left lanes are relative to the direction of increasing stations
[a] Warrant for no-passing zones

TABLE 6.6: Marking Using Profiles of Required and 3-D Available PSD.

Right Lane			Left Lane		
Station	Marking		Station	Marking	
	P or N	Warrant[a]		P or N	Warrant[a]
10+000			17+000		
	N	PSD		N	passing lane
10+0 ,0			16+420		
	P	-----		P	-----
10+640			15+300		
	N	passing lane		N	PSD
10+750			14+820		
	N	PSD		P	-----
11+300			14+520		
	N	passing lane		N	PSD
11+640			14+080		
	N	PSD		N	length of passing zone
11+950			13+896		
	N	passing lane		N	bridge
12+540			13+750		
	N	PSD		N	length of passing zone
12+990			13+680		
	P	-----		N	PSD
13+400			13+180		
	N	PSD		P	-----
13+880			12+670		
	N	length of passing zone		N	PSD
14+060			12+370		
	N	PSD		P	-----
14+600			11+980		
	P	-----		N	PSD
16+600			11+390		
				P	-----
			10+740		
				N	PSD
			10+560		
				P	-----
			10+400		

P = passing zone, N = no-passing zone
Right and left lanes are relative to the direction of increasing stations
[a] Warrant for no-passing zones

is not experienced on the left lane. Subsequently, the 2-D and 3-D marking does not yield large differences in the marking of passing and no-passing zone. This is due to the considerable length upon which a sufficient PSD is required. As a result, the short distances which have significant differences between 2-D and 3-D sight distances do not yield large differences in the marking. In addition, as shown in Figure 6.8, most of the differences between the 2-D and 3-D PSD are experienced at sections with available PSD less than the required PSD.

However, a more significant difference can be seen in comparing the marking based on the profiles of required and 3-D available PSD and the marking according to the MUTCD standards (Tables 6.6 and 6.3, respectively). As shown in the two tables, the MUTCD results a total of 350 m on the right lane (15.0% of the 2330-m total length of passing zones) and 1190 m (36.0% of the 3310-m total length of passing zones) on the left lane to be marked as passing while they are unsafe according to the marking based on the profiles of required and 3-D available PSD. Also, 1040 m on the right lane and 980 m on the left lane (44.6 and 29.6% of the corresponding total length of passing zones) are marked as no-passing while they are safe according to the marking based on the profiles of required and 3-D available PSD.

Comparing Tables 6.4 and 6.6, it can be seen that the field marking has a total of 30 m (5.4% of the 558-m total length of passing zones) on the right lane and 14 m (3.0% of the 474-m total length of passing zones) on the left lane are marked as passing although they are unsafe according to the marking based on the profiles of required and 3-D available PSD. On the other hand, 2492 m on the right lane and 2690 m on the left

lane (446.6 and 567.5% of the corresponding total length of passing zones) are marked as no-passing while they are safe according to the marking based on the profiles of 3-D available and required PSD.

6.4 Summary

It is shown in the 4-phase study presented in this chapter that the 2-D and 3-D computer programs, *MARKS* and *MARKC*, can determine the profile of available sight distance on real highway segments with complex alignments and variable side-slopes. The programs use the data that are already available in the highway agencies, and can reduce the time required to evaluate the sight distance significantly. In addition, using these computer programs reduces the cost, avoids human errors, and provides high flexibility to change the alignment and evaluate the resulting sight distance and the gains or losses in passing zones. Moreover, the decision for marking passing and no-passing zones is transferred to the engineers instead of the technicians in the field crew. However, when using the computer programs, users must be aware of the trade-offs between the computer run-time and the accuracy where both increase as the element size decreases. Generally, the element size can be set as large as 50 m if the alignment and the cross-section data are regular. As the irregularity in the side-slopes increases, smaller elements should be use.

Comparing the 2-D and 3-D sight distances shows that differences can be significant. Ignoring the 3-D nature of highway alignments may overestimate or underestimate the available sight distance. However, because of other warrants in the marking of passing and no-passing zones, the resulting marking using 2-D and 3-D

alignments would be close, and most of the differences are in the conservative side. On the other hand, comparing the marking according to MUTCD standards and that based on the profiles of available and required sight distance shows that the MUTCD can be too conservative or too liberal.

CHAPTER 7

ESTABLISHMENT OF DESIGN PROVISIONS FOR 3-D HIGHWAY ALIGNMENTS

In this chapter the three cases in which the 2-D and 3-D sight distances are significantly different are examined in more detail. As mentioned in Chapter 6, these cases are: (1) horizontal curve combined with crest vertical curve in cut section, (2) horizontal curve combined with sag vertical curve in cut section, and (3) horizontal curve combined with crest vertical curve in fill section. The model for 3-D available sight distance, presented in Chapter 5, is used to design combined horizontal and vertical alignments in cut and fill sections, and to examine the effect of considering the 3-D combined alignment on two highway design elements; namely the minimum radius of horizontal curves and the minimum length of crest vertical curves (Hassan et al, 1996*d*; 1996*e*).

7.1 Current and 3-D Design Practices

The current highway geometric design practice is explained in detail in Chapter 2. According to this design practice, the main design element of horizontal curves is the radius, R, which is determined so as to satisfy vehicle stability, driver comfort, and sight distance. The minimum radius required for vehicle stability and driver comfort can be determined using Equation 2.10 while the minimum radius required for sight distance can be determined using Equation 2.5. This latter radius should enable a driver with an h_1-eye height to see ahead an object of an h_2-height at a minimum of stopping sight distance

(SSD). Since the design requirements are based on SSD rather than PSD, h_2 in this case is taken as 0.38 m (TAC, 1986). However, h_1 recommended for design is still equal to that recommended for marking (1.05 m). Because the lateral clearance on a curve in a cut section varies with the height, the average height of h_1 and h_2 can be used to calculate the lateral clearance (AASHTO 1994). For a crest or sag vertical curve, the main design element is the curve length, L, or the length of vertical curve per percent change in grade, K; where $K = L/A$, and A is the algebraic difference of the curve grades in percent. The design values of K are given in the design guides to satisfy two criteria: sight distance and drainage (AASHTO 1994; TAC 1986). Also, when the sight distance is the governing criterion, the formulas in Equations 2.6 through 2.9 can be used.

As an alternative, the analytical model developed in this research and presented in Chapter 5 can be used to design combined alignments in 3-D projections. The software *MARKC* can be used iteratively to determine the minimum required R of a horizontal curve or L of a vertical crest curve to satisfy a specific SSD. Iterative loops have been added to *MARKC* to automate the calculation of minimum R or L. It should be noted, however, that the calculated R or L will satisfy only the sight distance, and other checks for other design bases are required. Nonetheless, only the required value for sight distance is used for a clear comparison between 2-D and 3-D designs.

7.2 Study Procedure

A horizontal circular curve combined with a vertical sag or crest curve is assumed as a typical combined alignment. The horizontal and vertical curves are positioned so that the

station of the midpoint of both curves coincide with each other. Long tangents are added at the end of either curve. Two distinct highway sections are considered: cut and fill. The design criteria and the parameters affecting the design may vary for either section as follows.

7.2.1 Cut Section

A highway cut section can be experienced if the natural ground level is higher than the level of the highway surface. Thus, an upward side-slope is used as a transition between the two levels. The slope, *SS*, is usually expressed as a ratio of horizontal to vertical and depends mainly on the stability of the side-slope soil (Figure 7.1). A vertical side-slope (*SS*=0:1) can be used if the soil is very stable, e.g. rock. Generally, cut side-slopes represent continuous lateral obstructions which may limit the available sight distance. As a result, sight distance is a controlling criterion in the design of horizontal curves. The procedure used to study the effect of 3-D consideration on the design elements can be summarized as follows:

1. A base case is used as a reference to study the effect of each element. The parameters of the base case are as follows:
   - The highway is a two-lane facility which represents the dominant component of the Canadian highway network.
   - The design speed, *V*, is equal to 110 km/h, which is the design speed of most rural arterial undivided highways in Canada, and the corresponding required SSD is 220 m (TAC 1986).

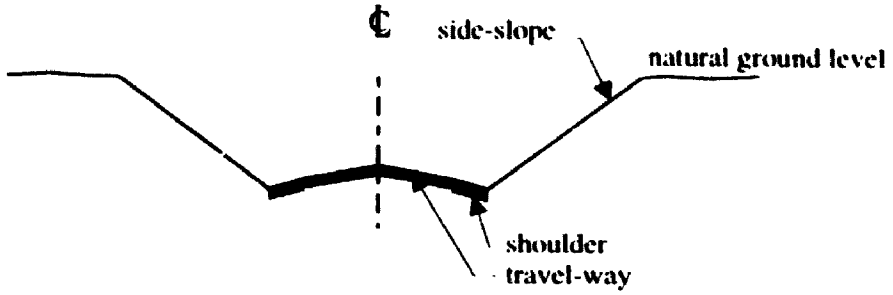

(a) Cut Section with No Down-Slope or Ditch.

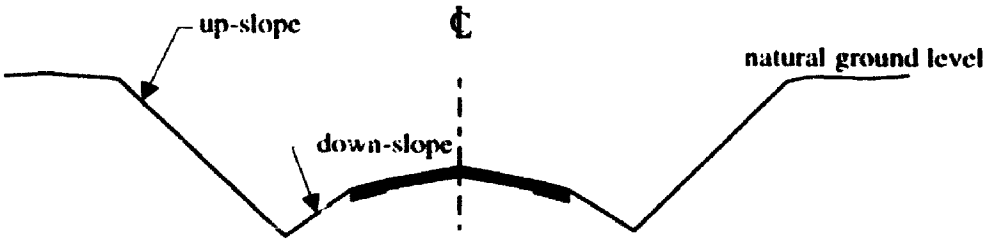

(b) Cut Section with Down-Slope.

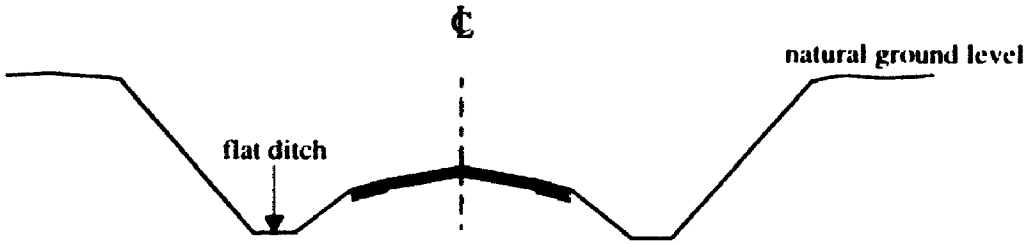

(c) Cut Section with Down-Slope and Ditch.

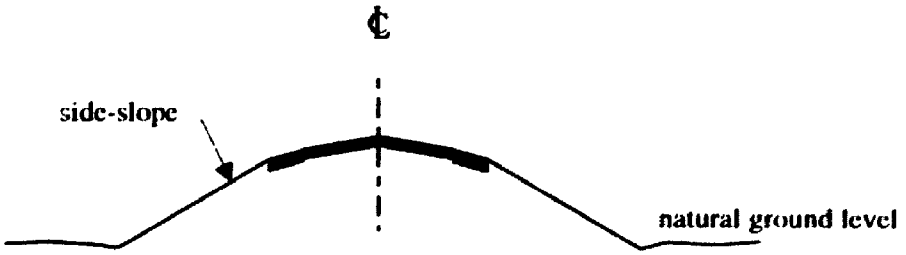

(d) Fill Section.

FIGURE 7.1: Highway Cut and Fill Sections.

- Lane and shoulder widths are 3.7 and 2.5 m, respectively (TAC 1986).
- The development of the superelevation is ignored; that is the entire alignment has a fully superelevated cross-section with a superelevation rate, e, of 6%.
- The shoulder cross-slope is equal to the pavement cross-slope.
- The side-slope, SS, is 2:1. The cut side-slope begins immediately at the end of the shoulder with no down-slope or drainage ditch.
- The horizontal curve is combined with either a crest or sag vertical curve.
- The algebraic difference of the vertical curve is variable. The grades of the two tangents have the same absolute value but different signs.
- Driver's eye height, h_1, and object height, h_2, are 1.05 and 0.38 m, respectively (TAC 1986). Thus, the lateral clearance, m, for current design practice is corresponding to an average height, h_{av}, of 0.715 m.

2. The required R of the horizontal curve and K of the vertical curve are determined according to the conventional design practice. These values will be referred to as the 2-D values. Then, due to the fact that both R and K depend on the sight distance, one of them, K, is designed conventionally and the other, R, is determined considering the 3-D interaction among design elements. This value will be referred to as 3-D R. In both cases, the object and the driver eye are positioned along the centerline of the inside lane.
3. The effect of each of the design elements on the required R is studied by changing the value of one parameter at a time, while other parameters have the base values. Namely:

- The range of V is 110 and 130 km/h. The corresponding values of SSD are 220 and 260 m, respectively (TAC 1986).
- The range of e is 6 and 8%.
- The range of SS is 2:1 and 3:1.
- The range of the algebraic difference of the vertical curve, A, is 2, 4, and 6% crest and sag. A seventh case corresponds to a separate horizontal curve, i.e. A=0, is also considered.
- An additional value for K is taken greater than the minimum value in the design standards.
- The range of the deflection angle of the horizontal curve, Δ, begins at 5° and increases with a 5°-increment until any further increase in Δ will not change the required R.
- A 1-m down-slope of SS=2:1, with and without 1-m flat ditch, is added before the up-slope to help as a drainage ditch (Figure 7.1).
- The superelevation is developed over 90-m superelevation runoff with and without spiral curve. In this case, the normal crown slope, q, is 2%.

7.2.2 Fill Section

If the natural ground level at the location of the highway is lower than the required level of the highway surface, a fill soil is used to reach the required levels forming a fill section (Figure 7.1). In this case, no lateral obstruction exists, and therefore horizontal sight distance is not a governing criterion for R, but K is still controlled by the sight

distance. The study approach is similar to that for the cut sections but with some differences:

1. The side-slope, *SS*, is not a parameter because it does not affect either *R* or *K*.
2. *R* is designed based on the stability condition only (Equation 2.10). Then, *K* is determined according to the current practice and considering the effect of the 3-D interaction.
3. The effect of the change in each parameter is studied with respect to the required 3-D *K*.
4. Both the inside and outside lanes are studied. The driver's eye and the object are positioned along the centerline of the lane being considered.

7.3 Results and Analysis

The design values based on the current design practice are shown in Table 7.1. In this table, a half of the lane width is added to the values of *R* for the sight distance calculated using Equation 2.5 because the equation gives the radius of the centerline of the inside lane while the design values are always expressed in terms of the radius of the highway centerline. These values are used as reference for studying the effect of 3-D consideration.

7.3.1 Cut Sections

As mentioned previously, the length of the vertical curve, *L*, in this case is taken as the 2-D value, that is $L = K\,A$, where the values of *K* are shown in Table 7.1. Then, the

TABLE 7.1: Minimum Horizontal Curve Radius, *R*, and Design Values of *K* According to Current Design Practice.

V (km/h)	SSD [a] (m)	f_s [a]	*R* (m) [b]		*K* (m) [a]	
			Vehicle Stability	Sight Distance [c]	Crest Curve	Sag Curve
110	220	0.10	595.5	960.9	85	55
130	260	0.08	950.5	1341.7	120	65

[a] From (TAC, 1986)
[b] Alignment parameters have the base values
[c] For fill section only. The lateral clearance, *m*, is equal to 6.302 m (corresponding to an average height of 0.715 m)

minimum 3-D *R* is determined by iterations to the nearest 0.1 m to satisfy the sight distance condition. It should be noted that these values should not be less than the minimum value for vehicle stability shown in Table 7.1. However, as mentioned earlier, to have a clear comparison with the 2-D values, only the values controlled by the sight distance are shown. Table 7.2 shows the percentage difference between the 2-D and 3-D radii, *Diff*, that is calculated as:

$$Diff = \frac{(3\text{-}D\ value) - (2\text{-}D\ value)}{(2\text{-}D\ value)} \times 100 \qquad (7.1)$$

As shown in the equation, the 2-D values are taken as the reference for comparison because designers and engineers are more familiar with them. Thus, a negative value of *Diff* indicates that the 2-D analysis overestimates the design, while a positive value indicates that the 2-D analysis underestimates the design.

TABLE 7.2: Difference Between 2-D and 3-D Radii for Horizontal Curves Combined with Vertical Curve.

Δ	*Diff* (%)						
	A (crest curves)			*A*=0	*A* (sag curves)		
	6%	4%	2%		2%	4%	6%
(a) *V* = 110 km/h (SSD = 220 m). 2-D *R* = 960.9 m.							
5	-100.00 (0)	-100.00 (0)	-100.00 (0)	-100.00 (0)	-100.00 (0)	-100.00 (0)	-100.00 (0)
10	29.84 (218)	29.84 (218)	27.72 (214)	-9.26 (152)	-54.56 (76)	-69.67 (51)	-69.76 (51)
15	29.88 (327)	29.88 (327)	27.90 (322)	0.35 (253)	-21.47 (198)	-28.25 (181)	-28.25 (181)
20					-16.00 (282)	-25.56 (250)	-25.82 (249)
25					-5.67 (396)	-22.39 (325)	-25.82 (311)
30					-0.30 (502)	-9.95 (453)	-25.16 (377)
35					0.35 (589)	-1.36 (579)	-18.21 (480)
40						0.36 (673)	-3.48 (648)
45							0.32 (757)
50							0.37 (842)
(b) *V* = 130 km/h (SSD = 260 m). 2-D *R* = 1341.7 m.							
5	-37.47 (73)	-37.47 (73)	-38.32 (72)	-100.00 (0)	-100.00 (0)	-100.00 (0)	-100.00 (0)
10	29.36 (303)	29.36 (303)	29.13 (302)	-0.84 (232)	-39.17 (143)	-51.99 (112)	-52.02 (112)
15				0.31 (352)	-23.17 (270)	-29.31 (248)	-29.31 (248)
20					-9.87 (422)	-27.65 (339)	-29.12 (332)
25					-0.69 (581)	-14.15 (503)	-28.99 (416)
30					0.32 (705)	-1.24 (694)	-22.87 (542)
35						0.33 (822)	-2.12 (802)
40							0.34 (940)

- e = 6%, SS = 2:1, K = 85 m (crest), K = 55 m (sag)
- Values between parentheses are the length of horizontal curve, L_c, in meters
- Below the solid line, further increases in Δ do not change the value of *Diff*

As shown in the table, three possibilities exist for the combined alignment. First, if the horizontal curve is combined with a crest vertical curve, the 3-D R is less than the 2-D value for small angles of deflection, Δ, where R can vanish indicating that the sight distance is not a controlling criterion. However, for larger Δ, the required 3-D R is greater than the required 2-D value. The reason for this increase is that the curvature of the crest curve reduces the effective h_{av} at which the sight line is tangent to the side-slope. This in turn reduces the lateral clearance, m, compared to the clearance at the average height of h_1 and h_2. The reduction in m is maximum when the vertical curve length, L, is equal to or greater than SSD. Therefore, the required 3-D R will not depend on L, and in turn on A. This can be observed by comparing *Diff* for A = 4 and 6%, where for SSD = 220 m, L is 340 and 510 m, respectively, and for SSD = 260 m, L is 480 and 720 m, respectively. However, if L is less than SSD, as A and L decrease, the reductions in m and h_{av} decrease, and thus the required 3-D R decreases. This trend can be observed by comparing *Diff* for A = 2 and 4, where for SSD = 220 m, L is 170 and 340 m, respectively, and for SSD = 260 m, L is 240 and 480 m, respectively. This trend continues until A vanishes, that is a case of no vertical curve, where the 3-D and 2-D values of R are basically the same. For the same value of A, the difference between the 3-D and 2-D values of R increases as Δ increases until the length of the horizontal curve is equal to SSD. This can be seen in the stabilization of *Diff* when the horizontal curve length, L_t, is greater than or equal to SSD.

Second, if a sag curve is combined with the horizontal curve, the effective h_{av} at which the sight line is tangent to the side-slope increases. Therefore, as shown in the

table, the 3-D R is less than the corresponding 2-D value. Also, the larger the A, the greater the difference between the 3-D and the 2-D values. For the same A, as Δ increases the 3-D R increases. However, unlike the case of a crest curve, the change of the 3-D R continues even after the length of the horizontal curve is greater than SSD. However, if $L \geq$ SSD and $L \geq L_t$, any further increase in A and L will not affect the required 3-D R. For example, for SSD = 220 m, *Diff* for A = 4% (L = 220 m) is equal to *Diff* for A = 6% (L = 330 m) up to Δ = 15° (L_t = 180.5 m). Similarly, for SSD = 260 m, *Diff* for A = 4% (L = 260 m) is equal to *Diff* for A = 6% (L = 390 m) up to Δ = 15° (L_t = 248.3 m). The reason for this is that the critical part of the curve is not the part combined with the vertical curve; but rather each of the two parts with no overlap with the vertical curve at both ends. When either of these parts equals SSD, this part will act as a separate horizontal alignment and will control the 3-D R. Therefore, R is practically equal to the value corresponding to A=0, and any further increase in Δ, and in turn in the length of the horizontal curve, has no effect on the 3-D R.

The same trend in both cases of crest and sag curves is valid regardless of the design speed. However, for the same Δ of the horizontal curve, the higher the design speed, the higher the effect of crest curves and the lower the effect of sag curves. For example, when Δ=10° and A=2%, as the design speed increases from 110 to 130 km/h, the difference between the 2-D and 3-D values of R increases from 27.72 to 29.13% for a horizontal curve combined with a crest curve while the difference decreases from 54.56 to 39.17% for a horizontal curve combined with a sag curve. Also, as the design speed increases, the value of Δ beyond which it has no effect decreases. For example, when

A=2% and V=110 km/h, the value of Δ has no effect beyond 15° for a horizontal curve combined with a crest curve and 45° for a horizontal curve combined with a sag curve while the corresponding values when V=130 km/h are 10° and 30°, respectively.

Third, if no vertical curve exists, i.e., A=0, the 3-D R for short horizontal curves, small Δ, is less than the 2-D R. As Δ and the length of the horizontal curve increase, Equation 2.5 will be more accurate, and therefore the difference between the 3-D and 2-D values of R decreases. This trend continues until the length of the horizontal curve is equal to SSD. However, as shown in the table, for horizontal curves longer than SSD, a slight difference between the 2-D and 3-D radii still exists. This is due to the fact that both the lateral obstruction by the side-slope and the sight line are sloped in the same direction (the sight line is sloped from a 1.05 m driver eye to a 0.38 m object). As a result, the point of tangency between the sight line and the obstruction is not at h_{as} exactly. Such difference is expected to decrease as SS decreases until it vanishes when SS is equal to 0:1 (vertical obstruction). To verify this hypothesis, Table 7.3 shows the 2-D and 3-D radii for separate horizontal curves with lengths longer than SSD using different values of SS (A = 0). As shown in the table, for a vertical side-slope, SS = 0:1, the difference between the 2-D and 3-D radii is 0.1 m which is the accuracy used to determine R. As SS increases, *Diff* increases. Yet, the difference is very minimal (less than 0.5%).

The effect of the remaining parameters on the difference between the 2-D and 3-D values of R can be seen by comparing Table 7.2*a* with Table 7.4. In each part of Table 7.4, all the parameters have the base values and only one parameter is changed.

TABLE 7.3: 2-D and 3-D Values of R for Separate and Long Horizontal Curves in Cut Sections (A = 0, L_c > SSD).

SS	2-D		3 D R (m)	Difference (m)	*Diff* (%)
	m (m)	R (m)			
0:1	4.350	1392.0	1392.1	0.1	0.0072
1:1	5.326	1136.9	1138.5	1.6	0.1405
2:1	6.302	960.9	964.3	3.4	0.3526
3:1	7.278	832.0	836.0	4.0	0.4785

Comparing the values of *Diff* in Tables 7.2*a* and 7.4*a* shows that for the same Δ and A, the effect of the combined alignment decreases as the vertical curve becomes flatter, that is K becomes larger. This finding is expected since as $K \rightarrow \infty$, the alignment will end up as a separate horizontal curve. On the other hand, Comparing Tables 7.2*a* and 7.4*b* shows that as the superelevation rate, e, increases, the effect of crest curves decreases slightly while the effect of sag curves increases slightly. The reason for this is that as e increases, the difference in elevation between the centerline of the inside lane (where the driver eye and the object are positioned) and the end of the shoulder (where the side-slope begins) increases. As a result, the effective height at the point of tangency between the sight line and the side-slope increases, and in turn the effective lateral clearance increases. This will reduce the increase of R on crest curves and will increase the reduction of R on sag curves. Comparing Tables 7.2*a* and 7.4*c*, it is shown that as SS increases, the effect of both crest and sag curves increases. This is due to the fact that for flatter slopes (higher SS), the difference in the effective h_{av} will result in higher difference in the lateral

TABLE 7.4: Effect of Vertical Curvature, Superelevation Rate, and Side-Slope on 3-D *R*.

Δ	*Diff* (%)						
	A (crest curves)			*A*=0	*A* (sag curves)		
	6%	4%	2%		2%	4%	6%
(a) *K* (crest) = 102 and *K*(sag) = 66. 2-D *R* = 960.9 m.							
10	23.31	23.31	23.12	-9.26	-51.59	-59.65	-59.65
20	23.79	23.79	23.62	0.35	-16.12	-22.44	-22.44
30					-0.88	-14.54	-22.43
40					0.36	0.11	-11.80
50						0.36	0.37
(b) Superelevation rate, *e*, =8%. 2-D *R* = 935.1 m.							
10	28.52	28.52	26.38	-11.68	-58.21	-73.77	-73.89
20	28.82	28.82	26.92	0.32	-16.73	-25.15	-25.32
30					-0.75	-11.68	-24.90
40					0.33	0.32	-5.35
50						0.34	0.34
(c) *SS* = 3:1. 2-D *R* = 832.0 m.							
10	42.20	42.20	38.69	-25.55	-100.00	-100.00	-100.00
20	42.79	42.79	39.69	0.48	-25.14	-31.88	-31.88
30					-5.28	-27.49	-31.11
40					0.50	-2.12	-28.10
50						0.49	-0.12
60							0.49

Below the solid line, further increases in Δ do not change the value of *Diff*

clearance, m, and in turn higher effect of the combined alignment. If the lateral obstruction is vertical (SS=0:1), the change in the effective $h_{a\lambda}$ will not cause any difference in m, and thus the combined alignment will have no effect.

Table 7.5a shows the effect of adding a 1-m down-slope (SS=2:1) without flat ditch before the up-slope, and Table 7.5b shows the effect of the same down-slope with a 1-m flat ditch (Figure 7.1). In the first case, the lateral clearance, m, at $h_{a\lambda}$ is 8.302 m and the required 2-D R is 729.3 m. When the flat ditch is added, m increases to 9.302 m and the required 2-D R decreases to 650.7 m. Comparing Tables 7.2a and 7.5 shows that the same trends discussed in the base case are still valid. However, the effect of the crest curve on the required 3-D R is reduced by the addition of the down-slope, and is reduced even more by the addition of the flat ditch. For example, for A = 6%, the corresponding maximum value of *Diff* in the base case is 29.88%, compared to 21.10% when the down-slope is added. This maximum value of *Diff* is further reduced to 18.52% when the flat ditch is added. This reduction in the effect of the crest curve can be due to the increase of the 2-D lateral clearance, m, at $h_{a\lambda}$ while the absolute decrease in the 3-D m due to the vertical curvature remains the same. As a result, the decrease in the 3-D m will represent a lower percentage and will have a lower effect on the 3-D R than that in the base case. In case of sag vertical curves, the same effect is noted for the large values of Δ. For example, for A = 6% and Δ = 30°, *Diff* decreases from -25.16% in the base case to -20.94% when the down-slope is added. The corresponding value of *Diff* decreases more to -19.16% when the flat ditch is added. However, for small values of Δ, both the down-slope and the ditch increase the effect of the sag curve. This can be

TABLE 7.5: Effect of Down-Slope and Drainage Ditch Before Up-Slope on 3-D *R*.

Δ	*Diff* (%)						
	A (crest curves)			*A*=0	*A* (sag curves)		
	6%	4%	2%		2%	4%	6%
(a) Down-slope before the up-slope. 2-D *R* = 729.3 m.							
10	-1.23	-1.23	-3.92	-52.86	-100.00	-100.00	-100.00
20	21.10	21.10	19.79	0.19	-16.66	-21.69	21.69
30					-7.54	-19.09	-20.94
40					-0.21	-6.68	19.44
50					0.21	[illegible]	5.59
60						0.21	0.21
(b) Down-slope and ditch before the up-slope. 2-D *R* = 650.7 m.							
10	-29.86	-29.86	-32.80	-87.51	-100.00	-100.00	-100.00
20	18.52	18.52	17.37	0.23	-16.74	-22.44	-22.44
30					-10.36	-18.43	-19.16
40					-1.87	-11.34	18.83
50					0.23	-1.80	12.66
60						0.25	1.71
70							0.25

- e = 6%, SS = 2:1, K = 85 m (crest), K = 55 m (sag)
- Down-slope: SS=2:1, width = 1m. Ditch width = 1 m
- Below the solid line, further increases in Δ do not change the value of *Diff*

seen by comparing the values of *Diff* for A = 6% and Δ = 15° (not shown in Table 7.5). The corresponding values for the base case, the base case with down-slope, and the base case with down-slope and ditch are -28.25, -37.76, and -48.26%, respectively. This is due to the fact that the large lateral clearances, m, when the down-slope and the ditch are added, accompanied with small Δ reduce the required R significantly, and may not require a curve at all.

Finally, Table 7.6 shows the minimum 3-D R for the horizontal curve with all parameters having the base values. However, in this case, the transition from a normal crown cross-section to a fully superelevated cross-section is considered with and without a spiral curve. In either case, a 90 m-transition is used so that the rate of change of the elevation of either the inside or the outside edges does not exceed 1:400 (TAC 1986). Figure 7.2 shows the development of the superelevation in both cases. As shown in the table, for smaller Δ, the consideration of the superelevation development raises the elevations of the driver eye and the object and thus the effective average height. Subsequently, the required R is reduced slightly. Therefore, the effect of the sag curve is slightly aggravated while the effect of the crest curve is slightly reduced. However, if the horizontal curve is long enough so that the development of the superelevation does not interact with the vertical alignment, the required R will not change whether the development is considered or not. This is reflected in the value of R which is required for large Δ.

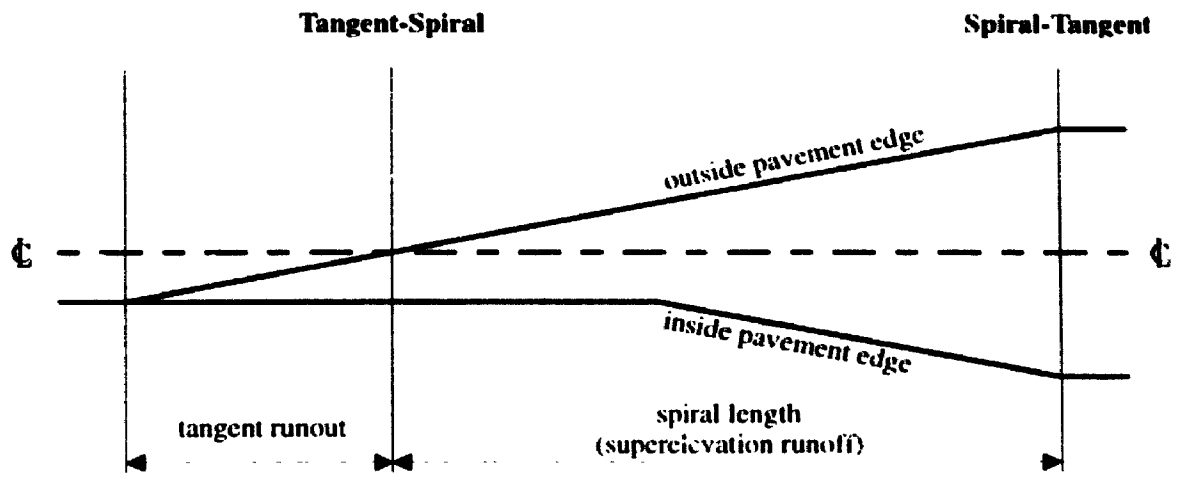

(a) Horizontal Curve with Spiral

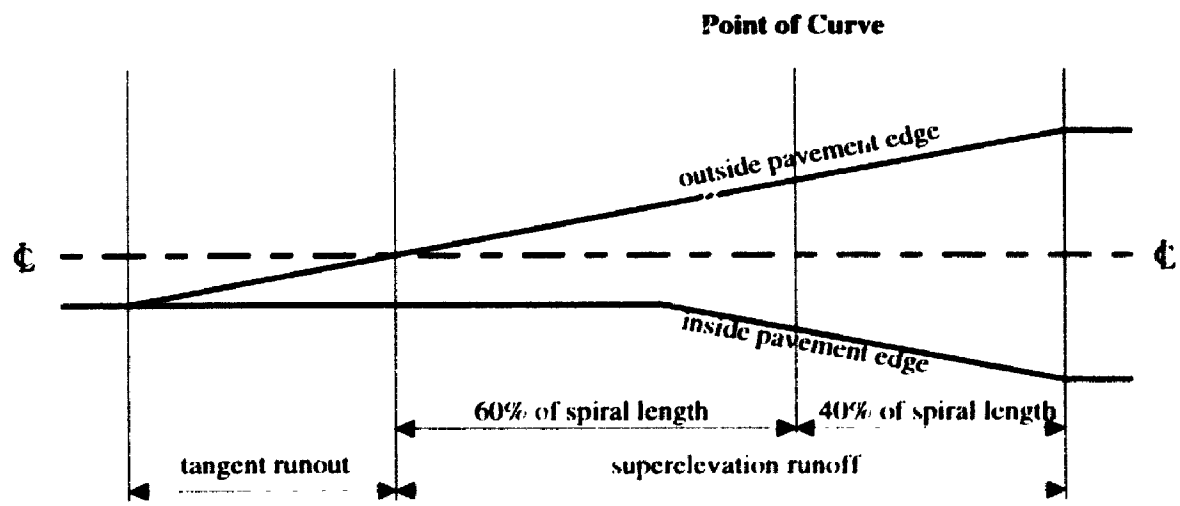

(b) Horizontal Curve without Spiral

FIGURE 7.2: Development of Superelevation.

TABLE 7.6: Minimum *R* for Horizontal Curve Considering the Superelevation Development.

Δ	*R* (m)						
	A (crest curves)			*A*=0	*A* (sag curves)		
	6%	4%	2%		2%	4%	6%
(a) Curves with spiral. 2-D *R* = 960.9 m.							
10	1156.6	1156.6	1130.2	709.8	N/A	N/A	N/A
20	1247.9	1247.9	1229.0	964.3	758.8	698.4	698.4
30					928.9	801.9	712.8
40					964.3	952.9	866.3
50						964.4	963.1
60							964.5
(b) Gradual change of cross-slope without spiral. 2-D *R* = 960.9 m.							
10	1221.8	1221.8	1201.1	832.7	N/A	N/A	N/A
20	1248.0	1248.0	1229.0	964.3	793.6	710.3	708.2
30					949.0	847.4	713.5
40					964.3	958.9	911.5
50						964.4	964.5

N/A = Not applicable (the length of the curve is not enough for the development of the superelevation)

- q = 2%, e = 6%, SS = 2:1, K = 85 m (crest), K = 55 m (sag)
- Below the solid line, further increases in Δ do not change the value of R

7.3.2 Fill Sections

As mentioned earlier, in this case, the main parameter is the length of the vertical curve, L, or the vertical curvature which is expressed in terms of, K. However, because the analytical model cannot consider the headlight sight distance, only crest curves are considered in this study. The range of the algebraic difference in grades, A, is 4 to 12%. The radius of the horizontal curve is controlled by the vehicle stability only. Therefore, R is taken as 600 and 950 m for the design speeds of 110 and 130 km/h, respectively (Table 7.1). The other design elements base values are the same as those used in cut sections. However, the degree of alignment overlap is changed by increasing the length of the horizontal curve, L_c, with 100 m-increments from zero (separate vertical alignment) until the required 3-D K does not change with the change of L_c. The minimum 2-D K corresponding to design speeds of 110 and 130 km/h, calculated using Equations 2.6 and 2.7, are 89.9 and 125.5 m, respectively. These values are slightly larger than those recommended in the design guides. Possibly this is due to the fact that the required SSD shown in the table are rounded while the design values of K are based on the exact SSD before approximation. Therefore, for consistency, the calculated values are used as the base of comparison with the 3-D K.

Table 7.7 shows the percentage difference between the 2-D and 3-D K values, *Diff*, calculated using Equation 7.1. As shown, when a portion of the vertical curve, of a length equal to or more than SSD, is not overlapping with the horizontal curve, the 2-D and 3-D K values are practically the same. This is due to the fact that this portion will act as a separate vertical alignment and will control the required vertical curvature.

TABLE 7.7: Difference Between 2-D and 3-D *K* Values for Crest Vertical Curves Combined with Horizontal Curve.

L_c (m)	*Diff* (%)				
	A=4%	*A*=6%	*A*=8%	*A*=10%	*A*=12%
Inside Lane					
0	0.00	0.00	0.00	0.00	0.00
100	-31.92	0.00	0.00	0.00	0.00
200	-66.52	-13.13	0.00	0.00	0.00
300	-71.64	-59.96	-0.22	0.00	0.00
400			-59.73	0.00	0.00
500				-1.56	0.00
600				-59.51	0.00
700					-59.29
Outside Lane					
0	0.00	0.00	0.00	0.00	0.00
100	-32.15	0.00	0.00	0.00	0.00
200	-50.17	-12.46	0.00	0.00	0.00
300	-50.83	-48.83	-0.22	0.00	0.00
400			-48.61	0.00	0.00
500				-1.22	0.00
600				-48.39	0.00
700					-48.16
Both Lanes					
0	0.00	0.00	0.00	0.00	0.00
100	-31.92	0.00	0.00	0.00	0.00
200	-50.17	-12.46	0.00	0.00	0.00
300	-50.83	-48.83	-0.22	0.00	0.00
400			-48.61	0.00	0.00
500				-1.22	0.00
600				-48.39	0.00
700					-48.16

2-D K = 89.9 m

Below the solid line, further increases in L_c do not change the value of *Diff*

However, when the entire vertical curve is combined with the horizontal curve, the 3-D K is reduced significantly relative to the 2-D K. The reduction may be as high as 70%. It is found also that the reduction in the required 3-D K is higher for the inside lane than that for the outside lane. For example, when A = 12%, the maximum *Diff* for the inside and outside lanes are -59.29 and -48.16%, respectively. A possible reason for this difference is that, for the inside lane, the sight line can be obstructed by the highway surface on the inside shoulder and half a lane. On the other hand, for the outside lane, the sight line can be obstructed by the inside shoulder, the inside lane, and half a lane. Subsequently, the potential of having a sight obstruction is higher when considering the inside lane than when considering the outside lane. The overall 3-D K required for the highway is the maximum for both lanes. Comparing the results for different values of A indicates that the 3-D K is slightly lower for curves with small A (4%). For curves with higher A (6 to 12%), the 3-D K is practically independent of the algebraic difference in grades of the vertical curve.

The effect of the other design elements on the required 3-D K is shown in Table 7.8. The results for a higher design speed, 130 km/h, have the same trend observed for 110-km/h speed. In addition, the results suggest that the length of the horizontal curve required for the 3-D K to be minimum increases as the design speed increases. Also, the difference between 2-D and 3-D K values decreases with the increase in the design speed. For example, when A = 12%, *Diff* and the length of the horizontal curve required for minimum 3-D K are -43.98% and 1100 m, respectively, for V = 130 km/h compared to -48.16% and 700 m for V = 110 km/h. It is also shown in the table that, expectedly, as

TABLE 7.8: Effect of Speed, Horizontal Curve Radius, and Superelevation Rate on 3-D *K* Values for Crest Vertical Curves Combined with Horizontal Curve.

Case	A=4%		A=6%		A=8%		A=10%		A=12%	
	L_t [e]	*Diff* [f]	L_t	*Diff*	L_t	*Diff*	L_t	*Diff*	L_t	*Diff*
(a)	300	-50.83	300	-48.83	400	-48.61	600	-48.39	700	-48.16
(b)	300	-44.46	500	-44.38	600	-44.22	800	-44.14	1100	-43.98
(c)	300	-40.49	400	-40.38	500	-40.27	600	-40.27	700	-40.14
(d)	300	-62.18	300	-55.73	400	-55.51	600	-55.39	700	-55.22

(a) Base case (V = 110 km/h, SSD = 220 m, R = 600 m, e = 6%, 2-D K = 89.9 m)
(b) V = 130 km/h (SSD = 260 m, R = 950 m). 2-D K = 125 5 m
(c) R = 800 m. 2-D K = 89.9 m
(d) e = 8%. 2-D K = 89.9 m
[e] The length of the horizontal curve (to the nearest 100 m) beyond which L_t does not have an effect on 3-D K
[f] The corresponding difference between the 2-D and 3-D K values (Equation 7.1)

the horizontal curve radius increases, *Diff* decreases. For example, for A = 12%, *Diff* changes from -48.16 to -40.14% as R increases from 600 to 800 m. Eventually, if $R \rightarrow \infty$, the combined alignment will be a separate vertical alignment. On the other hand, as the superelevation rate increases, *Diff*, and in turn the effect of the 3-D alignment, increases. For example, for A = 12%, *Diff* changes from -48.16 to -55.22% as e increases from 6 to 8%. This is due to the lowering of the highway surface, which represents a potential sight obstruction relative to the sight line.

Tables 7.9 and 7.10 show the required 3-D K when the development of the superelevation rate is carried out on a 90-m transition without and with spiral curves,

TABLE 7.9: 3-D *K* Values for Crest Vertical Curve Combined with Horizontal Curve with 90 m Superelevation Runoff Length (No Spiral Curve).

L_c (m)	*K* (m)				
	A=4%	*A*=6%	*A*=8%	*A*=10%	*A*=12%
Inside Lane					
200	29.1	94.9	94.9	94.9	94.8
400	24.7	36.0	94.6	94.7	94.7
600			36.2	93.8	94.5
800				36.4	36.6
Outside Lane (2-D *K* = 89.9 m)					
200	47.9	83.0	90.0	90.0	89.9
400	44.3	46.0	79.2	90.0	89.9
600			46.2	46.4	87.3
800				46.4	46.6
Both Lanes					
200	47.9	94.9	94.9	94.9	94.8
400	44.3	46.0	94.6	94.7	94.7
600			46.2	93.8	94.5
800				46.4	46.6

Below the solid line, further increases in L_c do not change the value of *K*

TABLE 7.10: 3-D *K* Values for Crest Vertical Curve Combined with Horizontal Curve with 90 m Spiral Curve at Both Ends.

L_c (m)	*K* (m)				
	A=4%	*A*=6%	*A*=8%	*A*=10%	*A*=12%
Inside Lane					
200	29.3	92.6	92.6	92.7	92.7
400	25.5	36.0	36.2	92.6	92.6
600				90.6	92.4
800				36.4	36.6
Outside Lane					
200	61.7	87.2	87.3	89.9	89.9
400	44.5	46.0	87.3	87.2	89.9
600			46.2	86.6	87.3
800				46.4	46.6
Both Lanes					
200	61.7	92.6	92.6	92.7	92.7
400	44.5	46.0	87.3	92.6	92.6
600			46.2	90.6	92.4
800				46.4	46.6

- L_c is the length of the original circular curve from point of curve to point of tangent. Actual circular curve is L_c - 90
- Below the solid line, further increases in L_c do not change the value of *K*

respectively. Comparing Table 7.7 to Tables 7.9 and 7.10, the effect of the development of the superelevation can be explained as follows. First, the inside lane has a 2% cross-slope (normal crown-slope) which increases gradually to 6% (full superelevation). If the driver eye is on the transition and the object is on a fully superelevated section, or vice versa, one of them will *sink* relative to the other. Therefore, the required 3-D *K* will increase relative to that if the cross-slope is constant. However, if the horizontal curve is long enough so that both the driver eye and the object will be on fully superelevated sections while the transition is not overlapping with the vertical curve, the superelevation development will not affect the 3-D *K*. This is illustrated by the same 3-D *K* for long horizontal curves.

Second, the outside lane has an adverse cross-slope of 2% which changes to a full superelevation of 6%. As a result, the lane surface will be warped and the elevations of the surface increase as the superelevation develops. Therefore, if the horizontal curve is very short, the driver's eye will be on a transition and the object will be on the other transition, and the sight line will pass over the outside lane. Therefore, the lane surface on the superelevated portion will be as a mount, and the 3-D *K* will increase relative to that if the cross-slope is constant. As the horizontal curve length increases, the driver's eye will be on a transition while the object is on a superelevated section, or vice versa, and the sight line will pass over the inside lane. As a result, the effective height of the driver's eye, or the object, will increase and the required 3-D *K* will decrease. However, the portion of the vertical curve that is not overlapping with the horizontal curve will produce a greater 3-D *K* that controls the curve. As a result, the 3-D *K* will be the same

like that for separate vertical alignment and for combined alignment with constant cross-slope. Finally, as the entire vertical curve is overlapping with the horizontal curve, the fully superelevated portion will control the 3-D K and the result will be identical to that in the case of a constant cross-slope.

7.4 Summary

It is shown in this chapter that the analytical model for 3-D sight distance can be very useful in establishing geometric design standards based on 3-D combined highway alignment. The model is used to design combined horizontal and vertical curves with the sight distance as the main controlling parameter. It is shown that the 2-D and 3-D designs may differ significantly with the result that the current 2-D-based design standards are compromising traffic safety or highway economy. The model is also used to study the effect of the different design elements on the 3-D design. It is shown that both the required R for horizontal curves and K for crest vertical curves depend on all other design elements (superelevation rate, SSD, side-slope, deflection angle and degree of horizontal curves, flatness of vertical curves, and degree of overlap between horizontal and vertical curves). Ignoring the interaction among these elements may lead to erroneous results.

The addition of down-slope and/or flat drainage ditch before the up-slope in cut sections reduces the impact of the 3-D sight distance on the design elements, and, intuitively, reduces the effect of aligament overlap on the 3-D sight distance. This explains in part the small difference between the marking of passing and no-passing zones using the 2-D and 3-D sight distances (Chapter 6). On the segment used in the marking application, down-slopes, with or without flat ditches, are always added before the up-

slopes in the cut sections, and thus the effect of the alignment overlap is relatively reduced. It should be noted, however, that sometimes the topography may not allow such provisions. For example, Figure 7.3 shows a horizontal curve combined with a crest vertical curve on Trans-Canada Highway (Highway 17). As shown in the figure, an up-slope is introduced immediately after the shoulder with no provision for down-slope or ditch.

FIGURE 7.3: Combined Alignment on Cut Section on Highway 17.

CHAPTER 8

CONCLUSIONS AND RECOMMENDATIONS

8.1 Summary

As has been demonstrated throughout this research, highway geometric design is a vital phase in the design of safe, pleasing, and efficient highways. However, the development of the current highway geometric design standards contains a number of rough assumptions, and many new research findings have not been adopted in the several revisions of the standards over the last forty years. Among these rough assumptions is ignoring the 3-D nature of highway alignment. Such an assumption has been introduced because of the anticipated difficulties associated with considering the 3-D interaction among the different design elements. As a result, the design standards can be inaccurate, and the resulting margin of safety or hazard cannot be estimated.

In this research, the subject of sight distance on rural highways is addressed comprehensively. Although sight distance is agreeably believed to be an important element in highway safety and efficiency, not much work has been done to determine the required or the available sight distance accurately. Even though, most of the work done has not been considered in the design standards. Therefore, the research presents a complete study of the required passing sight distance and other requirements for safe and efficient passing manoeuvres on two-lane highways (length, beginning, and end of passing zones). The sight distance required for stopping is being studied in the NCHRP Project 3-42 and is beyond the scope of this research.

In addition to the requirements for passing manoeuvres, the research presents comprehensive analytical models for available daytime sight distance on complex separate 2-D horizontal and vertical alignments. These models fill the gaps that currently exist in this area where the current models can deal only with simple and isolated horizontal or vertical curves. The developed models are coded into computer programs to determine the profile of available sight distance on complex 2-D alignments at a user-specified accuracy. Furthermore, an unprecedented analytical model to evaluate the available daytime sight distance in 3-D combined alignments is developed. The analytical model can be considered an application of the finite element technique in highway geometric design. The modelling proved to be very accurate, especially for straight segments and parabolic vertical curves where the modelling is exact. For circular and spiral horizontal curves and vertical spline grades, the modelling is approximate, and the smaller the element size used in the modelling the higher the accuracy. The model is also coded into a computer program that can determine the profile of available sight distance on 3-D complex alignments at a user-specified accuracy.

Finally, two applications for the developed models are presented; namely marking of passing and no-passing zones on two-lane highways and design of 3-D combined alignments. In the marking application, the 2-D and 3-D computer programs and the developed requirements for passing are used to determine the marking of passing and no-passing zones on a 7-km segment of Highway 61. In the design application, the minimum required radius of horizontal curves, R, and the minimum length of vertical crest curves, L, are determined in 3-D combined alignments. These 3-D values of R and

L are compared with the corresponding 2-D values according to the current standards. Thus, the effect of ignoring the 3-D interaction among the different highway design elements is quantified.

8.2 Conclusions

First, the literature review presented in Chapter 2 shows a number of deficiencies in the current highway geometric design standards. Among these deficiencies is the design of highway alignments in 2-D projections separately from the other elements. Even in this approximation, the design standards can deal only with a simple and isolated element at a time, e.g., a simple circular curve with long tangents and with a curve length greater than the required sight distance. Expectedly, the resulting formulas are simple but of limited value in practical applications (AASHTO, 1990; 1994).

Second, several discrepancies are encountered in the current design and marking standards regarding the requirements for passing manoeuvres on two-lane highways. Furthermore, the design standards are not free from self-discrepancies while the reasons behind the values recommended in marking standards are not clear. Other models have been developed to provide more accurate and realistic modelling for the passing manoeuvres. However, close investigations of these models show that revisions are still needed. Moreover, all of these models have focused on the minimum required passing sight distance, and none of them has investigated the minimum length of passing zones or the optimum beginning and end of passing zones. A revised analytical model is presented in Chapter 3 to overcome these setbacks. The model provides a comprehensive

modelling for the entire passing manoeuvre from its beginning to end. The resulting values of minimum required passing sight distance have been validated with field measurements, and they have showed superiority over the other existing models. A comparison with the current marking standards shows that these standards can be unsafe. The degree of hazard that may result from the marking standards increases with the increase of the design speed where the consequences of a collision are more severe.

Third, the analytical models and computer software for 2-D and 3-D sight distances, presented in Chapters 4 and 5, have proven to be accurate and comprehensive through graphical and field verifications. The software can consider virtually all possible types of sight obstructions; namely, highway surface, continuous lateral obstructions, single lateral obstructions, and overpasses. Moreover, the single lateral obstructions can be defined by one, two, or three points, and the overpasses can have variable vertical clearance and/or can be at skewed angle with the highway centerline. These models and software provide a very useful tool for marking passing and no-passing zones on two-lane highways and for designing combined alignments in 3-D projections.

Fourth, a marking application for a 7-km segment of Highway 61 is used in Chapter 6 to show the applicability of the developed 2-D and 3-D software. The software can determine the profile of available 2-D and 3-D sight distances using the alignment and cross-section data that are already available in the highway agencies. The maximum element size specified in the alignment modelling can affect the computer run-time and the modelling accuracy. The optimum size depends on the irregularities of the alignment and cross-section data. However, a maximum element size as large as 25 m does not

compromise the modelling accuracy in this application example. Interestingly, the modelling accuracy of the 3-D combined alignment is relatively insensitive to the maximum element size up to 50-m maximum element size. The profiles of available sight distance can be used for marking passing and no-passing zones according to the MUTCD standards or according to the requirements developed in this research. A comparison between the two methods of marking shows that the MUTCD standards can compromise the traffic safety by allowing passing on unsafe sections, and can compromise the highway level-of-service by disallowing passing on safe sections. The marking on the field is, however, more conservative but on the expense of the highway quality of service.

The profiles of 2-D and 3-D sight distances can differ significantly. The 2-D separate alignment tends to overestimate the available sight distance when a crest vertical curve overlaps with a horizontal curve in a cut section. On the other hand, the 2-D separate alignment tends to underestimate the available sight distance when a sag vertical curve overlaps with a horizontal curve in a cut section or when a crest vertical curve overlaps with a horizontal curve in a fill section. However, this difference does not translate into significant difference in the marking in this specific application. The reasons behind this are: (1) the 2-D and 3-D sight distances differ from each other along short distances while the sight distance for passing is required on long distances, (2) the 2-D and 3-D sight distances differ from each other on obstructed segments where the available sight distance is less than the required sight distance, and (3) the provision of

down-slopes and flat ditches before the up-slopes in cut sections reduces the effect of the combined alignment on the sight distance.

Finally, Chapter 7 presents an application for the use of the 3-D model and software in designing combined highway alignments. Because the design is based on the stopping sight distance which is considerably less than the passing sight distance, the differences between the 2-D and 3-D sight distances have a significant effect on the highway design. When a horizontal curve is overlapping with a crest curve in a cut section, the required radius, R, can be significantly higher than the 2-D value recommended in the design standards (up to 130%). On the other hand, the required R can be significantly lower than the 2-D value recommended in the design standards (no curve may be required for small deflection angles) when the horizontal curve is overlapping with a sag curve in a cut section. Also, when a crest vertical curve is overlapping with a horizontal curve in a fill section, the required length of the vertical curve, L, can be significantly lower than the 2-D value recommended in the design standards (up to 50%). It is also shown that the highway design elements; namely R and L depend on the values selected for the other design elements such as, deflection angle of horizontal curve, degree of alignment overlap, superelevation rate, required stopping sight distance, side-slope, and superelevation development.

8.3 Recommendations and Future Research

Based on the findings of this research, presented in the previous chapters and summarized above, the following can be recommended:

- The current standards for marking passing and no-passing zones on two-lane highways require major revisions to eliminate the discrepancies related to the passing manoeuvre and to ensure that the resulting marking can effectively assist drivers take a decision to pass or trail a slower vehicle without compromising the highway's level-of-service. The revised model presented in this research can provide a useful tool in such revisions.
- The current design standards require major revisions to enhance the design requirements based on 3-D combined alignments and to establish 3-D design standards. The analytical model and software developed in this research can provide a useful tool in the consideration of the daytime sight distance. However, further research is still needed for establishing a complete set of 3-D design standards.
- Designers should be aware of the effect of the combined alignment on the sight distance provisions. Ignoring this effect may lead to constructing roads with too liberal and too conservative sections, even though all of them are designed according to the current standards. In modifying existing roads, ignoring the interaction among the different highway design elements may lead to erroneous allocation of financial resources where safe sections may be modified and unsafe sections are overlooked.
- Highway agencies should survey the single lateral obstructions in addition to the horizontal and vertical alignments and cross-section data.

Because this research has focused mainly on daytime sight distance on rural highways, further research is still needed and can be very fruitful as follows:

- An accurate consideration of the nighttime sight distance (headlight sight distance) in highway design has not been modelled. At nighttime, drivers can see just as far as their vehicles' headlights cover. Although the design standards include provisions for designing sag vertical curves based on the headlight sight distance, only 2-D simple isolated sag is considered. Analytical models for 2-D and 3-D headlight sight distance are still lacking.
- The revised model for required PSD, minimum length of passing zones, and beginning and end of passing zones developed in this research was deterministic. That is a specific design value was assume to each parameter in the model. However, due to the wide variations in drivers' reactions and performances in the same situation, a probabilistic analysis should be carried out. Such an analysis would determine the required PSD, minimum length of passing zones, and beginning and end of passing zones that would be sufficient for a specific percentage of drivers and vehicles on each specific highway.
- In this research as in all current models, the driver of the passing vehicle is assumed to have a clear sight distance that can be obstructed by the alignment only. However, in reality, the impeding vehicle is by default ahead of the passing vehicle and may fall on the sight line of the passing driver. Therefore, the impeding vehicle may act as a moving obstruction that may block the passing driver's sight distance. Such possibility needs to be investigated closely to simulate the passing manoeuvre as accurate as possible.

- The developed models for 2-D and 3-D sight distance can be enhanced to consider the intersection sight distance. Since urban intersections are usually controlled, and speeds are relatively low, the intersection areas are usually small enough to be approximated into a 2-D plan. However, rural intersections are usually uncontrolled, and speeds are relatively high. Subsequently, approximating the intersection into a 2-D plan may lead to erroneous results.

REFERENCES

AASHO. 1954. *A Policy on Geometric Design of Rural Highways*. American Association of State Highway Officials, Washington, D.C.

AASHO. 1940. *A Policy on Sight Distance for Highways*. American Association of State Highway Officials, Washington, D.C.

AASHTO. 1994. *A Policy on Geometric Design of Highways and Streets*. American Association of State Highway and Transportation Officials, Washington, D.C.

AASHTO. 1993. *Highway Drainage Guidelines*. Vols. **1-11**, American Association of State Highway and Transportation Officials, Washington, D.C.

AASHTO. 1991. *Model Drainage Manual*. American Association of State Highway and Transportation Officials, Washington, D.C.

AASHTO. 1990. *A Policy on Geometric Design of Highways and Streets*. American Association of State Highway and Transportation Officials, Washington, D.C.

AASHTO. 1986. *AASHTO Guide for Design of Pavement Structures*. American Association of State Highway and Transportation Officials, Washington, D.C.

Adler, H.A. 1987. *Economic Appraisal of Transport Projects*. Published for the Economic Development Institute of the World Bank, The Jhons Hopkins University Press, Baltimore, U.S.A.

Agg, T.R. 1916. *Construction of Roads and Pavements*. First Edition. (Cited in Hall and Turner, 1989)

Allen, R.W., T.J. Rosenthal, and D.H. Klyde. 1995. Application of Vehicle Dynamic Modeling to Interactive Highway Safety Design. Presented at the *Transportation Research Board Annual Meeting*, January 22-27.

ASCE. 1977. *Practical Highway Aesthetics*. American Society of Civil Engineering, New York, N.Y.

Berg, W.D., J. Choi, and E.J. Kuipers. 1989. Development of Highway Alignment Information from Photolog Data. *Transportation Research Record* **1239**, TRB, National Research Council, Washington, D.C., pp. 54-61.

Blanchard, A.H., and H.B. Drowne. 1914. *Text-Book on Highway Engineering*. First Edition. (Cited in Hall and Turner, 1989)

BTS. 1996. *National Transportation Statistics*. Bureau of Transportation Statistics, U.S. Department of Transportation, Washington, D.C.

Cook, R.D., D.S. Malkus, M.E. Plesha. 1989. *Concepts and Applications of Finite Element Analysis*. Third Edition, John Wiley & Sons, Inc., New York, N.Y.

Drábek, K. 1969. Plane Curves and Constructions. Chapter 4: *Survey of Applicable Mathematics*. Edited by K. Rektorys, M.I.T. Press, Cambridge, Mass.

Dunlap, D.F., P.S. Fancher, R.E. Scott, C.C. MacAdam, and L. Segel. 1978. *Influence of Combined Highway Grade and Horizontal Alignment on Skidding*. National Cooperative Highway Research Program, NCHRP Report **184**, TRB National Research Council, Washington, D.C.

Easa, S.M. 1995. Geometric Design. Chapter 60: *Civil Engineering Handbook*. Edited by W.F. Chen, CRC Press, Boca Raton, Fla.

Easa, S.M. 1994*a*. Design Considerations for Highway Reverse Curves. *Transportation Research Record* **1445**, TRB, National Research Council, Washington, D.C., pp. 1-11.

Easa, S.M. 1994*b*. Design Considerations for Highway Sight-Hidden Dips. *Journal of Transportation Research*, Vol. **28A**, No. **1**, pp. 17-29.

Easa, S.M. 1993. Lateral Clearance Needs on Compound Horizontal Curves. *Journal of Transportation Engineering*, ASCE, Vol. **119**, No. **1**, pp. 111-123.

Easa, S.M. 1992. Sight Distance Relationships for Symmetrical Sag Curve with Noncentered Overpass. *Journal of Transportation Research*, Vol. **26B**, No. **3**, pp. 241-251.

Easa, S.M. 1991*a*. Lateral Clearance to Vision Obstacles on Horizontal Curves. *Transportation Research Record* **1303**, TRB, National Research Council, Washington, D.C., pp. 22-32.

Easa, S.M. 1991*b*. Sight Distance Model for Unsymmetrical Crest Curves. *Transportation Research Record* **1303**, TRB, National Research Council, Washington, D.C., pp. 39-50.

Easa, S.M. 1991*c*. Sight Distance Model for Unsymmetrical Sag Curves. *Transportation Research Record* **1303**, TRB, National Research Council, Washington, D.C., pp. 51-62.

Fambro, D.B., K. Fitzpatrick, and R. Koppa. 1995. A New Stopping Sight Distance Model for Use in Highway Geometric Design. Presented at the *International*

Symposium on Highway Geometric Design Practices. Boston, Massachusetts, USA, August 30-September 1.

FHWA. 1995. *Status Report: Strategic Highway Research Program Product Implementation*. Federal Highway Adminstration, U.S. Department of Transportation, Washington, D.C.

FHWA. 1972. *Economic and Social Effects of Highways*. Federal Highway Adminstration, U.S. Department of Transportation, Washington, D.C.

Fitzpatrick, K. 1994. Horizontal Curve design: An Exercise in Comfort and Appearance. *Transportation Research Record* **1445**, TRB, National Research Council, Washington, D.C., pp. 47-53.

French, A. 1982. Vehicle Operating Characteristics. Chapter 6 (B): *Transportation and Traffic Engineering Handbook*. Edited by S.H. Wolfgang, L.E. Keefer, and W.R. McGrath, Institute of Transportation Engineers, ITE, Second Edition, Prentice-Hall, Inc., Englewood Cliffs, New Jersey.

Gallaway, B.M., R.E. Schiller, and J.D. Rose. 1971. *The Effect of Rainfall Intensity, Pavement Cross Slope, Surface Texture, and Drainage Length on Pavement Water Depths*. Research Report No. **138-5**, Texas Transportation Institute. (Cited in Dunlap et al, 1978)

Garber, J.G., and L.A. Hoel. 1988. *Traffic and Highway Engineering*. West Publishing Company, St. Paul, MN.

Geissler, E.H. 1968. A Three-Dimensional Approach to Highway Alignment Design. *Highway Research Record* **232**, HRB, National Research Council, Washington,

D.C., pp. 17-28. (Also published as Report No. **RR138**, Ministry of Transportation of Ontario, MTO, Downsview, Ontario, 1968.)

Glauz, W.D., D.W. Harwood, and A.D. St. John. 1980. Projected Vehicle Characteristics Through 1995. *Transportation Research Record* **772**, TRB, National Research Council, Washington, D.C., pp. 37-44.

Glennon, J.C. 1989. Highway Sight Distance Design Issues: An Overview. *Transportation Research Record* **1208**, TRB, National Research Council, Washington, D.C., pp. 1-3.

Glennon, J.C. 1988. New and Improved Model of Passing Sight Distance on Two-Lane Highways. *Transportation Research Record* **1195**, TRB, National Research Council, Washington, D.C., pp. 132-137.

Glennon, J.C. 1987. Effect of Sight Distance on Highway Safety. *Transportation Research Board, State of the Art Report* **6**, National Research Council, Washington, D.C., pp. 65-77.

Glennon, J.C., and G.D. Weaver. 1972. Highway Curve Design for Safe Vehicle Operations. *Highway Research Record* **390**, HRB, National Research Council, Washington, D.C., pp. 15-26.

Good, D., J.B.L. Robinson, G. Sparks, and R. Neudrof. 1991. *The Effect of Vehicle Length on Traffic on Canadian Two-Lane, Two-Way Roads*. Transportation Association of Canada, Ottawa, Ontario.

Goult, R.J, R.F. Hoskins, J.A. Milner, and M.J. Pratt. 1973. *Applicable Mathematics: A Course for Scientists and Engineers*. The Macmillan Press Ltd, London, England.

Guillet, E.C. 1966. *The Story of Canadian Roads*. University of Toronto Press, Toronto, Canada.

Hall, J.W., and D.S. Turner. 1989. Stopping Sight Distance: Can We See Where We Now Stand? *Transportation Research Record* **1208**, TRB, National Research Council, Washington, D.C., pp. 4-13.

Harwood D.W., and J.M. Mason. 1994. Horizontal Curve Design for Passenger Cars and Truck *Transportation Research Record* **1445**, TRB, National Research Council, Washington, D.C., pp. 22-33.

Harwood, D.W., and J.C. Glennon. 1989. Passing Sight Distance for Passenger Cars and Trucks. *Transportation Research Record* **1208**, TRB, National Research Council, Washington, D.C., pp. 59-69.

Harwood, D.W., and J.C. Glennon. 1977. Framework for Design and Operation of Passing Zones on Two-Lane Highways. *Transportation Research Record* **601**, TRB, National Research Council, Washington, D.C., pp. 45-50.

Hassan, Y., S.M. Easa, and A.O. Abd El Halim. 1996*a*. Passing Sight Distance on Two-Lane Highways: Review and Revision, *Journal of Transportation Research* (in press).

Hassan, Y., S.M. Easa, and A.O. Abd El Halim. 1996*b*. Analytical Model for Sight Distance Analysis on 3-D Highway Alignments. *Transportation Research Record* **1523**, TRB, National Research Council, Washington, D.C., pp. 1-10.

Hassan, Y., S.M. Easa, and A.O. Abd El Halim. 1996*c*. Computer Model for Establishing No-Passing Zones on 3-D Highway Alignments. Proceedings, *1st*

Transportation Speciality Conference for the Canadian Society for Civil Engineering, CSCE, Edmonton, Alberta, May 29-June 1, Vol. IIIb, pp. 411-422.

Hassan, Y., S.M. Easa, and A.O. Abd El Halim. 1996*d*. Toward 3-D Highway Geometric Design Standards. Proceedings, *1st Transportation Speciality Conference for the Canadian Society for Civil Engineering*, CSCE, Edmonton, Alberta, May 29-June 1, Vol. IIIb, pp. 345-354.

Hassan, Y., S.M. Easa, A.O. Abd El Halim. 1996*e*. Design Considerations for Combined Highway Alignments. Accepted for Publication in the *Journal of Transportation Engineering*, ASCE.

Hassan, Y., A.O. Abd El Halim, and S.M. Easa. 1995*a*. Design Considerations for Passing Sight Distance and Passing Zones. Presented at the *International Symposium on Highway Geometric Design Practices*, August 30- September 1, Boston, Massachusetts, USA.

Hassan, Y., S.M. Easa, and A.O. Abd El Halim. 1995*b*. Sight Distance on Horizontal Alignments with Continuous Lateral Obstructions. *Transportation Research Record* **1500**, TRB, National Research Council, Washington D.C., pp. 31-42.

Hassan, Y., S.M. Easa, and A.O. Abd El Halim. 1995*c*. New Development for Establishing No-Passing Zones on Two-Lane Highways due to Vertical Alignments. Proceedings, *Annual Conference of the Canadian Society for Civil Engineering*, CSCE, Ottawa, Vol. IV, pp. 205-214.

Hassan, Y., S.M. Easa, and A.O. Abd El Halim. 1995*d*. New Methodology for Available Sight Distance in Two-Dimensional Horizontal and Vertical Alignments, Proceedings, *Al-Azhar Engineering Fourth International Conference*, Cairo, Egypt, December 16-19, 1995, Vol. 4, pp. 283-294.

Hassan, Y., S.M. Easa, and A.O. Abd El Halim. 1995*e*. *User's Guide of MARKC: A Program for Establishing No-Passing Zones on Two-Lane Highways due to Combined Horizontal and Vertical Alignments*. Research Report LU-TRC-RR-95-1, Transportation Research Centre, Lakehead University, Thunder Bay, Ontario.

Hassan, Y., S.M. Easa, and A.O. Abd El Halim. 1994*a*. *User's Guide of MARKV: A Program for Establishing No-Passing Zones on Two-Lane Highways due to Vertical Alignment*. Research Report LU-TRC-RR-94-3, Transportation Research Center, Lakehead University, Thunder Bay, Ontario.

Hassan, Y., S.M. Easa, and A.O. Abd El Halim. 1994*b*. *User's Guide of MARKH: A Program for Establishing No-Passing Zones on Two-Lane Highways due to Horizontal Alignment*. Research Report LU-TRC-RR-94-1, Transportation Research Center, Lakehead University, Thunder Bay, Ontario.

HCM. 1994. *Highway Capacity Manual*. Special Report **209**. Transportation Research Board, National Research Council, Washington, D.C.

Huang, Y.H. 1993. *Pavement Analysis and Design*. Prentice-Hall, Inc., Englewood Cliffs, New Jersey.

Jones, J.R. 1970. *An Evaluation of the Safety and Utilization of Short Passing Sections*. Texas A&M University, College Station, MS Thesis. (Cited in Harwood and Glennon, 1977)

Jull, D.E., and G.T. Murray. 1984. ITEDS: A Computer Aided Design System for Highway Engineering. Proceedings, *Annual Conference of the Canadian Society for Civil Engineering*, CSCE, Halifax, May 23-25, pp. 431-445.

Khisty, C.J. 1990. *Transportation Engineering: An Introduction*. Prentice-Hall, Inc., Englewood Cliffs, New Jersey.

King, C.L., and W.B. Harkins. 1982. Geometric Design. Chapter 19: *Transportation and Traffic Engineering Handbook*. Edited by S.H. Wolfgang, L.E. Keefer, and W.R. McGrath, Institute of Transportation Engineers, ITE, Second Edition, Prentice-Hall, Inc., Englewood Cliffs, New Jersey.

Kontaratos, M., B. Psarianos, and A. Yotis. 1994. Minimum Horizontal Curve Radius as Function of Grade Incurred by Vehicle Motion in Driving Mode. *Transportation Research Record* **1445**, TRB, National Research Council, Washington, D.C., pp. 86-93.

Kosasih, D., R. Robinson, and J. Snell. 1987. *A Review of Some Recent Geometric Road Standards and Their Application to Developing Countries*. Transport and Road Research Laboratory, TRRL, Research Report **114**, England.

Krammes, R.A., and M.A. Garnham. 1995. Review of Alignment Design Policies Worldwide. Presented at the *International Symposium on Highway Geometric Design Practices*, Boston, Massachusetts, USA, August 30-September 1.

Lamm, R. 1984. Driving Dynamic Consideration: A Comparison of German and American Friction Coefficients for Highway Friction. *Transportation Research Record* **960**, TRB, National Research Council, Washington, D.C., pp. 13-20.

Lamm, R., and B.L. Smith. 1994. Procedure for Detecting Errors in Alignment Design and Consequences for Safer Redesign. *Transportation Research Record* **1445**, TRB, National Research Council, Washington, D.C., pp. 64-72.

Larson, T.R. 1996. Application of 3D and 4D Visual Modeling for Transportation Systems (NCHRP Project 20-5). Presented at the *Transportation Research Board Annual Meeting*, January 7-11.

Lieberman, E.B. 1982. Model for Calculating Safe Passing Sight Distances on Two-Lane Rural Roads. *Transportation Research Record* **869**, TRB, National Research Council, Washington, D.C., pp. 70-76.

Mannering, F.L., and W.P. Kilareski. 1990. *Principles of Highway Engineering and Traffic Analysis*. John Wiley & Sons, Inc. New York, N.Y.

Meijer, F., and O. Van Nijf. 1992. *Trade, Transportation and Society in Ancient World*. Routledge, Chapman and Hall Inc., New York, N.Y.

Michael, H.L. 1960. Highway Planning. Section 2: *Highway Engineering Handbook*. Edited by K.B. Woods, D.S. Berry, and W.H. Goetz, McGraw-Hill, Inc., New York, N.Y.

Mori, Y., M. Kurihara, A. Hayama, S. Ohkuma. 1995. A Study to Improve the Safety of Expressways by Desirable Combinations of Geometric Alignments.

Presented at the *International Symposium on Highway Geometric Design Practices*, Boston, Massachusetts, USA, August 30-September 1.

MUTCD. 1995. *Manual of Uniform Traffic Control Devices.* Ministry of Transportation of Ontario, MTO, Downsview, Ontario.

MUTCD. 1988. *Manual of Uniform Traffic Control Devices.* Federal Highway Administration, FHWA, Washington, D.C.

MUTCD. 1976. *Manual of Uniform Traffic Control Devices for Canada.* Transportation Association of Canada, TAC, Ottawa, Ontario.

NAASRA 1980. *Interim Guide to the Geometric Design of Rural Roads.* National Association of Australian State Road Authorities., Sydney, Australia.

Neuman, T.R. 1989. New Approach to Design for Stopping Sight Distance. *Transportation Research Record* **1208**, TRB, National Research Council, Washington, D.C., pp. 14-22.

Neuman, T.R., and J.C. Glennon. 1984. Cost-Effectiveness of Improvements to Stopping Sight Distance. *Transportation Research Record* **923**, TRB, National Research Council, Washington, D.C., pp. 26-34.

Noble, C.M. 1960. Geometric Design. Section 22: *Highway Engineering Handbook.* Edited by K.B. Woods, D.S. Berry, and W.H. Goetz, McGraw-Hill, Inc., New York, N.Y.

Oglesby, C.H., and R.G. Hicks. 1982. *Highway Engineering.* Fourth Edition, John Wiley & Sons, Inc., New York, N.Y

Olson, P.L., D.E. Cleveland, P.S. Fancher, L.P. Koystyniuk, and L.W. Schneider. 1984. *Parameters Affecting Stopping Sight Distance*. National Cooperative Highway Research Program, NCHRP Report **270**, TRB, National Research Council, Washington, D.C.

Park, R.A., N.J. Rowan, and N.E. Walton. 1968. A Computer Technique for Perspective Plotting of Roadways. *Highway Research Record* **232**, HRB, National Research Council, Washington, D.C., pp. 29-45.

PCA. 1984. *Thickness Design for Concrete Highway and Street Pavements*. Portland Cement Association, Chicago, Illinois.

Persaud, B.N. 1992. *Roadway Safety - A Review of the Ontario Experience and Relevant Work Elsewhere*. Report **PAV-92-02**, Ministry of Transportation of Ontario, Downsview, Ontario.

Reagan, J.A. 1994. The Interactive Highway Safety Design Model: Designing for Safety by Analyzing Road Geometrics. *Public Roads*, Vol. **58**, No. **1**, pp. 37-43.

Reagan, S. 1995. Influence of Road Geometrics on Vehicle Dynamics. Presented at the *International Symposium on Highway Geometric Design Practices*, Boston, Massachusetts, USA, August 30-September 1.

Rillet, L.R., B.G. Hutchinson, and M. Whitney. 1990. Mechanics of the Passing Maneuver and the Impact of Large Trucks. *Journal of Transportation Research*, Vol. **24A**, No. **2**, pp. 121-128.

Ross, N.F., and K. Russam. 1968. *The depth of Rain Water on Road Surfaces*. Road and Research Laboratory, RRL, Report No. **LR 236**, England. (Cited in Dunlap et al, 1978)

Saito, M. 1984. Evaluation of the Adequacy of the MUTCD Minimum Passing Sight Distance Requirement for Aborting the Passing Maneuver. *Journal of the Institute of Transportation Engineers*, pp. 18-22.

Sanchez, E. 1994. A 3-Dimensional Analysis of Sight Distance on Interchange Connectors. *Transportation Research Record* **1445**, TRB, National Research Council, Washington, D.C., pp. 101-108

Smith, B.L., and R. Lamm. 1994. Coordination of Horizontal and Vertical Alignment with Regard to Highway Aesthetics. *Transportation Research Record* **1445**, TRB, National Research Council, Washington, D.C., pp. 73-85.

Sparks, G.A., R.D. Neudorf, J.B.L. Robinson, and D. Good. 1993. Effects of Vehicle Length on Passing Operations. *Journal of Transportation Engineering*, ASCE, Vol. **119**, No. **2**, pp. 272-283.

Staughton, G.C., and T. Williams. 1970. *Tyre Performance in Wet Surface Conditions*. Road and Research Laboratory, RRL, Report No. **LR 355**, England. (Cited in Dunlap et al, 1978)

TAC. 1990. *Canada's Roadway Infrastructure: Selected Facts and Figures*. Transportation Association of Canada, Ottawa, Ontario.

TAC. 1986. *Manual of Geometric Design Standards for Canadian Roads*. Transportation Association of Canada, Ottawa, Ontario.

Tanton, M.S., R.M. Prescott, N. Walji, W.B. Currie, D.R. Saunders, R.G. Charlwood, P.Salt, C.W. Baker, and S. Gray. 1986. *The Use of Computer-Aided Design Techniques in Highway Engineering*. Transportation Association of Canada, TAC, Ottawa, Ontario.

TRB. 1987. *Designing Safer Roads: Practices for Resurfacing, Restoration, and Rehabilitation*. Special Report **214**. Transportation Research Board, National Research Council, Washington, D.C.

Van Der Tak, H.G., and A. Ray. 1971. *The Economic Benefits of Road Transport Projects*. Occasional Paper No. **13**, World Bank.

Van Valkenberg, G.W., and H.L. Michael. 1971. Criteria for No-Passing Zones. *Highway Research Record* **366**, HRB, National Research Council, Washington, D.C., pp. 1-9.

Waissi, G.R., and D.E. Cleveland. 1987. Sight Distance Relationships Involving Horizontal Curves. *Transportation Research Record* **1122**, TRB, National Research Council, Washington, D.C., pp. 96-107.

Weaver, G.D., and J.C. Glennon. 1971. *Passing Performance Measurements Related to Sight Distance Design*. Research Report **134-6**, Texas Transportation Institute.

Wright, P.H., and R.J. Paquette. 1979. *Highway Engineering*. Fourth Edition, John Wiley & Sons, Inc., New York, N.Y.

Yeager, R.W. 1971. *The Depth of Rain Water on Road Surfaces*. Unpublished Report, Goodyear Tire & Rubber Co. (Cited in Dunlap et al, 1978)

Yeager, R.W., and J.D. Miller. 1971. *Actual Water Depths on Roadways and Its Relationship to Tire Testing*. Unpublished Report, Goodyear Tire & Rubber Co. (Cited in Dunlap et al, 1978)

Yoder, E.J., and M.W. Witczak. 1975. *Principles of Pavement Design*. John Wiley & Sons, Inc., New York, N.Y.

Young, J.C., R.D. Miles, and C.L. Miller. 1960. Route Selection, Airphoto Interpolation, Photogrammetry, and Digital Computers. Section 5: *Highway Engineering Handbook*. Edited by K.B. Woods, D.S. Berry, and W.H. Goetz, McGraw-Hill, Inc., New York, N.Y.

Zienkiewicz, O.C., and R.L. Taylor. 1991. *The Finite Element Method*. Fourth Edition, McGraw-Hill Book Company Limited, London, England.

END

1 3 0 6 - 9 7

FIN